KATHOLIEKE UNIVERSITEIT LEUVEN
FACULTEIT TOEGEPASTE WETENSCHAPPEN
DEPARTMENT. ELEKTROTECHNIEK (ESAT)
AFDELING ELEKTRISCHE ENERGIE EN
COMPUTERARCHITECTUREN (ELECTA)
Kasteelpark Arenberg 10 - 3001 Leuven (Heverlee)

IMPACT OF WIND ENERGY IN A FUTURE POWER GRID

Promotoren:
Prof. dr. ir. R. BELMANS
Prof. dr. ir. W. HEYLEN

Proefschrift voorgedragen tot
het behalen van het doctoraat
in de toegepaste wetenschappen

door

Joris SOENS

December 2005

KATHOLIEKE UNIVERSITEIT LEUVEN
FACULTEIT TOEGEPASTE WETENSCHAPPEN
DEPARTEMENT ELEKTROTECHNIEK (ESAT)
AFDELING ELEKTRISCHE ENERGIE EN
COMPUTERARCHITECTUREN (ELECTA)
Kasteelpark Arenberg 10 - 3001 Leuven (Heverlee)

IMPACT OF WIND ENERGY IN A FUTURE POWER GRID

Jury:
Prof. dr. ir. A. HAEGEMANS , voorzitter
Prof. dr. ir. R. BELMANS, promotor
Prof. dr. ir. W. HEYLEN, promotor
Prof. dr. ir. J. DRIESEN
Prof. dr. ir. J. MELKEBEEK (U. Gent)
Prof. dr. ir. C. HIRSCH (V.U.Brussel)
Prof. dr. ir. R. HANITSCH (T.U.Berlin, Germany)
Prof. dr. ir. N. HATZIAGYRIOU (N.T.U. Athens, Greece)

Proefschrift voorgedragen tot
het behalen van het doctoraat
in de toegepaste wetenschappen

door

Joris SOENS

ISBN 90-5682-652-2
Wettelijk depot D/2005/7515/86
UDC 621.548

December 2005

ISBN 90-5682-652-2
Wettelijk depot D/2005/7515/86
UDC 621.548

Preface

Finishing a doctoral thesis should awake feelings of satisfaction, conceit, and good hopes for a bright career. In other cases however, the author finds himself back in the gutter, hardly able to remember anything of the wild expressions of relief, that accompanied the end of his thesis. By an act of fate, being the sudden appearance of a vacancy that I could impossibly resist applying for, this work was written from scratch in a few months. It was an intense and severe journey. Looking back to it, the number and kind of anatomical parts, that I wished the thesis to be united with during the writing process, remained well within the limits of courtesy. Although this might by explained by the fact that the day and night labour made me simply forget about their existence.

My gratitude goes towards my promotors, Professor Belmans and Professor Heylen, for willing to support the ideas in this work. Also I'd like to thank the members of the Advisory Committee and the Jury, especially Prof. Johan Driesen, for the interest and feedback in this very 'windy' thesis. I further wish to thank Professor D'haeseleer for kindly permitting the use of PROMIX. Also I want to express my thanks to all the people I had the pleasure of working with at K.U.Leuven, Universiteit Gent, V.U.B., 3E and Elia. Public opinions about the highly trendy subject of wind power can generally be classified as either (extreme) pro or (extreme) con. With the support by this group of experts, I tried to set up a correct assessment of the real potential of wind power for the specific case of Belgium. I do hope that the nuanced outcome of this work will be considered by decision makers as a relevant opinion about the strategy to follow.

This work was realized with the financial support of the Fonds voor Wetenschappelijk Onderzoek (F.W.O.) – Vlaanderen, that is greatly acknowledged.

I sincerely wish to thank Professor Belmans again, for his cooperative and gentle attitude with regard to my new career step. A cynic observer might interpret his highly non-obstructive behaviour, during my applying for a new job, as an indication of esteem about my value for his own department. Nevertheless I stubbornly keep interpreting the friendly and easy conversations in which we agreed

about my leaving K.U.Leuven in two phases as a sign of mutual understanding, of which I am very grateful.

To my new colleagues at the VREG, I am very grateful for their provisionally being satisfied with the half of me. I will do my very best to prove that my other half was worth waiting for: the worst is yet to come.

To my 'old' colleagues at the K.U.Leuven, all apologies for my anti-social behaviour during the last months. I will always keep nostalgic memories on the interesting discussions about electrical things, as well as the more human aspects of collegiality: the sport tournaments (which the ELECTA team won most of the time), the Christmas parties, the cantuses, the many receptions and birthday cakes, the terraces on the Oude Markt, the conferences, the awful music in the neighbouring office… Thank you for the very nice four years of -among other things- working together.

The completion of a PhD-thesis, and the accompanying privilege to write this preface as the most-read and least-controlled part of it, also gives me the opportunity to set right an oblivion in the acknowledgements of my previous (master) thesis. With a delay of four-and-a-half years, I wish to express my gratitude to Inge for embellishing my master thesis with hundreds of commas, making it comprehensible for the slow reader. I further wish to thank my mother and Christiane for removing those commas again. After all, the world's wealths are traditionally preserved for fast readers.

A very big 'thank you' to my family for offering me all chances to reach this moment of becoming a Dr- Ir. Thank you!

Finally, it is my opinion that this thesis, being a – however modest - contribution to a world's better environment, deserves a compensation. Therefore I claim for myself the right to pollute the world with a bunch of CO_2-emitting, noisy and annoying kids. Together with my wife-to-be Elke we will work on this matter in a near future. Thank you, Elke, for the exquisite dinners, for keeping me alive during the final push-through of this thesis, for all nice moments we shared, and the many more yet to come!

Abstract

This thesis investigates on various levels the technical impact of wind power on a power system.

The first part develops detailed dynamic models of wind turbines or farms in software dedicated to power system simulation. These models are used to assess the impact of wind speed or power grid disturbances. The models are a suitable tool to investigate the turbine's ability to provide 'ancillary services', i.e. voltage control or other types of grid support, and to assess the impact of adapting grid connection requirements specifically for wind turbines.
The second part quantifies the hourly and daily power output fluctuations of an aggregated wind park for the specific case study of the Belgian control zone, for various scenarios. Furthermore, the potential contribution to the abatement of carbon dioxide emissions by the total power generation park is assessed.
The final part presents the results of a multidisciplinary study with regard to optimal offshore wind developments in the Belgian Continental Shelf, including aspects with regard to seabed properties, wind resources, turbine types and power system availability.

Samenvatting

Dit doctoraat onderzoekt op verschillende niveaus de technische impact van windenergie op een elektriciteitsnet.

Het eerste deel van het doctoraat ontwikkelt gedetailleerde dynamische modellen van windturbines of -parken in software, specifiek voor de dynamische simulatie van elektriciteitssystemen. Deze modellen worden gebruikt om de invloed van veranderingen in windsnelheid of storingen in het net te simuleren. Verder zijn ze een geschikt hulpmiddel om te evalueren in welke mate een windturbine ‘netondersteunende diensten’ zoals spanningscontrole kan bieden, en wat de invloed is van aangepaste netaansluitingsvoorwaarden voor windturbines.
Het tweede deel van het doctoraat beschrijft de uurlijkse en dagelijkse fluctuaties in energiegeneratie door een geaggregeerd windpark, en dit voor de specifieke gevalstudie van de Belgische regelzone, voor verschillende scenario’s. Bovendien wordt het potentieel van windenergie om de totale CO_2-uitstoot van het Belgisch centralepark te doen afnemen geëvalueerd.
In het laatste deel worden de resultaten voorgesteld van een multidisciplinaire studie met betrekking tot de optimale ontwikkelingen voor offshore windenergie in het Belgische deel van de Noordzee. Deze resultaten houden rekening met eigenschappen van de zeebedding, windkarakteristieken, turbinetypes en beschikbaarheid van een elektriciteitsnet.

Table of Contents

Nederlandstalige samenvatting

Impact van windenergie in het toekomstig elektriciteitsnet

I. Inleiding

Probleemstelling

Windenergie is samen met biomassa de snelst expanderende technologie voor hernieuwbare-energieproductie in Europa. Eind 2004 bedroeg het totaal geïnstalleerd windvermogen in de 15 oorspronkelijke lidstaten van de Europese Unie 34 GW, een cijfer dat alle oorspronkelijke doelstellingen overtrof.

Met deze steile groei van geïnstalleerd windvermogen in de bestaande energienetten gaan nieuwe uitdagingen voor robuust en betrouwbaar netbeheer gepaard. Energie-opwekking door windkrachtgeneratoren verschilt immers in meerdere aspecten van klassieke generatie.

- In vele gevallen wordt windenergie geproduceerd door alleenstaande turbines en geïnjecteerd in het distributienet, waaraan normaliter enkel afnemers van energie gekoppeld zijn. Hierdoor veranderen de klassieke vermogensstromen van transmissie- naar distributienet mogelijk van richting, wat nieuwe beveiligingsstrategieën nodig maakt.

- In andere gevallen worden windturbines gegroepeerd tot grote windparken, die hun energie rechtstreeks in het transmissienet injecteren zoals een klassieke centrale. Deze windparken worden gebouwd waar de

beschikbaarheid van ruimte en de te verwachten windsnelheden het grootste zijn; dit is meestal ver van stedelijke of industriële centra met hoge energievraag (bijvoorbeeld in zee). Het transport van windenergie naar de verbruikers moet derhalve over grote afstanden gebeuren, wat mogelijk een aanpassing van het transmissienet noodzakelijk maakt.

- De generatoren in windturbines verschillen van generatoren in klassieke centrales, vooral omwille van de vereiste dat een windturbine sterk fluctuerende mechanische belastingen moet kunnen ondergaan. Van de verschillende generatortypes voor windturbines is het transiënt gedrag tijdens netstoringen vrij complex en soms niet precies gekend. Een goede kennis ervan is nochtans cruciaal voor de stabiliteit van het energiesysteem. Het volgend scenario illustreert dit: de uitschakeling van een windturbine door haar eigen beveiligingscircuit tengevolge van een netstoring betekent een plots verlies aan energie-injectie. Dit is op zich een nieuwe netstoring die de uitschakeling van andere turbines in de nabijheid kan induceren. Op die manier kan een cascade-effect ontstaan waarbij een groot aantal windturbines en andere generatoren op korte tijd van het net gekoppeld worden, wat een aanzienlijk verlies van energieproductie veroorzaakt, en waarbij de stabiliteit van het energiesysteem in het gedrang komt. Het is dus belangrijk dat windturbines tijdens een netincident binnen de mate van het technisch mogelijke hun energieproductie niet onderbreken, en daarbij ook nog extra netondersteuning bieden, zoals spannings- en frequentiecontrole, om de invloed van een netstoring op andere netgebruikers te beperken.

- Omwille van de variabiliteit van de wind zelf is de energieproductie moeilijk voorspelbaar en nauwelijks controleerbaar. Fluctuaties in de productie van windenergie moeten opgevangen worden door andere generatoren in het energiesysteem. Een groot gebruik van windgeneratoren maakt de beschikbaarheid van extra regelvermogen dus noodzakelijk. Hierdoor wordt het economisch en ecologisch voordeel van windenergie enigszins afgezwakt.

Dit doctoraat onderzoekt in welke mate en onder welke voorwaarden windenergie een belangrijk deel van de totale elektriciteitsproductie kan uitmaken. Stabiel en robuust netbeheer is hierbij het voornaamste criterium.

Inhoud van het doctoraat

Het eerste deel van het doctoraat licht de recente vernieuwingen in het beheer van Europese elektriciteitsnetten toe: met name de deregulering van de elektriciteitsmarkt en de toenemende interesse voor hernieuwbare energie wordt behandeld. De nieuwe technologieën voor de productie van hernieuwbare energie worden meestal onder de vorm van verspreide generatie (dit zijn generatoren van relatief laag vermogen die aan het distributienet gekoppeld worden) geïmplementeerd. In een literatuurstudie wordt het toenemende belang van aangepaste netaansluitingsvoorwaarden voor verspreide generatie-eenheden, met in

het bijzonder windenergie, aangetoond. Deze specifieke netaansluitingsvoorwaarden werden reeds geïmplementeerd in enkele Europese landen, en moeten garanderen dat het elektriciteitsnet niet minder stabiel wordt wanneer grote conventionele generatoren vervangen worden door verspreide generatie-eenheden. Onder meer het gevaar voor het cascade-effect, zoals hierboven toegelicht, legt hoge technische eisen op aan deze generatoren. In deze nederlandstalige samenvatting wordt hier verder niet op ingegaan.

In het tweede deel worden de karakteristieken van windenergie overlopen, en worden dynamische modellen van een windturbine met al haar componenten ontwikkeld. De nadruk ligt hierbij op de elektrische karakteristieken. Deze modellen worden gebruikt voor dynamische simulaties van elektriciteitsnetten in daartoe specifiek ontwikkelde software. Na de ontwikkeling van een gedetailleerd windturbinemodel wordt een vereenvoudigd dynamisch model, bestaande uit een transferfunctie die windsignalen rechtstreeks omzet in vermogensignalen, voorgesteld. Deze modellen laten toe om een inschatting te maken van de dynamische effecten van geïnstalleerd windvermogen in een elektriciteitsnet. Dit kan onder meer gebruikt worden om de technische haalbaarheid en de impact van specifieke aansluitingsvoorwaarden voor windturbines, opgelegd door de netbeheerder, in te schatten.

Een derde deel van het doctoraat kwantificeert de verwachte fluctuaties in generatie door een geaggregeerd windpark in de Belgische regelzone, door middel van Markov-matrices. Daarop verder bouwend wordt ook een evaluatie gemaakt van de waarde van windenergie, volgens verschillende criteria: de capaciteitsfactor, het capaciteitskrediet, de gemiddelde betrouwbare energieproductie, en de potentiële vermindering van CO_2-uitstoot door het Belgisch elektriciteitscentralepark.

Het laatste deel bespreekt de resultaten van een multidisciplinair onderzoeksproject dat tot doel had de krijtlijnen uit te tekenen voor de optimale ontwikkelingen van offshore-windenergie in het Belgisch deel van de Noordzee. De bijdrage van de auteur in dit onderzoeksproject bestaat voornamelijk uit een evaluatie van de beschikbaarheid van een hoogspanningsnet voor de opname van offshore-windenergie, en een evaluatie van de technologische ontwikkelingen van de turbines zelf.

II. Karakteristieken van windenergie

Wind

Figuur 1a toont een histogram voor de gemeten uurlijkse windsnelheden in Oostende in de periode 2001-2003, met de best passende Weibull-curve gesuperponeerd als schatting van de kansdichtheid. Weibull-curves, met het typisch trager afnemend verloop voor hogere x-waarden, worden algemeen beschouwd als

een goede benadering voor de kansdichtheid van de windsnelheid op een bepaalde plaats.

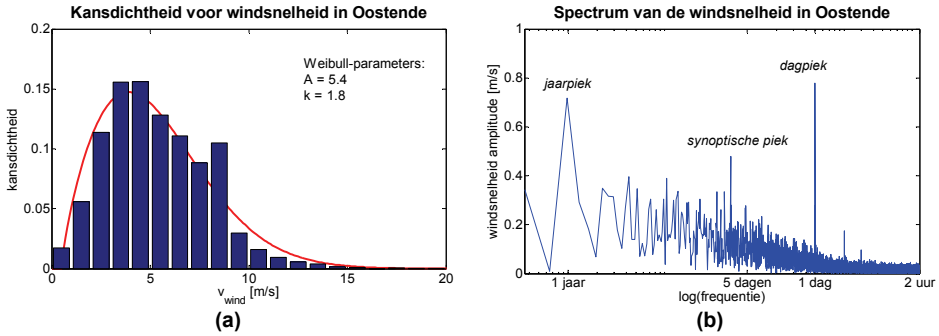

Figuur 1. histogram voor de gemeten uurlijkse windsnelheden in Oostende in de periode 2001-2003 (a), en spectrum van dezelfe windmetingen (b)

Figuur 1b toont het spectrum voor dezelfde gemeten windsnelheden. De jaar-, synoptische en dagpiek kunnen duidelijk onderscheiden worden:

- de *jaarpiek* wordt verklaard door de seizoensafhankelijkheid van de windsnelheid, met de hoogste gemiddelden in februari, en de laagste in augustus;

- de *dagpiek* wordt verklaard door de dagelijkse periodiciteit van de windsnelheid, met een hoogste gemiddelde in de namiddag en een laagste in de vroege ochtend;

- de *synoptische* piek is eerder een uitgestreke zone met hogere frequentie-inhoud dan een scherpe piek, en wordt verklaard door de cyclische weerpatronen met een typische periode van een dag tot een week.

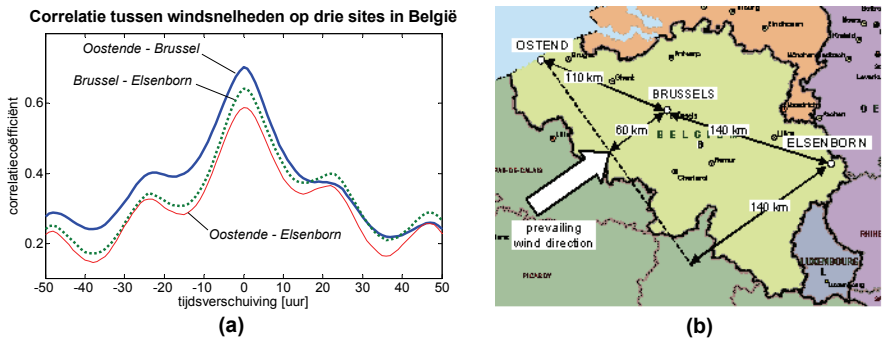

Figuur 2. Correlatie tussen uurlijkse windsnelheden op drie sites in België (a): Oostende, Brussel en Elsenborn (b)

Figuur 2a toont de correlatie tussen uurlijkse windsnelheden, gemeten op drie sites in België (Oostende, Brussel en Elsenborn - Figuur 2b). Deze toont aan dat de correlatie tussen windsnelheden over vrijwel het hele Belgische gebied erg groot is, en het grootst wanneer gelijktijdige windsnelheden op de verschillende sites worden beschouwd. Dit impliceert dat de gunstige invloed van een sterke ruimtelijke spreiding van de turbines op de fluctuaties van het geaggregeerde windvermogen beperkt is. Dit wordt verder besproken in hoofdstuk IV van deze samenvatting.

Turbine- en generatortypes

De verschillende types windturbines onderscheiden zich van elkaar voornamelijk door hun snelheidsregeling en bladhoekregeling. De keuze van het generatortype wordt grotendeels bepaald door het gewenste snelheidsbereik van de turbine.

De constante-snelheidturbines gebruiken meestal een inductiegenerator met kooirotor. De inductiegenerator is rechtstreeks verbonden met het net zonder vermogenelektronische tussenkring. Deze turbines hebben een uiterst beperkt snelheidsbereik rond het synchroon toerental van de generator. De generator verbruikt steeds reactieve energie, en kan geen netondersteunende diensten, zoals spanningsregeling, leveren.

Variabele-snelheidturbines kenmerken zich door een hogere energieproductie bij lage windsnelheden, door het verhoogd aerodynamisch rendement bij laag turbinetoerental. Bovendien zijn deze turbines beter bestand tegen de mechanische belastingsstoten bij variërende windsnelheden: deze belastingen worden deels opgevangen door een verandering in het turbinetoerental, wat ook in een meer gelijkmatige energieproductie resulteert. De meest gebruikte generatortypes bij variabele-snelheidturbines zijn de dubbelgevoede inductiegenerator en de synchrone generator: deze types zijn beter geschikt voor de levering van netondersteunende diensten dan de inductiegenerator. De vermogenelektronische componenten beïnvloeden het transiënt gedrag tijdens netstoringen, wat een grondige studie noodzakelijk maakt.

De bladhoekregeling kan voor zowel constante- als variabele-snelheidturbines van het type *stall-control* of *pitch-control* zijn.

Bij *stall-control* zijn de turbinebladen niet verstelbaar om hun as. Door een aangepaste vormgeving van de turbinebladen ontstaat turbulentie bij hoge windsnelheden. Dit vermindert aanzienlijk het mechanisch koppel op de rotor, waardoor de turbine intrinsiek beschermd is tegen overbelasting. Voor windsnelheden groter dan de nominale waarde daalt de energieproductie bij toenemende windsnelheid.

Bij *pitch-control* zijn de turbinebladen wel verstelbaar om hun as. Bij hoge windsnelheden worden de turbinebladen deels uit de wind gedraaid, zodat het aerodynamisch rendement van de turbine daalt. Op deze manier kan de turbine haar nominaal vermogen blijven produceren bij windsnelheden groter dan de nominale windsnelheid.

III. Dynamische modellering van een windturbine

Gedetailleerd model

Modelstructuur

Een gedetailleerd dynamisch model van een volledige windturbine is ontwikkeld in Eurostag, een softwareplatform voor dynamische simulaties van elektriciteitsnetten. Figuur 3 toont de modelstructuur van een bladhoekgecontroleerde turbine, uitgerust met een dubbelgevoede inductiegenerator. Dit is de meest complexe combinatie van turbine en generator. Modellen van turbines met of zonder bladhoekregeling en met andere generatortypes kunnen eenvoudig bekomen worden door weglating of lichte aanpassing van een aantal modelblokken.

Het model heeft als ingangssignalen de netspanning *(u_R, u_l)*, de windsnelheid v_{wind} en een referentiewaarde voor het reactief vermogen. Het uitgangssignaal is de stroomfasor *(i_R, i_l)* die door de turbine in het net geïnjecteerd wordt. Voor de uitvoerige beschrijving van dit model wordt verwezen naar hoofdstuk 5 van dit doctoraat.

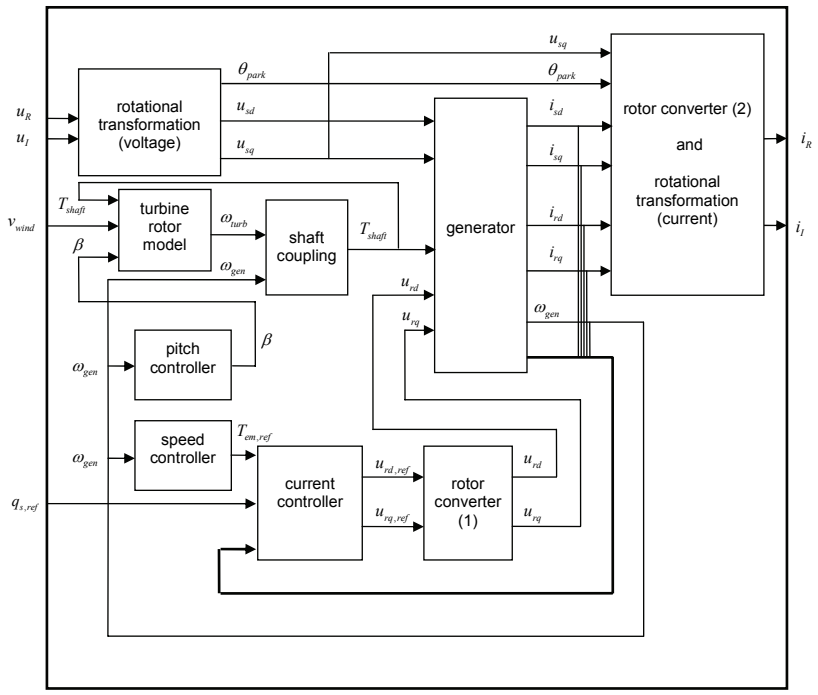

Figuur 3. Modelstructuur van een bladhoekgecontroleerde windturbine met dubbelgevoede inductiegenerator

Simulaties

Met het dynamisch model van Figuur 3 kan het effect van een windsnelheidsveranderingen of netstoringen nauwkeurig bestudeerd worden. Figuur 4 toont de als invoersignaal gebruikte windsnelheid, stapsgewijs veranderend van 6 m/s naar 20 m/s in stappen van 2 m/s.

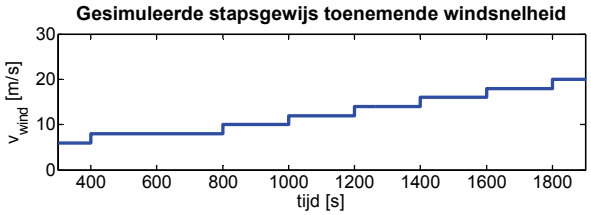

Figuur 4. Windsnelheid, gebruikt als invoersignaal voor dynamische simulaties

Figuur 5a toont de resulterende generatorsnelheid. De versnelling van de constante-snelheidturbine bij toename van de windsnelheid is uiterst gering, en wordt bepaald door de (steile) koppel-toerentalkarakteristiek van een inductiemachine. De variabele-snelheidturbine versnelt bij toenemende windsnelheid tot het maximaal toerental bereikt is, in dit voorbeeld gelijk aan 1.1 per unit. Figuur 5b toont een detailopname van de snelheidsverandering van turbinerotor en generator bij een stapsgewijze windsnelheidstoename. De generatorsnelheid in stationair bedrijf verschilt uiterst weinig voor en na de windsnelheidstoename. De figuur toont wel de torsionele oscillaties tussen turbinerotor en generator, meteen na de windsnelheidstoename.

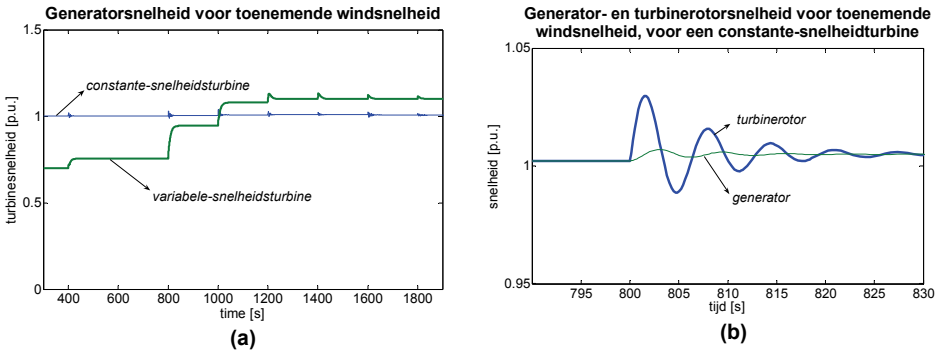

Figuur 5. Generatorsnelheid bij toenemende windsnelheid (a), en close-up op generator- en turbinesnelheid bij toenemende windsnelheid voor een constante-snelheidturbine (b)

De eerder genoemde voordelen van variabele-snelheidturbines kunnen afgeleid worden uit Figuur 6a. Deze toont het geproduceerd actief vermogen voor een variabele-snelheidturbine met bladhoekregeling enerzijds, en een constante-snelheidturbine zonder bladhoekregeling anderzijds. Bij de variabele-

snelheidturbine wordt de rotorsnelheid zodanig geregeld dat het aerodynamisch rendement maximaal is over een breed windsnelheidsbereik. Dit levert vooral bij lage windsnelheid hogere energie-opbrengsten op. De figuur toont verder ook het voordeel van bladhoekregeling: een turbine met bladhoekregeling is in staat haar volledig nominaal actief vermogen te produceren over een breed windsnelheidsbereik boven de nominale windsnelheid, terwijl de energie-opbrengst van een turbine zonder bladhoekregeling daalt bij toenemende windsnelheid boven de nominale waarde, omwille van de daling van het aerodynamisch rendement. Deze daling is een intrinsieke bescherming tegen mechanische overbelasting op de turbine.

Figuur 6b toont het torsiekoppel in de koppeling tussen turbinerotor en generator, die als een gedempte torsieveer werd gemodelleerd. De koppeltransiënten zijn prominent aanwezig bij de constante-snelheidturbine, terwijl deze in het andere geval gedempt worden door de gelijktijdige versnelling van de turbine.

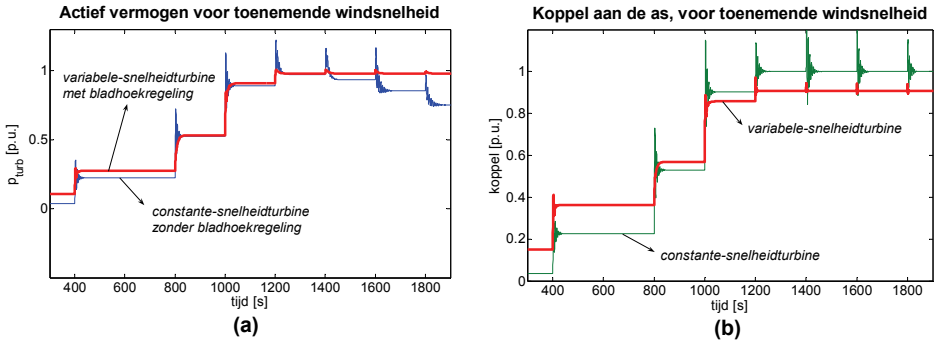

Figuur 6. Actief vermogen voor toenemende windsnelheid (a), en koppel aan de as voor toenemende windsnelheid (b)

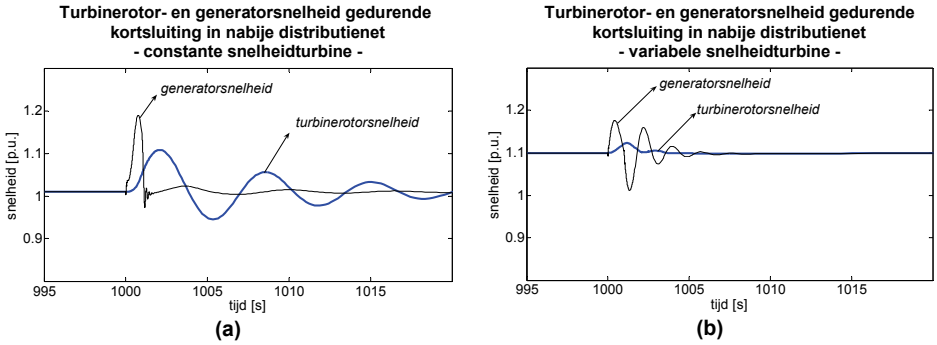

Figuur 7. Turbinerotor- en generatorsnelheid gedurende een kortsluiting in het nabije distributienet, voor een constante- (a) en variabele-snelheidturbine (b)

Figuur 7 toont de generator- en turbinesnelheid in het geval van een kortsluiting in het distributienet, resulterend in een spanningsdaling tot 60% van de nominale spanning gedurende 1 seconde aan de klemmen van de turbinegenerator, voor een

constante-snelheidturbine (a) en een variabele-snelheidturbine (b). De variabele-snelheidturbine is hierbij uitgerust met een dubbelgevoede inductiegenerator met actieve spanningsregeling. De amplitude en duur van de snelheidstransiënten zijn duidelijk groter voor de constante-snelheidturbine.

Figuur 8 toont het actief (a) en reactief (b) vermogen voor dezelfde kortsluiting, voor beide turbinetypes. Ook in deze figuur blijkt dat de transiënten bij een constante-snelheidturbine met inductiegenerator een grotere amplitude en een langere duur hebben dan bij een variabele-snelheidturbine.

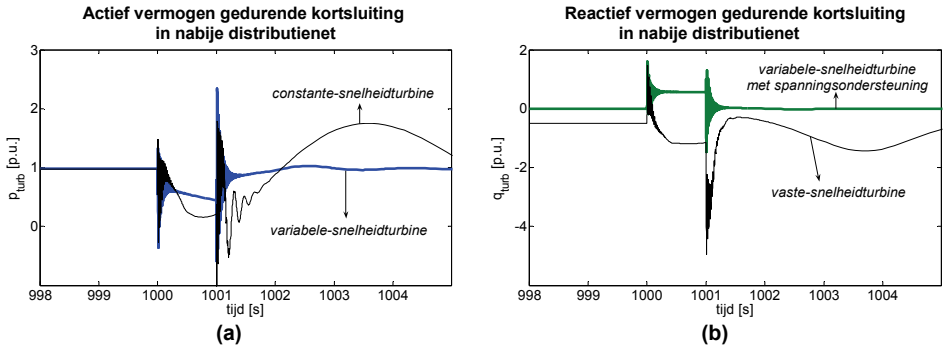

Figuur 8. Actief (a) en reactief (b) vermogen gedurende een kortsluiting in het nabije distributienet, voor een constante- en variabele-snelheidturbine

Vereenvoudigd equivalent model

Modelstructuur

Voor de opbouw van een vereenvoudigd equivalent model wordt vertrokken van een gedetailleerd model zoals hierboven beschreven. Een reeks simulaties wordt uitgevoerd, waarbij signalen voor de windsnelheid worden gegenereerd als een superpositie van een constante waarde met een sinusgolf. Enkele simulatievoorbeelden worden getoond in Figuur 9. Het actief vermogen, door het turbinemodel berekend, bestaat ook uit een superpositie van een constante waarde en een sinusgolf, met dezelfde frequentie als deze van de windsnelheid. Dit suggereert dat het hele systeem lineair is.

Figuur 10 toont de amplitude van de vermogenfluctuaties, in functie van de gemiddelde waarde en frequentie van het windsnelheidssignaal. In de figuur worden twee curvensets onderscheiden. De curves horende bij de lage waarden voor de gemiddelde windsnelheid (lager dan de nominale waarde) vertonen een constant en daarna dalend verloop, dit is de karakteristiek van een laagdoorlaatfilter van de eerste orde. De curves horende bij de hogere waarden voor de gemiddelde windsnelheid vertonen een stijgend en daarna dalend verloop, dit is de karakteristiek van een transferfunctie van een hogere orde.

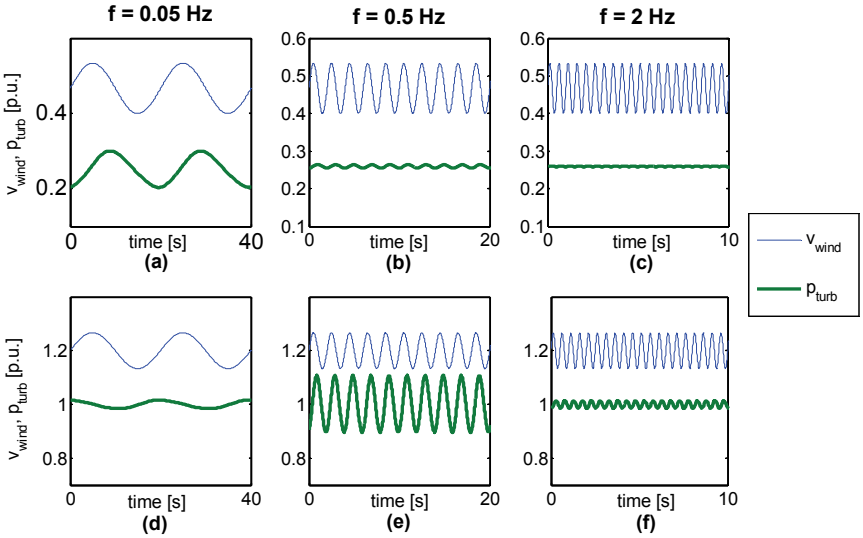

Figuur 9. Enkele simulatievoorbeelden met een sinusoïdale windsnelheid gesuperponeerd op een constante waarde

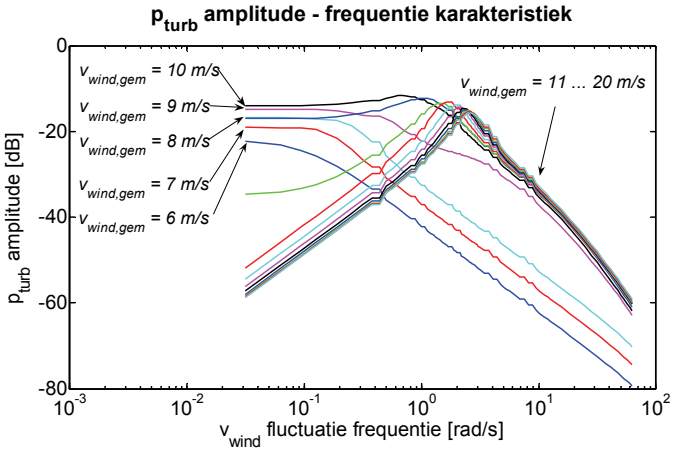

Figuur 10. Amplitude van de vermogenfluctuaties in functie van de frequentie van het windsnelheidssignaal

Het vereenvoudigd dynamisch model, dat het beschikbaar turbinevermogen $p_{beschikb}$ rechtstreeks uit de windsnelheid berekent, is weergegeven in Figuur 11. De twee transferfuncties die overeenstemmen met de twee curvensets uit Figuur 10, namelijk de laagdoorlaatfilter en de bijkomende transferfunctie voor hoge-windsnelheidregime, kunnen teruggevonden worden in het model. Verder is de vermogencurve van de betreffende turbine ook opgenomen in het model. Bij windsnelheden groter dan de nominale waarde is de bovenste invoer van de sommator die $p_{beschikb}$ berekent constant en gelijk aan het nominale turbinevermogen.

De onderste invoer van de sommator vertegenwoordigt de tweede curvenset uit Figuur 10, en wordt vermenigvuldigd met een factor die gelijk is aan 0 bij lage windsnelheden, en gelijk aan 1 bij hoge windsnelheden, met een geleidelijke overgang van 0 naar 1 voor windsnelheden in de buurt van de nominale windsnelheid.

Het vereenvoudigd dynamisch model vervangt de complexe modellen van de turbinerotor, de toerentalregeling, de bladhoekregeling en de generator uit Figuur 3, met dezelfde resultaten voor het berekend actief vermogen, zowel in stabiele als in transiënte toestand.

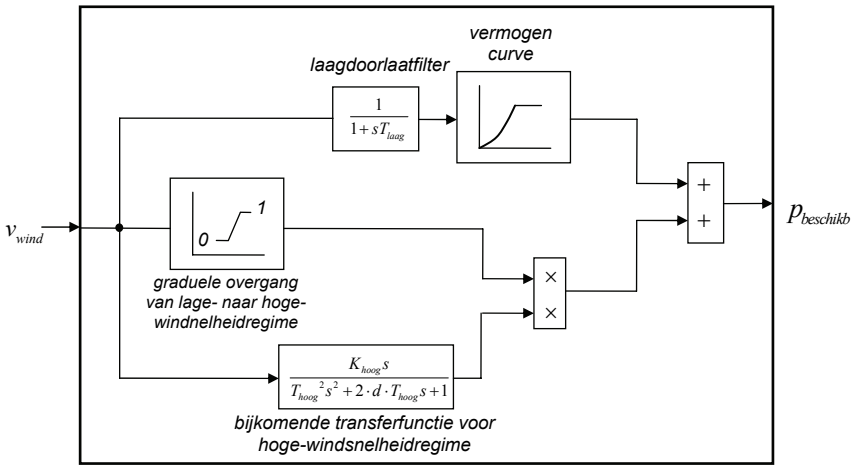

Figuur 11. Vereenvoudigd dynamisch actief-vermogenmodel van een windturbine

Het actief-vermogenmodel wordt verder nog uitgebreid met een module die toelaat te kiezen tussen verschillende controlemodi (Figuur 12). Deze uitbreiding reflecteert de strengere netaansluitingsrichtlijnen, opgelegd door steeds meer netbeheerders, voor windturbines en –parken, in verband met de regelbaarheid van actief vermogen. Drie modi kunnen geselecteerd worden.

- In de '*fractie*'-modus wordt slechts een fractie α van het beschikbaar vermogen geproduceerd, de fractie (1- α) wordt door bladhoekregeling als reservevermogen voor frequentieregeling ingezet.

- In de '*begrensd*'-modus wordt het maximaal geproduceerd vermogen, door voortdurende regeling van de bladhoek, niet hoger dan de waarde p_{lim}, ook indien de ogenblikkelijke waarde van $p_{beschikb}$ hoger is. Dit kan opgelegd worden door de operator van de windkrachtinstallatie of door de netbeheerder, bijvoorbeeld indien er overbelasting dreigt van een bepaalde hoogspanningslijn.

- De meest voorkomende mode, de '*100%*'-modus, is diegene waarbij alle beschikbaar mechanisch turbinevermogen $p_{beschikb}$ wordt omgezet in

elektrisch vermogen. Dit wordt in het model uit Figuur 12 ingesteld door α gelijk aan 1 te kiezen in de '*fractie*'-modus, of door p_{lim} gelijk aan het nominaal turbinevermogen te kiezen in de '*begrensd*'-modus.

De hellingsbegrenzer ('rate limiter') reflecteert de begrensde regelsnelheid van de turbinebladhoeken, en de daaruitvolgende equivalente vertraging bij de overschakeling tussen twee modi.

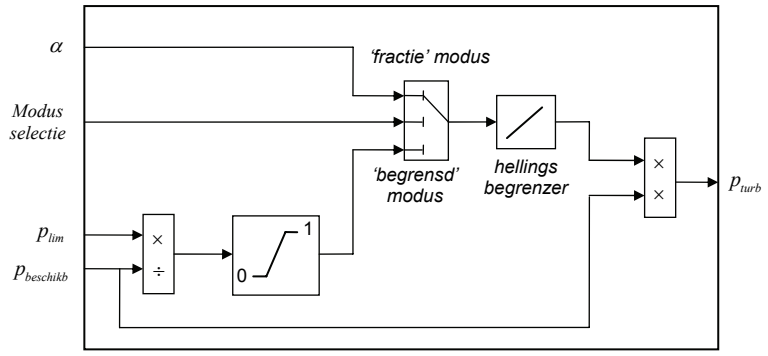

Figuur 12. Dynamisch model voor de overgang tussen de verschillende modi voor actief-vermogenproductie

Het vereenvoudigd equivalent dynamisch model voor reactief vermogen wordt getoond in Figuur 13. Twee modi worden hier gebruikt: in de '*vaste arbeidsfactor*'-modus wordt de arbeidsfactor, of $\cos\phi$, op een constante waarde gehouden, bijvoorbeeld 1. De ogenblikkelijke referentiewaarde voor reactief vermogen of stroom wordt berekend uit de gewenste arbeidsfactor en het ogenblikkelijk actief vermogen.

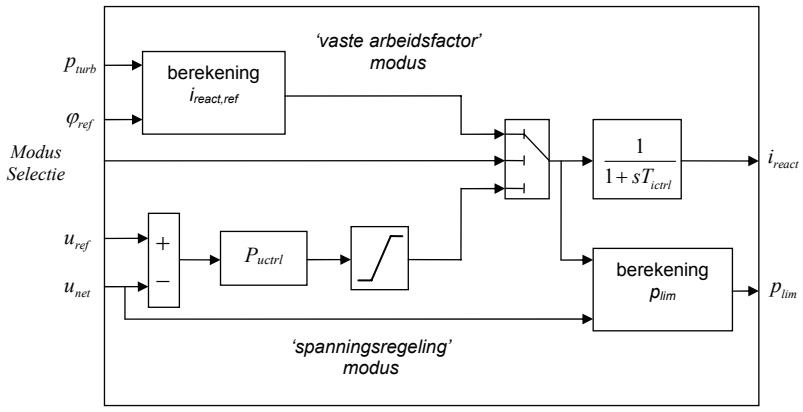

Figuur 13. Equivalent dynamisch reactief-vermogenmodel van een windturbine

In de '*spanningsregeling*'-modus wordt het reactief vermogen geregeld om de netspanning u_{net} een bepaalde referentiespanning u_{ref} te laten bereiken. In het

voorbeeld uit Figuur 13 wordt een proportionele regelaar gebruikt, met versterking P_{uctrl}.

In beide regelmodi wordt ook een limietwaarde p_{lim} berekend voor het actief vermogen, die ten allen tijde moet gerespecteerd worden en die dient als invoerwaarde voor de '*begrensd*'-modus, de standaardmodus voor de actief-vermogenregeling. Deze limietwaarde volgt uit de vereiste dat de totale machinestroom haar nominale waarde niet mag overschrijven. Voorrang wordt gegeven aan de reactieve stroom, zodat de actieve stroom naar beneden moet bijgesteld worden indien de totale stroom te hoog wordt. In normaal bedrijf is de hier berekende p_{lim} niet lager dan het nominale turbinevermogen, wat neerkomt op de toepassing van de '*100%*'-modus voor de actief-vermogenregeling.

Gebruik van het vereenvoudigd equivalent model

Figuur 14 toont het actief (a) en reactief (b) vermogen, berekend door het vereenvoudigd equivalent dynamisch model, voor de stapsgewijs toenemende windsnelheid van Figuur 4. De resultaten stemmen zowel in stationair als in transiënt bedrijf in hoge mate overeen met de berekeningen met het gedetailleerd turbinemodel, wat de equivalentie van het vereenvoudigd model bewijst.

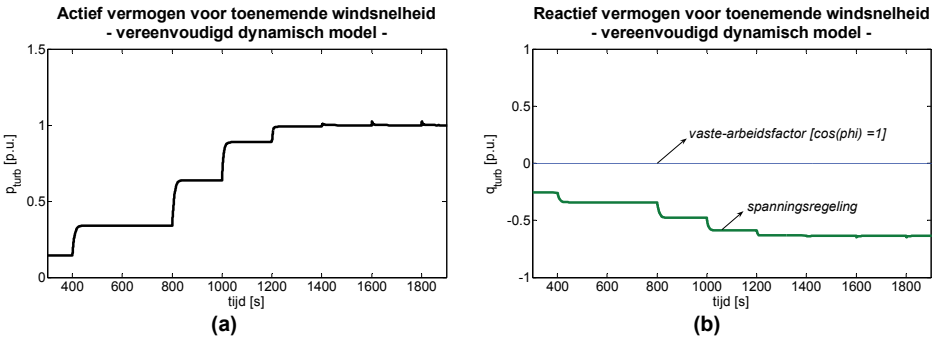

Figuur 14. Simulatie van actief (a) en reactief (b) vermogen, berekend met het vereenvoudigd equivalent dynmaisch model

Met deze en andere simulatieresultaten kan als besluit worden gesteld dat berekeningen met het vereenvoudigd equivalent turbinemodel zowel in stationaire als transiënte nettoestanden tot dezelfde resultaten leiden als deze met het gedetailleerd turbinemodel.

Het gebruik van het vereenvoudigd model levert een grote besparing op, zowel wat betreft het rekenwerk voor de simulator als het modelleerwerk voor de gebruiker. Het model is toepasbaar voor alle variabele-snelheidturbines met bladhoekregeling, onafhankelijk van het precieze generatortype. De parameters van het model, voor een specifieke turbine, zijn geen standaard constructeurgegevens, maar kunnen uit simulatieresultaten met een gedetailleerd model bepaald worden. De modelparameters hebben bovendien rechtstreeks betrekking op het gedrag van de

turbine in het elektrisch net. De parameters in het vereenvoudigd model zijn bovendien heel nauw verwant met de parameters in een typisch netaansluitingsreglement, door de netbeheerder opgesteld.

IV. Geaggregeerde windenergie in België

Werkwijze

Dit hoofdstuk berekent de uurlijkse energieproductie van het geaggregeerd windpark in de regelzone beheerd door Elia (d.i. België en een deel van Luxemburg). Op basis van windsnelheidsgegevens op drie sites in België met een uurlijkse resolutie over een periode van drie jaar worden tijdreeksen berekend voor de totaal geproduceerde windenergie per uur, als percentage van het geïnstalleerd windvermogen. Deze drie sites zijn Oostende, Brussel en Elsenborn, en liggen verspreid in de beschouwde regelzone zoals reeds getoond in Figuur 2b.

Voor de berekening van deze energietijdreeksen is een algoritme ontwikkeld dat vertrekt van een willekeurig aantal turbinetypes met een eigen vermogencurve en gondelhoogte, een geografische beschrijving van de landschapsruwheid ('*roughness length*') en windturbulentie. Verder vraagt het algoritme ook een beschrijving van de ruimtelijke spreiding van de turbines als invoer, als functie van de positie op de as Oostende-Brussel-Elsenborn. De resolutie van de data kan door de gebruiker vrij gekozen worden.

In dit hoofdstuk wordt de berekening uitgevoerd met twee turbinetypes:

- *type I*: variabele-snelheidturbines met bladhoekregeling, gondelhoogte 80 m of 90 m;
- *type II*: constante-snelheidturbines zonder bladhoekregeling, gondelhoogte 40 m;

en voor vier scenario's in verband met de ruimtelijke spreiding van de turbines (Figuur 15):

- *scenario I*: alle turbines regelmatig verspreid over het hele gebied, 50% van het geïnstalleerd vermogen is van *type I* en 50% van *type II*;
- *scenario II*: een grotere concentratie turbines in West-Vlaanderen waar de windcondities het gunstigst zijn, 60% van het geïnstalleerd vermogen is van *type I* en 40% van *type II*;
- *scenario III*: één windpark in de Noordzee (*type I*, gondelhoogte 110 m);

- *scenario IV*: 40% van het totaal geïnstalleerd vermogen aan land zoals in *scenario II*, en 60% in zee zoals in *scenario III*.

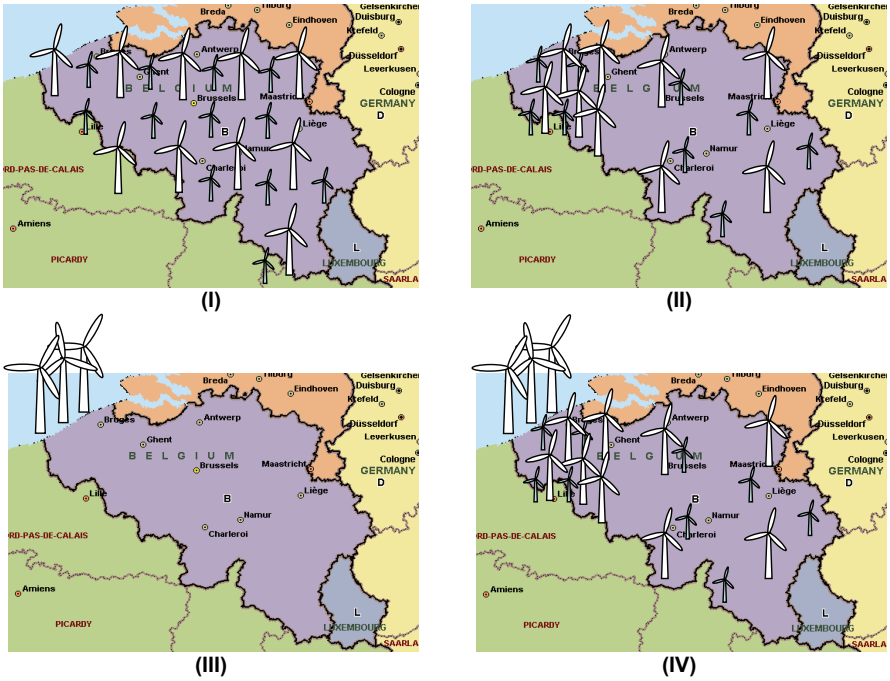

Figuur 15. Vier scenario's voor de ruimtelijke spreiding van turbines in de Belgische regelzone

Als verdere invoerdata voor het algoritme wordt een windturbulentie aangenomen van 15% over de hele regelzone, en een breedte van de regelzone loodrecht op de as Oostende-Brussel-Elsenborn variërend tussen 50 km en 200 km.

Het algoritme berekent voor elk punt op de Oostende-Brussel-Elsenborn de uurlijkse windsnelheid door lineaire interpolatie van de beschikbare meetdata voor hetzelfde uur. De windsnelheid op elke plaats wordt ook herrekend als functie van de gondelhoogten van de turbines die op deze plaats aanwezig zijn, gebruik makend van de volgende vergelijking:

$$v_{wind,h2} = v_{wind,h1} \cdot \frac{\ln \frac{h_2}{z_0}}{\ln \frac{h_1}{z_0}}$$

met $v_{wind,h}$ de windsnelheid op hoogte h, en z_0 de landschapsruwheid.

Vertrekkende van de vermogencurves van de verschillende turbinetypes worden multiturbinevermogencurves berekend, die de breedte *D* van de regelzone in rekening brengen voor de gezamenlijke productie van windturbines verspreid over deze breedte. Met deze curves en de uit de meetdata berekende windsnelheden wordt uiteindelijk het beschikbare vermogen uit windturbines berekend voor elk punt op de as Oostende-Brussel-Elsenborn. De vermogens op al deze punten worden dan gesommeerd om voor elk uur het geaggregeerd beschikbaar vermogen in de Belgische regelzone te bekomen.

De resulterende vermogentijdreeksentijdreeksen met uurlijkse resolutie worden daarna verder statistisch verwerkt. De verwachte productie van windenergie en haar fluctuaties worden in enkele kernfiguren en -matrices samengevat. De resultaten worden verder ook gebruikt om de waarde van windenergie in België te schatten.

Resultaten

Figuur 16 toont een voorbeeld van tijdreeksen van geaggregeerd windvermogen gedurende 72 uur, voor de vier scenario's. Van alle scenario's vertoont *scenario III* (het windpark in zee) de hoogste productiepieken maar ook de meeste fluctuaties.

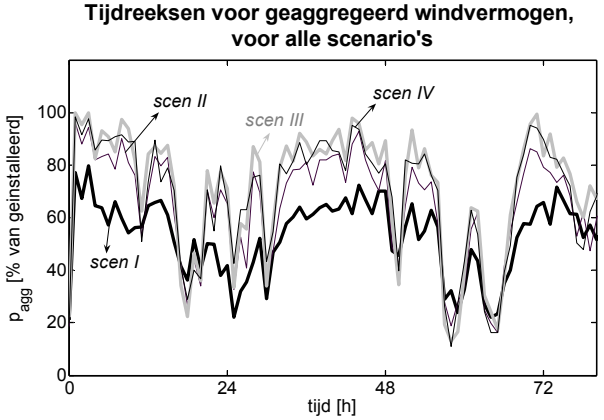

Figuur 16. Tijdreeksen voor geaggregeerd windvermogen voor alle scenario's

scenario	*capaciteitsfactor [%]*	*equivalent aantal vollasturen*
I	20	984
II	26	1519
III	31	1755
IV	29	1660

Tabel 1. Capaciteitsfactor en equivalent aantal vollasturen voor de vier scenario's

De gemiddelde productie over een jaar, als percentage van het geïnstalleerd vermogen, is de *capaciteitsfactor*. Deze is voor de vier scenario's weergegeven in Tabel 1, samen met het equivalent aantal vollasturen.

Figuur 17 toont hoe de gemiddelde generatie van windenergie afhangt van de maand in het jaar. Voor alle scenario's is de hoogste generatie in februari en de laagste in augustus.

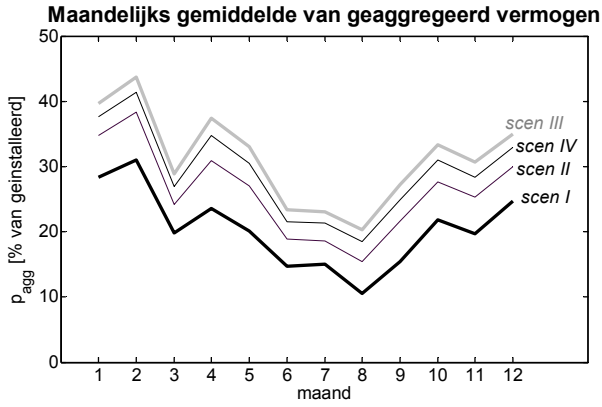

Figuur 17. Maandelijks gemiddelde van het geaggregeerd vermogen voor de vier scenario's

De gemiddelde productie van windenergie verandert ook met het uur van de dag. Figuur 18 toont het gemiddeld vermogen per uur van de dag voor de winter (december, januari en februari) en zomer (juni, juli, augustus), voor *scenario III*. De dagelijkse periodiciteit is veel sterker uitgesproken in de zomer dan in de winter. De resultaten voor herfst en lente liggen tussen de twee extremen van winter en zomer. De resultaten voor de andere scenario's zijn gelijkaardig.

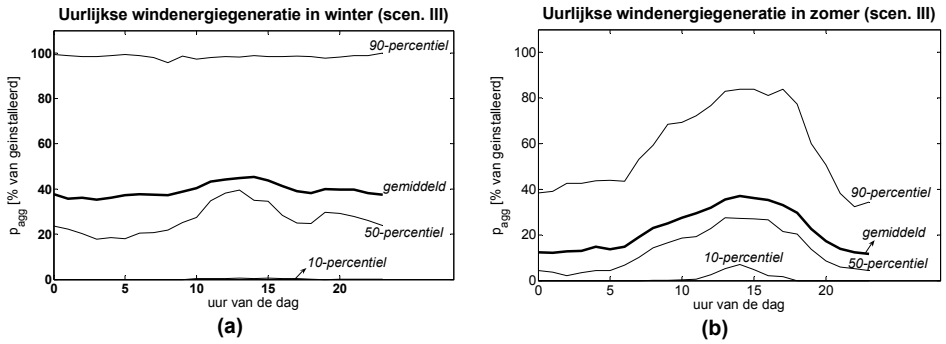

Figuur 18. Gemiddeld vermogen per uur van de dag voor *scenario III*, winter (a) en zomer (b)

De verwachte uurlijkse variaties in geaggregeerde productie worden gekwantificeerd in Tabel 2 (*scenario I*) en Tabel 3 (*scenario III*). Bijvoorbeeld, in de resulterende vermogentijdreeksen voor *scenario I* komt het in drie jaar tijd 365 keer voor dat het geaggregeerd vermogen zakt van 60-80% van het geïnstalleerd vermogen in het uur H – 1 naar 40-60% in het daaropvolgend uur H. De onderliggende grijstinten in de tabellen zijn een grafische voorstelling van dezelfde matrix, met breedte van de vermogenintervallen gelijk aan 1%. De diagonaalelementen in Tabel 3 zijn beduidend groter dan deze in Tabel 2, wat erop wijst dat de uurlijkse fluctuaties voor *scenario I* minder sterk zijn dan in *scenario III*. Niettemin komen uurlijkse fluctuaties rond 20% van het geïnstalleerd vermogen ook in *scenario I* veelvuldig voor.

scen. I		Hour H				
		0%-20%	20%-40%	40%-60%	60%-80%	80%-100%
Hour H-1	0%-20%	15024	1207	57	0	0
	20%-40%	1206	3132	794	28	1
	40%-60%	58	792	1806	367	5
	60%-80%	1	27	365	1031	115
	80%-100%	0	2	6	113	142

Tabel 2. Aantal uurlijkse variaties van geaggregeerde productie, voor *scenario I*

scen. III		Hour H				
		0%-20%	20%-40%	40%-60%	60%-80%	80%-100%
Hour H-1	0%-20%	12199	1253	308	96	113
	20%-40%	1281	1462	741	270	101
	40%-60%	313	748	734	513	239
	60%-80%	95	292	507	557	540
	80%-100%	82	99	257	555	2924

Tabel 3. Aantal uurlijkse variaties van geaggregeerde productie, voor *scenario III*

Deze matrices kunnen ook voor de andere scenario's, of per seizoen afzonderlijk, berekend worden. Daar wordt in deze samenvattende tekst niet verder op ingegaan.

De algemene besluiten zijn de volgende:

- De gelijktijdige windsnelheden zijn sterk gecorreleerd (Figuur 2). Het gunstig effect van geografische spreiding van turbines (*scenario I*) is aangetoond, maar mag niet overschat worden. In het scenario met gelijke spreiding van de turbines komen grote sprongen in de uurlijkse generatie van windenergie nog veelvuldig voor.

- De productie van windenergie hangt af van het seizoen. De gemiddelde productie is hoger in de winter dan in de zomer. Ook de dagelijkse periodiciteit van windenergiegeneratie hangt af van het seizoen: deze periodiciteit is sterk uitgesproken in de zomer, en quasi onbestaand in de winter. Zowel de dagelijkse als de jaarlijkse periodiciteit vallen vrijwel

samen met de normale belastingssfluctuaties in een elektriciteitsnet, met de hoogste belasting in de winter en in de vooravond.

- Bij deze besluiten moet vermeld worden dat steeds een beschikbaarheid van 100% wordt aangenomen voor de windturbines. Vooral voor moeilijk toegankelijke windparken in zee kan een defect leiden tot een maandenlange onbeschikbaarheid, dewelke hier niet in rekening gebracht is. Ook wordt voor alle turbines een optimale foutbestendigheid (ride-through capability) verondersteld, zodat de turbines niet uitschakelen in geval van een netstoring. Alle vermogenfluctuaties die in dit hoofdstuk gevonden werden, zijn dus louter te wijten aan windsnelheidsveranderingen.

Waarde van windenergie

De waarde van windenergie in het bilan van een energiesysteem is niet eenduidig te bepalen. Deze waarde kan gekwantificeerd worden door middel van de capaciteitsfactor, het capaciteitskrediet, de gemiddelde betrouwbare windenergie en de potentiële vermindering van de CO_2-uitstoot door het totale elektriciteitscentralepark.

Capaciteitsfactor

De *capaciteitsfactor* van een windturbine of van een geaggregeerd windpark is de procentuele verhouding van het gemiddeld geproduceerd vermogen tot het nominaal turbine- of parkvermogen. De capaciteitsfactor voor de vier hierboven beschouwde scenario's werd reeds gegeven in Tabel 1. De capaciteitsfactor vermenigvuldigd met 8760 uur geeft het aantal equivalente vollasturen per jaar.

De capaciteitsfactor is een interessante waardemeter voor de uitbater van een windturbinepark wanneer diens inkomsten recht evenredig zijn met de hoeveelheid geproduceerde energie, onafhankelijk van het moment van productie en eventuele regelbaarheid. Voor het beheer van energiesystemen geeft de capaciteitsfactor echter onvoldoende informatie om windenergie te valueren, omdat niets bekend is over het tijdstip en de fluctuaties van windenergieproductie.

Capaciteitskrediet

Het *capaciteitskrediet* wordt via de volgende stappen gedefinieerd:

- de *betrouwbare capaciteit* is de hoeveelheid geïnstalleerde capaciteit in een energiesysteem die met een gegeven betrouwbaarheid ogenblikkelijk beschikbaar is om de totale energievraag te dekken;

- de *loss of load probability* (LOLP) is de waarschijnlijkheid dat de totale energievraag groter is dan de betrouwbare capaciteit;

- het *capaciteitskrediet* van windenergie is de hoeveelheid conventionele generators die kunnen vervangen worden door windturbines, zonder dat de LOLP toeneemt.

Uit de definitie volgt dat het capaciteitskrediet van windenergie afhangt van de betrouwbare capaciteit van het geïnstalleerde conventionele productiepark, en de actuele waarde van de LOLP. Hierbij wordt volgende uitdrukking aangenomen:

$$H(D) = H(0) \cdot \exp\left(-\frac{\lambda D}{Q_{peak}} \right)$$

waarbij *H(D)* de waarschijnlijkheid is dat de totale energievraag de betrouwbare capaciteit overtreft met meer dan *D* MW (Figuur 19a). Negatieve waardes voor *D* duiden op een beschikbaarheid van surpluscapaciteit. Per definitie is *H(0)* gelijk aan de LOLP, gelijk verondersteld aan aan 4 uur per jaar of 0,05% voor de verdere berekeningen. Q_{peak} is de piekvraag in de Belgische regelzone, gelijk aan 13.500 MW, en λ een vervalfactor, gelijk aan 30.

De toevoeging van een nieuwe centrale in het productiepark leidt tot een nieuwe functie, $H_2(D)$, volgens de uitdrukking:

$$H_2(D) = \sum_{P_{plant}} H(D + P_{plant}) \cdot p\left(P_{plant}\right)$$

waarbij $p(P_{plant})$ de waarschijnlijkheid is dat de nieuwe centrale tenminste het vermogen P_{plant} levert. In de sommatie bestrijkt P_{plant} het hele vermogenbereik van de nieuwe centrale.

Het geaggregeerd windpark, geografisch verspreid volgens een van de vier hierboven vermelde scenario's, wordt aanzien als een enkele centrale, waarvan de cumulatieve waarschijnlijkheidsverdeling voor elk productieniveau kan berekend worden uit de vermogentijdreeksen.

Figuur 19b toont als voorbeeld $H_2(D)$ voor het geval waarbij het productiepark wordt uitgebreid met een geaggregeerd windvermogen van 1000 MW, evenwichtig verspreid over de regelzone zoals in *scenario I*. Het capaciteitskrediet van het windpark is aangeduid op de figuur, en is gelijk aan de horizontale afstand tussen *H(D)* en $H_2(D)$ op het niveau van de oorspronkelijke LOLP (4 u/jaar). Op de figuur is ook de verbetering in LOLP door de invloed van het windpark aangeduid, en ook de hoeveelheid extra geïnstalleerd conventioneel vermogen om dezelfde verbetering in LOLP te realiseren. Deze laatste grootheden kunnen eveneens aanzien worden als een kwantificatie van de waarde van geïnstalleerd windvermogen. In dit werk wordt echter enkel het capaciteitskrediet verder besproken.

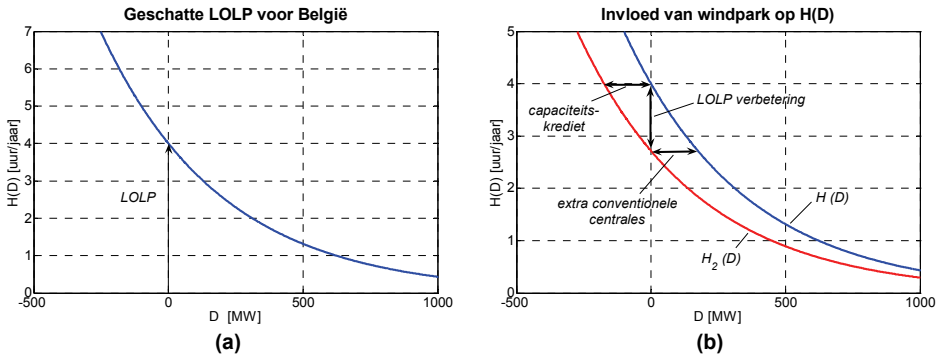

Figuur 19. Aangenomen verloop van *H(D)*(a), en invloed van een windpark op *H(D)* (b)

Figuur 20a toont het absoluut capaciteitskrediet van het geaggregeerd windpark voor de vier scenario's, als functie van de totale hoeveelheid geïnstalleerd windvermogen. Figuur 20b toont dezelfde resultaten in relatieve grootheden. Het capaciteitskrediet van het geaggregeerd windpark daalt monotoon voor stijgende vermogens. Voor lage waarden van geïnstalleerd vermogen wordt het capaciteitskrediet goed benaderd door de capaciteitsfactor.

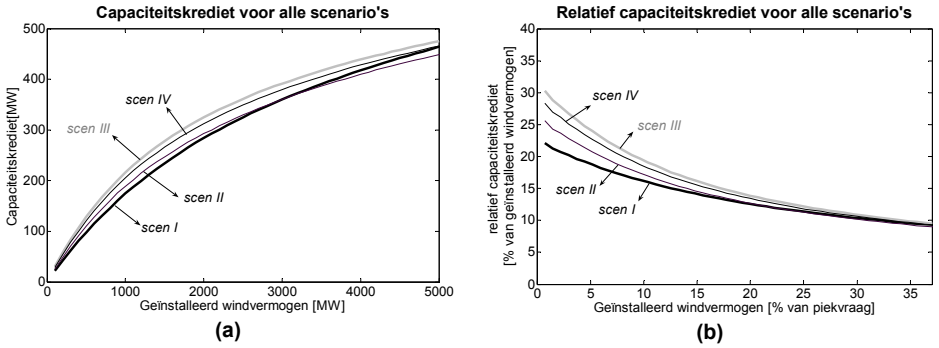

Figuur 20. Capaciteitskrediet van windenergie voor de vier scenario's, in absolute (a) en relatieve (b) termen

Voor lage waardes van geïnstalleerd vermogen is het capaciteitskrediet het grootst voor *scenario III*, het offshore windpark. Dit wordt verklaard door de gemiddeld grotere jaarlijkse energieopbrengst van het offshore windpark. Voor grotere waardes van geïnstalleerd vermogen toont *scenario I* het hoogste capaciteitskrediet. Dit wordt verklaard door de lagere fluctuaties in uurlijkse energieproductie, wat de betrouwbaarheid van de beschikbare windenergie verhoogt. Dit effect is echter pas zichtbaar voor geïnstalleerde vermogens vanaf ongeveer 5000 MW. Voor lagere vermogens wegen de voordelen van de hogere energie-opbrengst door een offshore windpark sterker door dan de lagere vermogenfluctuaties bij een grotere spreiding van de turbines.

Het capaciteitskrediet kan voor elk scenario berekend worden per afzonderlijk seizoen. Dit wordt verder uitgewerkt in hoofdstuk 6 van het doctoraat. In het algemeen is het capaciteitskrediet van windenergie in de winter hoger dan in de zomer.

Betrouwbare windenergiegeneratie gedurende een gegeven tijdsduur

De waarde van windenergie is sterk afhankelijk van de betrouwbaarheid van een zeker productieniveau gedurende een gegeven tijdsspanne.

	scen. I	0%-20%	20%-40%	40%-60%	60%-80%	80%-100%
t = 1 hour	0%-20%	100	8	0	0	0
	20%-40%	100	77	16	1	0
	40%-60%	100	98	72	12	0
	60%-80%	100	100	98	74	7
	80%-100%	100	100	99	97	54

(a)

	scen. I	0%-20%	20%-40%	40%-60%	60%-80%	80%-100%
t = 6 hours	0%-20%	100	3	0	0	0
	20%-40%	100	39	4	0	0
	40%-60%	100	71	30	3	0
	60%-80%	100	91	68	33	1
	80%-100%	100	99	89	64	5

(b)

Tabel 4. Betrouwbaarheidsmatrices voor *scenario I*, voor een betrouwbaarheid van 90% gedurende een tijdsspanne van 1 uur (a) of 6 uur (b)

Tabel 4 toont de windenergiebetrouwbaarheidsmatrices voor *scenario I*, voor een tijdsspanne van 1 uur (a) en 6 uur (b). Deze matrices kunnen berekend worden uit de hierboven berekende vermogentijdreeksen.

Het volgend voorbeeld illustreert het gebruik van Tabel 4: indien het geaggregeerd geproduceerd windvermogen in een gegeven uur tussen 60% en 80% van het geïnstalleerd vermogen ligt, is er een waarschijnlijkheid van 7% dat het vermogen in het volgende uur tenminste 80% is, 74% voor een vermogen van tenminste 60%, 98% voor een vermogen van tenminste 40% enz. Verder is er een waarschijnlijkheid van 1% dat het vermogen gedurende de zes volgende uren permanent tenminste 80% bedraagt, 33% voor een vermogen van tenminste 60% enz.

Vertrekkende van deze matrices (weliswaar in een hogere resolutie) en de vermogentijdreeksen kunnen nieuwe tijdreeksen worden opgesteld, die op elk uur het beschikbaar vermogenniveau aanduiden dat met een gegeven betrouwbaarheid gedurende de volgende x uren niet zal onderschreden worden. Figuur 21 toont het voorbeeld voor een zomerdag (windsnelheidsgegevens van 1 juni 2001) voor *scenario I*. Het ogenblikkelijk beschikbaar vermogen van het geaggregeerd windpark wordt getoond, evenals het vermogenniveau dat gedurende de volgende 2, 6 en 24 uur met een betrouwbaarheid van 90% niet zal onderschreden worden.

De gemiddelde waarde van betrouwbare windenergiegeneratie, in functie van het betrouwbaarheidsniveau en de beschouwde tijdsduur, wordt getoond in Figuur 22 voor de winter- en zomermaanden van *scenario I* (a,b) en *III* (c,d).

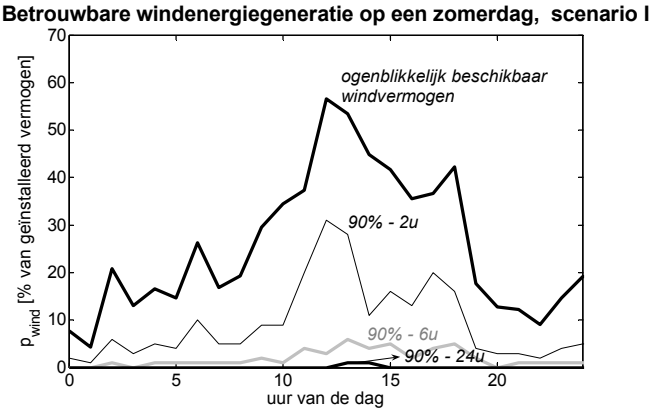

Figuur 21. Betrouwbare windenergiegeneratie op een zomerdag *(scenario I)*

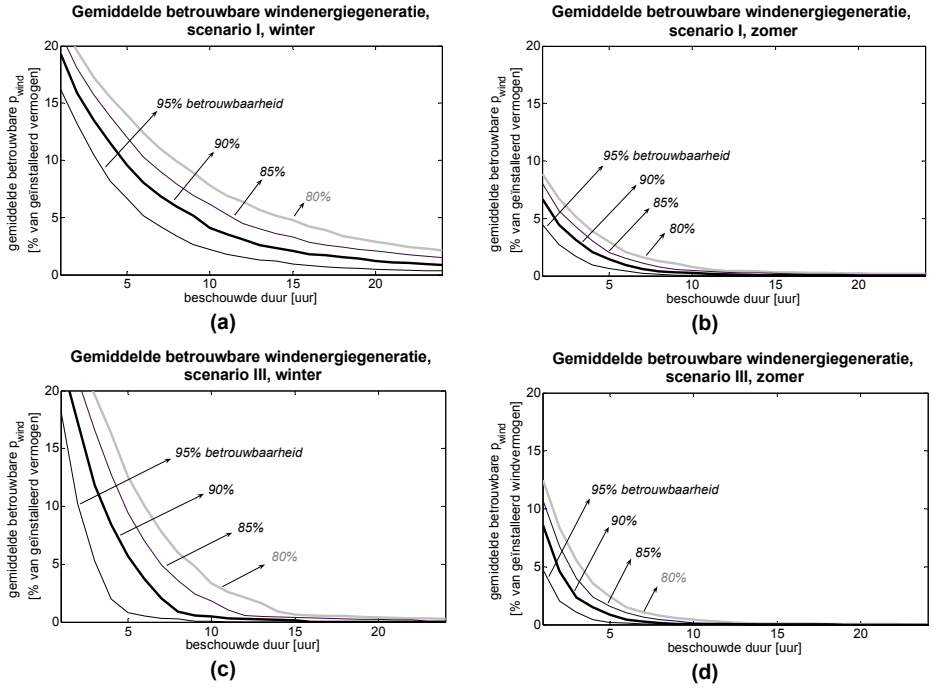

Figuur 22. Gemiddelde betrouwbare windenergiegeneratie, voor winter en zomer in *scenario's I* en *III*

De figuur leidt tot de volgende besluiten:

- de gemiddelde betrouwbare windenergiegeneratie is hoger in de winter dan in de zomer, voor alle scenario's en betrouwbaarheidsniveau's;

- de gemiddelde betrouwbare windenergiegeneratie is hoger in *scenario III* dan *I* voor lage betrouwbaarheidsniveau's en korte tijdsduren. De afname bij toenemende betrouwbaarheidsniveau's en tijdsduren is weliswaar veel sterker in *scenario III* dan in *I*;

- voor alle scenario's is de gemiddelde betrouwbare windenergiegeneratie gedurende een interval van 24 uur erg laag.

Potentiële vermindering in CO_2-uitstoot dankzij windenergie

Methodologie

Een laatste benadering van de waarde van windenergie is haar bijdrage in de potentiële vermindering van CO_2-uitstoot door het gehele elektriciteitscentralepark van België. Om dit te berekenen wordt de simulatietool *PROMIX* gebruikt. *PROMIX* staat voor '*Production Mix*' en verwijst naar de samenstelling van het elektriciteitsgeneratiesysteem in een specifieke regelzone. Gebaseerd op de primaire energieverbruiken, de brandstofkosten en andere zonespecifieke parameters berekent *PROMIX* de optimale verdeling van elektriciteitsproductie door het beschikbare park om te beantwoorden aan de elektrische energievraag. Ook de totale brandstofkosten en CO_2-emissies worden berekend. Hiervoor zijn een uitvoerige beschrijving van het productiepark en een tijdreeks van de geaggregeerde energievraag met uurlijkse resolutie nodig als invoerdata.

PROMIX houdt rekening met starttijden en –kosten voor elk type centrale, zodat het generatiepatroon op een dynamische manier (met tijdstappen van een uur) gesimuleerd en geoptimaliseerd wordt.

De vermogentijdreeksen voor het geaggregeerd windenergiepark volgens een van de vier scenario's, zoals hierboven berekend, worden toegevoegd aan de invoergegevens van *PROMIX* om de invloed op de totale CO_2-uitstoot te evalueren. De manier waarop deze tijdreeksen moeten worden beschouwd is echter niet eenduidig. Voor kleine waarden van geïnstalleerd windvermogen kunnen de tijdreeksen van beschikbare windenergie beschouwd worden als een even grote afname van de geaggregeerde energievraag. Voor grotere waarden is de equivalente afname van de energievraag minder groot dan de onmiddellijk beschikbare windenergie: gezien de relatief lage betrouwbaarheid van windenergie voor langere tijdsduren moeten andere elektriciteitscentrales stand-by blijven wanneer windenergie geproduceerd wordt. De tijdreeksen voor de equivalente afname van de energievraag worden dan beter benaderd door de betrouwbare windenergiegeneratie, zoals hierboven berekend, dan door het ogenblikkelijk beschikbaar windvermogen.

Resultaten

Figuur 23 toont de relatieve afname van CO_2-uitstoot door het totale elektriciteitsgeneratiepark, voor s*cenario I* en *III*. De resultaten voor *scenario II* en *IV* liggen tussen deze twee extreme scenario's.

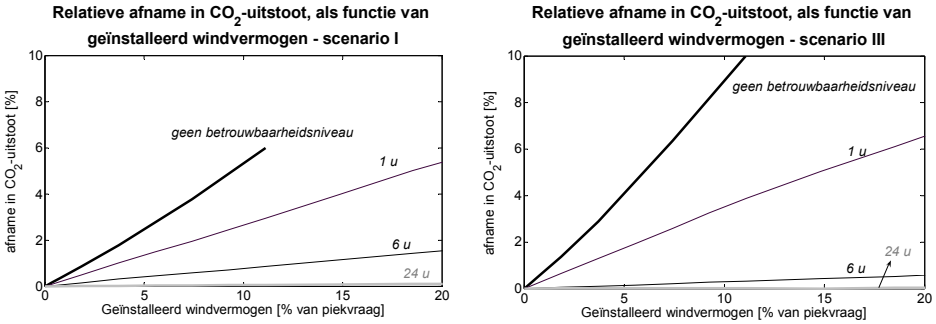

(a) (b)

Figuur 23. Relatieve afname van CO_2-uitstoot door het totale elektriciteitsgeneratiepark, voor *scenario I* en *III*

De figuur leidt tot de volgende conclusies:

- de geschatte potentiële vermindering van CO_2-uitstoot hangt sterk of van de vereiste betrouwbaarheidsniveau's voor de continue windenergieproductie. De absolute bovengrens voor de relatieve afname van CO_2-uitstoot is 10%. Deze bovengrens wordt bereikt in het geval met een offshore windpark (*scenario III*) met een geïnstalleerd vermogen van 10% van de piekvraag, zonder vereisten voor de betrouwbaarheid van continue windenergieproductie.

- Wanneer alle ogenblikkelijk beschikbare windenergie als een equivalente afname van de belasting wordt beschouwd biedt *scenario III* steeds het hoogste potentieel voor reductie van CO_2-uitstoot. Wanneer hogere betrouwbaarheidsniveaus vereist zijn daalt het potentieel enorm, en wordt het hoogste potentieel bereikt in *scenario I* (1.7% voor een geïnstalleerd vermogen van 20% van de piekvraag, en een vereiste betrouwbaarheid van 90% gedurende 6 uur).

De waarde van geïnstalleerd windvermogen vanaf wanneer een zekere betrouwbaarheid vereist is, is niet eenduidig te bepalen. De auteur is van mening dat, gegeven de samenstelling van het Belgisch productiepark met onder meer de pompcentrale van Coo als belangrijkste regeleenheid, hoogstens 1,3 GW ogenblikkelijk beschikbaar windvermogen als equivalente afname van de last kan beschouwd worden. Deze waarde komt overeen met het maximaal vermogen van de pompcentrale van Coo. Deze pompcentrale wordt echter nu al belast voor 'peak load shaving', zodat een meer realistische schatting voor het regelvermogen van Coo, beschikbaar voor de compensatie van windenergie, de helft bedraagt van haar

nominaal vermogen, dit is 0.7 GW. Voor deze geïnstalleerde hoeveelheid windenergie ligt de potentiële vermindering van CO_2-uitstoot tussen 2% (*scenario I*) en 4% (*scenario III*). Hogere waarden van geïnstalleerde windenergie vereisen hogere betrouwbaarheidsniveau's voor de productie. Voor deze niveau's wordt slechts bij enorm hoge waarden van geïnstalleerde windenergie opnieuw een potentieel van 2% tot 4% CO_2-afname verwacht. 2-4% is dus een realistische schatting van de maximale reductie van CO_2-uitstoot.

V. Optimale ontwikkelingen voor offshore windenergie in België

Dit hoofdstuk vat de resultaten samen van een multidisciplinair onderzoek dat de krijtlijnen voor offshore windenergie in het Belgisch deel van de Noordzee (het Belgisch Continentaal Plat) beoogt uit te zetten. Het onderzoek behandelt de volgende aspecten:

- eigenschappen van de zeebodem en geschiktheid voor de constructie van offshore-turbines;
- de beschikbare ruimte in het Belgisch Continentaal Plat;
- de voorkomende windsnelheden;
- de beschikbare technologieën voor windturbines;
- beschikbaarheid van een elektriciteitsnet;
- berekening van het totaal en economisch potentieel van offshore windenergie in België.

De volledige resultaten van het onderzoek zijn gepubliceerd in [XVI].

De voornaamste verwezenlijkingen en besluiten worden hieronder opgesomd.

- Een kennisplatform voor de eigenschappen van de zeebedding is opgesteld, met betrekking tot de geschiktheid voor turbinefunderingen voor verschillende technologieën.
- De windsnelheid neemt snel toe in functie van de afstand tot te kust, tot 20 km van de kust (jaarlijks gemiddelde 10,1 m/s voor 20 km in zee en hoogte 150 m). Vanaf 20 km verhoogt de windsnelheid niet meer met toenemende afstand tot de kust. De windsnelheid neemt ook toe in functie van de hoogte boven het zee-oppervlak. Vanaf een hoogte van 70 m is dit effect minder uitgesproken. Vanuit economisch oogpunt is het dus aangewezen om windturbines niet te ver offshore te bouwen, en de

gondelhoogte te beperken. Het optimaal geïnstalleerd vermogen per km² wordt op 10 MW geschat.

- Het Belgisch Continentaal Plat heeft een oppervlakte van 3600 km². Met het actuele ruimtegebruik (scheepvaart, stortplaatsen, militaire oefengebieden, visuele hinder van windparken op minder dan 3 km van de kust...) blijft theoretisch 2100 km² over voor offshore windturbines. Het gebied in het Belgisch Continentaal Plat dat de regering op dit moment reserveert voor offshore windenergie heeft een oppervlakte van 270 km².

- De capaciteit van het hoogspanningsnet aan de Belgische kust om offshore windenergie op te nemen hangt sterk af van het actuele productie- en belastingspatroon en België en haar buurlanden. Een heel algemeen besluit is dat slechts kleine versterkingen in het hoogspanningsnet nodig zijn tot een geïnstalleerd offshore vermogen van 600 MW. Vanaf grotere vermogens dient het 400 kV uitgebreid te worden naar de kust, wat een enorme investering betekent.

Het potentieel van offshore windenergie in het Belgisch Continentaal Plat wordt samengevat in Tabel 5. Voor de berekening van het economisch potentieel wordt ervan uitgegaan dat 15% tot 30% van de beschikbare ruimte waar de waterdiepte maximaal 20 m is en die zich op maximaal 40 km van de kust bevindt op een economisch verantwoorde manier kan worden ingevuld. Ter duiding geeft de tabel ook het totaal geïnstalleerd elektrisch vermogen en het totaal jaarlijks verbruik van elektrische energie in België weer.

Potentieel aan windenergie		**Geïnstalleerd vermogen [GW]**	**Jaarlijkse energieproductie [TWh]**
Potentieel in Belgisch Continentaal Plat	Totaal	21	66 - 79
	Economisch	2.1 – 4.2	6 - 13
Potentieel in zone bestemd voor offshore wind	Totaal	2.7	8.5 - 10.1
	Economisch	0.3	0.9 - 1.1
Belgisch centralepark		**Geïnstalleerd vermogen [GW]**	**Jaarlijks elektrisch energieverbruik [TWh]**
		15.7	83.7

Tabel 5. Offshore windenergie: potentieel in Belgisch Continentaal Plat

VI. Besluiten en aanbevelingen

Dit doctoraat behandelt de impact van windenergie op een elektriciteitsnet waarin het beheer van productie, transport en distibutie van elektrische energie ontvlochten is, zoals opgelegd door de Europese directieven met betrekking tot de liberalisering van de elektriciteitsmarkt.

In een eerste deel worden de technische eigenschappen van een enkele windturbine of windpark besproken en gemodelleerd. Hierbij ligt de nadruk op het transiënt gedrag van alle componenten in het elektriciteitsnet. Ook wordt aandacht besteed aan de levering van 'netondersteunende diensten' door windturbines, en aan het belang van specifieke netaansluitingsvoorwaarden voor windturbines, opgelegd door de netbeheerder. De ontwikkelde dynamische modellen zijn een nuttig instrument voor de evaluatie van de technische mogelijkheid van deze specifieke aansluitingsvoorwaarden, en van de impact ervan op het net.

In een tweede deel worden de fluctuaties van de geaggregeerde opgewekte energie door windturbines in een volledige regelzone, in casu België, gekwantiseerd. Vertrekkende van windsnelheidstijdreeksen met uurlijkse resolutie voor drie plaatsen in België, wordt aangetoond dat de uurlijkse schommelingen in geproduceerde windenergie regelmatig 20% van het geïnstalleerd vermogen of meer bedragen, zelfs voor het scenario waarin alle windturbines ruimtelijk gelijk verspreid worden over de hele regelzone. Verder wordt de invloed van windenergie op de potentiële vermindering van CO_2-uitstoot van het hele Belgische centralepark geschat op maximaal 4%. Deze waarde komt voor wanneer 700 MW aan windenergie geïnstalleerd is in België, op de plaatsen waar de gemiddelde windsnelheid het hoogst is.

De turbines kunnen ook ruimtelijk gespreid worden naar plaatsen waar de gemiddelde windsnelheid minder hoog is, met de bedoeling om de fluctuaties van geaggregeerde windenergieproductie te verminderen en het totale capaciteitskrediet van windenergie te verhogen. Echter, de geschatte vermindering van CO_2-emissies bereikt dan pas 4% voor onrealistisch hoge waarden van geïnstalleerd windturbinevermogen.

Het laatste deel van het doctoraat stelt de resultaten van een multidisciplinair onderzoek voor met betrekking tot het potentieel van offshore windenergie in België. Als besluit wordt een economisch potentieel van 2.1 tot 4.2 GW vooropgesteld, waarvan 300 MW in het op dit moment (december 2005) daartoe bestemd gebied in de Noordzee. Vanaf een geïnstalleerd offshore vermogen van ca. 600 MW dienen grote versterkingen van het elektriciteitsnet uitgevoerd te worden, zowel in de buurt van de kust als verder in het binnenland. Deze waarde hangt echter sterk af van het generatie- en verbruikspatroon van elektriciteit op een gegeven moment, zowel in België als haar buurlanden.

Gegeven de resultaten in dit doctoraat, pleit de auteur ervoor dat de installatie van windenergiegeneratoren aangemoedigd wordt tot een totaal geïnstalleerd vermogen van ca. 500 tot 700 MW in België, bij voorkeur op de plaatsen waar de beschikbare

windsnelheden het grootst zijn (bijvoorbeeld in zee). Met de huidige explosieve groei van windenergie aan land (ca. 100 MW geïnstalleerd tegen eind 2004 waarvan 28 MW in 2004) en een verwacht offshore windpark van 216 MW wordt deze grens mogelijk spoedig bereikt.

De resultaten in dit doctoraat houden geen rekening met de invloed van betrouwbare windsnelheidsvoorspellingen op het beheer van een elektriciteitsnet. De huidige beschikbare windsnelheids- en windenergievoorspellingen zijn nog niet performant genoeg om te gebruiken voor robuust netbeheer. De ontwikkeling van nieuwe modellen in deze sector zijn op dit moment onderwerp van intens wetenschappelijk onderzoek, wat aanmoediging verdient.

De resultaten in dit doctoraat houden ook geen rekening met mogelijke andere technische oplossingen dan snel inzetbare elektriciteitsgeneratoren, om de nood aan meer regelvermogen omwille van windenergie op te vangen. Deze andere technische oplossingen zijn onder meer energie-opslag en ‘demand side management’.

De opslag van elektrische energie is sinds lang een onderwerp van veel onderzoek, de vooruitgang in deze sector is traag, en maakt steeds gebruik van dure technologieën met relatief laag nominaal eenheidsvermogen (behalve pompcentrales). Op korte en middellange termijn wordt het economisch potentieel van energie-opslag in België door de auteur zeer laag geschat.

‘Demand side management’ (het actief controleren van de vraag naar elektrische energie, in functie van de actueel beschikbare energie) wordt door de auteur wel beschouwd als een realistische alternatieve invulling van de nood aan regelvermogen. Dit concept is reeds lang bekend, maar in de vernieuwde context van geliberaliseerde elektriciteitsmarkten met een grote participatie van hernieuwbare energie is verder onderzoek in die sector ten zeerste aan te bevelen.

Abbreviations

AC	Alternating Current;
ARP	Access Responsible Party;
BCS	Belgian Continental Shelf;
CHP	Combined Heat and Power (cogeneration);
DC	Direct Current;
DSO	Distribution System Operator;
DFIG	Doubly-fed Induction Generator;
DG	Distributed Generation;
EU	European Union;
EU-15	European Union (15 Member States);
EU-25	European Union (25 Member States);
EUA	European Union Emission Allowance;
EU ETS	European Union Emission Trading Scheme;
IEA	International Energy Agency;
IGBT	Insulated Gate Bipolar Transistor;
ISET	Institut für Solare Energieversorgungstechnik (Kassel);
LOLP	Loss of Load Probability;
LOLE	Loss of Load Expectation;

PCC	Point of Common Coupling;
p.u.	per unit (i.e. referred to normalised value);
PV	Photovoltaic;
PWM	Pulse Width Modulation;
RES-E	Renewable Energy Sources for the generation of Electricity;
SCIG	Squirrel Cage Induction Generator;
SG	Synchronous Generator;
SVC	Static Var Compensator;
TGC	Tradable Green Certificate;
TREC	Tradable Renewable Energy Certificate;
TSO	Transmission System Operator;
UCTE	Union for the Coordination of Transmission of Electricity;
UPS	Uninterruptible Power Supply;
WTP	Willingness to Pay.

Symbols

General conventions

- Phasors (voltages, currents…) are written **boldface**.
- Values in real units (voltages, currents…) are written in CAPITALS.
- Normalised values (voltages, currents) are written in small fonts.
- Machine parameters and constants are written in *italic font*.
- The following subscripts are frequently used:

  $\square_{max}$: maximum value for the considered variable;

  $\square_{min}$: minimum value for the considered variable;

  $\square_{ref}$: reference value for the considered variable;

  $\square_{err}$: error value for the considered variable;

  $\square_{rated}$: rated value for the considered variable;

  $\square_{base}$: base value for the considered variable (as reference for normalisation to per unit system).

- The following operators are frequently used:

  $\square^{*}$: complex conjugate;

  $|\square|$: absolute value of complex (phasor) variable.

List of symbols

Chapter 3

P_{flow}	local active power flow on radial feeder line;
P_L	total active load on radial feeder line;
P_G	total active power generation on radial feeder line;
$\mathbf{I_{LOAD}}$	current supplying load on PCC;
$\mathbf{I_{DG}}$	current supplied by distributed generation on PCC;
Z_{LOAD}	(equivalent) load impedance on PCC;
Z_{DG}	(equivalent) generation impedance on PCC;
Z_{GRID}	(equivalent) grid impedance on PCC;
$\mathbf{U_{PCC}}$	voltage at PCC;
$\mathbf{U_{GRID}}$	grid voltage source (from equivalent grid model);
$\mathbf{S_{SC}}$	short-circuit power at PCC;
$\mathbf{I_{SC}}$	short-circuit current at PCC;
p_p	pole-pair;

Chapter 4 and 5

P_{wind}	kinetic energy of wind, flowing through turbine propeller, per unit of time;
S_{rotor}	turbine propeller area;
P_{turb}	mechanical energy in turbine propeller;
P_R	rotor active power;
s	slip;

P_δ	air-gap power;
n_s	synchronous speed ;
P_S	stator active power;
Q_S	stator reactive power;
$\mathbf{I_S}$	stator current phasor;
$\mathbf{U_S}$	stator voltage phasor;
$\mathbf{I_R}$	rotor current phasor;
$\mathbf{U_R}$	rotor voltage phasor;
$\mathbf{I_R'}$	rotor current phasor (referred to stator quantities);
$\mathbf{U_R'}$	rotor voltage phasor (referred to stator quantities);
R_S	stator resistance;
$X_{\sigma S}$	stator leakage reactance;
R_R	rotor resistance;
R_R'	rotor resistance (referred to stator quantities);
$X_{\sigma R}$	rotor leakage reactance;
$X_{\sigma R}'$	rotor leakage reactance (referred to stator quantities);
N_S	number of stator windings;
N_R	number of rotor windings;
X_M'	machine mutual reactance (referred to stator quantities);
X_S	stator reactance;
X_R	rotor reactance;
$\mathbf{S_R}$	rotor apparent power phasor;
$\mathbf{u_s}$	stator voltage phasor [per unit];
u_{sR}	stator voltage, *R*-component in *(R,I)*-reference frame [per unit];

u_{sI} stator voltage, *I*-component in *(R,I)*-reference frame [per unit];

u_{sd} stator voltage, *d*-component in *(d,q)*-reference frame [per unit];

u_{sq} stator voltage, *q*-component in *(d,q)*-reference frame [per unit];

u_{rd} rotor voltage, *d*-component in *(d,q)*-reference frame [per unit];

u_{rq} rotor voltage, *q*-component in *(d,q)*-reference frame [per unit];

i_R equivalent machine current (stator and rotor), *R*-component in *(R,I)*-reference frame [per unit];

i_I equivalent machine current (stator and rotor), *I*-component in *(R,I)*-reference frame [per unit];

i_{sd} stator current, *d*-component in *(d,q)*-reference frame [per unit];

i_{sq} stator current, *q*-component in *(d,q)*-reference frame [per unit];

i_{rd} rotor current, *d*-component in *(d,q)*-reference frame [per unit];

i_{rq} rotor current, *q*-component in *(d,q)*-reference frame [per unit];

p_s stator active power [per unit];

q_s stator reactive power [per unit];

ω_b rotational speed base value for per unit-reference;

ω_s generator synchronous speed (stator flux rotational speed) [per unit];

ω_{gen} generator rotational speed [per unit];

ω_{turb} turbine propeller rotational speed [per unit];

λ tip-to-speed ratio (propeller tip speed divided by wind speed);

θ_{park} Park's angle (angle of rotational transformation between reference frames in generator model);

r_s stator resistance [per unit];

r_r' rotor resistance [per unit];

x_{md} generator mutual reactance, *d*-component in *(d,q)*-reference frame [p.u.];

x_{mq} generator mutual reactance, *q*-component in *(d,q)*-reference frame [p.u.];

x_{rq}	generator rotor reactance, *d*-component in *(d,q)*-reference frame [p.u.];
x_{sd}	generator stator reactance, *d*-component in *(d,q)*-reference frame [p.u.];
x_{sq}	generator stator reactance, *q*-component in *(d,q)*-reference frame [p.u.];
x_{rd}	generator rotor reactance, *d*-component in *(d,q)*-reference frame [p.u.];
x_{rq}	generator rotor reactance, *q*-component in *(d,q)*-reference frame [p.u.];
ψ_{sd}	generator stator flux, *d*-component in *(d,q)*-reference frame [p.u.];
ψ_{sq}	generator stator flux, *q*-component in *(d,q)*-reference frame [p.u.];
ψ_{rd}	generator rotor flux, *d*-component in *(d,q)*-reference frame [p.u.];
ψ_{rq}	generator rotor flux, *q*-component in *(d,q)*-reference frame [p.u.];
T_{em}	electromagnetic generator torque;
T_{shaft}	mechanical torque in shaft (between propeller and generator);
β	propeller pitch angle [degrees];
v_{wind}	wind speed [m/s];
ρ_{air}	air mass density [kg/m³];
R_{turb}	turbine radius [m];
C_p	coefficient of performance (propeller aerodynamic efficiency);
J_{turb}	propeller inertia [kgm²];
H_{turb}	propeller normalised inertia constant [s];
H_{gen}	generator normalised inertia constant;
T_{turb}	propeller drive torque by wind;
θ_{turb}	propeller angular position;
θ_{gen}	generator rotor angular position;
K_{shaft}	normalised shaft stiffness [torque p.u. / electrical radian];
C_{shaft}	normalised shaft stiffness [torque p.u. / base speed];

K_ω	proportional constant of PI-speed controller;
T_ω	time constant of PI-speed controller;
PI_ω	output of PI-speed controller before bounding;
K_β	proportional constant of PI-pitch controller;
T_β	time constant of PI-pitch controller;
PI_β	output of PI-pitch controller before bounding;
K_{irq}	proportional constant of PI-controller for rotor q-current;
T_{irq}	time constant of PI-controller for rotor q-current;
PI_{irq}	output of PI-controller for rotor q-current, before bounding;
T_{conv1}	equivalent rotor converter time constant (delay for voltage creation);
T_{conv2}	equivalent rotor converter time constant (filter time constant for active power transfer from rotor to grid or vice versa);
η_{conv}	rotor converter efficiency for active power transfer from rotor to grid or vice versa;
p_r	rotor active power [per unit];
i_{totq}	equivalent active machine current (stator and rotor), *q*-component in *(d,q)*-reference frame [per unit];
$u_{under,1}$	first undervoltage threshold value, to activate tripping equipment [p.u.];
$u_{over,1}$	first overvoltage threshold value, to activate tripping equipment [p.u.];
$t_{u\_under,1}$	critical activation time for tripping at first undervoltage threshold value [s];
$t_{u\_over,1}$	critical activation time for tripping at first overvoltage threshold value [s];
r_{cb}	crowbar resistance [p.u];
$i_{r,over}$	rotor overcurrent threshold value, for crowbar switching [p.u.];
$t_{ir,over}$	critical activation time for crowbar switching at rotor overcurrent [s];
t_{cb}	delay between crowbar switching and turbine tripping [s];
T_{low}	time constant for equivalent 1st-order wind-to-power transfer function, low wind speed regime (simplified model);

T_{high}	time constant for equivalent 2nd-order wind-to-power transfer function, high wind speed regime (simplified model);
K_{high}	proportional constant for equivalent 2nd-order wind-to-power transfer function, high wind speed regime (simplified model);
d	damping constant for equivalent 2nd-order wind-to-power transfer function, high wind speed regime (simplified model);
p_{avail}	available active power for energy production by wind turbine [p.u.] (simplified model);
p_{lim}	limit value for active power production by wind turbine, in '*Limited*' mode [p.u.] (simplified model);
α	fraction of available power to be produced by wind turbine, in '*Balancing*' mode (simplified model);
T_{ictrl}	equivalent time constant for current controller [s] (simplified model);
i_{react}	total turbine reactive current [p.u.] (simplified model);
i_{act}	total turbine active current [p.u.] (simplified model);

Chapter 6

D	width of area of over which turbine are (evenly) spread, as input parameter the multi-turbine power curve calculation [km];
I	wind turbulence intensity [p.u];
$v_{wind,h1}$	wind speed at given height h_1 [m/s];
z_0	roughness length [m/s];
p_{agg}	total aggregated active power generation by all wind turbines in one control area [p.u. or % of installed];
$H(D)$	probability function for electrical demand in a control area exceeding the instantaneously available capacity by more then D MW;
$Qpeak$	peak power demand in control area (Belgium) [MW];
λ	decay factor, as parameter in the probability function $H(D)$;
P_{plant}	power produced by a power plant in a control area;

Chapter 1

Introduction

1.1. Context of the thesis

Wind power is, together with biomass, the fastest growing renewable energy technology in Europe. During the last decade, the fast development of both the amount of installed wind power as the technological properties of the turbines has continuously exceeded the most ambitious targets. The target for total installed wind power in the 15 Member States of the European Union (EU-15) for the year 2000 was set at 4 GW in 1991 and revised to 8 GW in 1997. Finally, in 2000, the real value exceeded 13 GW. Also for the year 2010, the targets have already been modified upwards: from 40 GW (set in 1997) to 60 GW (set in 2000) and further to 75 GW (set in 2003). The actual installed wind power at the end of 2004 was 34 GW [1]. The wind power targets are driven by European legislation on renewable energy, which will be discussed in the next chapter.

Given the high presence of wind power in the electricity systems of the European Union, especially in Germany, Denmark and Spain, wind power can no longer be considered as a marginal contribution to the generation of electricity. It must be regarded as a generation technology bearing the same responsibilities for contributing to power system management as conventional power generation does. This is a huge challenge, as wind power generation differs fundamentally from conventional generation in various ways:

- the power generation, as a function of time, is intermittent, unpredictable and hardly controllable. This has implications on the operation of the power system in the context of a liberalised market, as is explained below.

- Individual wind turbines are mostly installed in the distribution grid, to which traditionally only loads are connected. A high penetration in the distribution grid may cause power flows to reverse: from the distribution grid up to the transmission grid. This has impact on the distribution system in various ways, as is discussed in Chapter 3;

- On the other hand, large wind farms are mostly located where wind resources and space availability are high, i.e. in rural or mountainous areas or even offshore, thus relatively far from urban centres with high electrical demand. This implies transports of high amounts of power over long distances, necessitating reinforcements of the transmission grid.

- The technology of wind turbines is different from conventional generators: their controllability and their reaction to grid disturbances are relatively complex and sometimes not exactly known. With the given high penetration of wind power, its behaviour during normal and abnormal grid conditions is however crucial for designing and operating a stable and reliable power system. This consideration applies to all distributed generation technologies, and is discussed in Chapter 3, and further specifically for wind power in Chapter 4 and Chapter 5.

The fast growth of wind power coincides with another process severely affecting the European power system: the liberalisation of the electricity market. Whereas generation, transmission, distribution and supply of electricity in each country or part of it was in the hands of one electricity company before liberalisation, those different handlings are performed by unbundled companies now. This makes the integration of wind power rather difficult, as it has to participate in the electricity market, however not disposing of the same flexibility and reliability of its power generation as other generators do. However, in most countries, political incentives ensure that all available wind power is injected into the system, facilitating its development and integration, but jeopardising a solid and stable power market operation. This might lead to high price volatility and unpredictable power flows through the European system.

On a large scale, wind power affects the European power flows. Especially the power exchanges between Germany and France, being respectively the highest producer of wind power and the highest net electricity exporter in Europe [2], take very high values in both directions, putting severe loads on the power system not only in Germany and France, but also in every country that is on a parallel path for electricity between them. Unless the European grid is highly reinforced to cope with international power exchanges, it is therefore important that every transmission system operator maintains the real-time power balance in its control area to avoid high unexpected international power flows, without shifting too much the centre of gravity of the generation pattern even in one control area. The large integration of

wind power may jeopardize this real-time power balance, as discussed in Chapter 6 of this thesis for the Belgian case.

The fast development of wind power in Europe has induced a number of research projects on its large-scale integration in power systems. The two most recent are the Wilmar [3] and the DENA study [4].

- The Wilmar study is a German-Scandinavian research project supported by the European Commission under the Fifth Framework Program. One part of the study consists in an investigation of the issue of system stability. It evaluates wind integration aspects with regard to the fast (less than 10 minutes) fluctuations in the wind power generation. Secondly the study investigates the wind integration ability of large electricity systems with substantial amounts of power trade in power pools. The results claim that the aggregated wind power in a large region is smoothened to such an extent that the need for extra balancing power is very low, which is however contested in this thesis for the Belgian case and fluctuations on hourly base. Furthermore, the Wilmar Study develops a market model, in which wind power is explicitly modelled as a stochastic variable with parameters defined by the user. The results on e.g. price volatility seem widely depending on the assumed scenarios and parameters.

- The DENA study entitled 'Economic planning for the grid integration of wind power in Germany, on- and offshore, until 2020' explores how wind power can be integrated into the German electric power system, and shows how this is technically and economically feasible until 2015. The findings are that wind energy installations in Germany can expand from almost 17 GW today to 36 GW in 2015, and 48 GW in 2020. It is noted that the total electrical peak load in Germany was 72 GW in December 2004 [2]. In this scenario, the cumulative costs for extension of the 400 kV-grid will mount to 1.1 billion euro, yet excluding the costs for grid upgrades at lower voltage levels. In relative terms, the further extension of wind energy capacities until 2015 would rise the costs for private household customers in Germany by 0.385 to 0.475 eurocents per kWh.

Also in Belgium, various studies on the integration of large scale wind energy or distributed generation in general were initiated. The author of this PhD-thesis participated in the following research projects, of which the results are integrated in the thesis:

- 'Optimal offshore wind energy developments in Belgium': a multidisciplinary study describing the resources and potential, the technological options and related costs of offshore wind power in Belgium, funded by the Belgian *Federal Science Office* [5].

- 'The role of renewable energy in the security of supply in Belgium': a multidisciplinary study handling on how 'security of supply' is influenced by renewable energy in Belgium, funded by the Belgian Federal Science Office.

- 'Embedded generation: a global approach to energy balance and grid power quality and security' handles technical and economical aspects of distributed generation in general, funded by the *Institute for the promotion of Innovation by Science and Technology in Flanders* (IWT-Flanders [6]).

- 'Estimation of fluctuation of wind power in Belgium', a joint study by the Belgian Transmission System Operator *Elia* [7] and K.U.Leuven, dealing with the fluctuations of the aggregated wind power in Belgium, on hourly or daily time scale.

- Finally the author performed individual research, funded by the *Fund for Scientific Research - Flanders (Belgium)* [8], resulting in this doctoral thesis.

This work brings my most relevant contributions with regard to wind power together, with its last chapters focusing on wind power in Belgium specifically.

1.2. Overview of the thesis

Chapter 2 describes the general structure of a liberalised power market according to European legislation. It makes the user familiar with the role of generators and suppliers of electric energy, transmission and distribution system operators, and regulatory authorities.

Chapter 3 describes the technical aspects of distributed generation in general. The different distributed generation technologies are reviewed, and the various technical consequences of integration of distributed generation in the power system are summed up. It also fundamentally studies the bases for the new grid connection requirements, issued by power system operators, who anticipate on the role of distributed generation, not only generating power but contributing to the power system stability as far as technological limits allow to.

Chapter 4 describes the technical aspects of wind power specifically. The characteristics of wind speed, wind turbines and their generators are discussed. The three most chosen generator types for wind turbines are reviewed. Furthermore, the value of wind power is discussed: existing definitions are given and commented.

In Chapter 5, new dynamic models of wind turbines are developed, for specific use in power system simulations with dedicated software. The models allow a power system operator to test and develop the grid connection requirements of which some are discussed in Chapter 3. Wind turbine models vary from highly detailed, including a physical description of every component, to highly simplified, generated

by means of the equivalent time constants of the total wind-to-power transfer function.

Chapter 6 describes the results of the joint study by the Belgian transmission system operator Elia and K.U.Leuven. Time series for the aggregated wind power in the Belgian control zone are calculated for various scenarios of installed wind power. This allows quantifying the fluctuation of wind power. The study results in a tool needed by Elia to estimate the increased need for balancing power, due to wind. Furthermore, the wind power time series are used to estimate the value of aggregated wind power in Belgium according to the definitions from Chapter 4. Recommendations are given concerning the amount of wind power that can be installed in Belgium, and the resulting benefits on CO_2-emission abatement.

Chapter 7 discusses the results of the study project entitled 'Optimal offshore wind developments in Belgium'. This multidisciplinary study leads to an estimation of the theoretical and economical potential of offshore wind power in the Belgian North Sea territory. The study takes into account the available wind resources, and constraints concerning available area in the North Sea, geotechnical properties of the sea bed, and availability of the high voltage grid.

Chapter 8 summarises the conclusions of this work, and gives recommendations for further research.

Chapter 2

Renewable energy in new power systems

2.1. Introduction

Over the last years, the structure of power systems has changed immensely, as a consequence of the liberalisation of the electricity market, driven by EU-legislation. This chapter briefly describes the 'new' power systems with its various players, being among others the transmission and distribution system operators, generators and suppliers, and regulatory authorities.

This chapter further describes the EU-policy on renewable energy, indicating the targets for the Member States. Wind power is by many Member States considered as an important contributor for achieving these targets, as can be concluded from the impressive amounts of installed wind power by them.

This chapter makes the reader familiar with the role of the transmission and distribution system operators. Given the renewable energy targets and the potential of wind power, it is understood that renewable energy and specifically wind power cannot be assumed to remain a marginal part of power generation, but may actually influence the total power system's behaviour. This statement indicates the need of understanding well all aspects of wind power by all players in the electricity market.

2.2. ‘New’ power systems

2.2.1. Unbundling of power systems

The EU Treaties of Rome (1957) and Maastricht (1993) laid the foundation of an internal market, with free movement of people, goods and capital. For the specific good being electricity, the European Directive 96/92/EC [9], in 2003 replaced by the Directive 2003/54/EC [10], defines the framework of a liberalised market. This framework aims at unbundling the existing vertically integrated electricity companies managing the entire electricity supply chain: generation, transmission and distribution.

In order to unbundle this chain, the Directive charges the Member States to appoint one or more independent *transmission system operators* (*TSOs*), *distribution system operators* (*DSOs*) and *regulatory authorities* that are competent in well specified control areas. Generators and suppliers of electrical energy are not appointed, but operate in a free market context.

The tasks of the TSO are to keep the balance between power generation and consumption in its control area, and to keep the voltage in the transmission system at the correct frequency and amplitude. Contrary to the vertically integrated electricity companies, the TSO does not own the physical equipment to fulfil these tasks. Therefore, he contracts and procures *ancillary services*, which can be delivered by both generation and demand side. Ancillary services are a general denomination for a number of services securing a safe, reliable, stable and economically manageable system operation. This includes frequency and voltage control, and support for black start capability [11]. Frequency control is closely linked to balancing generation and consumption of active power, while voltage control is closely linked to reactive power generation or consumption. Reactive power markets are not further discussed in this work.

To maintain the balance between load and generation in the control area at real time, the TSO purchases balancing power, i.e. dispatchable generation and interruptible loads. The TSO is further qualified to charge *ARP*s (*Access Responsible Parties*, being power traders, generators or suppliers) deviating too much from their power generation or consumption programs. ARPs thus are stimulated not to cause unbalance in the system. In most EU Member States, a tolerance margin is defined in which deviations from generation or consumption programs are only moderately charged. Beyond the tolerance margin, which may for example be set to 10% of contracted power, deviations are more severely penalised. This balance has to be kept within the frame of 15 minutes by each individual ARP in principle, although some TSOs allow pooling of balances. At the moment of writing, the balancing

market is not internationally organised, which is why every TSO has to purchase balancing power in its own control area [12].

As a further task, the TSO must invest in the grid to secure the supply on short and long term, and to facilitate the power market operation. The TSO ensures non-discrimination between system users or classes of system users. An exception can be made for generators using sources from renewable energy (RE), waste burning or combined heat and power (CHP).

The *distribution system operators* (DSOs) have to ensure a secure and reliable operation of the distribution grids in the control area for which they are appointed.

The *regulatory authorities* are fully independent bodies and guard the non-discrimination, the effective competition, the efficient functioning and the transparency of the market. In most EU Member States, the regulatory authorities that supervise the electricity market also supervise the gas market.

The concept of unbundling implies that the TSOs and DSOs are neither administratively nor legally linked with generation or supply companies in their control area. The sources of income for TSOs and DSOs are the network access tariffs, which are regulated and approved by the regulatory authorities in each Member State individually. Tariffs can be determined according to different systems, among which the Cost+ and Price cap system are the most used.

- The *Cost+ system* determines the tariffs as a function of the validated costs and a reasonable profit by TSOs and DSOs. However, basing the tariffs on the real costs has the disadvantage of not creating incentives to system operators to reduce costs, thus leading to a higher overall energy price for the consumer.

- The *Price cap system* is based on ex-ante benchmark studies for the necessary costs, and stimulates the system operators to work as cost-efficiently as possible. It has the disadvantage that the focus on cost efficiency might cause system operators being reluctant for necessary long-term investments and grid reinforcements.

It is the task of the regulator to unambiguously determine the tariff system applied. The regulator must be well informed about the necessary grid costs and investments, in order to create incentives for system operators to work cost-efficiently, without jeopardising the necessary long-term investments.

The status of market implementation in the EU Member States can be consulted in the Benchmarking Report of the European Commission [13].

For Belgium, the transmission system operator is Elia. Elia is qualified to operate the high voltage grid at voltage levels ranging from 400 kV down to 30 kV, in Belgium and a part of Luxemburg. The distribution grids are operated by DSOs, each appointed for a specific area.

As the energy policy in Belgium is partially a national and partially a regional competence, different regulatory authorities exist. The federal regulator is CREG, while the regional regulators are VREG in Flanders, CWaPE in Wallonia and BIM in the Brussels region.

2.2.2. Market operation

A general electricity market structure is shown in Figure 2.1, taken from [12].

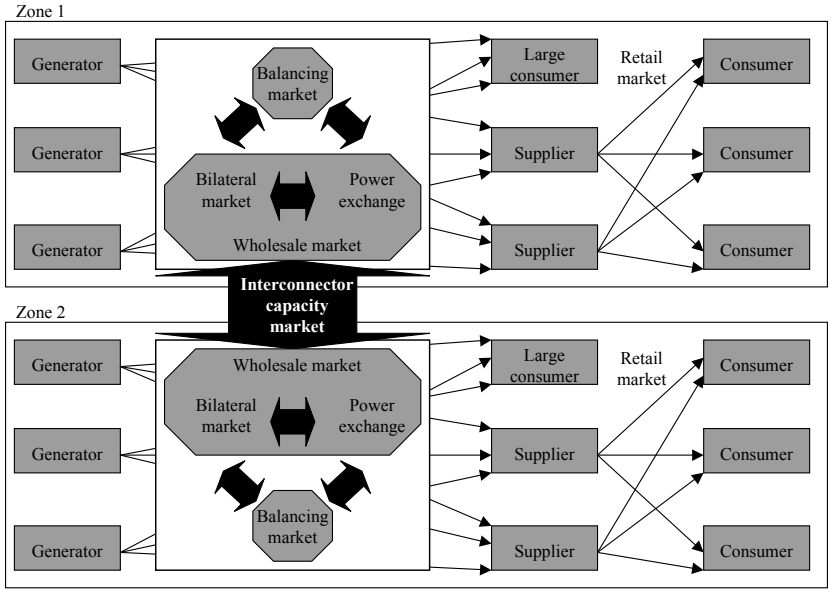

Figure 2.1. Electricity market structure [12]

The *wholesale market* covers the trading of electrical energy between producers and consumers. Distinction is made between *bilateral markets* and *power exchanges*. Most wholesale volume in the electricity market is traded bilaterally by long-term and forward contracts, based on the expected generation and consumption portfolios. When the real-time approaches, the conditions for generators and consumers may change, due to unexpected events, machine outages or new business opportunities. To cover the difference between long-term contracted and real-time generation and consumption, there is need for additional daily and hourly contracts in spot markets.

The spot market is in many Member States organised via *power exchanges*, i.e. trading platforms, operating day-ahead and facilitating anonymous trade in hourly or multi-hourly contracts. Thanks to these platforms, power traders do not need to search an adequate partner for bilateral trading in a short timeframe, which is a costly operation and forces to reveal information of their actual market position. The

power exchange matches the bids of generation and load to define a price on an hourly basis, ensuring that the total contracted power generation equals the total contracted demand. Even though only a small fraction of total trade goes via power exchanges, their public hourly price index may be seen as a reference for the contracts negotiated in other markets such as forward markets [12].

In the balancing market, balancing power is traded. The TSO purchases balancing power and procures it to ensure that the equilibrium between generation and consumption is satisfied at all instances of time.

Apart from the wholesale and balancing markets, an *interconnector capacity market* exists. This market finds it origin in the technical limits of the European high voltage transmission grid, which was initially only designed to allow assistance between control zones in case of emergencies. Liberalisation of electricity markets lead to an increased use of the cross-border interconnections, resulting in large power flows over the borders. As a consequence, the physical interconnections between different control zones are often heavily loaded or even congested. In order to allow a fair and equal access to the interconnections, an interconnector capacity market is introduced, where the limited transfer capacity is allocated based on some previously agreed upon procedure. It must be noted that the physical flows in the European power grid are determined by the load and generation pattern as a whole. Therefore the identification of transactions actually using capacity or causing congestion on a specific interconnector is not straightforward. This is not discussed in this work, but is further elaborated in [14] and [15].

2.3. Renewable energy

2.3.1. Context

Since the last decades, the interest and political support for electricity generation from renewable sources has much increased in Europe. This was part of a strategic response, after the traumatic experiences of the global oil crisis in 1973: renewable energy is considered as a long-term alternative to fossil fuel resources, contributing to the security of energy supply in Europe. Another motive is the creation of employment opportunities in the renewable energy industry, in which Europe maintains the world leader position. Furthermore, the widely assumed causal relation between greenhouse gas emissions and climate change is an important incentive for renewable energy development. Worldwide concern about climate change resulted in the agreements of Rio de Janeiro (1992), Kyoto (1997) and Marrakech (2001), aiming to decrease the global greenhouse gas emissions. Finally, nuclear energy, although not emitting greenhouse or toxic gases in the atmosphere,

also faces a public and political opposition, resulting in the increased interest for renewable energy as part of an alternative electricity supply [16].

2.3.2. European targets and support mechanisms for renewable energy

European Union policy on renewable energy

In the last decade, the European Union has done efforts to develop a supportive and coherent framework towards the use of *Renewable Energy Sources for the generation of Electricity* (*RES-E*) in the entire EU. Milestones in the European renewable energy policy were the following:

Green paper COM/96/576: 'Energy for the future: renewable sources of energy - Green paper for a Community strategy'

The Green Paper [17] opened up the debate on the most urgent and important measures relating to renewable sources of energy, identifying objectives, obstacles and means to be deployed. The Paper rose for the first time quantified propositions for Renewable Energy (RE) targets in the European Union, i.e. 12% of the gross inland energy consumption in the EU must come from renewables. The paper confirmed on-going European support and research programs, and called for regional policies in favour of renewable energy.

White Paper COM/97/599: 'Energy for the future: renewable sources of energy - White Paper for a Community strategy and action plan'

The White Paper [18] confirmed the statements of the preceding Green Paper, and drew up a list of priority measures, including:

- non-discriminatory access to the electricity market for renewable energies;
- fiscal and financial incentives for renewable energies;
- new initiatives regarding bio-energy for transport, heat and electricity and, in particular, specific measures to increase the market share of bio-fuels, promote the use of biogas and develop markets for solid biomass;
- promotion of the use of renewable energy sources (such as solar energy) in the construction industry, both in retrofitting and for new buildings.

The already existing ALTENER support program was indicated as the support and follow-up program for the resulting actions, including European campaigns for 10.000 MW of wind energy, one million of photovoltaic installations and 10.000 MWth of electricity generation plants from biomass.

Directive 2001/77/EC of the European Parliament and of the Council of 27 September 2001 on the promotion of electricity from renewable energy sources in the internal electricity market

The European Directive 2001/77/EC [19] is the legislative result of the preparative Green and White Paper. The national RE-targets were confirmed, as presented in Figure 2.2. At a later stage, targets for the 10 new Member States were defined, also shown in Figure 2.2.

The Directive calls for national support actions to meet the targets. It does not impose specific implementations or support mechanisms.

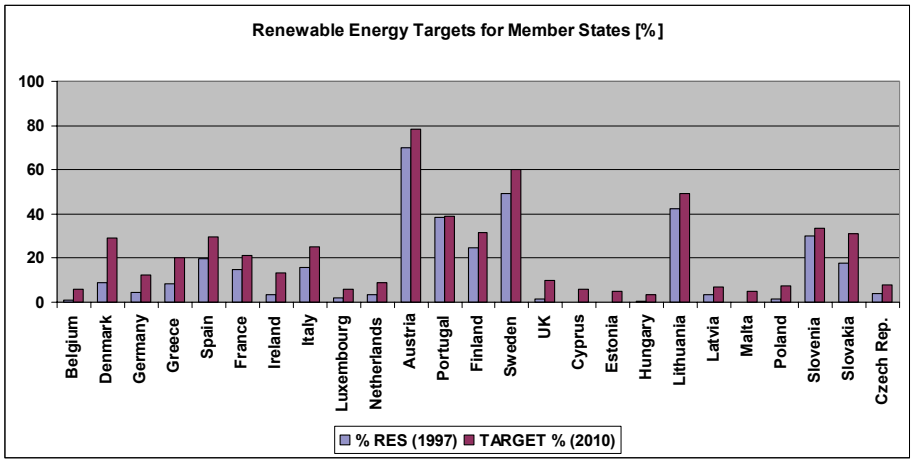

Figure 2.2. National targets for electricity generation share by renewable sources: targets for 2010 for the EU-25 Member States

Overview of support mechanisms

The most applied mechanisms for financial support of RES-E are [16]:

- feed-in tariff systems;
- quota system with tradable green certificates;
- tendering procedures;
- investment subsidies
- fiscal and financial incentives;
- green pricing.

Feed-in tariff systems

Feed-in systems stimulate electric power generators, by offering them a minimum price per kWh produced: the feed-in tariff. As generation costs differ across renewable energy technologies, the feed-in tariff usually differs for various technologies. It is provided for a limited period of time. The feed-in tariff can either be the only revenue, or it can be a supplement to the power price or other subsidies.

Feed-in tariffs are set by national or regional legislation. In theory, by setting the price but not the quantity produced, it is a priori not entirely certain how much RES-E will be promoted. Furthermore, it is a difficult task to estimate an appropriate feed-in tariff for each RES-E technology. Too low tariffs lead to not achieving the RES-E targets. Too high tariffs lead to market distortion, as they keep technology prices artificially high.

Quota system with tradable green certificates

The system of '*Tradable Green Certificates*' (*TGC*s) or '*Tradable Renewable Energy Certificates*' (*TREC*s) is an attempt to support RES-E without creating market distortion as feed-in tariffs do. The system is applied in some European countries, although differences in the exact implementation occur.

Briefly, the system works as follows:

- A generator of electricity from renewable sources receives a certificate for a given quantity of energy produced (e.g. 1 MWh). This certificate is issued by an independent 'issuing body', mostly the regulator. Apart from obtaining this certificate, the producer can sell the electrical energy at the actual market price.

- At regular times, e.g. annually, every supplier of electricity has to redeem TGCs, representing a given quota of his total electric supply, to the issuing body. The supplier may obtain these TGCs by generating electricity from renewable sources using own power plants, or by purchasing TGCs on the 'certificate market', in which electricity suppliers, generators of green energy and brokers participate. The supplier who does not submit the required amount of TGCs is given a fine by the issuing body, proportional to the amount of lacking TGCs. The magnitude of this fine determines the upper limit for the market price of a TGC.

- TGCs are thus an extra source of income for electricity generators from renewable sources. This income depends on the actual market price of the certificates.

Compared to the feed-in tariff system, the TGC-system has the following advantages.

- There is a clear distinction between the income from energy sales and from certificate sales. The energy market is thus not distorted by the presence of RES-E generators.

- The actual market price of a TGC reflects the actual extra costs for generating electrical energy from renewable sources, compared to generation from conventional sources. It offers thus a view on the maturity of renewable energy. This statement is however only valid if the number of available certificates on the market is higher than the demand, determined by the quota. If there is a shortage of certificates, its market price is determined by the fine for not redeeming them.

- The quotas that determine the amount of required TGCs allow specifically envisaging the national targets for RES-E. The number of redeemed TGCs allows the regulator to evaluate whether the national targets for RES-E are met. The magnitude of the fine reflects the eagerness with which policy makers are willing to comply with the targets.

- For each RES-E technology, a minimum certificate price can be set. This avoids that all new RES-E generators focus on the actually cheapest form of renewable energy (e.g. wind) without developing a long-term policy towards other RES-E sources (e.g. photovoltaic). If the minimum price is higher than the market price that suppliers are willing to pay, another party, mostly the TSO or DSO, can be obliged to purchase the certificates at the minimum price and sell them further on the market, probably at a lower price. The resulting financial losses for the TSO or DSO are compensated by the tariffs for grid access.

- Separate certificate systems may be set up for different purposes, for instance the promotion of renewable energy (‘green certificates’), combined heat and power (*CHP* – ‘blue certificates’), the promotion of CO_2-emission abatement (‘black certificates’), or the promotion of rational use of energy (‘white certificates’).

A disadvantage of the TGC-system is the limited exchangeability of TGCs between regions with different regulators. Although the liberalisation of the electricity market should allow free transfer of electric energy across the European Union within the technological limits, the redemption of the certificates to a regulator in a region different from the one where the certificates were issued is confronted with technical and legal barriers. An international market for certificates, parallel with the international market for electricity, is thus difficult to implement.

Apart from the feed-in tariffs and TGC systems, other support mechanisms for RES-E are applied in the EU -Member States, described below.

Tendering procedures

In tendering, a public institution invites generators to compete for a specific financial budget or capacity. There are usually separate tenders for different RES-E technologies. These procedures, which stimulates strong competition between RES-E generators and hence cost-efficiency and price reduction, have not shown great success in promoting RES-E, probably due to the complexity of the procedures involved in a tendering system.

Investment subsidies

RES-E plants are often capital intensive projects with relatively low marginal costs. Therefore, governments may offer subsidies on investment for RES-E technologies in terms of €/MW or as a percentage of total investment costs. Investment subsidies are the oldest, and still the most common type of support. This may be explained by the fact that it probably is the most feasible political way to introduce non-competitive technologies into the market. However, a major disadvantage of this instrument is that it gives no incentive to install and operate the plant as efficiently as possible.

Fiscal and financial incentives

Fiscal and financial incentives represent a wide range of specific measures to promote RES-E. Among them are: exemption of RES-E from energy taxes, tax refund for RES-E, lower VAT rates for RES-E, exemption of investments in RES-E plants from income or corporate taxes etc. Fiscal and financial incentives are a very widespread policy, probably because they are usually easy to implement. Mostly they represent an additional support scheme, apart from feed-in tariffs or quota systems. Like investment subsidies, fiscal and financial incentives alone often do not encourage installing and operating the plant as efficiently as possible.

Green pricing

Green pricing means that a surplus on the energy bill is voluntarily paid by customers when it is guaranteed that the purchased energy comes from renewable sources. The success of this system depends on the willingness to pay (WTP) for renewable energy on the part of consumers, which differs from country to country. Obviously, green pricing provides the least guarantees for RES-E generators, who will be very reluctant to invest if no other support is provided.

Increased tolerance margin for unbalance

As described in paragraph 2.2.2, the TSO can charge ARPs causing unbalance by too highly deviating from the contracted quantity of energy generation or

consumption. The power generation of RES-E generators, such as wind turbines, is often hardly predictable. Therefore their market introduction is jeopardised, as power market operation requires mostly a 24h – forecast with hourly resolution. To facilitate market participance of RES-E generators, the tolerance margin, in which the power generation may vary from the contracted power without being severely penalised, may be broadened.

This support system is however often negatively commented, and also difficult to implement. It neglects the need for incentive to RES-E generators to assist in power system balance, however essential for stable power system operation with high contribution of renewable energy.

Furthermore, it is feared that generation companies owning both RES-E and conventional generators may use the allowed broadened tolerance margin for their aggregated power generation to smoothen the generation pattern of the conventional generators, leading to a higher overall efficiency of these generators. This is considered as unfair competition.

Categorisation of support mechanisms

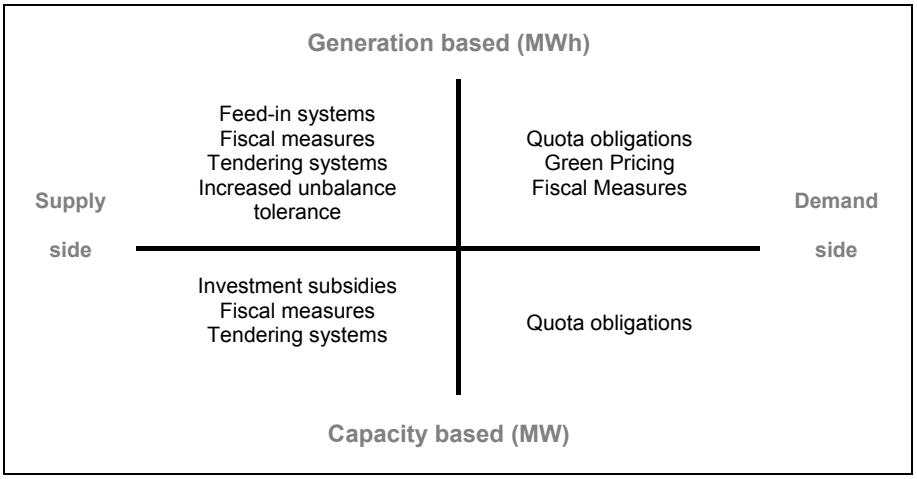

Figure 2.3. Classification of support mechanisms for renewable energy [16]

The support mechanisms discussed above can be categorised as in Figure 2.3 [16].

An overview of the support mechanisms applied in the EU Member States is given in Table 2.1 [16]. Especially in some of the 10 new Member States, the support strategies are in an early stage of development. It is recommended to check for updated information before using Table 2.1 as a reference.

	Feed –in tariff	Investment subsidies	Fiscal incentives	Financial incentives	Quota obligations / TGC	Tendering systems	Green pricing
Austria	X	X	X	X			
Belgium	X	X	X		X		X
Denmark	X	X	X				
Finland		X	X				X
France	X	X	X			X	
Germany	X	X		X			X
Greece	X	X	X	X			
Ireland						X	
Italy	X		X		X		
Luxembourg	X	X	X	X			
Netherlands	X	X	X	X			X
Portugal	X	X	X	X			
Spain	X	X		X			
Sweden	X	X			X		
UK		X	X		X	X	
Cyprus	X	X	X				
Estonia	X		X				
Hungary	X	X	X	X			
Lithuania	X	X	X	X			
Latvia	X						
Malta			X	X			
Poland		X	X	X	X		
Slovenia	X	X	X				
Slovakia							
Czech Rep.	X		X	X	X		

Table 2.1. Overview of national support policies in the EU-25 Member States [16]

2.3.3. Installed wind power in the European Union

The amount of already installed renewable energy in each Member State is shown in Figure 2.2 for 1997. Considering wind power only, Table 2.2 [1] shows the total installed amount by the end of 2003, the new installed wind power in 2004, and the total installed by the end of 2004.

	Total [MW] end 2003	New [MW] 2004	Total [MW] end 2004		Total [MW] end 2003	New [MW] 2004	Total [MW] end 2004
Austria	415	192	606	Latvia	26	0	26
Belgium	68	28	95	Lithuania	0	7	7
Cyprus	2	0	2	Luxembourg	22	14	35
Czech Republic	9	9	17	Malta	0	0	0
Denmark	3.115	9	3.117	Netherlands	910	197	1.078
Estonia	2	3	6	Poland	63	0	63
Finland	52	30	82	Portugal	296	226	522
France	253	138	386	Slovakia	3	3	5
Germany	14.609	2.037	16.629	Slovenia	0	0	0
Greece	375	90	465	Spain	6.203	2.065	8.263
Hungary	3	3	6	Sweden	399	43	442
Ireland	33	148	191	UK	648	240	888
Italy	904	221	1.125				
EU-15		**28.460 (end 2003)**		**5.678 (new 2004)**		**34.073 (end 2004)**	
EU-25		**28.568 (end 2003)**		**5.703 (new 2004)**		**34.205 (end 2004)**	

Table 2.2. Installed wind power in the European Union [1]

Denmark, Germany and Spain are by far the countries in which wind power penetration is highest. While wind power in Denmark seems to be saturated, the growth in Germany and Spain has continued in 2004. The fastest growth of wind power in 2004 was in Portugal and the UK. Especially in the UK, the willingness to further increase the actual growth of wind power is noted.

Until now, most installed wind power is *onshore*, i.e. on land. Existing *offshore* wind farms vary from single turbines located some meters in the sea (also called *near shore*) to large wind farms in water depths up to 20 m. The largest installed wind farms until now are shown in Table 2.3 [20]. The offshore projects that are in the permitting procedure are numerous; most of them are situated in UK, Ireland and Germany. In Belgium, an offshore project of 216 MW is scheduled to start construction in 2006 [21]. An application for another 150 MW was submitted on May 31, 2005.

Wind farm	year of commissioning	number of turbines	total power [MW]
Middelgrunden (DK)	2001	20	40
Horns Rev (DK)	2002	80	160
North Hoyle (UK)	2003	30	60
Nysted (DK)	2004	72	158
Scroby Sands (UK)	2004	30	60

Table 2.3. Largest (> 40 MW) commissioned offshore wind farms until 2004 [20]

2.4. Conclusion

This chapter briefly describes the operation of the 'new' power system, being restructured due to the electricity market liberalisation process driven by European legislation. Also the European drive towards more energy generation from renewable energy sources is outlined, and the various existing support mechanisms for renewable energy are briefly commented. Finally the status of wind power in Europe at the end of 2004 is provided.

The chapter demonstrates that the political drive for increasing energy generation from renewable energy sources is immense. Wind power is considered as a main contributor to this. This is demonstrated by the high amount of installed wind power in Europe, still increasing annually.

The chapter has made the reader familiar with the role of the *Transmission System Operator* (TSO) and *Distribution System Operators* (DSO). In general, the chapter describes in broad outline the context in which the following chapters are to be situated, as described below.

In Chapter 3, the technical impact of *distributed generation* on the grid is discussed. Distributed generation and renewable energy often coincide. Chapter 3 describes, amongst others, the role of the transmission and distribution system operators to issue grid connection requirements that demand assistance for voltage control and stability by distributed generators. Chapter 4 then handles the technical aspects of wind power in particular, and Chapter 5 deals with the dynamic modelling of wind power, which is an important tool for the system operators to estimate the need and impact of the grid connection requirements for wind turbines in particular.

In Chapter 6, the fluctuations of wind power within a control region are quantified, for the example of Belgium. Considering the commitment of the TSO to guard the system power balance within its control area for which it is appointed, a correct estimate of fluctuations of wind power is of fundamental importance. It is reminded from this chapter that policy makers have the option to decide in favour of widely increased unbalance tolerance margins for wind power generators, thus forwarding the risk of unbalance and the related costs from the wind power generators to the TSO and via increased tariffs further to every system user. Chapter 6 will estimate the fluctuation of the aggregated wind power output in Belgium. Although it makes abstraction of the market mechanisms that drive the decisions of generators and consumers, the results are considered as valuable information for the TSO, as it estimates the impact of wind power on the balancing power that must be purchased. The results in Chapter 6 further allow estimating the total value of aggregated wind power in Belgium.

Chapter 3

Technical aspects of grid-connected distributed generation

3.1. Introduction

This chapter is dedicated to the technical aspects on distributed generation. During the last decade, a renewed interest for distributed generation has arisen. This is confirmed by the International Energy Agency (IEA) that lists five major factors contributing to this evolution, i.e. developments in distributed generation technologies, constraints on the construction of new transmission lines, increased customer demand for reliable electricity, the electricity market liberalisation and concerns on climate change ([22], [23]).

After an attempt to define distributed generation, this chapter gives a brief overview of the existing types and technologies. Distributed generation technologies are classified as reciprocating engines, gas turbines, micro turbines, fuel cells, wind turbines, PV-cells or other generators from renewable sources.

The focus is on the technical impact of grid-connected distributed generation on the power system. Distributed generation changes the traditional grid behaviour with respect to:

- line loading and line losses;
- steady-state voltage and voltage control;
- safety and protection;
- power system stability and ride-through behaviour;
- power quality.

All are discussed in this chapter. For the aspects of voltage control and ride-through behaviour, an overview of the grid connection requirements in some selected European regions is provided. In this way, the recognition of the growth in distributed generation - more particular wind energy - by various grid operators in Europe is illustrated. Especially the grid operators that were confronted with a large increase of distributed generators in their power system introduced adapted rules for them. This implies that distributed generation is not any more to be considered as a 'negative load' (not influencing the grid behaviour, undispatched and hence practically unknown), but as actively contributing to the grid management. The Danish and German transmission system operators Eltra and E.ON have played a leading role in developing renewed grid connection requirements. They take the technological limits of distributed generators into account, but also indicate the appropriate responsibility to assist in ensuring a solid grid management.

3.2. Definitions and types of distributed generation

3.2.1. Definition of distributed generation

The definition of distributed generation is not unambiguous. Observers may base their judgment whether a generator of electrical energy is considered as a distributed generator on location, rating, technology, operation or dispatch modus, ownership, purpose, environmental impact etc.

The final report by the CIRED Working Group on Dispersed Generation (1999) showed a large variety in view points put forward by questionnaire respondents. As a conclusion, the Working Group selected the following criteria that a generator must comply with to be considered as 'distributed generator' [24]:

- not centrally planned;
- not centrally dispatched;
- usually connected to the distribution network;
- rated power smaller than 50-100 MW.

These criteria were also already mentioned in the final report on the CIGRE working group on the impact of increasing contribution of dispersed generation on the power system.

Other aspects such as ownership, technology, environmental impact and intermittency were not included in the criteria as it might lead to exclusion of generators that should be seen as distributed generators. The upper limit of the power range is somewhat arbitrary: the proposed 50-100 MW was a compromise between the respondents.

A more general definition for DG is suggested by Ackermann et al. [25], and maintained by Pepermans et al. [23]:

> *Distributed generation is an electric power source connected directly to the distribution network or on the customer site of the meter.*

This and many other definitions are commented in [23]. The definition by Ackermann excludes criteria as planning and dispatch, technology, ownership etc, which are all not considered as determining factors. Ackermann suggests however to further subdivide all DG according to the power range as in Table 3.1, or according to environmental impact in *'Renewable'*, *'CHP'* or *'Other'*. Note that the upper limit in Table 3.1 is extended to 300 MW, compared to the 50 – 100 MW from the CIGRE definition. 300 MW is however considered as highly exceptional for distributed generation units.

Category	Power Range
Micro	1 W – 5 kW
Small	5 kW – 5 MW
Medium	5 MW – 50 MW
Large	50 MW – 300 MW

Table 3.1. Categories of distributed generation, according to rating [25]

Formulating an unambiguous, complete, and sufficiently specific definition for distributed generation, universally valid, is virtually impossible.

For the specific case of Belgium, it is considered by the author that distributed generation mainly consists of CHP, wind power, small biomass generators, small hydrogenerators, photovoltaic modules and UPS-equipment (e.g. diesel generators). UPS-equipment normally only operates during emergency situations from the point of view of the consumer (e.g. a hospital), but is sometimes also used for load peak

shaving purposes. The following criteria are then considered as relevant for the definition of distributed generation:

- not centrally planned;
- not centrally dispatched;
- usually connected to the low voltage or medium voltage distribution network (400 V up to 36 kV)
- rated power smaller than 100 MW.

With the power range up to 100 MW, on-shore wind farms are included, while large offshore wind farms are not. These are not considered as distributed generators, also because of the voltage level criterion.

3.2.2. Types and technologies of distributed generation

Attempts to classify the types and technologies of distributed generation are amongst others made in [23], [25] and [26]. A summary is presented in Table 3.2 [23].

Technology	Power Range	Fuel
Reciprocating engines	*diesel:* 20kW – 10+ MW *gas:* 5 kW – 5+ MW	diesel, heavy fuel, bio diesel, natural gas, landfill gas, biogas…
Gas turbines	1 – 20 MW	natural gas, kerosene
Micro turbines	30 kW – 200 kW	natural gas, flare, landfill gas, biogas
Fuel Cells	*see Table 3.3*	*see Table 3.3*
Photovoltaic	20 + kW, *every range possible when using more cells*	sun
Wind	*wind turbine*: 200 W – 5 MW *wind farm*: 100+MW onshore	wind
Other Renewables (small hydro, tidal, thermal solar, geothermal…)		various renewable sources

Table 3.2. Classification of distributed generation technologies

The fuel cells are further classified in Table 3.3 ([27], [28]).

	Low temperature			High temperature	
	AFC	**PEMFC**	**PAFC**	**SOFC**	**MCFC**
Electrolyte	alkali hydroxide	polymer	phosphoric acid	ceramic	molten carbonates salt
Working Temperature	80 °C	80 °C	100 °C	850 °C	650 °C
Fuel	H_2	H_2	H_2	H_2/CO/CH_4	H_2/CO/CO_2/ CH_4
Oxidant	O_2 / air	O_2 / air	O_2 / air	O_2 / air	O_2 / air
Efficiency	40 %	40-50 %	40 %	50-60 %	50-60 %
Power Range	1 kW – 250 kW	1 kW – 250 kW	250 kW – 2 MW	1 kW – 5 MW	50 kW – 2 MW
Properties	CO poisons Pt-catalyst	CO poisons Pt-catalyst smaller volume than AFC	little CO-pollution allowed (1% - 2%)	Ni-catalyst i.o. Pt (resistant to CO-pollution)	Ni-catalyst i.o. Pt (resistant to CO-pollution)

AFC *alkaline fuel cell*
PEMFC *proton exchange membrane fuel cell*
PAFC *phosphoric acid fuel cell*
SOFC *solid oxides fuel cell*
MCFC *molten carbonates fuel cell*

Table 3.3. Fuel cell types

Apart from the types mentioned in Table 3.3, also the direct methanol and the regenerative fuel cell are worth mentioning.

The direct methanol fuel cell uses methanol instead of hydrogen as fuel, having the practical advantage of being liquid at room temperature and thus easily transportable. Operating temperature is ca. 100°C and the efficiency reaches 40%. This fuel cell type is still in a very early development stage, but is especially promising for mobile applications.

Regenerative fuel cells can be of any type mentioned in Table 3.3, in which both electrolysis and electricity generation can occur, depending on the need. The water

that is formed during electrical energy generation serves as input for the electrolysis: it then splits into hydrogen and oxygen. No external supply of hydrogen is thus necessary. The energy necessary for the electrolysis may be provided by a photovoltaic module. The regenerative fuel cell is a suitable energy source for stand-alone applications.

In some references (e.g. [26]), also storage devices are considered as distributed generation. These devices can then further be subdivided into batteries, flywheels, capacitors and inductors. Also regenerative fuel cells are sometimes considered as storage devices: hydrogen is seen as a medium to store energy.

From the electrical point of view, the distributed generation technologies can be subdivided into rotating and non-rotating generators. Rotating generators are driven by reciprocating engines, gas and micro turbines and wind turbines. They are equipped with an electrical generator that can be an induction or synchronous generator type. This generator can be directly grid connected or via a power electronic converter. For wind turbines, this is extensively discussed in Chapter 4.

The non-rotating generators are PV-systems and fuel cells. They deliver their electrical power as a DC-voltage and -current, and must be grid connected through a DC-AC inverter.

3.3. Technical impact on grid

3.3.1. Line loading and losses

In a distribution grid with radial feeder lines and without distributed generation, the distribution transformer connecting the line with the higher voltage level must transfer all necessary power to supply the total load. This may result in high losses and heating of the transformer and the first segment of the feeder line. These losses may be highly alleviated when distributed generation is installed along the feeder line [29].

Figure 3.1a shows the theoretical case where the load is equally distributed along the feeder line. The active power flow through the line decreases linearly as a function of the distance from the distribution transformer. Figure 3.1b shows the same network with a distributed generator. Obviously, with a good choice of generator size and location, the average power flow through the line is considerably reduced, resulting in a reduction of the losses as well.

In Appendix I is calculated that a generator with rated power equal to 2/3 of the total load on the feeder line, and installed at 2/3 of the line lengths, leads to the highest theoretical line loss reduction, being 89%. Also the cases with more generators on one feeder line is discussed in Appendix I.

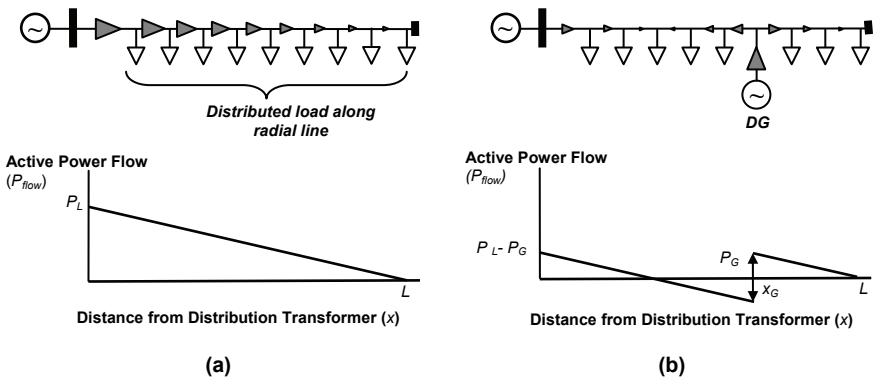

Figure 3.1. Line loading along radial feeder line, without (a) and with DG (b)

3.3.2. Steady state voltage

Theoretical considerations

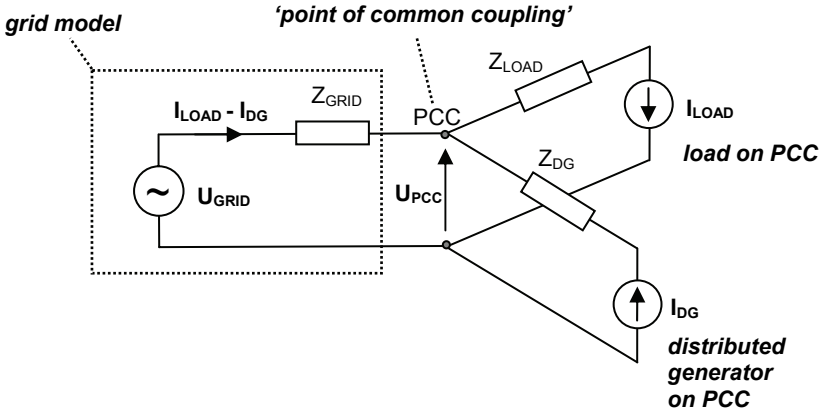

Figure 3.2. Grid model with load and generator connected at PCC

To analyze the impact of a distributed generator on the grid voltage, it is important to know the characteristics of the 'Point of Common Coupling' (PCC), i.e. the grid point at which the distributed generator is connected to the grid, optionally together with other grid users at that location.

The most simple grid model, as seen from the PCC, is a constant voltage source $\mathbf{U_{GRID}}$ in series with an impedance Z_{GRID}. The single-phase equivalent model is shown in Figure 3.2. The figure shows, as an example, one load and one distributed generator connected to the grid at the PCC. Depending on its behaviour, a load can be modelled as an impedance, a current source, a series connection of both (as in Figure 3.2) or a more detailed model. Also the distributed generator is represented as a current source in series with an impedance: $\mathbf{I_{DG}}$ and Z_{DG}. More detailed dynamic models for generators are discussed in Chapter 5.

An important characteristic is the short-circuit power $\mathbf{S_{SC}}$ of the grid at the PCC. Assuming that load and generator at the PCC have a negligible influence on the short-circuit power, $\mathbf{S_{SC}}$ (for one phase) can be written as:

$$\mathbf{S_{SC}} = \mathbf{U}_{\mathbf{GRID}} \cdot \mathbf{I_{SC}}^{*} = \frac{\mathbf{U_{GRID}} \cdot \mathbf{U_{GRID}}^{*}}{Z_{GRID}} \quad \text{or} \quad \left|\mathbf{S_{SC}}\right| = \frac{\left|\mathbf{U_{GRID}}\right|^{2}}{Z_{GRID}} \tag{3.1}$$

with $\mathbf{I_{sc}}$ the current that would flow through a metallic short-circuit at the PCC (Figure 3.3). 'Metallic' means that the impedance between PCC and ground at the fault location is zero.

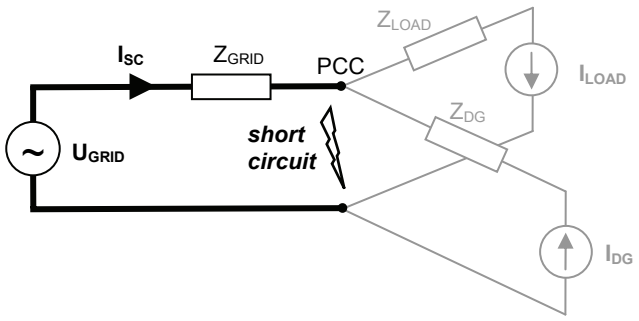

Figure 3.3. Short circuit at PCC

Table 3.4 lists typical three-phase short-circuit powers for substations in the Belgian high voltage grid.

Substation voltage	Typical value for $\|S_{sc}\|$
400 kV	30.000 MVA
150 kV	10.000 MVA
70 kV	2.500 MVA
30 kV	1.300 MVA
15 kV	500 MVA
10 kV	400 MVA
400 V	16 MVA

Table 3.4. Typical short-circuit values

It follows from (3.1) that $|\mathbf{S_{sc}}|$ is inversely proportional to Z_{GRID}. The voltage at the PCC, $\mathbf{U_{PCC}}$, during normal grid operation is (Figure 3.2):

$$\mathbf{U_{PCC}} = \mathbf{U_{GRID}} - (\mathbf{I_{LOAD}} - \mathbf{I_{DG}}) \cdot Z_{GRID} \tag{3.2}$$

It appears from (3.2) that, the lower Z_{GRID} (i.e. the higher $|\mathbf{S_{sc}}|$), the lower the influence of the load and generator current on $\mathbf{U_{PCC}}$. Thus, a higher short-circuit power at the PCC implies that varying load or generator currents (e.g. due to a load switching action or varying generator output) cause only small voltage disturbances at the PCC, and a grid user will notice less voltage disturbances caused by other grid users at the same PCC. Therefore, the short-circuit power is an important parameter to estimate the 'strength' of the grid. For a given load (generator), connected at a given node, *'grid strength'* is defined as the short-circuit power divided by the rated power of the load (generator):

$$grid\ strength = \frac{|\mathbf{S_{sc}}|}{P_{DG}} \tag{3.3}$$

A rule of thumb states that the grid strength should always be higher than 50. Taking the typical short-circuit power values from Table 3.4 into account, the maximal installed distributed generation power, on a single radial line, is given in Table 3.5 as a function of the voltage level.

Voltage level	70 kV	30 kV	15 kV	10 kV	400 V
Max. DG	50 MW	26 MW	10 MW	8 MW	320 kW

Table 3.5. Indicative values for maximum distributed generation power on one radial branch, as a function of voltage level

The values in Table 3.5 are only indicative. They do not reflect considerations on line ratings, safety devices and dynamic criteria. These aspects should be evaluated for every specific case.

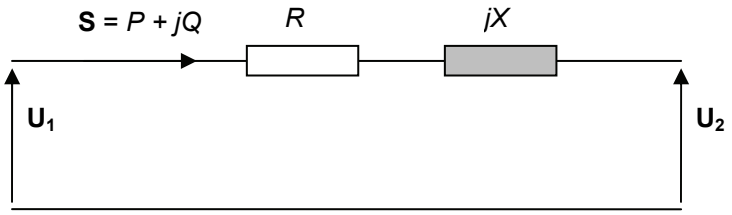

Figure 3.4. Voltages at extremities of power transferring line

To examine how the voltage can be controlled locally by distributed generators, Figure 3.4 is used. It shows a branch with impedance $R + jX$ and supplying an apparent power $\mathbf{S} = P + jQ$. The voltages at the extremities of the branch are $\mathbf{U_1}$ and $\mathbf{U_2}$ respectively. The relation between voltages, line parameters and transmitted power is, with good approximation ([30], [31]):

$$\left|\mathbf{U_1}\right| - \left|\mathbf{U_2}\right| \approx \frac{\left(R \cdot P + X \cdot Q\right)}{\left|\mathbf{U_1}\right|} \tag{3.4}$$

For most transformers and open-air lines, the following is valid:

$$X >> R \tag{3.5}$$

From (3.4) and (3.5) follows that the voltage can be controlled by controlling the reactive power injection at the branch extremities. Reactive power control is therefore considered as a means for voltage control in high-voltage grids and other grids where $X >> R$. Applying (3.4) in Figure 3.2 indicates that the voltage control capability by a generator depends on Z_{DG} and Z_{GRID}.

For underground cables, the X/R - ratio varies between 0.1 and 10, depending on material choice, conductor cross-sections and distances between phase conductors. Urban distribution grids are mostly built using underground cables, thus limiting the voltage control capability by reactive power.

Notwithstanding this last consideration, some TSOs have defined ranges for reactive power, that distributed generators – and wind turbines in particular - must be able to supply on a continuous basis. This is further discussed below. The reactive power control may be required for voltage control or compensation of other reactive loads in the network. Active voltage control can optionally remove the upper limits for the amount of distributed generation stated in Table 3.5.

Voltage profile along a line

To illustrate the impact of a distributed generator on the voltage profile along a line, the distribution grid of Haasrode, a semi-industrial site near Leuven (Belgium), is considered (Figure 3.5). The 70 kV-substation '*SUB*' is in reality connected to the high voltage grid. Here it is considered as the reference node with short-circuit power $|\mathbf{S}_{sc}| = 2.500$ MVA. The grid consists of 4 radial branches in an open-ring structure: the switches between the second, third and fourth branch and bus 111 are normally open. The rated voltage is 10 kV.

On average, the *X/R* ratio of the distribution lines in the studied grid is approximately 5.

The total active load is 10 MW, assumed equally divided among the four branches.

A generator is assumed to be connected to bus 406. Figure 3.6 shows the voltage along the fourth branch for active power injection in bus 406 being 2 MW or 8 MW. The voltage profile for the case without a generator is also shown. The figure makes further distinction between the case without reactive power exchange between generator and grid (a), capacitive behaviour, $\cos\varphi = 0.9$ (b), and inductive, $\cos\varphi = 0.9$ (c).

As can be seen in the figure, the distributed generator has impact on the voltage profile along the line. By the active power injection in node 406, the voltage around this node increases (Figure 3.6a).

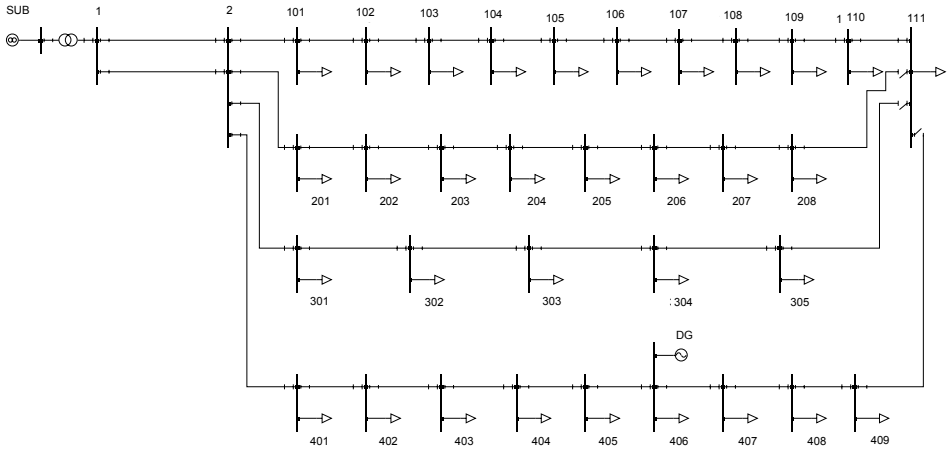

Figure 3.5. Distribution grid of Haasrode (Leuven; Belgium)

Because of the relatively reactive nature of the grid ($X/R \approx 5$), the case (b) with capacitive generator behaviour tends to increase the voltage the most, while the voltage rise due the active power injection is compensated by the voltage drop due to the inductive consumption by the generator in case (c). In this grid, the reactive

power behaviour of the generator has thus a significant impact on the voltage profile along the line.

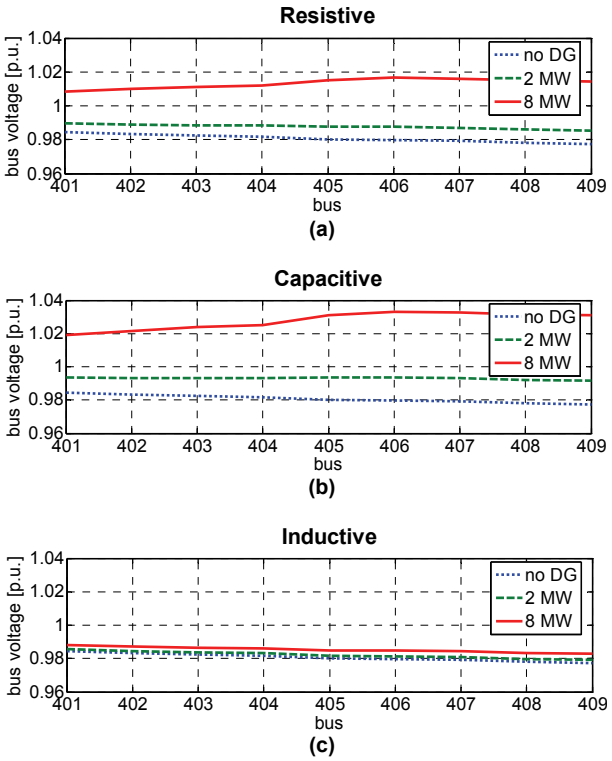

Figure 3.6. Voltage profile along line 4, with a generator connected to bus 406, cos φ = 1 (a), cos φ = 0.9 capacitive (b) and cos φ = 0.9 inductive.

The highest impact on the voltage is for this example seen in case (b) at bus 406, where the difference between the voltages for the case with an 8 MW generator and the case without generator is approximately 5%.

Reactive power control requirements issued by TSOs

Figure 3.7 shows the required reactive power ranges for continuous operation, issued by some European grid operators ([32] - [40]). Generators must be able to regulate their reactive at every value between the upper and lower limits shown.

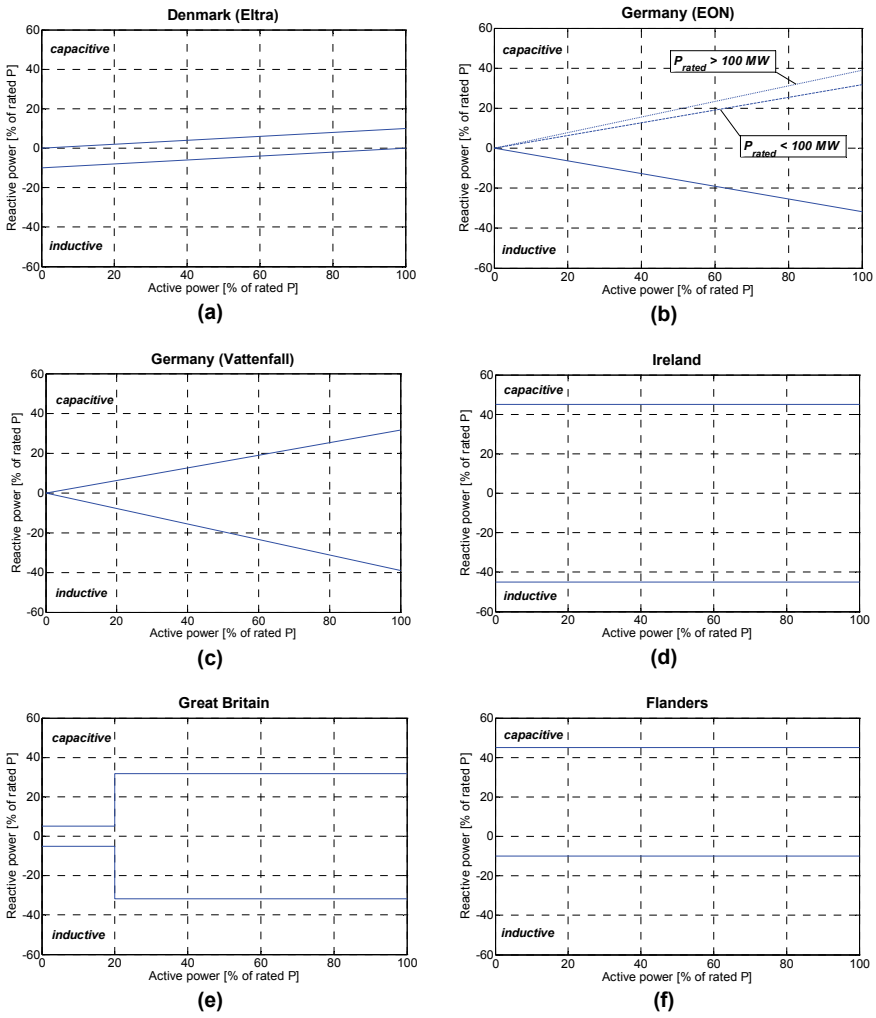

Figure 3.7. Reactive power ranges for continuous operation, for various European grid operators

Some remarks on Figure 3.7 should be given:

- The requirements on reactive power ability frequently change. Consultation of updated information is thus necessary. Also, most grid operators leave the possibility to impose bilaterally agreed requirements for particular cases.

- Some grid operators put demands on the extreme values for the power factor (E.ON and Vattenfall in Germany), while in Ireland and Flanders fixed reactive power ranges, independent – or only stepwise dependent for Great Britain - of instantaneous active power generation, are demanded.

- Figure 3.7e is the proposed reactive power range requirement specifically for wind turbines in Great Britain, i.e. United Kingdom excluding Northern Ireland. It is at the moment of writing yet to be validated by the British regulator Ofgem. Although different TSOs are active in England & Wales on the one hand, and Scotland on the other, Figure 3.7e is a proposition for common reactive power range requirements in Great Britain.

- The requirements in Flanders (Belgium) for distributed generation are to be bilaterally agreed between the power generator and the operator of the distribution grid. Figure 3.7f shows the minimal requirement, imposed by the Flemish Technical Regulation [40], applying however only to generators with grid connection at voltages between 30 kV and 70 kV.

- In the Swedish regulations, specifically for wind farms (not shown in Figure 3.7), the demand for reactive power control is expressed in terms of permissible voltage range. According to these regulations, wind farms should be able to maintain automatic regulation of reactive power with voltage as reference value. The reference value should be adjustable within at least ±10% of rated operating voltage [32]. The required range of reactive power capabilities thus depends on the local short-circuit power, as the grid impedance determines the impact of a given amount of reactive power on the voltage at the PCC.

- The specifications for the reactive power ranges in the Spanish grid are not obligatory, but wide control ranges for reactive power result in extra premiums. Table 3.6 [38] gives the premiums, as a percentage of the reference or average tariff (‘Tarifa Media de Referencia’ or TMR). Positive values indicate premiums, negative penalties. The premiums depend on the time of the day (peak, normal and off-peak: these periods vary between Summer and Winter and between the different autonomous regions in Spain). Table 3.6 indicates that the optimal reactive power behaviour depends on the grid loading. During off-peak hours, the generators preferentially have an inductive behaviour to compensate for the capacitances of the cables. During peak hours, capacitive behaviour is rewarded, compensating for the inductive energy consumption by most of the loads in the grid.

Power Factor		Peak	Normal	Off-peak
	< 0.95	-4%	-4%	8%
	0.95 … 0.96	-3%	0%	6%
INDUCTIVE	0.96 … 0.97	-2%	0%	4%
	0.97 … 0.98	-1%	0%	2%
	0.98 … 1.00	0%	2%	0%
	1.00	0%	4%	0%
	0.98 … 1.00	0%	2%	0%
	0.97 … 0.98	2%	0%	-1%
CAPACITIVE	0.96 … 0.97	4%	0%	-2%
	0.95 … 0.96	6%	0%	-3%
	< 0.95	8%	-4%	-4%

Table 3.6. Premiums for reactive power control, as a percentage of the TMR

3.3.3. Safety and protection mechanisms

The impact of distributed generation on the following three aspects of safety and protection is qualitatively discussed below:

- unintentional islanding;
- relay selectivity;
- fault detection.

Unintentional islanding

'Islanding' can be defined as the continued operation of a distributed generation unit that is tripped from the main grid due to a grid fault or for grid maintenance purposes. The grid section including the embedded generation in islanding is referred to as a power island [41].

Intentional islanding is possible without causing difficulties if the power island contains at least one generation unit that controls the voltage of the energised grid section. This is for example the case for uninterruptible power supply systems where a power island is maintained intentionally in order to securely supply critical loads.

Unintentional islanding can occur if a grid section is disconnected from the mains with its power balance approximately in equilibrium. This compromises the safety of maintenance staff working on the disconnected grid section. It is part of line

working procedures in most countries to take all reasonable steps to check that the circuit is not energised.

The transition to islanding mode is mostly detected by a disturbance in voltage magnitude or frequency on the power island. However, these transition phenomena may be minimal if the power island was in equilibrium for both active and reactive power before disconnection from the grid. A rigorous implementation of island detection is not straightforward. In [41], a report of laboratory testing with four inverters from different manufacturers indicates that for every inverter, conditions can be provoked in which unintentional islanding is not detected. The exact conditions under which islanding occur depend on the inverter type, and on whether specific island detection schemes are implemented or not. However, also with specific islanding detection schemes, unintentional islanding may still occur in specific conditions, e.g. when the instantaneous load and generated power in the power island is very small, i.e. less than 20% of the rated values.

Selectivity

'Selectivity' refers to the protection system ability to isolate the faulted zones, with the smallest possible disruption to other zones [42].

Figure 3.8 illustrates the principle of selectivity. As an example, a distribution grid with two radial branches is shown. The circuit breaker *D* is normally open: this is a typical *open ring layout*, widely used in distribution grids.

Figure 3.8a shows the occurrence of a grid fault between *A* and *B*. The fault current is supplied by the main grid. Figure 3.8b shows the normal grid reaction to the fault: circuit breakers *A* and *B* are opened and the grid fault is isolated. The remaining part of the lower radial branch can be supplied through *D*, being temporally closed. Only a very small part of the total load on the distribution grid is isolated due to the opening of *A* and *B* (plotted in grey).

Figure 3.8c shows the situation when *A* fails to open. In this case, the circuit breaker *C*, further upstream the fault, is opened, resulting in an isolation of the distribution grid from the main grid. The 'selectivity' principle, implying for this case that *C* only operates after a failure of *A*, guarantees that the smallest possible amount of grid users in case of a fault is isolated, only isolating a larger amount if the security equipment nearer to the fault suffers from failures.

However, when distributed generators are installed in the grid, the opening of *C* does not guarantee a total isolation of the grid fault (Figure 3.8d).

The general rule of thumb for implementing selectivity is to increase the relay switching time delays after fault detection in a radial branch with decreasing distance from the main grid. The presence of distributed generators however, as in Figure 3.8d, implies that this principle cannot be applied any more, as it does not

guarantee a total disruption of current towards the fault. In general, an increased amount and performance of switching relays are necessary in the presence of distributed generators.

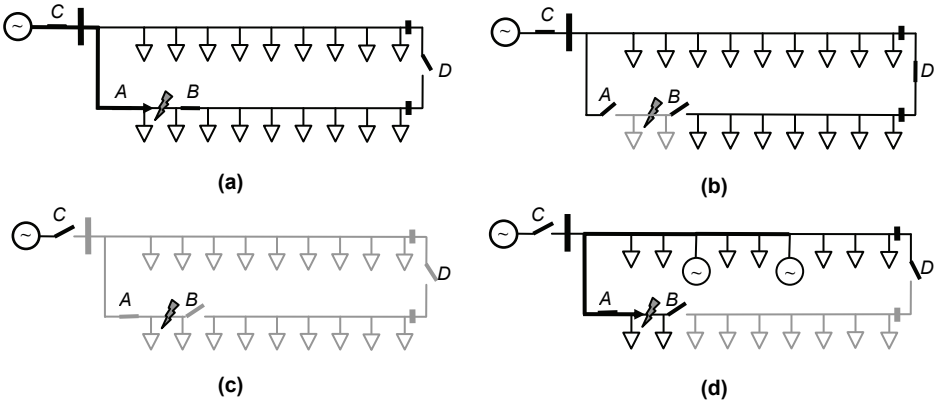

Figure 3.8. Principle of 'Selectivity': fault in distribution grid (a), fault isolated by circuit breakers *A* and *B* (b), fault isolated by circuit breaker *C* (c), fault not isolated by *C* in case of installed distributed generators (d)

Fault detection

The magnitude of a fault current depends on the local short-circuit power and the fault impedance, but is mostly an order of magnitude larger than the rated line current. In a radial grid, this fault overcurrent is detected by all relays upstream the fault. Their switching order is determined by the selectivity principle, as discussed above.

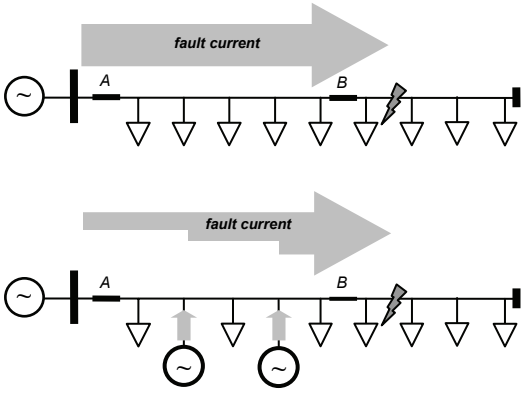

Figure 3.9. Fault current in line without (upper), and with distributed generation (lower)

In the case with installed distributed generation on a line, the fault current is to some extent supplied by the distributed generators. Figure 3.9 shows qualitatively the fault current without (upper part) and with (lower part) distributed generation. In both cases, the current at the fault location is the same, and the fault is detected by the circuit breaker *B*. If *B* fails to isolate the fault, the circuit breaker further upstream the fault, e.g. *A* in Figure 3.9, has to isolate it. The detection of the fault by *A* in the case with distributed generation is however not guaranteed. The fault current that is supplied from the main grid may be a very small fraction of the total fault current, not exceeding the rated current of the line, and thus not considered as being abnormal.

3.3.4. Stability and ride-through behaviour

Context

Until recently, the relative amount of distributed generators in the total generation park of a power system has been relatively small in most power systems. Distributed generators were then considered as negative loads, only alleviating the total system load but not contributing actively to the system power balance or voltage control. Distributed generators were free to choose the instants of connection and disconnection, according to their own needs and possibilities. Their protection devices prevented them from any overcurrent, overspeed or other instable behaviour, by disconnecting them from the grid in case of grid disturbances such as voltage or frequency transients.

In general, generators that are grid-connected through power electronic interfaces need very fast tripping in case of grid disturbances, as the power electronic interfaces are easily damaged by overcurrents or overvoltages.

With grid-connected induction generators, unstable behaviour may result from a grid disturbance. As an example, Figure 3.10 shows the reaction of an induction generator, operating at rated power, to a voltage drop to 15% of rated voltage, lasting 50 ms (a) or 150 ms (b). The voltage imposed for the simulation is shown in the upper part; the lower part shows the generator speed.

During the voltage drop, the electromechanical generator torque disappears, resulting in an acceleration. In this simulation, the generator is able to return to a stable behaviour in case of a voltage restoration after 50 ms, but continues to accelerate if the voltage drop lasts for 150 ms. The dynamic modelling and simulation details of the induction generator are extensively discussed in Chapter 5.

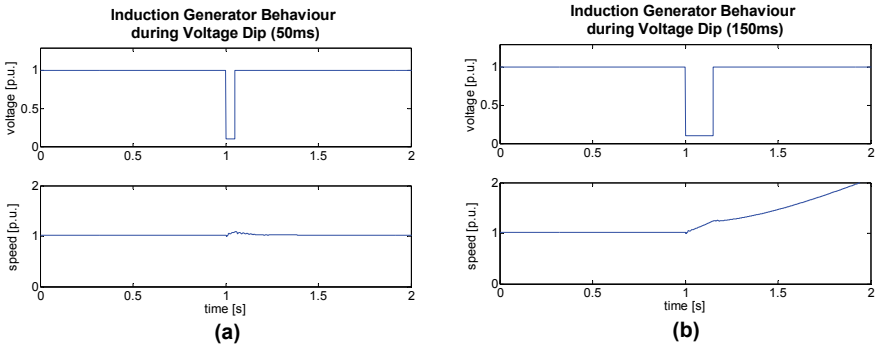

Figure 3.10. Induction generator behaviour during voltage dip lasting 50 ms (a) and 150 ms (b)

This example shows that induction generators are vulnerable to instable behaviour in case of grid disturbances of a certain extent. Operators of distributed induction generators thus traditionally choose for a very conservative protection scheme, tripping the generator already in case of small disturbances.

However, tripping a generator implies loss of power injection, causing another grid disturbance. When a large amount of distributed generators is installed nearby, this fast reaction might result in a cascaded tripping of other generation units, resulting in a considerable generation loss.

In the Spanish power grid, some historical incidents with cascaded tripping of wind turbines are reported for the first semester of 2004. They are listed in Table 3.7 [43]. Furthermore, the German transmission system operator (TSO) E.ON rang the alarm bell, stating that grid faults at specific locations could result in the loss of more than 3000 MW of wind power, thus surpassing the maximum power for immediate assistance that is available in from the UCTE-grid in case of emergencies [44]. Sudden losses of more than 3000 MW generation are likely to lead to a black-out of the power system.

Date	***Incident***	***Loss of Wind Power***
January 17-18, 2004	Various grid faults due to storms	465 MW
February 26, 2004	2-phase fault in 400 kV bus bar	600 MW
April 1st, 2004	Two 3-phase faults in 400 kV grid	500 MW
April 18, 2004	3-phase fault in 400 kV grid	400 MW

Table 3.7. Incidents with loss of wind power in the Spanish high voltage grid

To prevent such incidents, distributed generators are required to remain grid-connected during (or to 'ride through') grid faults, in order to actively support the grid and maintain its stability. The extent of the grid faults that may not lead to a disconnection is defined by the TSO or technical regulations in each control zone.

Voltage drop ride-through requirements issued by TSOs

Specific grid connection requirements and fault ride-through requirements for distributed generators were first issued by Eltra[1] and E.ON[2]. These two TSOs were the first to be confronted with large amounts of distributed generation, mainly wind power. Their connection requirements were used as a reference for other TSOs facing the same challenges. Some TSOs issue specific ride-through requirements for wind power only, as of all distributed generation technologies, wind power has known the fastest increase in both installed power and technical generator capabilities.

Fault ride-through requirements specify the extent and duration of a voltage or frequency drop or rise that may not lead to a disconnection of the generator. Research institutes, TSOs and generator manufacturers recognise that the most critical grid disturbance is a voltage drop, as this is a disturbance that regularly occurs, but also provokes most easily unstable generator behaviour and cascaded tripping.

Figure 3.11 ([32] - [40]) gives an overview of the voltage drop profiles as defined by various grid operators or regulators in Europe, specifically for distributed generators or in some cases only for wind power generators. Any voltage that does not cross the lines should not lead to a disconnection of the generator.

Some remarks are to be made for Figure 3.11:

- As for the reactive power range requirements, ride-through requirements for distributed generators are changed frequently by TSOs. The reader may want to check for updates before using Figure 3.11 as a reference.

- Figure 3.11a is elaborated by the two Danish TSOs Eltra (Western Denmark) and Elkraft System (Eastern Denmark). The requirements concern wind farms connected after July 2004 to networks with voltage levels lower than 100 kV [32].

[1] Eltra is the TSO for the Danish peninsula Jutland and Funen, since 2005 merged with Elkraft Transmission, Elkraft System and Gastra into *Energinet.dk*.
[2] E.ON-Netz is the TSO for the German provinces Schleswig-Holstein, Lower Saxony, Hesse, Bavaria, and parts of North Rhine-Westphalia.

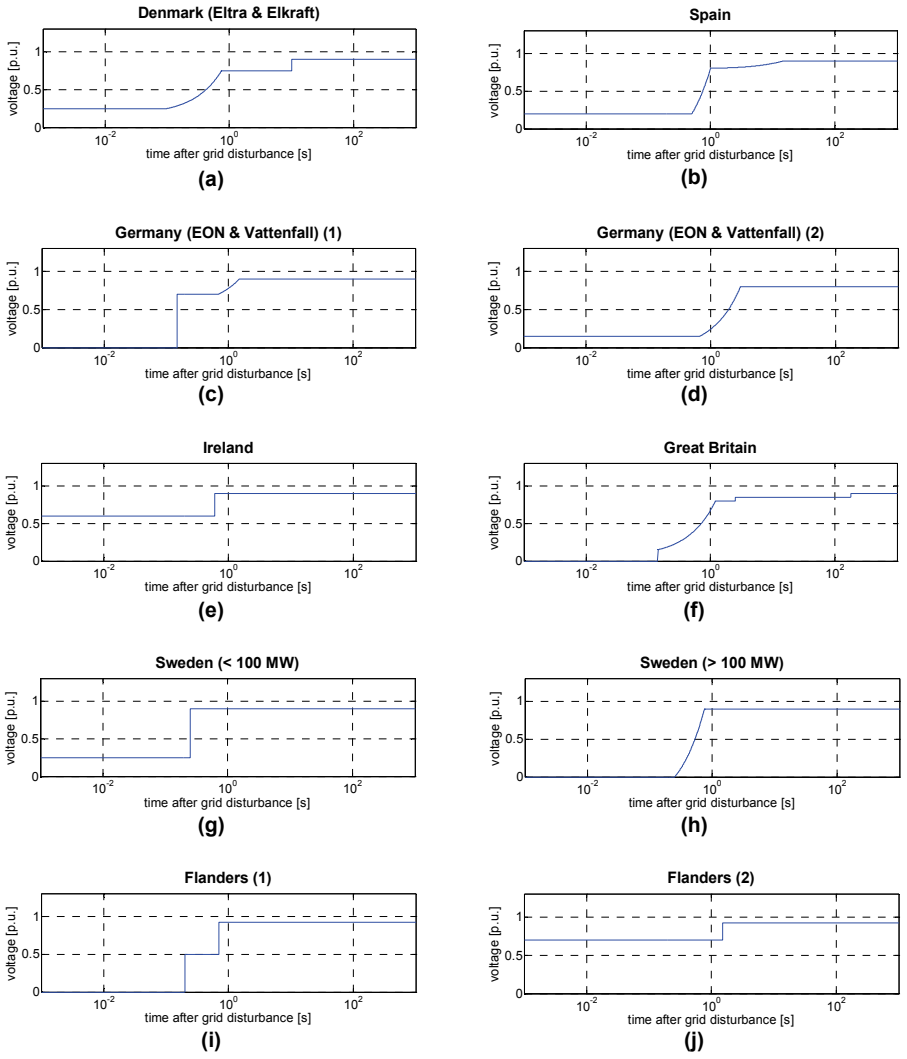

Figure 3.11. Voltage drop ride-through requirements from various European grid operators

- As for the reactive power range, the voltage drop ride-through requirements are mandatory for all generators envisaged, except in Spain (Figure 3.11b), where fulfilment of the ride-through requirements is facultative, but leading to a higher retribution for the energy produced [38]. Like Figure 3.11a, Figure 3.11b also applies for wind turbines only, in Spain.

- The German TSOs E.ON and Vattenfall make distinction between generators with high symmetrical short-circuit current component (if the

contribution of the generator at the network connection point to a short-circuit is higher than twice the rated line current for longer than 150 ms) and with low (all other). The first have to satisfy the ride-through requirement from Figure 3.11c, the other from Figure 3.11d. Those requirements apply for all generators, large and distributed, thermal and other, all falling in one of the two categories. As a rule of thumb, Figure 3.11c applies for large synchronous generators, and Figure 3.11d for distributed generators or generators connected through power electronic interfaces.

- Figure 3.11d was the first voltage drop profile issued by E.ON as a specific ride-through requirement for wind turbines (December 2001) [35], later generalised for all generators with low symmetrical short-circuit component (August 2003) [36].

- As for the reactive power range, Figure 3.11f is the proposed voltage drop ride-through requirement specifically for wind turbines in Great Britain, yet to be validated by the British regulator.

- The Swedish grid operator makes a distinction between generators with rated power higher or lower than 100 MW, as seen in Figure 3.11(g) and (h), not distinguishing further for different generator technologies such as wind power.

- As for the reactive power range requirements, distributed generation ride-through is to be bilaterally agreed between power producer and operator of the grid in Flanders. However the Flemish Technical Regulation imposes Figure 3.11i and Figure 3.11j as minimum ride-through requirement for respectively short and long voltage drops, applying however only for generators with grid connection at voltages between 30 kV and 70 kV.

- Apart from these predefined voltage drop profiles, most TSOs leave room for bilateral agreements for particular generators (e.g. large or offshore wind farms).

Similar ride-through requirements exist for frequency disturbances. A good overview of these requirements for some selected countries can be found in [32].

Figure 3.11 illustrates the differences in regulations by various grid operators, making it difficult for generator manufacturers to standardise their products. As for the reactive power requirements, it is concluded that the ride-through requirements lack uniformity in the various European zones. This is partially explained by different grid structures in different control zones, but is also a result of historical coincidences. Furthermore, national strategies to influence the market access by national or foreign manufacturers of electrical generators, by making the requirements more or less adapted to the capabilities of one specific manufacturer, is an often heard accusation from competing manufacturers.

3.3.5. Power quality

Overview

The denomination 'Power Quality' refers to the extent to which the voltage at the PCC is close to the ideal voltage, being in the case of three-phase AC-grids a perfectly balanced sine wave with amplitude and frequency equal to their rated values and not varying in time.

Power quality distortion phenomena can be subdivided into [45]:

- harmonic distortion;
- transients;
- voltage dips;
- voltage swells;
- flicker;
- voltage asymmetry (unbalance);
- frequency variations.

Whereas paragraph 3.3.2 and 3.3.4 briefly illustrated the idea that deteriorated power quality (voltage and frequency deviations) by any external cause should not jeopardise the stability of distributed generators, this paragraph reviews power quality deteriorations that may be caused by the generators themselves.

Harmonic distortion

Harmonic distortion, i.e. the presence of higher-order harmonics and interharmonics in the voltage or current sine waves, is mainly caused by loads and generators that are grid-connected through power electronic interfaces. It may cause computers to malfunction and motors, transformers and wires to heat up excessively.

The measurement procedures and quantification of harmonic current emissions by distributed generators is defined by international standards. Specifically for wind turbines, the standard IEC 61400-21 [46] defines the measurement procedures for every power quality aspect. The measurement of harmonic emissions is only compulsory for wind turbines with power electronic interfaces. The standard prescribes that the amplitude of every harmonic current until the 50^{th} order is to be measured as a percentage of the rated current, at the generator output power resulting in the highest amplitude of every individual harmonic.

The converters in modern wind turbines and other generation types are mostly equipped with an active front-end with *Pulse Width Modulation* (*PWM*), implying that the conversion from the grid voltage to the DC voltage on the capacitor in the

converter is done by an active rectifier bridge (consisting of e.g. '*Insulated Gate Bipolar Transistors*' or *IGBT*s), rather than a thyristor bridge. Apart from other benefits, IGBT-converters can filter out the harmonic content of the current exchanged with the grid. Modern power electronic interfaces are thus well equipped not to cause harmonic distortion in the grid. Therefore, harmonic distortion is not further discussed in this work.

Transients

Transients are sudden and significant deviations from normal voltage and current, usually having a short duration (μs or ms). Transients may be caused, amongst others, by short-lasting but relatively high inrush currents during switching actions. Inrush currents may be an order of magnitude higher than the machine's rated current, and occur for instance if a squirrel cage induction generator or transformer is magnetised when switched on, or if the capacitor in a converter of a PV-array is loaded.

It will be shown in Chapter 5 that switching operations of directly grid-connected induction generators may cause heavy transients in weak distribution grids. Therefore, a soft-starter is often used as an interface between generator and grid. A soft-starter consists of two anti-parallel thyristors per phase and aims at limiting the inrush current and thus the grid transients. It is bypassed if steady operation is reached. For generators connected through power electronic interfaces, manufacturers make sure that switching transients are reduced to the minimum, by applying appropriate switching procedures.

Voltage dips and swells

Voltage dips and swells are decreases, respectively increases, of short duration in voltage values. The distinction between voltage dips or swells and transients is rather vague. In general, 'dips' and 'swells' refer to voltage disturbances lasting longer than one period, while 'transients' refers to shorter phenomena. As for transients, voltage dips may be caused by switching actions. Also grid faults (short-circuits) may cause voltage dips in neighbouring bus bars.

As for transients, voltage dips caused by switching actions are in practice limited by either soft-starters or the power electronic interfaces between generators and grid.

Voltage dips and swells may also be caused by simultaneous excessive power output fluctuations from a set of distributed generators. Strong wind gusts may cause simultaneous power output fluctuations by a series of wind turbines concentrated in a small area. As distributed generation is by definition not centrally dispatched,

these phenomena are preferentially countered by basic control and peer-to-peer communication algorithms, implemented locally [47].

Flicker

Flicker consists of small periodic voltage amplitude changes, occurring at frequencies between 0.5 Hz and 25 Hz. It is rarely harmful to electronic equipment, but supplying an incandescent lamp by a voltage suffering from flicker causes annoying changes in lightning levels. Figure 3.12a shows a typical voltage waveform, polluted by flicker.

Flicker is caused by rapidly fluctuating loads or generators such as wind turbines. Especially the 'tower effect' of fixed speed wind turbines, i.e. the slight decrease in mechanical torque (and thus power generation) each time a turbine blade passes the tower front, may cause flicker.

Flicker is quantified according to the *IEC61000-4-15* standard [48]. The so-called *UIE flicker meter* is a measurement device in which this standard is implemented. The principle is as follows: through a series of filters, defined in the standard, the amplitudes of the frequency components of the voltage in the range 0.5 – 25Hz are normalised and summed. A weighting function is hereby taken into account, which reflects the level of irritation that an average person experiences from a light bulb supplied by a flicker-polluted voltage.

Flicker is quantified by the variable *Pst* ('Probability short term'), and is measured within a time span of 10 minutes. *Pst* = 0 indicates a flicker-free voltage; *Pst* = 1 indicates that the flicker pollution has reached the tolerance limits of the average person. The variable *Plt* ('Probability long term') quantifies the flicker pollutions within a longer time span, generally two hours. Basic values in medium-voltage grids are 0.35 (*Pst*) and 0.25 (*Plt*) [49].

Figure 3.12b ([48], [50]) shows the normalised amplitude *dU/U* of the periodic voltage variation that results in *Pst* = 1, for the case with only one voltage frequency component present apart from the fundamental frequency. It shows that a fluctuation frequency of 8-9Hz causes the most irritation to humans, as even a very low amplitude at this frequency results already in *Pst* = 1.

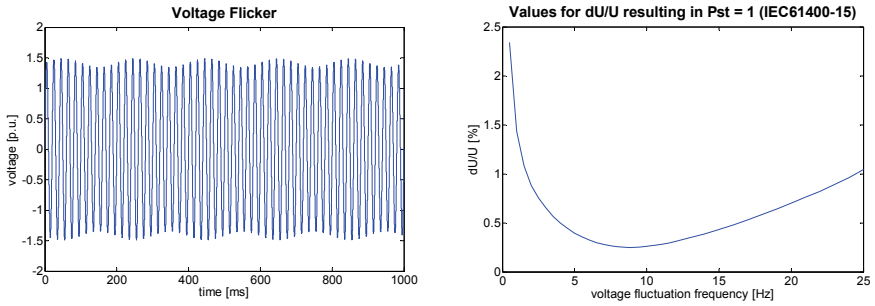

Figure 3.12. Voltage polluted by flicker (a), and relative voltage fluctuation amplitudes resulting in Pst = 1 (b)

The *IEC61400-21* standard gives a specific measurement procedure to calculate the impact of wind turbines on grid voltage flicker. The procedure is elaborated in such a way that a measurement report for a single wind turbine is independent of the characteristics of the grid on that site, and allows a quantification of the turbine impact on grid flicker for every location [46].

Voltage asymmetry (unbalance)

Voltage asymmetry refers to differences in phase-to-neutral or phase-to-phase voltage magnitudes or phase angles of the three-phase system. This is mainly caused by the uneven distribution of single-phase loads. Also asymmetrical impedances in three-phase lines or transformers may cause unbalance. Single-phase generators are assumed to cause unbalance to the same extent as single-phase loads. This is not further evaluated in this work.

Frequency disturbances

In contrast to voltage amplitude, being a local quantity, the voltage frequency is a quantity almost equal across the entire interconnected UCTE-grid. Frequency disturbances indicate temporary unbalances between generation and load in a power system. Distributed generators are thus very unlikely to cause frequency disturbances in the entire interconnected grid. However, some TSOs require distributed generators, or more specifically wind turbines, to assist in frequency control by tuning their active power output down in case of frequency rises.

In smaller power systems, e.g. islands grids with on-site generators, frequency disturbances may frequently occur, possibly also caused by power output fluctuations by the generators. In this case, specific measures must be taken to make

generators control the frequency, rather than causing additional frequency disturbances. Isolated grids will not be further discussed in this work.

3.4. Conclusions

This chapter has dealt with the technical aspects of distributed generation relevant for power system operation. The chapter intended to summarise a vast amount of literature, standards and grid codes in a comprehensive overview. The literature review was extended with own considerations about the potential line loss reduction by distributed generation, further elaborated in Appendix I.

While Chapter 2 briefly reflected the political support systems for increasing renewable energy, thus illustrating the recognition by decision makers of the need for renewable energy generators, this chapter has shown that also the system operators have taken distributed generation – which is to some extent overlapping with 'renewable energy' – seriously. Through specific grid connection requirements for distributed generators, it is illustrated that system operators recognise the increasing impact of these technologies, and also their technological specificity and limits. However, power system operators also want to confront distributed generators with their responsibilities to keep the power system stable. This requires a change in mentality for generator manufacturers and operators, but the far stage of specific grid connection requirements in some European countries illustrates the already present awareness.

While this chapter was mainly dedicated to distributed generation in general, the following chapter will focus on the aspects of wind power specifically.

Chapter 4

Technical Aspects of Wind Power

4.1. Introduction

This chapter describes the technical aspects of wind power relevant for the power system. It is subdivided in a review on wind speed characteristics, wind turbine characteristics and then more specific wind turbine generator types. Finally, common definitions for estimating the value of wind power are provided and commented.

The study and explanation of the physical mechanisms that cause wind is not the aim of this work. Paragraph 4.2 briefly describes the various aspects of wind speed that have an impact on power system operation. These are respectively: wind speed probability distribution function, wind speed fluctuations, correlations between wind speeds at different sites and forecasting of wind speed or wind power. Paragraph 4.2 is a mixture of literature review and presentation of statistical results of own wind speed measurements. A more extensive discussion on the estimates of aggregated wind *power* in Belgium, based on these wind speed data, is done in Chapter 6.

Paragraph 4.3 gives a review of the technical aspects of wind turbines, with special focus on generator types. For the doubly-fed induction generator, one paragraph is dedicated to a closer view on its operating ranges, going beyond existing literature. Further description of the behaviour of wind turbine generators, and their dynamic

modelling in dedicated power system simulation software, is discussed in Chapter 5 where simulation results are presented.

Paragraph 4.4 gives a brief review of how the value of wind power in a power system is estimated. The terms '*capacity factor*' and '*capacity credit*' are often used. Their definitions are commented with regard to the influence of fluctuations on wind power value. This is further worked out in Chapter 6 for the specific case of Belgium.

4.2. Wind Characteristics

4.2.1. Probability distribution of wind

Wind speed

The probability distribution for the wind speed at a given site is best described by a Weibull probability distribution function [51]. The 2-parameter Weibull probability distribution function is defined by:

$$p(x) = kA^{-k}x^{k-1}e^{-\left(\frac{x}{A}\right)^k} \tag{4.1}$$

Figure 4.1 shows as an example the normalised histogram of hourly recorded wind speeds in Ostend (Belgium) at 10 m anemometer height, during the period 2001 - 2003. The best fitting Weibull-curve is also shown.

The Weibull parameter estimates for Ostend are A = 5.4 and k = 1.8.

The average wind speed in Ostend is 5.0 m/s, while the most probable wind speed is 4.0 m/s. It is a typical property of a Weibull-distributed variable that the average value is higher than the most probable value, due to the asymmetrical probability distribution function, with a more slowly decaying behaviour in the high region. This implies a low number of occurrences of high wind speeds, but over a large range of wind speed values.

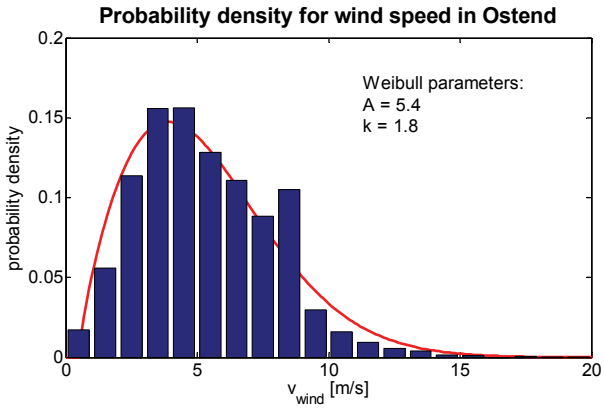

Figure 4.1. Histogram of measured wind speeds in Ostend, and fitted Weibull probability density function

Wind direction

A representation of the probability distribution for wind directions is given in the *wind rose* [51].

Systematic measurements of wind directions, covering a long time span, were not available. However from [52], it is known that the by far prevailing wind direction in nearly all Belgium is west – southwest.

4.2.2. Wind speed fluctuations

Wind speed varies continuously as a function of time and space. The frequency spectrum of the wind speed in Ostend is shown in Figure 4.2, indicating the time scales of wind speed variations. The frequency axis is logarithmic.

The resolution of the spectrum in the region of very low frequencies (period around one year) is very low, as measurement data for only three years are available. Also the frequency spectrum in the region of fast fluctuations (period less than 2 hours) could not be calculated, as the sample period of the available wind speed data is one hour.

The following spectral peaks are visible in Figure 4.2 and documented in [53]:

- *annual peak*: explained by the seasonal dependency of the wind speed. In Belgium, the wind speed is generally highest in late Winter (February) and lowest in late Summer (August);

- *synoptic peak zone*: explained by changing weather patterns, which typically vary daily to weekly [53];

- *diurnal peak*: explained by the daily periodicity of wind speeds, caused by the daily periodical temperature changes.

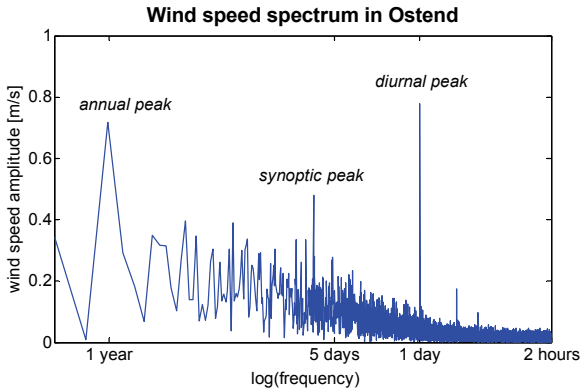

Figure 4.2. Wind speed spectrum in Ostend (average wind speed is 5 m/s)

The annual and diurnal peaks are pronounced spectral peaks at one specific frequency, while the synoptic peak zone is rather an extended zone of high spectral content, in the frequency range between days and weeks.

Apart from the three spectral peaks mentioned, also the existence of a *turbulent peak* is reported in literature [53]. This peak is mainly caused by gusts, and covers the seconds to minutes spectral range, impossible to be distinguished in the available wind speed time series with an hourly resolution.

4.2.3. Correlation between wind speeds at various sites

Context

The *correlation coefficient cor(x, y)* is:

$$cor(x,y) = \frac{\mathrm{cov}(x,y)}{\sigma_x \sigma_y} \tag{4.2}$$

with covariance:

$$\mathrm{cov}(x,y) = \left\langle \left(x - \langle x \rangle\right) \cdot \left(y - \langle y \rangle\right) \right\rangle \tag{4.3}$$

where x and y represent the variables between which the correlation is investigated, <..> represents the *mean* operator and σ_x and σ_y are the standard deviations of respectively x and y.

The correlation coefficient is a measure of linear dependency between the variables x and y. A correlation equal to 0 indicates that there is no linear dependency between the variables. A positive correlation indicates that when x increases, y is likely to increase too. A negative correlation means that y is likely to decrease if x increases. A correlation of 1 or -1 indicates a perfectly determined linear dependency between x and y.

From the point of view of power system balancing, it is a matter of high interest to know the correlation between wind speeds at various sites in a control area. When wind speeds at various sites in one control area are highly correlated, the aggregated wind power generation in this zone fluctuates almost as much as the generation of a single turbine, thus putting higher demands on the power system's reserves (mainly secondary reserves, in the minutes to hours range).

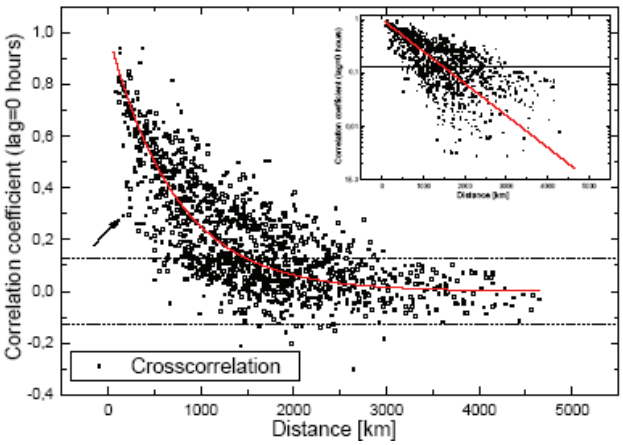

Figure 4.3. Correlation coefficient for every pair of 51 weather stations distributed over Europe, with time lag = 0 hours. In the inset, the same plot is scaled logarithmically [54].

Correlations between wind speeds at various sites have been the subject of much research [54], [55]. Figure 4.3, taken from Giebel [54], shows the correlation coefficient between any pair of 51 weather stations distributed all over Europe. The figure shows widely scattered correlation coefficients. The arrow in the figure marks the very low correlation between the wind speeds at the nearby measurement sites of Alghero and Cagliari. These stations are in the northwest and south of the island of Sardinia in the Mediterranean, and hence have different microclimates. This

example proves that sites, although very near to each other, may have relatively uncorrelated wind speeds.

The general conclusion from Figure 4.3 is however that correlations less than 0.3 occur rarely for distances below 1000 km. These dimensions are far above the extent of the Belgian control zone. It is thus expected from Figure 4.3 that the wind speeds at all sites in Belgium are strongly correlated. This is further discussed in the next paragraph.

Correlation between measured wind speeds in Belgium

Wind speed measurements with hourly resolution are available from three sites in Belgium (Ostend, Brussels and Elsenborn), for the period 2001-2003. These three sites are geographically well spread in Belgium, approximately on a straight line, and respectively 110 km and 140 km apart (Figure 4.4). As mentioned above, the prevailing wind speed direction in Belgium is west – southwest. Roughly estimated, the components of the distance between the measurement sites along the prevailing wind direction are 60 km and 140 km.

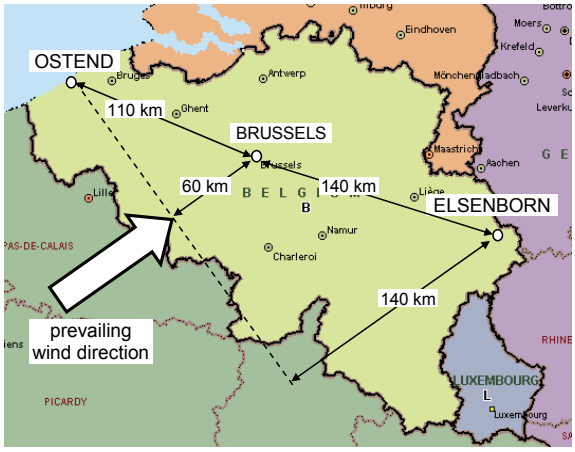

Figure 4.4. Wind speed measurement sites in Belgium

Figure 4.5 shows the measured wind speeds at the three sites during the first three days of January 2001. The simultaneous wind speed rises and drops seem highly correlated.

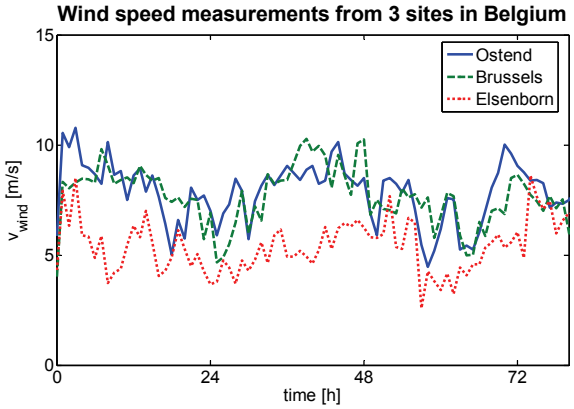

Figure 4.5. Measured wind speeds at the three sites for the first days of January 2001

This is confirmed in Figure 4.6, showing the correlation coefficients between each pair of measured time series from two of the three sites, as a function of relative time shift between them. The correlation has a clear maximum, for all three pairs, for a time shift equal to zero. This means that, for example, if the wind speed rises in Ostend, the wind speed in Elsenborn is likely to rise in the same hour, rather than some hours later or earlier. The periodical behaviour for larger time shifts in Figure 4.6 is explained by the natural daily periodicity of the wind speed.

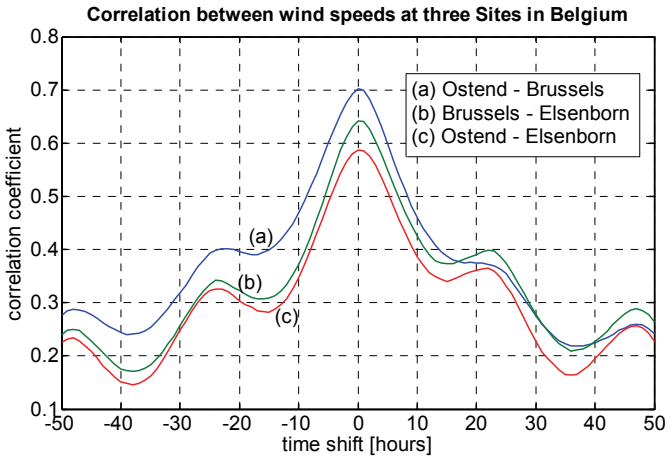

Figure 4.6. Correlation coefficients between wind speeds at three sites, as a function of time shift

Figure 4.6 contradicts the often made assumption that wind speed rises and drops are propagated at a speed equal to the wind speed itself, and that a wind speed time series at one site is a delayed version of the time series at another, at some distance upwards the wind direction ([3], [56], [57]). This assumption may be valid for very

small areas (up to some km²), such as within a single wind farm, but is not valid when considering the entire Belgian region.

Estimating the aggregated wind power output in a large control area has been the subject of much research (e.g. in [3], [56] and [57]). The above mentioned assumption has often lead to the proposal to calculate the sliding average of a wind speed time series (measured at the beginning of the control region), with a block-averaging window of several hours, depending on the wind speed, location of installed wind power and size of the control area. This methodology usually leads to strongly smoothened power time series, compared to the actually measured wind speed fluctuations. The outcoming results are mostly very much in favour of wind power, as they lead to the conclusion that the aggregated wind power output in a control area is smoothened to such in extent that the need for additional secondary power reserves in a power control zone is only very low, which is however contested in Chapter 6 of this work.

The estimation of the aggregated wind power in Belgium and its fluctuations, based on the available wind speed measurements, is further extensively discussed in Chapter 6.

4.2.4. Wind speed forecasting

From the point of view of system operators and wind power traders, forecasting of wind speed and power is of fundamental importance. In the deregulated electricity market, power generators may be penalised if their actual generation in a given time span is too far below or above the generation level contracted. Political support systems may broaden the tolerance margins specifically for wind power plants, before penalties are induced. However, with increasing penetration of wind power, accurate forecasting will increase the economical and ecological value of wind power considerably.

As stated in [53], the requirements regarding wind power prediction accuracy and time span depend on the specific power market system in the considered zone, rather than on physical criteria. In Denmark and Germany, for instance, predictions are used mainly for the day-ahead market closing at noon in Denmark (i.e. 12 to 36 hours before time of delivery) and at 3 p.m. in Germany (9 to 33 hours). Contrarily, the spot market in Great Britain closes only one hour before the time of delivery, according to the *NETA* (the British '*New Electricity Trading Arrangement*'). In Scandinavia, the market operation requires a 36-hours forecast horizon, which is however technically not strictly necessary as the hydro system (mostly in Sweden) can adjust generation within a fraction of an hour.

Various wind speed and power forecast systems exist, developed by different research institutes [53]. Basically wind speed forecast systems use either a physical or a statistical method, or a combination of both.

- The physical method simulates large-scale wind flows starting from *numeric weather predictions* (NWP), and further predicts local wind power generation using physical equations. This method offers the advantage that insight in the physical processes is given, allowing a solid theoretical basis for predictions.

- The statistical method mostly also starts from NWP, and further uses statistics, artificial neural networks or fuzzy logic instead of physical equations to calculate local wind power generation. They have the advantage to be able to learn from experience. The disadvantage is that they need a large dataset to be trained properly, and that extreme values of wind power will be more difficult to foresee.

Actual existing forecast tools are listed in Table 4.1 (taken from [53]).

	Method		**Input Data**	
	Physical	Statistical	NWP	Measurement
Prediktor	X		X	
Wind Power Prediction Tool		X	X	X
Zephyr	X	X	X	X
Previento	X		X	
e Wind ™	X		X	
SIPREÓLICO		X	X	X
Advanced Wind Power Prediction Tool		X	X	X
HONEYMOON	X		X	

Table 4.1. Overview of wind prediction systems [53]

The performance of wind prediction systems is improving fast during the last decades. For the Advanced Wind Power Prediction Tool, developed by the *Institut für Solare Energieversorgungstechnik* (ISET, Kassel) and used in the German power system, it is reported in [53] that for a forecast horizon of 24 to 48 hours, a wind power prediction error larger than 20% of installed wind power in Germany occurs during no more than 3% of the time. This performance may be considered as very high, given the immense complexity of the physical processes that eventually lead to wind power generation, but on the other hand it is far too low for solid power system management and stable energy prices on the market.

The most frequent cause of forecast errors is not the wrong estimation of wind power values as such, but the exact moment of wind power increases and decreases. This is a very heavy barrier for participating in power trades. Most wind power prediction tools foresee a system of on-line monitoring and continuous adaptation of the predictions, but this is not yet taken into account in the existing power trade mechanisms.

Wind speed forecasting is considered by the author as yet having a too low performance for solid grid management. In Chapter 6, wind power time series for Belgium are estimated using measured wind speeds, and some statistical operations are performed on the results to distinguish general trends. Wind speed forecasting is not further discussed in this thesis.

4.3. Wind Turbine Characteristics

4.3.1. Energy conversion formulas

Wind turbines extract kinetic energy from moving air, and convert it to mechanical energy in the turbine rotor, and further to electrical energy through the generator.

The kinetic energy of the wind, flowing through the turbine rotor (propeller), is per unit of time the power P_{wind}:

$$P_{wind} = \frac{1}{2}\rho_{air} S_{rotor} v_{wind}^{3} \tag{4.4}$$

with:

- ρ_{air} the mass density of air;
- S_{rotor} the propeller area;
- v_{wind} the wind speed.

The mechanical energy P_{turb} that is taken by the turbine from the wind is equal to:

$$P_{turb} = \frac{1}{2} C_p(\lambda, \beta) \rho_{air} S_{rotor} v_{wind}^{3} \tag{4.5}$$

with $C_p(\lambda,\beta)$ - further denoted as C_p - the 'coefficient of performance', i.e. the fraction of the kinetic energy of the air captured as rotational energy by the propeller.

C_p is a rather complex function of propeller design, the *tip-speed ratio* λ and the *blade pitch angle* β. The *tip-speed ratio* λ is defined as:

$$\lambda = \frac{R_{turb} \cdot \Omega_{turb}}{v_{wind}} \tag{4.6}$$

with R_{turb} the turbine propeller radius and Ω_{turb} the mechanical propeller speed.

The dependence of C_p on λ and β cannot be analytically described. C_p is calculated from measurements, approximate equations or numerical methods using e.g. the theory of the 'Blade Element Method' [51]. A possible approximate equation for a three-bladed horizontal axis turbine is [58]:

$$C_p(\lambda,\beta) = 0.22\left(\frac{116}{\lambda_i} - 0.4\beta - 5\right)\cdot e^{\frac{-22.5}{\lambda_i}} \tag{4.7}$$

$$\text{with: } \frac{1}{\lambda_i} = \frac{1}{\lambda + 0.08\cdot\beta} - \frac{0.035}{\beta^3 + 1} \tag{4.8}$$

This approximation is valid for λ in the range 4 – 8, and β in the range 0° – 30°.

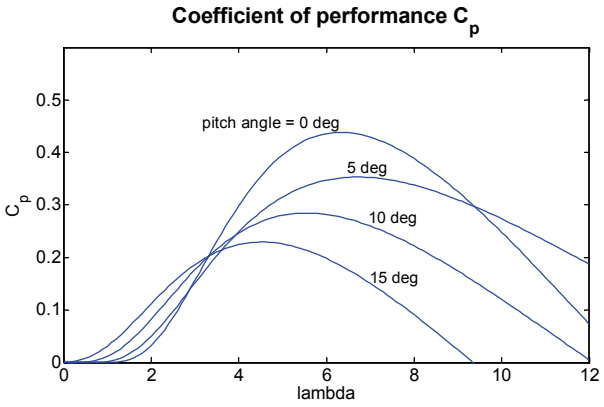

Figure 4.7. Coefficient of performance for a three-bladed turbine, approximate equation

Figure 4.7 plots C_p as a function of λ and β, according to (4.7) and (4.8).

The theoretical upper limit for C_p is 59%, i.e. the 'Betz-limit' [51]. This limit is not reached in Figure 4.7.

4.3.2. Turbine power curve and basic turbine control options

The power curve of a specific wind turbine gives the electrical power output as a function of wind speed at hub height (i.e. rotation centre of the rotor). It is the most important characteristic of a specific turbine.

The exact appearance of the power curve depends on the wind turbine technology and control options, more precisely:

- fixed speed or variable speed;
- pitch, active-stall or passive-stall controlled;
- operational settings.

Two typical power curves are shown in Figure 4.8. Figure 4.8a is the power curve of a fixed-speed, stall-controlled turbine. Figure 4.8b is the power curve of a variable-speed pitch-controlled turbine.

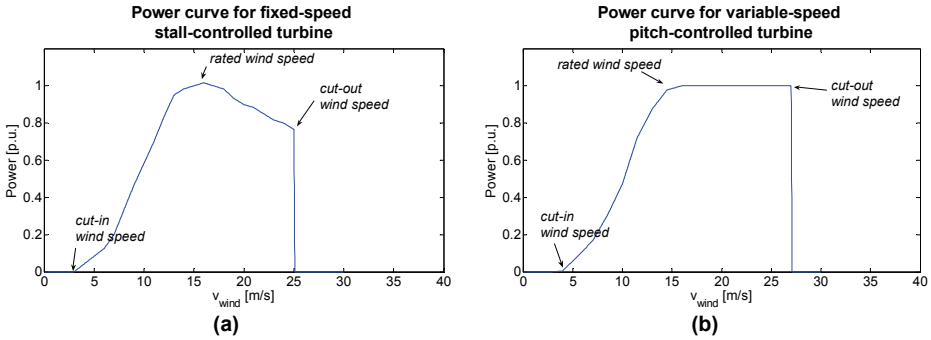

Figure 4.8. Typical power curve of a fixed-speed stall controlled turbine (a), and a variable speed pitch-controlled turbine (b)

The following wind speeds are typical characteristics for a specific turbine:

- *cut-in wind speed*: lowest wind speed at which the turbine can produce net electrical power, typical value 4 m/s;

- *rated wind speed*: lowest wind speed at which the turbine produces its rated electrical power, typical values around 13-16 m/s;

- *cut-out wind speed*: highest wind speed at which the turbine produces power. In case of higher wind speeds the turbine operation must be stopped because of too high mechanical loads on the turbine components. Typical values are around 25-30 m/s.

Regarding speed control, distinction can be made between fixed-speed turbines and variable-speed turbines.

- *Fixed-speed turbines* cannot control their rotational speed or λ. As can be derived from Figure 4.7, the aerodynamic efficiency is thus slightly lower at low wind speeds (high λ) or high wind speeds (low λ). Fixed speed turbines are mostly equipped with a squirrel cage induction generator type (see paragraph 4.3.3).

- *Variable-speed turbines* can optimise the aerodynamic efficiency C_p for every wind speed. Figure 4.7 shows that the optimal C_p occurs for a fixed value of λ, i.e. a fixed ratio between turbine and wind speed. Variable-

speed turbines thus decrease their rotational speed at lower wind speeds, and also have the advantage that the turbine, through acceleration and deceleration, can be used as a flywheel in case of sudden wind speed drops or rises, thus damping the power output fluctuations. Variable-speed turbines are mostly equipped with a doubly-fed induction (limited speed range) or synchronous generator (wide speed range - see paragraph 4.3.3).

Regarding blade angle control, three systems can be distinguished.

- *Passive stall-controlled* turbines (or 'stall controlled' turbines) have blades fixed on the rotor, i.e. they are not able to rotate around their longitudinal axis. The blades are designed in such a way that 'stall' (i.e. the loss of lift force due to turbulence of the wind on the top of the blade) starts to occur when the wind speed exceeds its rated value. The rotor torque and the electrical power are thus by design limited to their rated value, the turbine is inherently safe for wind speeds up to the cut-out wind speed. However, the power output for wind speeds between rated wind speed and cut-out wind speed decreases for increasing wind speed due to this stall effect (Figure 4.8a).

- *Pitch controlled* turbines have pitchable blades that allow to modify the aerodynamic efficiency of the turbine. This is especially useful during high wind speeds, when the blades are partially pitched out of the wind, in such a way that the steady-state power output is maintained at the rated value, for all wind speeds above rated and lower than cut-out wind speed. Figure 4.7 shows that C_p decreases more or less linearly for increasing values of β.

- *Active stall-controlled* turbines also have pitchable blades, and provoke actively the stall effect by rotation of the turbine blades and increasing the angle of attack at high wind speeds, in order to induce stall, and to limit the mechanical torque and electrical power to their rated values. The output power is better controlled than with passive-stall turbines. Both pitch controlled and active-stall controlled turbines have a power curve similar to Figure 4.8b.

4.3.3. Generator types for wind turbines

Grid-connected Squirrel Cage Induction Generator

For a long time, the *squirrel cage induction generator* (SCIG) has been the most used generator type for wind turbines.

The generator is mostly directly grid connected, as in Figure 4.9a. The torque-speed characteristic is shown in Figure 4.9b, in motor sign convention. The motor or

generator operation is only stable in the narrow range around the synchronous speed n_s. In this zone, the machine speed n varies only very little with varying torque, and cannot be controlled. Turbines equipped with this generator type are often called fixed-speed systems, although the speed slightly varies over a narrow range. The range becomes broader with increasing rotor resistance.

The induced rotor currents cause dissipation of electrical energy in the rotor bars. It can be proven that this dissipated rotor power P_R obeys the following equation:

$$P_R = sP_\delta \tag{4.9}$$

with:

- P_δ the air-gap power: the electromagnetic power crossing the air gap from stator to rotor or vice versa;
- s the slip, being equal to $n - n_s$ [p.u.], with n_s the synchronous speed. The slip is mostly not higher than 5% for SCIGs.

Generator operation only occurs for speeds higher than n_s (equal to 1 p.u. if n_s is chosen as the base speed). As the pole pair number p_p is mostly equal to 2 or 3 in commercial wind turbine generators with SCIGs, the synchronous speed in a 50Hz-grid is equal to 1500 or 1000 rpm.

The advantages of the SCIG are:

- well-known and robust technology, easy and relatively cheap mass production of the generator possible;

- no electrical connection between rotor and fixed system required: the mechanical power of the rotor is transferred to the stator by the magnetic field phenomena.

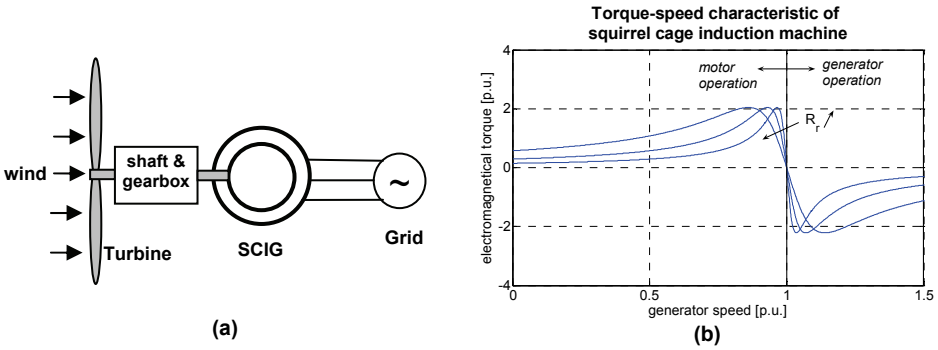

Figure 4.9. Grid connection scheme of squirrel cage induction generator (a) and torque speed characteristic (b)

The drawbacks of this generator type are multiple.

- The speed is not controllable and varies only over a very narrow range, having certain implications.

    - Wind speed fluctuations are directly translated into electromechanical torque variations, rather than rotational speed variations. This causes high mechanical and fatigue stresses on the system (turbine blades, gearbox and generator), and may result in swing oscillations between turbine and generator shaft. Also the periodical torque dips due to the tower shadow and shear effect are not damped by speed variations, and result in high flicker values. Fluctuations in power output are hardly damped, compared to wind speed fluctuations.

    - The turbine speed cannot be adjusted to the wind speed to optimise the aerodynamic efficiency. For every wind speed, there exists one turbine speed resulting in the highest C_p. This optimal speed cannot be continuously achieved with a squirrel cage induction generator. It must be mentioned however that many commercial wind turbines can switch between two pole-pair numbers, e.g. p_p= 2 or 3, by a rearrangement of the stator windings connection. This allows setting up one turbine speed for low wind speeds (p_p = 3 or higher) and one for high wind speeds (p_p = 2), but it does not provide continuous speed variation.

- A gearbox in the drive train is required: the generator speed is mostly around 1500 rpm or 1000 rpm. Common turbine speeds are 10 - 25 rpm, hence the need for a gearbox, mostly in three stages amongst which one planetary. Gearboxes represent a large mass in the nacelle, and also a large fraction of the investment costs. They are relatively maintenance intensive and are a possible source of failure.

- The machine always consumes reactive power, of which the value cannot be controlled. There is a fixed relation between reactive and active power. This makes it impossible to support grid voltage control. More general, it is hardly possible for an induction generator to provide any grid support. In most cases, capacitors are grid-connected parallel to the generator to compensate for the reactive power consumption.

Doubly-fed induction generator

General description

The connection scheme of a *doubly-fed induction generator* (DFIG) is shown in Figure 4.10. The stator is constructed in the same way as in the SCIG. The rotor is no longer a squirrel cage rotor, but equipped with a three phase winding, connected to the power system through a power electronic IGBT converter. The basic

operation principle is the same as for a squirrel cage generator: equation (4.9) still holds. However, P_R can be controlled now, by controlling the current flowing through the converter. Instead of dissipating the rotor energy, it can be fed into the grid.

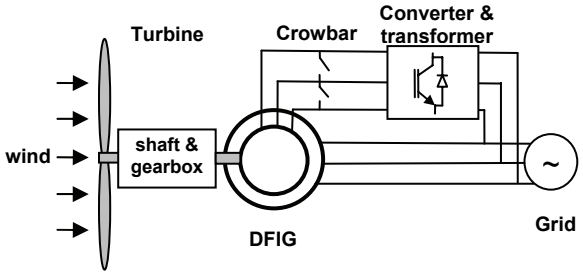

Figure 4.10. Connection scheme of a doubly-fed induction generator

Modern converters allow the rotor power P_R to flow in both directions, i.e. from grid to rotor and from rotor to grid. By controlling P_R and thus the slip s (4.9), the speed can be controlled above and below synchronous speed. Table 4.2 summarises the power flow directions for the various operation modes of the doubly-fed induction machine.

		motor operation (supplies mechanical torque)	generator operation (receives mechanical torque)
subsynchronous $n < n_s$; $s > 0$	P_S	*grid → stator*	*stator → grid*
	P_R	*rotor→ grid (or dissipation)*	*grid → rotor*
supersynchronous $n > n_s$; $s < 0$	P_S	*grid → stator*	*stator → grid*
	P_R	*grid → rotor*	*rotor → grid (or dissipation)*

Table 4.2. Power flow directions for various operation modes of doubly-fed induction machine

The choice for the rated power of the rotor converter $P_{conv,rated}$ is a trade-off between costs and speed range desired. The cost of power electronic converters increases fast with increasing rating. Mostly its rating is around 30% of the total generator rated power. The stator power P_S is – apart from the stator losses – equal to the air gap power P_δ. It follows from (4.9) that the range for s is then between -30% and 30%. The obtained range in which variable speed is possible is thus from 70% of the synchronous speed up to 130%.

The advantages of a DFIG are:

- the speed is variable within a sufficient range, with limited converter costs;

- the stator reactive power Q_S can be controlled by controlling the rotor currents with the converter. Furthermore, the grid-side of the rotor converter can control its reactive power $Q_{R,grid}$ independently of the generator operation. This allows the performance of voltage support towards the grid.

Some drawbacks are:

- a gearbox is still necessary in the drive train. The speed range for the generator is far from sufficient to obtain a generator speed of 10-25 rpm (common turbine speeds);

- the control of the rotor power by means of a grid-connected converter requires an electrical connection between a rotating and fixed system. Such a connection is given by carbon brushes (on the fixed system) pressing against slip rings (rotating system). These brushes require regular maintenance, are a potential cause of machine failure and increase the electrical losses.

- Also the power electronic converter is a fragile component: it is very sensitive to overcurrents. In case of a grid voltage dip, the stator and rotor currents may dramatically increase for a short time (~100 ms). To protect the converter from overcurrents, it is bypassed by a 'crowbar' (Figure 4.10), which is normally open. In case of rotor overcurrents, the rotor winding is short-circuited by closing the crowbar switch, resulting in the same behaviour as a SCIG for a short time. Normally, the crowbar switching is followed by the shut-down of the entire turbine. However, the high machine currents during the switching operations may cause high torque loads on the drive train.

- The dynamic behaviour of the installation in case of grid disturbances (especially in case of crowbar switching) is very complex. Detailed dynamic models and good knowledge of the machine parameters are required to make a correct estimate of occurring torques and speeds, and also of the impact of the machine behaviour on the grid. Dynamic modelling aspects will be discussed in Chapter 5.

The precursor of the DFIG is the OptiSlip generator, developed by Vestas [59]. This system is basically a single-fed induction generator, with the same characteristics as a SCIG, but with a power electronic device on the rotor that controls dynamically the rotor resistance R_R. This way, the most suitable torque-speed characteristic from Figure 4.9b can be chosen to obtain the optimal speed at the operating point. Only speeds higher than synchronous speed are possible for generator operation, and the rotor power is not fed back into the grid.

Closer view on the DFIG steady-state operating range

Equivalent circuit and steady-state machine equations

As illustrated above and following from (4.9), the basic rule of thumb is that if $P_{conv,rated} = k \cdot P_{S,rated}$, then the speed range is $(1 \pm k) \cdot n_s$. However, this does not take into account that also the stator reactive power output has its influence on the rotor electrical load. Furthermore, as the frequency converter (mostly consisting of IGBTs) is at least equally sensitive to too high values of currents as of power, considerations about the maximum rotor current and apparent power are of equal importance to determine the operating limits of a DFIG.

The equivalent circuit of a doubly-fed induction machine in steady-state operation is shown in Figure 4.11 [60]. Subscripts S and R refer to stator and rotor respectively, σ and M to leakage and mutual reactance. Iron losses are neglected, thus the only parallel element is X_M, the magnetising mutual reactance.

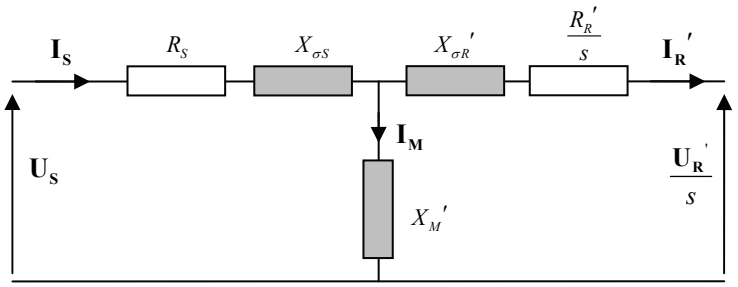

Figure 4.11. Equivalent scheme of doubly-fed induction machine

The rotor quantities are referred to the stator quantities. This means:

$$\mathbf{I_R}' = \frac{N_R}{N_S}\mathbf{I_R} \qquad (4.10) \qquad R_R' = \frac{N_S^2}{N_R^2}R_R \qquad (4.11)$$

$$\mathbf{U_R}' = \frac{N_S}{N_R}\mathbf{U_R} \qquad (4.12) \qquad X_{\sigma R}' = \frac{N_S^2}{N_R^2}X_{\sigma R} \qquad (4.13)$$

with

- N_S and N_R the number of stator windings and rotor windings respectively;
- $\mathbf{I_R}$, $\mathbf{U_R}$, R_R, $X_{\sigma R}$ the real phase-equivalent rotor quantities;
- $\mathbf{I_R}'$, $\mathbf{U_R}'$, R_R', $X_{\sigma R}'$ the rotor quantities referred to stator quantities.

From Figure 4.11, the following voltage equations are written:

$$\mathbf{U_S} = \left(R_S + j \cdot X_S\right) \cdot \mathbf{I_S} + j \cdot X_M \cdot \mathbf{I_R}' \tag{4.14}$$

$$\mathbf{U_R}' = \left(R_R' + j \cdot s \cdot X_R'\right) \cdot \mathbf{I_R}' + j \cdot s \cdot X_M \cdot \mathbf{I_S} \tag{4.15}$$

with $X_S = X_M + X_{\sigma S}$ and $X_R' = X_M + X_{\sigma R}'$ (4.16)

the total stator and rotor reactance respectively.

After some algebraic manipulations, $\mathbf{U_R}$' and $\mathbf{I_R}$' are written in terms of $\mathbf{U_S}$' and $\mathbf{I_S}$' [60]:

$$\mathbf{I_R}' = \frac{\mathbf{U_S} - \left(R_S + j \cdot X_S\right) \cdot \mathbf{I_S}}{j \cdot X_M} \tag{4.17}$$

$$\mathbf{U_R}' = \left(\frac{R_R' + j \cdot s \cdot X_R'}{j \cdot X_M}\right) \cdot \mathbf{U_S} - \left(\frac{\left(R_S + j \cdot X_S\right) \cdot \left(R_R' + j \cdot s \cdot X_R'\right) + s \cdot X_M^{\,2}}{j \cdot X_M}\right) \cdot \mathbf{I_S} \tag{4.18}$$

Equations (4.17) and (4.18) show the dependency of rotor current and voltage on stator quantities and machine parameters.

In the following considerations, the stator voltage $\mathbf{U_S}$ is assumed constant and equal to 1 p.u. The stator current $\mathbf{I_S}$ contains then two terms: the active (real) current $\mathbf{I_{S,a}}$ and the reactive (imaginary) $\mathbf{I_{S,r}}$, being numerically equal to respectively the stator active power P_S and reactive power Q_S.

The following plots examine the dependency of $|\mathbf{I_R}|$ and $|\mathbf{U_R}|$ as a function of the speed range, P_S and Q_S. As an example, the machine parameters of a 850 kW GAMESA wind turbine are used [61]:

P_{rated}	= 850 kW (i.e. $P_S + P_R$)	$\lvert\mathbf{U_{S,rated}}\rvert$	= 690 V
n_s	= 1500 rpm (p_p = 2)	$\lvert\mathbf{I_{S,rated}}\rvert$	= 670 A

The machine impedances are (in per unit notation):

R_S	= 0.027	$X_{\sigma S}$	= 0.125	X_M	= 11.403
R_R'	= 0.021	$X_{\sigma R}$'	= 0.204		

Rotor current

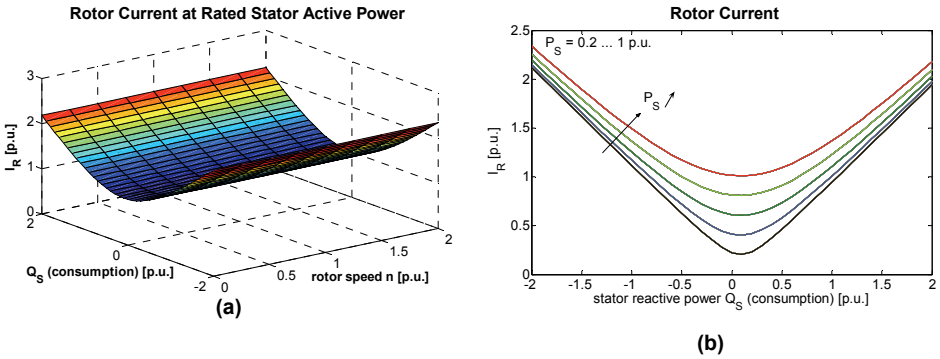

Figure 4.12. Rotor current as a function of speed and stator reactive power at rated stator active power (a), and as function of stator reactive power for various values of stator active power (b).

A main cost determining parameter for the rotor frequency converter is its rated current. The rotor current magnitude $|\mathbf{I_R}'|$ is therefore plotted as a function of speed and stator reactive power. This is shown in Figure 4.12a, for the case when $P_S = 1$ p.u. It is seen that the rotor current is independent of the rotor speed, as can also be derived from (4.17).

Figure 4.12b shows $|\mathbf{I_R}'|$ as a function of Q_S, for P_S varying from 0.2 p.u. to 1 p.u. The impact of P_S on $|\mathbf{I_R}'|$ is relatively high in the zone around $Q_S = 0$.

It is concluded that the maximum values of P_S and Q_S determine the rating of the rotor current. Limitations on the rotor current do not have impact on the speed range of the machine.

Rotor voltage

Figure 4.13a shows the rotor voltage magnitude $|\mathbf{U_R'}|$ as function of speed and Q_S for the case when $P_S = 1$ p.u.

It is seen that $|\mathbf{U_R}'|$ changes with speed and stator reactive power. This can be explained by (4.18): $\mathbf{U_R}'$ linearly depends on the slip s, and for constant slip values also on $\mathbf{I_S}$.

In Figure 4.13b the lines of equal $|\mathbf{U_R}'|$ are plotted for different values of P_S.

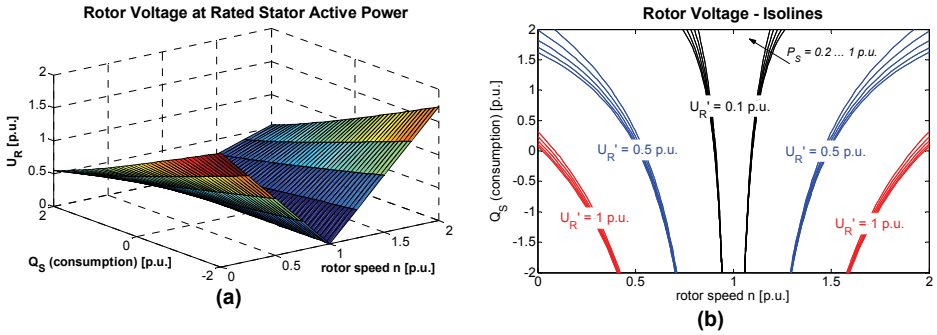

Figure 4.13. Rotor voltage as function of speed and stator reactive power (a), and rotor voltage - isolines as function of speed, stator active and reactive power (b).

It can be concluded that the dependency of the rotor voltage on both P_S and Q_S is low, compared to the dependency on the speed, especially near the synchronous speed. The exact coefficients can be derived from (4.18) and are function of the machine design (mainly the various reactances). For common machine designs such as the example used here, the rotor rated voltage for a DFIG is largely determined by the required speed range, and only slightly by the required stator active/reactive power range.

Rotor apparent power

The conclusions until now are:

- the maximum value for $|\mathbf{I_R'}|$ is the limiting factor for P_S and Q_S;
- the maximum value for $|\mathbf{U_R'}|$ is the limiting factor for the speed range

Both $\mathbf{I_R'}$ and $\mathbf{U_R'}$ are stator referred quantities, i.e. they depend on the effective stator-rotor winding ratio N_R/N_S. For the design of a specific machine, the winding ratio can be chosen in such a way that the working region is optimised as a function of power electronic converter costs.

The rotor apparent power $\mathbf{S_R}$, calculated as

$$\mathbf{S_R} = \mathbf{U_R}' \cdot \mathbf{I_R}'^{*} \quad [\text{p.u.}] \tag{4.19}$$

does however not depend on the winding ratio. Plots of $|\mathbf{S_R}|$ provide an indication for operating limits that cannot be crossed for any choice of N_R/N_S.

Figure 4.14a shows $|\mathbf{S_R}|$ as a function of speed and stator reactive power for the case when $P_S = 1$ p.u. Figure 4.14b shows the lines of equal $|\mathbf{S_R}|$ ($|\mathbf{S_R}| = 0.3$ p.u.) for different values of P_S. Those isolines define, as a function of rated value for $|\mathbf{S_R}|$, the contours of the range for combinations of n and Q_S.

It is seen that:

- in the capacitive region ($Q_S < 0$), the speed range is more limited than in the inductive; furthermore the dependency of the speed range on P_S decreases rapidly when moving further into the capacitive region;

- in the zone around $Q_S = 0$, the speed range becomes very broad for low values of P_S.

This last property is especially useful for wind turbines, where the aerodynamic efficiency at low wind speed (and thus low active power) is largely increased with reduced turbine speed.

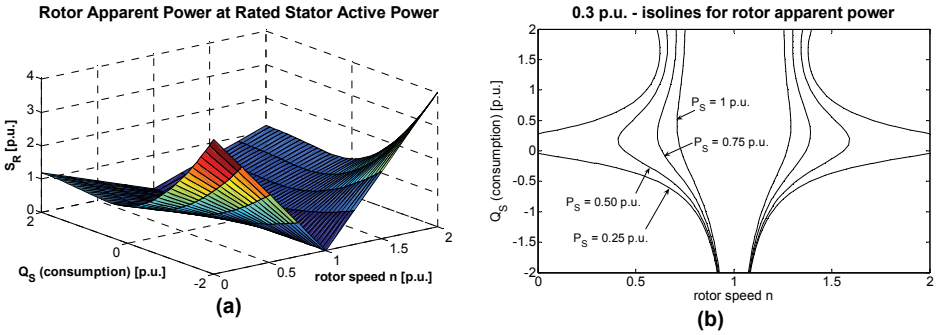

Figure 4.14. Rotor apparent power as function of speed and stator reactive power (a), and $|\mathbf{S_R}|$-isolines as function of speed and stator active and reactive power (b)

Figure 4.14b indicates that the isolines for $|\mathbf{S_R}|$ are approximately symmetrical around the synchronous speed n_s. A given range around n_s puts the same demands on the rating of the rotor converter for subsynchronous and supersynchronous operation.

An alternative way to present the results from Figure 4.14 is given in Figure 4.15: for rotor speeds, ranging from 10% to 50% above or below n_s, and for a given value of rotor apparent power ($|\mathbf{S_R}| = 0.3$ p.u.), all possible combinations of stator active and reactive power are plotted. The resulting lines are the contours of the zone of stator active and reactive powers feasible for a given rotor converter rating and speed range. As the isolines in Figure 4.14b are approximately symmetrical around n_s, the speed range isolines in Figure 4.15 are equally valid for deviations above or below n_s.

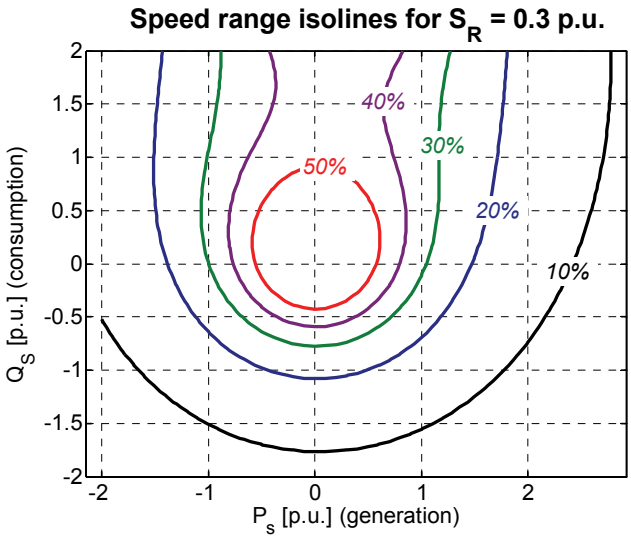

Figure 4.15. Stator active and reactive power ranges for given speed ranges and rotor converter apparent power

Note that in Figure 4.15, the 30%-isoline contains the points with (P_S, Q_S) approximately equal to (1,0) and (-1,0). Bearing in mind that the assumed rotor apparent power S_R is 0.3 p.u. in Figure 4.15, this confirms the well-known rule of thumb, that if $P_R = k \cdot P_{S,rated}$, the speed range is $(1 \pm k) \cdot n_s$. It appears however that this rule of thumb assumes that no reactive power is exchanged between stator and grid.

Concluding, the rule of thumb is now extended in two ways:

- $|\mathbf{S_R}|$ rather than P_R is taken into account;
- considerations about the speed range are extended towards the combined range of speed, stator active and stator reactive power.

The following conclusions are drawn:

- high deviations from the synchronous speed are possible for low values of P_S. (e.g. the 50%-line in Figure 4.15). This is especially useful for wind turbines where low wind speeds require low turbine speeds, far under the synchronous speed, for optimal aerodynamic efficiency;
- supplying high values of capacitive power puts more limits on the speed range than inductive, as can be seen in the asymmetry along the Q_S-axis in Figure 4.14 and Figure 4.15. This is explained by the fact that DFIGs, as SCIGs, are inductive by nature. In most grids, capacitive power is most needed at moments of high electrical load, as illustrated e.g. in Table 3.6. In these cases, the DFIG may be confronted with its limits.

Obviously, other limits than those in Figure 4.15 are to be taken into account for the operating region of a DFIG. Those aspects are however not typical for DFIGs, but valid for every turbine or generator:

- mechanical loading on the rotor bearings and blades limit the maximum torque and thus active power;
- centrifugal forces on the rotor limit the maximal speed;
- rated stator currents limit the stator active and reactive power.

Finally, it must be noted that the discussion above only concerned the stator active and reactive power. The rotor converter is in most cases also able to control its grid-side reactive power output within a given range. The converter may thus act as a Static Var Compensator (SVC). The grid-side reactive current in the converter is independent of the generator behaviour, and was not further investigated here.

Synchronous generator (direct drive)

General description

Like the SCIG and the DFIG, the synchronous generator (SG) is also equipped with a three-phase winding on the stator. For the rotor, there are two main possibilities:

- a rotor winding supplied by a DC current from a separate circuit;
- permanent magnets attached to the rotor.

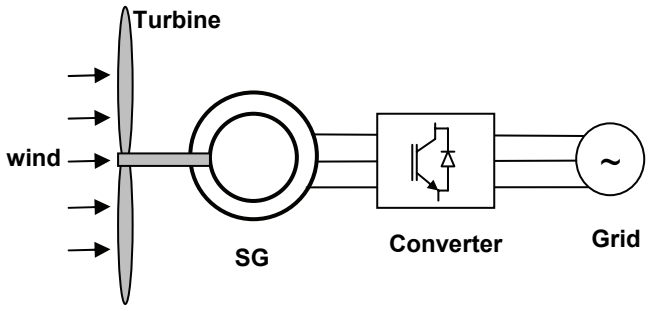

Figure 4.16. Grid connection scheme for a wind turbine with synchronous generator (direct drive)

The grid connection is shown in Figure 4.16. All power of the generator is processed through a power electronic converter, the interface between generator and grid. At the generator side of the converter, amplitude and frequency of the voltage can be fully controlled by the converter, independently of the grid characteristics. The

generator speed is fully controllable over a wide range, even to very low speeds. The gearbox can thus be omitted. The generator is directly driven by the turbine, hence the denomination ‘direct drive’.

The advantages are:

- a gearbox is no longer required: this is advantageous because this component normally has a non-negligible manufacturing cost, generates some acoustic noise, requires regular maintenance (lubrication) and is also a potential cause of mechanical failure;

- the converter permits very flexible control of the entire system: speed, active and reactive power can be fully controlled in case of normal and disturbed grid conditions. In highly disturbed grid conditions, the generator still has to be disconnected for safety reasons.

The main drawbacks are:

- the converter costs are considerable, as it has to process all the generator power: this requires more expensive power electronic components, needing intensive cooling;

- the generator needs a specific design: compared to normal electrical machines, it has to supply high electrical torques at low speeds. This is discussed below.

Design options

As stated above, the generator for direct drive wind turbines has to supply high electrical torques at low speeds. This requires a design that is fundamentally different from classical generator designs. Direct drive generators typically have a large rotor diameter (nearly 12 m for the Enercon E-112 direct drive 4.5 MW turbine [62]).

The electrically excited synchronous generator leaves most opportunities for control of the flux, thus allowing loss minimalisation in different power ranges. Furthermore, it does not require the use of permanent magnets, which would represent a large fraction of the generator costs, and might quickly suffer from performance loss in harsh atmospheric conditions. Therefore, it is the most used generator type by the manufacturers of large direct-drive wind turbines.

The permanent-magnet synchronous generator however allows a more compact design, which makes the use of generators with smaller diameters and smaller mass possible. Studies of design options for permanent magnet synchronous generators, specifically for wind turbines, are done in [63]-[69]. An overview of the most promising design options is given in Figure 4.17.

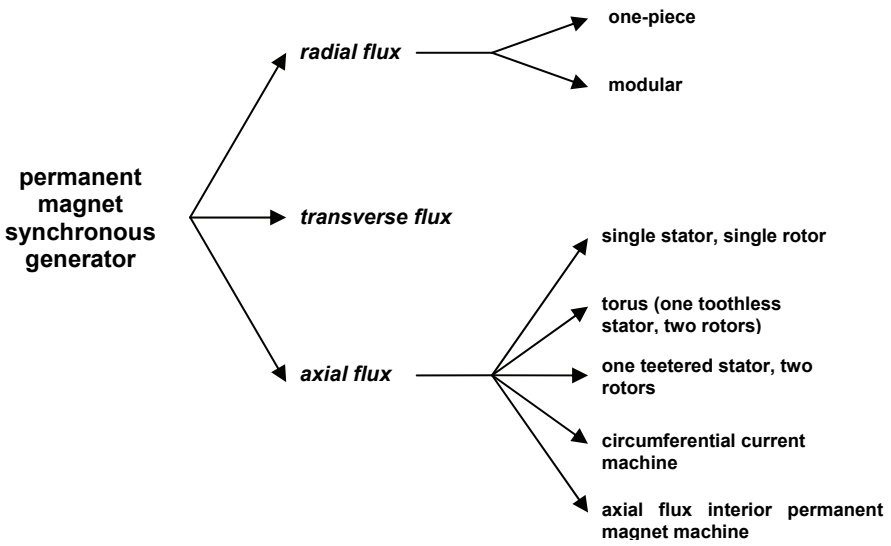

Figure 4.17. Design options for permanent magnets synchronous generators

Quantitative comparisons between the performances of all generator designs are difficult, as many numeric results for torque density found in literature are only calculated results from finite element software, rather than experimental data. Only as an indication, it is mentioned here that for a generator diameter of 2.5 m the highest torque density per generator volume unity has been estimated at 75 kNm/m³ for transverse flux machines, and 40 kNm/m³ for torus and radial flux designs [64]. Torque densities generally increase with increasing generator diameter, up to 100 kNm/m³ for a torus with 4.5 m diameter [64].

For comparison, the torque density for the Enercon E-112 generator (electrically excited, 12 m diameter) is estimated at 30 kNm/m³, given the rated speed of 13 rpm, a rated power of 4.5 MW, and generator diameter and length respectively equal to 12 m and approximately 1 m.

The permanent magnet synchronous generators thus offer a high potential increase in torque density, and are thus a promising technology for future turbines. However, the commercial applications for large turbines are nowadays very limited. The following barriers for commercial development of these generator types can be identified:

- relatively new and unknown technology for applications in the MW-range;
- difficult assembly of the generator;
- high material costs of the magnets;
- low material reliability in harsh atmospheric conditions (offshore);
- need for very specific power electronic interface for the grid connection.

Other generator types

Many other generator types or turbine designs are mentioned in literature. Among them are:

- SCIG with full power electronic grid interface;
- SG with gearbox (optionally reduced to one stage);
- linear induction generator ([69]);
- switched reluctance generator ([70], [71]);
- brushless doubly-fed induction generator ([72] - [78]).

Amongst them, the *brushless doubly-fed induction generator* (BDFIG) is the most innovative type. It has two separate three-phase windings on the stator, amongst which one directly grid-connected and one through a power electronic interface, and a double-cage rotor. The machine has the same properties as a DFIG concerning speed range and reactive power range, with the additional advantage not to have electrical connections between the fixed and rotating system. However the machine operation principle and its assembly are very complex. Also, to the author's knowledge, experiences with the DFIG have shown that the slip rings and brushes are not the most critical components of the generator. Technical solutions to avoid them are thus not a prior concern of manufacturers. Therefore, the BDFIG is not likely to be a commercial success within the years to come.

Manufacturers and generator types

Manufacturer	Worldwide market share (2002 [%]	Power range for given generator type [MW]		
		SCIG	DFIG	SG (direct drive)
Vestas	22.2		0.85 – 4.5	
Enercon	18.5			0.3 – 4.5
NEG-Micon (now Vestas)	14.3	0.75 – 1.65	2.75 – 4.2	
Gamesa (now Vestas)	11.8		0.66 – 2	
GE Wind	8.8		1.5 – 3.6	
Bonus (now Siemens)	7	0.6 – 2.3		
Nordex	7	0.6 – 1.3	1.5 – 2.5	

Table 4.3. Wind turbine manufacturers and their generator types

Table 4.3 gives a brief overview of the recent designs of the most important manufacturers of large turbines. For the three main generator types (SCIG, DFIG, SG-direct drive), the power range in which the manufacturers offer products, is given. The manufacturers are sorted according to the fraction of worldwide sold capacity in 2002 [79].

Apart from these manufacturers, Jeumont is mentioned as the only manufacturer of large turbines (up to 1.5 MW) using a discoidal, axial flux synchronous machine with permanent magnets [80].

From Table 4.3 it is concluded that the DFIG is the by far most used generator for turbines in the MW-range. This generator type will be extensively discussed in Chapter 5, dealing with dynamic modelling aspects of turbines and generators for use in power system simulations.

4.4. Value of wind power

Quantifying the value of wind power in a power system is subject to many discussions. An extensive discussion includes concerns about active power generation and its forecasting and probability distribution, reactive power control and other ancillary services, power market mechanisms, the possible need for grid investments and the assignment of investments towards TSOs and wind farm operators. This paragraph gives an overview of definitions for wind power value with regard to its active power generation, making abstraction of power market mechanisms that could possibly influence wind power generation in case of high penetration ratio.

Concerning the active power of wind power in a power system, one quantity that indicates the value of a wind turbine or aggregated wind park is the *capacity factor*:

$$\textit{capacity factor [\%]} = \frac{\textit{produced energy in one year [MWh]}}{\textit{rated power [MW]} \times \textit{8760 [h]}} \tag{4.20}$$

This quantity gives information about the annual energy delivery, and is thus an important parameter for the owners of wind power installations paid for the amount of energy supplied. Estimates for Belgium are between 31% (offshore) and 20% (onshore), which corresponds with 2716 to 1752 equivalent full-load hours per year. This will be further detailed in Chapter 6.

The knowledge of the capacity factor is however insufficient from the point of view of a power system operator, whose prior concern includes maintaining the stability of the system and the instantaneous power balance. The fluctuating nature of wind

power may jeopardise this power balance. Also a power trader cannot accurately estimate the value of wind power using the capacity factor only.

Intuitively, it is understood that both the economical and ecological value of wind power are not quantified by its total energy delivery as such, but rather by the amount of conventional generation capacity that can be replaced by wind power.

Therefore, a more correct valuation of wind power uses the term '*capacity credit*', defined through the following steps ([81] - [84]):

> *The **reliable capacity** is the amount of installed capacity in a power system available with a given reliability to cover the system load.*
>
> *The **loss of load probability (LOLP)** is the probability that the system load exceeds the reliable capacity.*
>
> *The **capacity credit** of wind power is the amount of installed conventional power generation capacity that can be replaced by wind power generators, without an increase of the LOLP.*

The capacity credit of a single wind turbine is virtually zero, as, due to the intermittent and relatively unpredictable nature of instantaneous wind speeds, one wind turbine cannot replace an amount of controllable conventional power generation without increasing the LOLP.

The capacity credit of wind power depends on the extent of the considered zone in which the aggregated wind power is evaluated. To the author's opinion, evaluation of capacity credit of wind power makes most sense when considering the aggregated wind power within an entire power control zone (e.g. Belgium), or within a zone that has limited power exchange capability with other zones because of transmission bottlenecks.

The correlation between wind speeds at different sites must be low to obtain a high aggregated capacity credit. Furthermore the capacity credit also depends on the actual LOLP, which on its turn depends on the reliability of the conventional power plants and on the load uncertainty.

The following definitions are given.

> *The **surplus capacity** is the difference between reliable capacity and maximal demand in a power system.*
>
> *The **increase in surplus capacity** due to wind power is the difference between surplus capacity of the total power system and the surplus capacity of the power system minus wind power.*

The value of the aggregated wind park in a control zone may thus be given by:

- the capacity credit of the aggregated wind park;
- the amount of installed conventional power that would realise the same decrease of the LOLP as the aggregated wind park does;
- the increase of surplus capacity by the aggregated wind park;
- the amount of installed conventional power that would allow a same increase of the load as the aggregated wind park does, given the maximal LOLP.

In [84], the value of wind power was calculated for a small network according to the definitions above. Capacity credit of wind power was rated to above 45% of installed wind power for very low wind power penetration, decreasing to 20% for a wind power penetration of 35% of installed power. These values seem very high, partially explained by the relatively low reliability assumed for the conventional power plants in the grid.

The capacity credit of the aggregated wind power in Belgium is calculated in Chapter 6. However, it is already mentioned here that, to the author's point of view, the definitions related with capacity credit take insufficiently the time dependency of both the LOLP and the wind power generation into account. Most implementations of the definitions above use static probability distribution functions, and do not sufficiently take the aspect of fluctuation into account.

The LOLP is mostly given in a percentage or as a given number of hours per year (also called the '*loss of load expectation*' or *LOLE*). However, the LOLP in fact depends on:

- the instantaneous load level and its uncertainty;
- the power plant types actual in operation and their reliability;
- the actual level of wind power generation (regardless of the amount of wind power installed), relevant for determining the probability distribution for wind power injection in the next time sample, as discussed in Chapter 6.

Taking the time dependency into account, the definition of *capacity credit* is not considered sufficient anymore. Especially the word '*replaced*' calls for further elaboration. Estimates of capacity credit will dramatically diverge, depending whether the estimated investments on constructing new power plants that can be totally avoided due to replacement by wind power are considered, or whether the amount of power plants that must be in operation (either producing active power or providing primary and secondary reserves) at the considered moment can be decreased due to replacement by wind power. For the last interpretation, knowledge is needed about:

- the instantaneous power system load and generation, the load uncertainty and the actual power plants in operation;

- the instantaneous wind power generation;

- the season and time of day, as it is an input parameter for the estimated probability of load and wind power production;

- the sample time length considered: for how many consecutive hours can wind power replace instantaneously operating power plants?

An attempt to estimate the value of wind power, with regard to the considerations above, is done in Chapter 6.

An alternative valuation of wind power can be done by estimating the avoided CO_2-emission by all power plants in a control zone, thanks to wind power. An estimation of the avoided CO_2-emission requires good knowledge of the expected wind power generation, as well as the characteristics of the available power plants and their CO_2-emission in steady regime and starting/stopping regime. This is further elaborated in Chapter 6.

4.5. Conclusions

After Chapter 2 described the state of the art concerning the organisation of power systems, and the political drives, and Chapter 3 described technical aspects of distributed generation with special focus on the point of view of power system operators, Chapter 4 treats the technical aspects of wind power, including a review of the characteristics of wind speed characteristics, wind turbines and their generators, and the wind power capacity credit. Although this chapter has already presented some own considerations from the author, it is the last chapter in this thesis that is dedicated to the review of state-of-the-art.

The following two chapters build on the reviews from the previous chapters.

Chapter 5 focuses on the dynamic modelling of wind turbine generators, starting from the equations that describe the physical generator operation, and then further simplifying towards more abstract but numerically simpler models. By means of dynamic simulations of typical grid events, Chapter 5 elaborates the considerations from Chapter 3 concerning ride-through behaviour and voltage control.

Chapter 6 treats the statistical modelling of wind power time series with hourly resolution, for the specific case of Belgium. The results in Chapter 6 allow further

elaborating the considerations about wind power value and capacity credit mentioned in this chapter.

Chapter 5

Dynamic modelling of wind power generators

5.1. Introduction

This chapter presents the development of a model of a wind turbine generator, to be used for dynamic simulations of power systems with dedicated software. The dynamic modelling of wind turbines has been the subject of much research. The importance of the dynamic behaviour of wind turbines, during normal and abnormal grid conditions, was illustrated in Chapter 3. Especially the capability of supplying voltage control and remaining connected during (or 'riding through') grid disturbances is an important criterion for the value of distributed generation in general and wind power in particular. Rather than performing expensive experiments to test the turbine behaviour at various events, the accurate simulation of these events is preferred.

In the first part of this chapter, a detailed model of a wind turbine generator is developed. The model components correspond with real elements: turbine propeller, gearbox, generator, power electronic components and various control modules are modelled corresponding with how they behave in reality. The result is a rather complicated detailed turbine model which can be used for the accurate simulation of individual events. Simulation examples of wind speed changes and grid disturbances due to switching transients and grid faults are included in this chapter.

In the next part, a simplified generic dynamic turbine model is developed, based on the frequency response characteristic of the detailed model. It aims at alleviating the programming and computational effort, while maintaining a satisfying accuracy to correctly estimate the impact of wind turbines in the overall power system. Simulation results for the same events as simulated with the detailed turbine model suggest that the simplified model can be used for estimating the impact of wind speed changes and 'light' transients, i.e. transients due to switching events etc. For the simulation of 'heavy' transients, i.e. transients due to grid faults relatively close to the turbine, the simplified model may neglect too many aspects of the turbine behaviour to provide reliable results.

5.2. Detailed dynamic wind turbine model

5.2.1. General description

Detailed models for wind turbines for power system simulations are described, amongst others, in [85]-[92]: two recent PhD-theses are almost entirely focused on the subject ([85]-[86]); [87] focuses on turbines with squirrel-cage induction generators, while [58] and [88]-[91] treat doubly-fed induction generators and [92] synchronous generators.

Wind turbine models generally consist of the following elements, which can all be elaborated with a high or low level of detail:

- *Wind speed model*: mostly a time series of measured or well-chosen wind speed values. However, wind speeds can also be generated by a stochastic model, based on a power spectral density function. Also methods based on Markov chains or wavelet decomposition are used to generate wind speed time series of various time resolutions [93].

- *Aerodynamic model of the turbine propeller*: mostly an approximate equation for the coefficient of performance C_p, as a function of wind speed, propeller speed and propeller design. For more detailed models, the Blade Element Method (BEM) can be used.

- *Model for the shaft coupling and gearbox*: mostly modelled as a torsional spring between two rotating inertias (propeller and generator). The equivalent spring stiffness is relatively low [87]. This may result in large torsional vibrations between propeller and generator, considerably affecting the electrical and mechanical behaviour.

- *Generator model,* containing the voltage differential equations and flux equations, mostly in a rotor- or stator-flux oriented *(d,q)*-reference frame, as well as the torque and motion equation.

- *Models for the power electronic circuits*, mostly simplified to some extent for the simulation of the entire power system, due to the much smaller time scales for transients in power electronic devices.

- *Controller models*, including pitch control, speed control, generator active and reactive power and current control and maximum power tracker

- *Protective relays*: for switching off the turbine after a given duration of a given over- or undervoltage or –frequency.

- *Grid model*: for assessment of the wind turbine behaviour alone, it is sufficient to model the grid as a voltage source with given short-circuit power. When the impact of the turbine on the grid is to be investigated as well, the existing power lines need to be represented in the grid model, using dedicated power system simulation tools.

5.2.2. Turbine block model components

Model overview

Figure 5.1 shows the global model of a pitch-controlled wind turbine with doubly-fed induction generator. This turbine type will be used as a basis for the detailed model, as it contains the most features. Other turbine types (for instance stall controlled turbines or turbines with squirrel cage induction generators) are easily obtained from it, by simplifying part of the model.

The figure shows all model components with their inputs and outputs. The inputs of the global model are grid voltage, wind speed and reference reactive power. They are given by the user or calculated by other models (e.g. the grid voltage is calculated from the grid model by the power system simulation software). The output of the model is the machine total current from both rotor and stator, referring to the reference frame used for the rest of the grid in the power system simulation software.

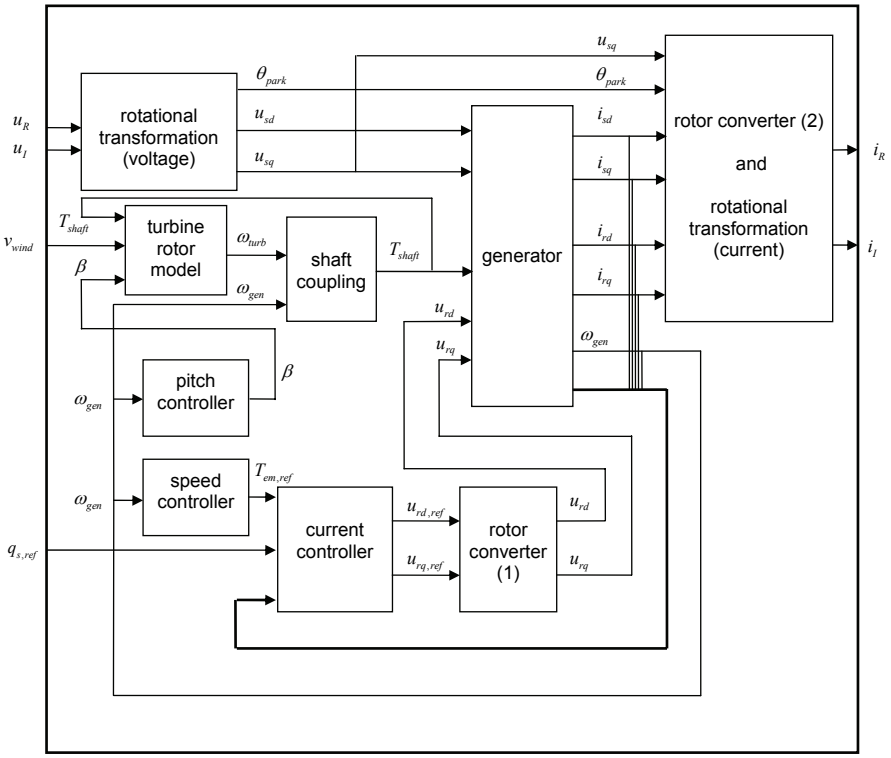

Figure 5.1. Turbine model overview

Turbine propeller model

The aerodynamic model calculates the mechanical propeller torque from the wind speed. It consists of the equations from paragraph 4.3.1. In this work, the numerical approximate expression for C_p from (4.7) and (4.8) is used. The mechanical propeller torque is then calculated as:

$$T_{turb} = \frac{1}{2}\pi R_{turb}{}^3 \rho_{air} v_{wind}{}^2 \frac{C_p}{\lambda} \tag{5.1}$$

The motion equation for the propeller is:

$$\frac{d}{dt}\omega_{turb} = \frac{1}{2H_{turb}}\left(T_{turb} - T_{shaft}\right) \tag{5.2}$$

with H_{turb} [s] the propeller inertia constant, i.e. the normalised propeller inertia, calculated as the stored energy at rated speed divided by the rated power [30]. An

example of how H_{turb} is calculated from the propeller inertia J_{turb} is given in Appendix II.

The aerodynamic model of the propeller is shown in Figure 5.2.

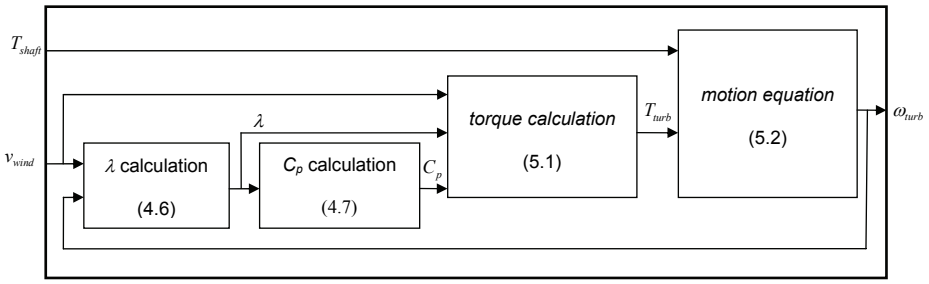

Figure 5.2. Turbine propeller model

The tower effect can be taken into account by assuming a periodical dip in the wind speed of 20%, three times per propeller revolution (for 3-bladed propeller).

Shaft coupling and gearbox

The combination shaft-gearbox can be regarded as a torsional spring, with a relatively low stiffness compared to shafts in thermal power plants. This is due to the relatively long shaft between driver and generator in wind turbines. K_{shaft} is typically in the range of 0.15 – 0.40 p.u. for wind turbines, while K_{shaft} is in the range of 20-80 p.u. for conventional power plants with synchronous generators [87]. An example of how the normalised K_{shaft} is calculated from the real shaft stiffness in Nm/rad, either at the low speed or high speed side of the gearbox, is given in Appendix II.

Also a damping torque, proportional to the difference between generator and propeller speed is taken into account, with a damping constant C_{shaft}.

The model equations thus are:

$$T_{shaft} = K_{shaft} \cdot \left(\theta_{turb} - \theta_{gen}\right) + C_{shaft} \cdot \left(\omega_{turb} - \omega_{gen}\right) \tag{5.3}$$

in which $$\theta_{turb} - \theta_{gen} = \int \left(\omega_{turb} - \omega_{gen}\right) dt \tag{5.4}$$

with

- T_{shaft} the mechanical torque transferred by the coupling from turbine propeller to generator;
- θ_{turb} angular position of the propeller;
- θ_{gen} angular position of the generator;
- θ_{turb} - θ_{gen} the torsion on the coupling between propeller and generator (i.e. the shaft and gearbox);
- ω_{turb} and ω_{gen} the rotational speed of respectively propeller and generator;
- K_{shaft} the stiffness of the assumed elastic coupling between propeller and generator;
- C_{shaft} the damping coefficient of the same coupling.

The shaft and gearbox block model is shown in Figure 5.3.

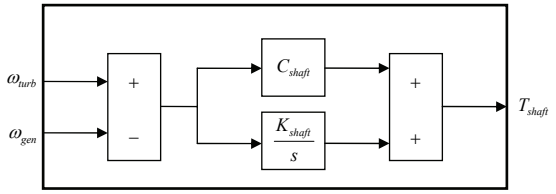

Figure 5.3. Turbine shaft and gearbox model

For constant speed wind turbines (equipped with squirrel cage induction generators), the shaft is about the only flexible element to absorb the torque fluctuations due to wind speed or grid voltage fluctuations. Therefore, it is recommended to include a model of a flexible shaft in the wind turbine model. For variable speed turbines, the torque oscillations are to a large extent absorbed by speed variations of the propeller and generator, and the shaft torsion is less relevant. In that case, the shaft model may be omitted as a first approximation. However, even for a variable speed turbine, the relatively low shaft stiffness is not negligible in case of short-circuits or other events causing severe transients.

Rotational transformation

Choice of reference frame

Before the voltage, given by the grid model, is applied to the generator model, it is first transformed to a reference frame more easily to use in the generator model.

The power system simulation software EUROSTAG uses an orthogonal *(R,I)*-reference frame for voltage and current phasors for the entire simulated power system. This means that three-phase voltages and currents are transformed to phasors, by the 3-to-2 power-invariant transformation [95]. It is hereby assumed that voltages and currents do not contain homopolar components, implying that the generator must be Y-connected without neutral conductor. The choice of the *(R,I)*

reference frame is done by the power system simulation software and is somewhat arbitrary.

Before applying this voltage as input to the generator model, it is first transformed to a *(d,q)*-reference frame (Figure 5.4) related to the generator itself, allowing easy algebraic manipulation and alleviating computational efforts. The transformation equations are, e.g. for the stator voltage $\mathbf{u_s}$:

$$u_{sd} = u_{sR} \cdot \cos\theta_{park} + u_{sI} \cdot \sin\theta_{park} \tag{5.5}$$

$$u_{sq} = -u_{sR} \cdot \sin\theta_{park} + u_{sI} \cdot \cos\theta_{park} \tag{5.6}$$

with θ_{park} Park's angle, i.e. the angle of the rotational transformation.

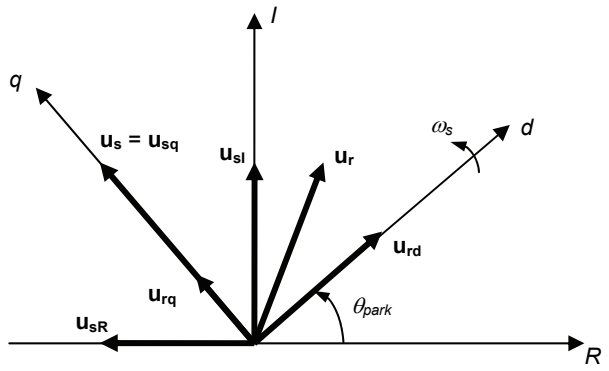

Figure 5.4. Stator and rotor voltage vector, and *(d,q)*-frame orientation

The often used approach when modelling an induction machine for drive applications is to align the *d*-axis with the rotor flux. This allows optimal decoupling between the *d*- and *q*-current control schemes, an important feature for high-performance speed controlled drives [95]. A better approach for the particular case of DFIGs is to align the *(d,q)*-frame with the stator voltage (Figure 5.4). This implies that u_{sd} = 0 and u_{sq} = $|\mathbf{u_s}|$. The rotor voltage is referred to the same frame, and consists in general of two non-zero *(d,q)*-components.

This is a particularly useful approach for doubly fed machines. The control is done by means of the rotor voltage. The stator voltage is the grid voltage, and can be regarded as a 'disturbance factor'. In stable grid conditions, the grid voltage is constant. As a result, with the chosen orientation the disturbance factor is zero in the *d*-axis and a DC-quantity in the *q*-axis. Another advantage of the chosen *(d,q)*-frame orientation is that the expressions for the instantaneous stator active power p_s and reactive power q_s become very simple:

$$p_s = u_{sq} \cdot i_{sq} \quad and \quad q_s = u_{sq} \cdot i_{sd} \tag{5.7}$$

The chosen reference framework is the most easy to control active and reactive stator power independently.

It must be mentioned that some authors already noticed the importance of an appropriate choice for the reference frame. The use of the stator-flux oriented frame has also been suggested for a doubly fed machine (i.e. $\psi_{sq} = 0$) [96]. If flux transients and stator resistance are neglected, this is exactly the same frame as used here, as can be seen in the equations (5.9) and (5.10) below.

When the reference frame is aligned with the stator voltage, θ_{park} is directly calculated from the input phasor (u_{sR}, u_{sI}) (Figure 5.4):

$$\theta_{park} = \arctan \frac{-u_{sR}}{u_{sI}} \tag{5.8}$$

The transformation angle θ_{park} is thus also calculated from the voltage phasor *(u_{sR}, u_{sI})*. This is in contrast with the cases where the reference frame is aligned with the machine flux, e.g. the rotor flux, and where θ_{park} must be calculated from a flux model, which can be regarded as a reverse motor model.

The block model of the rotational transformation of the voltage phasor is thus straightforward (Figure 5.5):

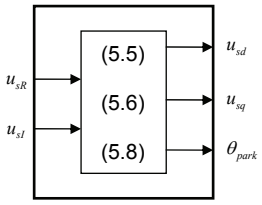

Figure 5.5. Rotational transformation, block model

Generator Model

As mentioned in paragraph 4.3.3, the generators most used by wind turbines are the squirrel cage induction generator (SCIG), the doubly-fed induction generator (DFIG) and the synchronous generator (SG). The most complex generator type, with regard to modelling aspects, is the DFIG. Its modelling is elaborated below. This model can easily be adapted towards a SCIG-or SG-model, as discussed below.

Stator and rotor voltage equations

For the stator and rotor voltage equations, the following assumptions are made:

- iron losses are neglected;
- saturation is neglected;
- homopolar voltage and current components do not exist; this implies that the generator is Y-connected without neutral conductor;

The equations are the following [94].

$$u_{sd} = r_s \cdot i_{sd} - \omega_s \cdot \psi_{sq} + \frac{1}{\omega_b} \cdot \frac{d}{dt} \psi_{sd} \tag{5.9}$$

$$u_{sq} = r_s \cdot i_{sq} + \omega_s \cdot \psi_{sd} + \frac{1}{\omega_b} \cdot \frac{d}{dt} \psi_{sq} \tag{5.10}$$

$$u_{rd} = r_r \cdot i_{rd} - \left(\omega_s - \omega_{gen}\right) \cdot \psi_{rq} + \frac{1}{\omega_b} \cdot \frac{d}{dt} \psi_{rd} \tag{5.11}$$

$$u_{rq} = r_r \cdot i_{rq} + \left(\omega_s - \omega_{gen}\right) \cdot \psi_{rd} + \frac{1}{\omega_b} \cdot \frac{d}{dt} \psi_{rq} \tag{5.12}$$

with ψ_{sd} and ψ_{rd} the stator and rotor flux component along the d-axis, respectively

$$\psi_{sd} = x_{sd} \cdot i_{sd} + x_{md} \cdot i_{rd} \quad \text{and} \quad \psi_{rd} = x_{rd} \cdot i_{rd} + x_{md} \cdot i_{sd} \tag{5.13}$$

and analogously for the q-component, with all *r*- and *x*-quantities equal to stator or rotor resistance and reactance in *d*- or *q*-orientation, indicated by the subscript.

ω_b is a constant, equal to the base frequency, which has been chosen equal to the rated grid frequency: $2\pi \cdot 50$ rad/s.

ω_s is the rotational speed of the *(d,q)*-reference frame, normalised with ω_b. ω_{gen} is the mechanical speed of the generator [p.u.].

Generator torque and motion equation

The equation for the electromechanical torque T_{em} is:

$$T_{em} = i_{sq} \cdot \psi_{sd} - i_{sd} \cdot \psi_{sq} \tag{5.14}$$

Several expressions for the torque in terms of stator and/or rotor fluxes and/or currents can be written. It is a complication caused by the choice of the reference frame that the torque equation always consists of two non-zero terms.

The mechanical motion equation is (motor sign convention):

$$\frac{d}{dt}\omega_{gen} = \frac{1}{2H_{gen}}\left(T_{em} - T_{shaft}\right) \tag{5.15}$$

with T_{em} and T_{shaft} the electromechanical torque and shaft torque respectively, and H_{gen} equal to the generator inertia constant.

Speed Controller

A block model of the speed control is shown in Figure 5.6. Inputs are v_{wind} and ω_{gen}, and output is $T_{ref,em}$, i.e. the reference value for the generator electromechanical torque.

From the expressions for C_p follows that there is an optimal λ (λ_{opt} is equal to 6.3 when using the approximate equation (4.7) and (4.8)) and thus an optimal $\Omega_{turb,opt}$ for a given wind speed, resulting in the highest aerodynamic efficiency. This $\Omega_{turb,opt}$ is calculated and normalised by $\Omega_{turb,base}$, and then used as a reference value for ω_{turb}, the normalised turbine propeller speed, being equal to ω_{gen} apart from the transient torsional oscillations between generator and propeller. It is also taken into account that $\omega_{gen,ref}$ is limited between a minimal and maximal value $\omega_{gen,min}$ and $\omega_{gen,max}$, corresponding to the speed range of the propeller, depending of the machine parameters, e.g. between 0.7 and 1.2 p.u. for a turbine with DFIG.

The actual speed control is then performed by a PI-controller with anti-windup. The output of the PI-speed controller is the reference electromechanical torque $T_{em,ref}$. The anti-windup block sets the input of the integrator in the PI-controller on inactive as long as the output of the PI-controller PI_{out} is out of the valid range for $T_{em,ref}$. The valid range for $T_{em,ref}$ is determined by the maximal electrical currents and the mechanical design, and is for instance equal to [-1 p.u. ; 1 p.u.].

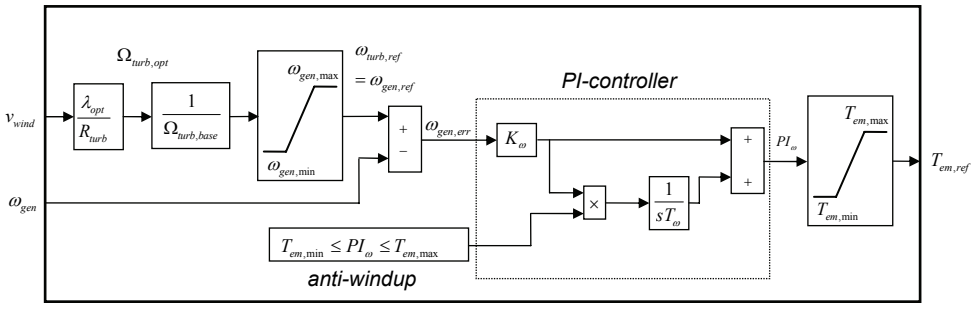

Figure 5.6. Turbine propeller speed control

Pitch control

A block model of the pitch control is shown in Figure 5.7. The model inputs are the actual propeller (or generator) speed and maximal (i.e. rated) propeller speed. The pitch controller tries to control the propeller speed at its maximal value using a PI-controller with anti-windup. Furthermore, a rate limiter is included, taking into account the limited speed of the pitch drive motors.

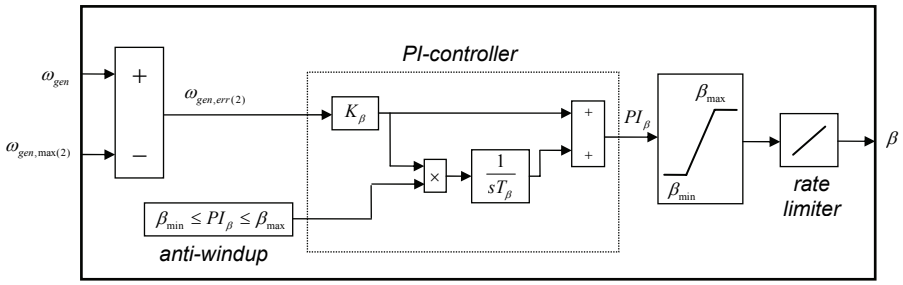

Figure 5.7. Turbine pitch controller

For low wind speeds, the propeller speed is controlled by the speed controller at a speed lower than the maximal speed. As ω_{gen} is smaller than $\omega_{gen,max(2)}$, and $\omega_{gen,err(2)}$ is negative in Figure 5.7, the pitch controller sets $\beta = 0°$ and is then inactive, due to the anti-windup, even if $\omega_{gen,err(2)}$ in Figure 5.7 remains non-zero. This model simulates the real behaviour of a pitch controller: it only becomes active at wind speeds above rated value.

In order to avoid oscillating interference between speed and pitch controller, the value for $\omega_{gen,max(2)}$ in Figure 5.7 must be slightly higher than $\omega_{gen,max}$ in Figure 5.6 (e.g. around 1% difference). Then speed and pitch controller are perfectly decoupled.

Current control

The reference values for the stator and rotor current are calculated from the reference reactive power and electromechanical torque respectively.

For a doubly-fed, grid-connected induction generator (Figure 4.10), the reactive power exchange with the grid can be controlled in two ways.

- The front end of the rotor frequency converter may operate as a kind of *Static Var Compensator* (SVC) and control the grid-sided reactive power. This is not modelled in this work, as the range for reactive power exchange by the converter is only limited, due to its limited rating;

- By means of controlling the stator current, the stator reactive power can be controlled too: this results in a much wider control range than what the converter is able to, as elaborated in paragraph 4.3.3 when discussing the DFIG. In the following, the control of stator reactive power is further elaborated.

With the given *(d,q)* frame orientation, the reference value for i_{sd} is calculated from the reference stator reactive power:

$$i_{sd,ref} = \frac{q_{s,ref}}{u_{sq}} \tag{5.16}$$

The reference value for i_{sq} follows from the reference value of the torque:

$$i_{sq,ref} = \frac{T_{em,ref} + i_{sd} \cdot \psi_{sq}}{\psi_{sd}} \tag{5.17}$$

(5.16) and (5.17) are respectively derived from (5.7) and (5.14).

The stator currents are controlled via the rotor currents. The relation between stator and rotor currents is, for the *d*-component:

$$i_{rd,ref} = \frac{\psi_{sd}}{x_{md}} - i_{sd,ref} \cdot \frac{x_{sd}}{x_{md}} \tag{5.18}$$

and analogously for the *q*-component.

The rotor currents are then controlled via the rotor voltage, through a classical PI-controller with anti-windup and decoupling terms for optimal dynamical behaviour.

The decoupling terms are added to the output of the PI-integrator, and compensate for the influence of i_{rd} on the *q*-current control and vice versa. From the rotor voltage equations (5.11) and (5.12), it is derived that the decoupling terms for the *d*-current control and *q*-current control respectively are:

$$-\left(\omega_s - \omega_{gen}\right)\psi_{rq} \tag{5.19}$$

and

$$\left(\omega_s - \omega_{gen}\right)\psi_{rd} \tag{5.20}$$

Figure 5.8 shows the control scheme for i_{rq}. The control scheme for i_{rd} is analogous, where (5.16) and (5.19) replace (5.17) and (5.20) respectively, with the appropriate model inputs for executing (5.16) and (5.19).

The output of the current controller is $u_{rd,ref}$ and $u_{rq,ref}$, and is in reality transformed to the real three-phase reference voltage by the three-phase converter on the rotor windings. For modelling purposes however, the transformation from the reference rotor voltages to three-phase voltages does not provide any added value, as the three-phase output voltages of the converter must be transformed back to the *(d,q)*-system as input for the generator model. The transformation from *(d,q)* to three-phase and back to *(d,q)* is thus skipped.

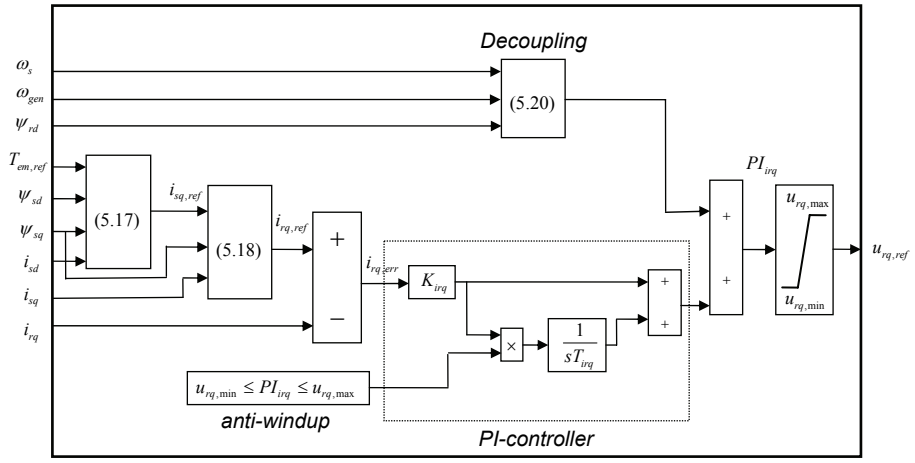

Figure 5.8. Rotor *q*-current controller

Rotor frequency converter

The rotor frequency converter is modelled in a simplified way. As can be derived from the grid connection scheme of a DFIG (Figure 4.10) and from the model overview (Figure 5.1), the converter behaviour has an impact on the voltage applied to the rotor and the rotor current exchanged with the grid.

The converter influence from $u_{rd,ref}$ to u_{rd} is modelled as a first-order time delay with time constant T_{conv1} (Figure 5.9). It represents the small delay (T_{conv1} = 0.005 s) for realising the reference voltages at the output.

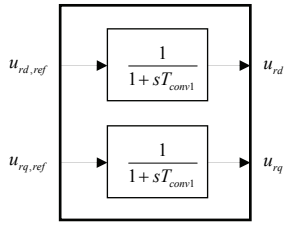

Figure 5.9. Rotor converter (1) model

With regard to the impact of the converter on the exchanged rotor current, it is assumed that:

- no reactive power is exchanged between grid and converter; this is independent from the reactive power exchange between converter and rotor;

- the active power exchanged between rotor and grid is assumed to be transferred by the frequency converter, with an efficiency η_{conv}, and with a time delay T_{conv2}, representing the damping effect of the converter capacitor.

The rotor active power is:

$$p_r = u_{rd} \cdot i_{rd} + u_{rq} \cdot i_{rq} \tag{5.21}$$

The total active current, referred to the stator voltage u_{sq} (equal to the grid voltage considering the grid connection scheme of a DFIG and the chosen reference frame), exchanged between the wind turbine generator and the grid is the stator active current i_{sq} plus the rotor active power, filtered by a first-order delay with time constant T_{conv2}, and divided by u_{sq}. The total active current, referred to the stator voltage, is called i_{totq}.

The total exchanged reactive current is the stator reactive current i_{sd}, as the rotor converter is assumed not to exchange reactive power with the grid.

The currents are then transformed back to the *(R,I)*-reference frame. The (i_R, i_I)-current phasor is the final output of the wind turbine model, further processed by the grid model. The back-transformation is done by the following equations, being the inverse of (5.5) and (5.6):

$$i_R = i_{sd} \cdot \cos\theta_{park} - i_{totq} \cdot \sin\theta_{park} \tag{5.22}$$

$$i_I = i_{sd} \cdot \sin\theta_{park} + i_{totq} \cdot \cos\theta_{park} \tag{5.23}$$

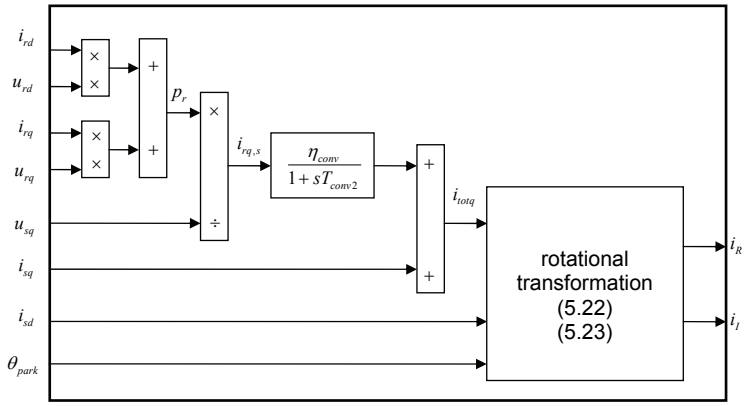

Figure 5.10. Motor converter (2) and rotational current transformation model

Turbine tripping settings

The turbine is disconnected from the grid in case of:

- severe grid voltage rises;
- severe grid voltage dips or short-circuits;
- severe overcurrents;
- propeller overspeed.

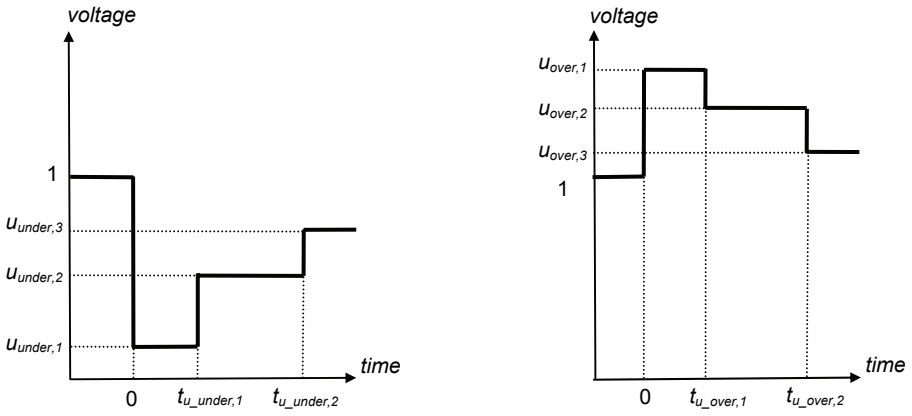

Figure 5.11. Under- and overvoltage tripping settings

The extent and duration of the voltage and current rises and dips that must lead to a disconnection can be specified by the user. Various gradations of current or voltage

deviations may be defined with various tripping time delays, as shown in Figure 5.11 for the example of under- and overvoltage. This way, the tripping settings can be defined, referring to a predefined voltage dip shape like those in Figure 3.11. The number of steps in the tripping curves from Figure 3.11 can be chosen arbitrarily.

Furthermore, in case of rotor overcurrents with a doubly-fed induction generator, a rotor crowbar with resistance r_{cb} short-circuits the rotor windings, with similar time settings as in Figure 5.11. The machine then behaves for a short time as a squirrel cage induction generator. The switching of the crowbar is mostly followed by a total disconnection of the turbine. However, scenarios where the crowbar opens to let the machine again operate as a DFIG can be thought of. This is presented in the simulation results.

In the model developed here, the crowbar action is described as follows: if the rotor current exceeds an upper limit $i_{r,over}$ for longer than $t_{ir,over}$, the crowbar short-circuits the rotor windings. After the crowbar switching, the entire turbine is tripped after t_{cb}.

5.2.3. Modification of model towards other turbine and generator types

The model discussed above is the full model of a variable speed and pitch-controlled wind turbine equipped with a doubly-fed induction generator. This model is the most complex. Models of other turbine and generator types can be easily derived from the model discussed above.

Fixed speed stall-controlled turbine with squirrel cage induction generator

The model of a fixed-speed stall-controlled turbine with SCIG is obtained by omitting the current, speed and pitch controller and converter model. The rotor voltage u_{rd} and u_{rq}, as input for the generator model, are set to zero. Only stator currents are considered as output of the model, as the rotor power is dissipated in the squirrel cage.

The pitch angle β, as input for the turbine model, is also constant and equal to zero. Tripping settings for rotor overcurrents are not necessary, as the rotor is a robust squirrel cage. The stator tripping settings are similar to those from the turbine with DFIG.

With these model adaptations, the propeller speed automatically follows the torque-speed characteristic from Figure 4.9b. In case of high wind speeds, the propeller torque is automatically limited due to the decreasing behaviour of C_p for decreasing λ (increasing v_{wind}) (Figure 4.7): this is the principle of passive stall control.

Fixed speed pitch-controlled turbine with squirrel cage induction generator

The model of a fixed-speed pitch-controlled turbine with SCIG is also obtained by omitting the current and speed controller and converter model. The pitch controller remains. However, as the propeller speed only varies in a very narrow range above synchronous speed which cannot be controlled (Figure 4.9b), it is recommended to use the generator active power as controlled variable for the pitch control, rather than speed. The reference active power is set to 1 p.u., or a lower value if the grid operator would demand a limit in output power in order to avoid hazardous grid situations, e.g. line overload or overvoltage. The pitch angle β is then automatically set by the controller at 0° if the reference active power is not reached, in case of too low wind speed, or is set at the correct value to obtain the reference active power.

5.2.4. Simulation results

Simulation parameters

Turbine

The turbine considered is a 2 MW turbine with doubly-fed induction generator. The parameters are given in Appendix II. The parameters are not referring to any specific commercially available turbine, but represent a 'typical' turbine.

Grid

The considered grid in which the turbine is installed is the distribution grid of Haasrode, a semi-industrial site near Leuven (Belgium). The grid lay-out is shown in Figure 5.12.

The distribution grid is supplied by the transformer in the substation *SUB*, transforming from 70 kV to 10 kV, the distribution grid voltage. The short-circuit power $|\mathbf{S}_{sc}|$ at the 70 kV-node *SUB* is 2500 MVA, a typical value for $|\mathbf{S}_{sc}|$ (Table 3.4).

The rated power of the distribution transformer is 14 MVA. This is an indication of the maximum demand from the entire distribution grid. The total instantaneous load in the distribution grid is assumed to be 10 MW active and 6 MVAr reactive power, more or less evenly distributed at the various 10 kV substations. All loads are assumed to have an impedance behaviour, this means that the active and reactive power consumption is proportional to the square of the grid voltage.

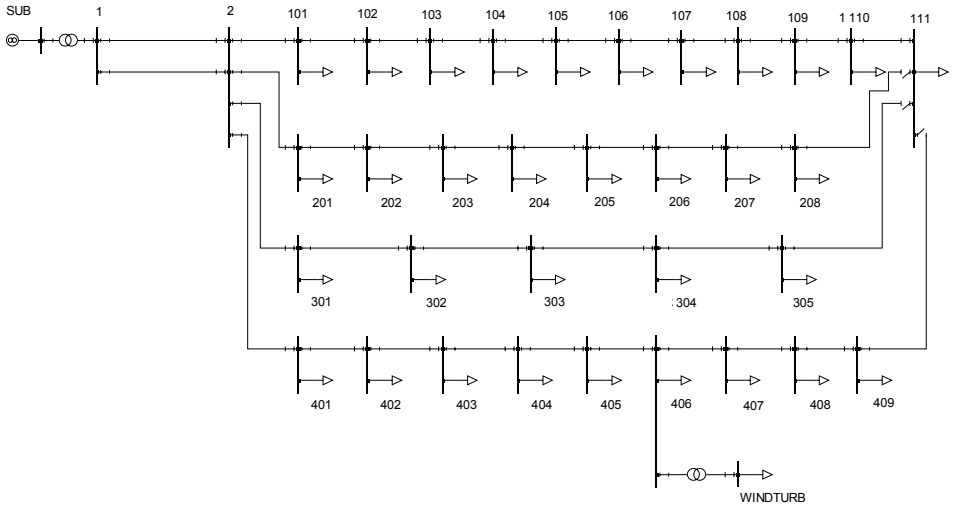

Figure 5.12. Distribution grid of Haasrode, with assumed wind turbine

A 2 MW wind turbine is assumed at node 406 via a 10kV-3kV transformer.

Considered cases

Four cases for the turbine type are considered in the following scenarios (Table 5.1).

	speed control	pitch control	generator type	reactive power control
case 1	fixed speed	passive stall control	SCIG	no
case 2	fixed speed	pitch control	SCIG	no
case 3	variable speed	pitch control	DFIG	cos φ = 1 always
case 4	variable speed	pitch control	DFIG	voltage control

Table 5.1. Cases considered for simulations with the turbine model

Simulation events and results

Wind speed variations

Figure 5.13 shows the wind speed at hub height, used as input for the simulation. The wind speeds varies step-wise from just over cut-in wind speed (6 m/s) to a value far above rated wind speed (20 m/s). At the beginning of the simulation, the turbine is considered operating steady state, with v_{wind} = 6 m/s.

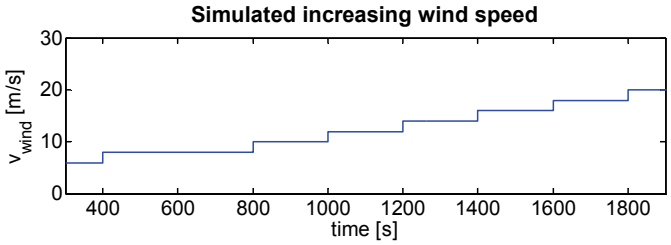

Figure 5.13. Assumed wind speed, as input for the simulation

Figure 5.14a shows the propeller speed during simulation. In *cases 1 & 2*, the propeller speed is determined by the SCIG torque-speed characteristic from Figure 4.9b. The speed varies only in a very narrow range above synchronous speed. The propeller with DFIG, from *cases 3 & 4*, controls its speed as a function of the wind speed, to obtain a maximal aerodynamic efficiency.

Figure 5.14b shows a close-up of the propeller speed behaviour, on the wind speed step change from 10 to 12 m/s. Both propeller and generator speed are shown, for *cases 1 & 2* and *cases 3 & 4* respectively. For *cases 1 & 2*, relatively high and oscillating differences are noted between propeller and generator speed. This is explained by the step-wise change of the wind speed, which is, due to the nearly fixed speed, directly translated into a step-wise change of the propeller torque, twisting shaft and gearbox.

For *cases 3 & 4*, the differences between propeller and generator speed are much lower. It is also noted that the transition towards a new steady state speed occurs relatively slow, explained by the choice of the parameters of the speed PI-controller. With the chosen parameters, both propeller speed and torque variations, as well as the active power that is injected in the grid, are well damped, as will be seen in the following figures.

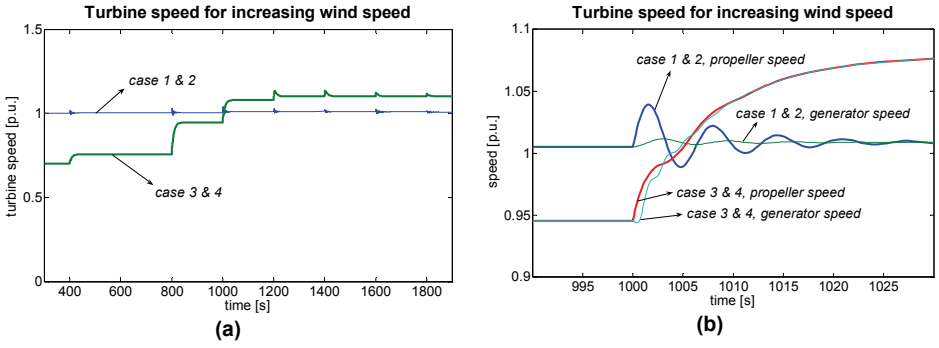

Figure 5.14. Propeller speed for all cases during the entire simulation (a), and close-up on propeller and generator speed on wind speed step change at t = 1000 s (b)

Figure 5.15 shows the turbine pitch angle and coefficient of performance C_p. For *case 1*, the turbine is not pitch-controlled, the pitch angle remains fixed at 0° (Figure

5.15a). For *cases 2*, *3* & *4*, the pitch angle is increased to reduce the aerodynamic efficiency at high wind speeds, in order to control the active power output permanently at its rated value.

In Figure 5.15b is shown that C_p is higher for *cases 3* & *4* at the beginning of the simulation, when wind speed is below rated value. This is explained by the variable speed operation, where the propeller speed, and thus λ, is controlled within the available speed range to optimise C_p. At higher wind speeds, C_p is decreased by the pitch angle controller in *cases 2*, *3* & *4* to control the power at 1 p.u, and decreases automatically in *case 1* due to the decreasing behaviour of C_p for decreasing λ (constant propeller speed and increasing wind speed) (Figure 4.7). This decrease of C_p automatically protects the turbine from overloads, but results in a decrease of power output at high wind speeds, as was already stated when discussing the power curve of the passive stall controlled turbine (Figure 4.8a).

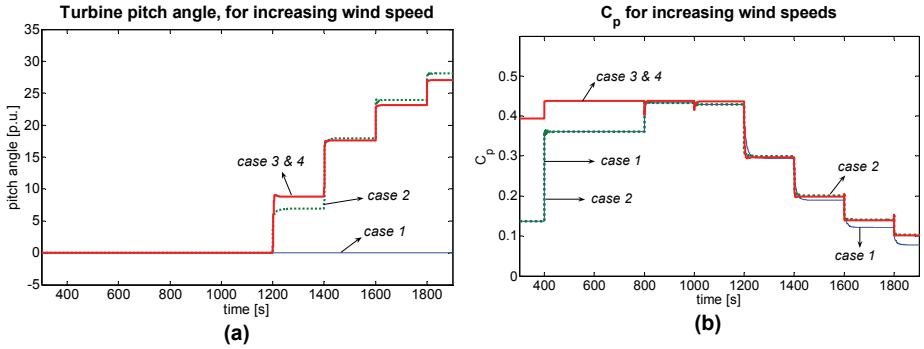

Figure 5.15. Turbine pitch angle (a), and coefficient of performance C_p (b) during simulation

Figure 5.16a shows the active power output of the turbine (stator plus rotor power). This figure confirms the results from Figure 5.15b and the above considerations about C_p. Also it is noted that the active power output at the moment of step-wise wind speed changes is far better damped in *cases 3* & *4* (variable speed turbine) than in *cases 1* & *2* (fixed speed turbine). By accelerating and decelerating, the turbine operates as a flywheel during wind speed variations, absorbing fast torque and power fluctuations. This is also seen in Figure 5.16b, where T_{shaft} is plotted as a function of time.

Above rated wind speed, T_{shaft} = 1 p.u. in *case 2* and 0.9 p.u. in *cases 3* & *4*, both resulting in a power output of 1 p.u. at a propeller speed of respectively 1 p.u. (approximately) and 1.1 p.u. The generator synchronous speed was taken as base value for normalisation, rather than the rated speed. This results in the rated generator speed being equal to 1.1 p.u. and rated torque to 0.9 p.u.

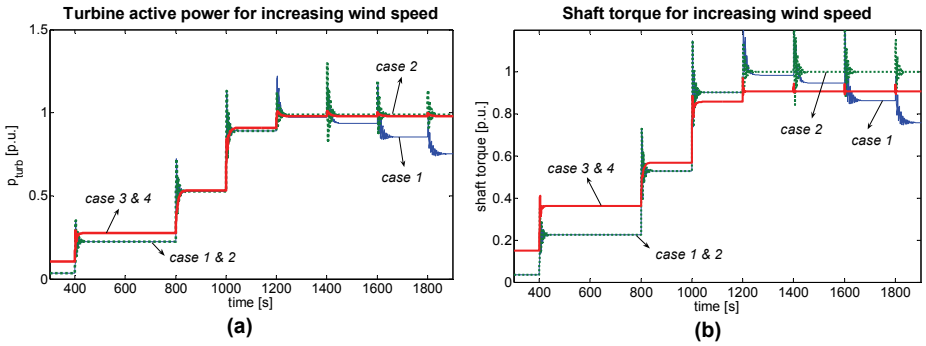

Figure 5.16. Turbine active power (a) and shaft torque T_{shaft} (b)

Finally, Figure 5.17 shows the turbine reactive power output and voltage at turbine node. The voltage in *case 4* is controlled to 1 p.u. by a PI-controller. In many cases, a voltage P-controller (often called a *droop* controller), leaving a small steady-state error in the voltage, is considered as satisfactory adequate.

The reactive power output of a SCIG (*cases 1* & *2*) cannot be controlled. The reactive power output is always negative (inductive behaviour), its absolute value increases with increasing active power (Figure 5.17a). The reactive power for *case 3* is permanently controlled to zero. The reactive power for *case 4* varies with varying active power, to control the turbine voltage towards 1 p.u.

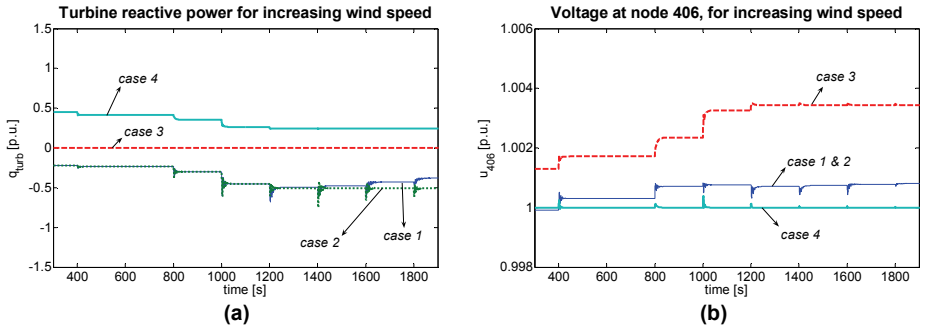

Figure 5.17. Turbine reactive power output (a), and voltage at node 406 (b)

The voltage at node 406 of the studied grid, to which the turbine transformer is connected, is shown in Figure 5.17b. The use of the DFIG with reactive power controlled to zero (*case 3*) leads to the highest voltage fluctuations. In *cases 1* & *2*, the active power generation and the reactive power consumption of the SCIG compensate each other's effect on the voltage, leading to voltage deviations with smaller amplitude, but still with much faster transients as for the cases with DFIG due to its lack of damping.

However, in general, the turbine causes only very small voltage fluctuations in all cases. This is explained by the relatively high strength of the grid: a high short-circuit power at the distribution transformer, and relatively short cables (thus impedances) in the radial lines.

Voltage transient due to motor start

For the next simulation, a 1 MW induction motor is assumed at node 403. The 3rd-order induction motor model from the Eurostag library is used as dynamic motor model. The 3rd-order model uses the same machine equations as in (5.9) - (5.15), hereby neglecting the stator flux transients in the stator voltage equations (5.9) and (5.10). Three differential equations thus remain in the machine model: the rotor voltage equations and the motion equation. This approximation is justified if the exact machine behaviour itself is not the subject of research, but its impact on the grid and on other machines, as is the case here.

At t = 1000 s, a start-up of the induction motor is simulated. The wind speed at t = 1000 s is assumed constant and equal to 14 m/s, and the turbine is assumed operating steadily at rated power.

During start-up, large inrush values of active and mainly reactive power consumption by the motor are noted (Figure 5.18). After the start-up transients, the motor operates at rated power.

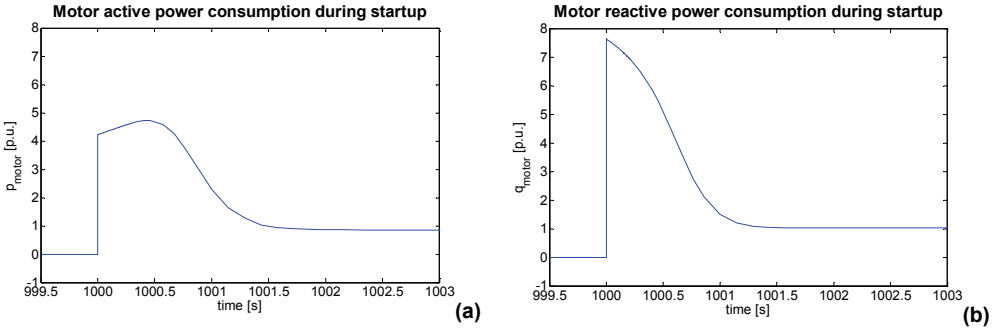

Figure 5.18. Motor active (a) and reactive (b) power consumption during start-up

The motor start-up transients cause a voltage dip in the distribution grid (Figure 5.19a). The duration and depth of the voltage dip are less severe in *case 4*, where an active voltage control is performed by the turbine generator. The reactive power injection by the turbine generator is shown in Figure 5.19b. In *cases 1, 2 & 3*, the reactive power is only passively influenced by the voltage transient at the turbine node, while in *case 4*, the reactive power generation by the turbine is severely increased to compensate for the reactive power consumption peak by the starting motor. The effect on the voltage dip alleviation is however relatively low, due to the relatively high grid strength. The extent of the voltage dip for the uncompensated situation is also only 1.5%.

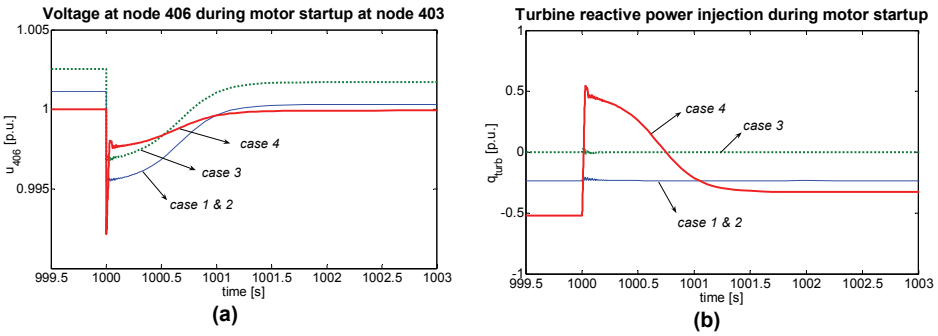

Figure 5.19. Voltage at node 406 during motor start (a), and turbine reactive power injection during motor start at node 403 (b)

Grid fault without turbine tripping

A quasi-metallic short-circuit is simulated at node 104 of the Haasrode grid, at t = 1000 s. The fault is cleared after 1 s. The wind speed is assumed constant and equal to 14 m/s. The voltage at node 104 is shown in Figure 5.20. No circuit breakers are assumed in this simulation. The fault results in a voltage dip at the turbine node, lasting 1 s. Also the tripping settings of the turbine are disabled. As a consequence, the turbine remains grid-connected for every value of current and voltage. This allows examining electrical and mechanical loading on the turbine during severe grid conditions.

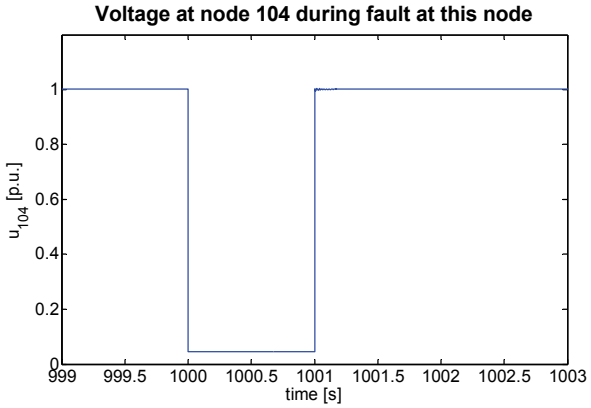

Figure 5.20. Voltage at node 104 of the Haasrode grid, during fault at this node

Figure 5.21a shows the voltage at node 406, the node at which the wind turbine is connected, for all cases from Table 5.1. The voltage drops below 60% of its rated value due to the grid fault. It is not much influenced by the type or control mode of the turbine. At the moment of fault clearance, a close-up of which is shown in Figure 5.21b, it is clearly seen that the voltage restoration is slightly delayed with a SCIG. This is mainly due to the high peaks of reactive power of a SCIG (Figure 5.23).

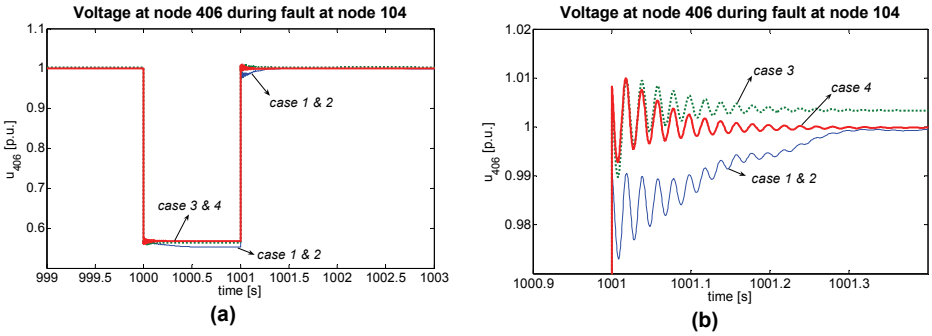

Figure 5.21. Voltage at node 406 (a) of the grid studied, during grid fault at node 104, and close-up at fault restoration (b)

Figure 5.22 shows the propeller and generator speed during the grid fault, for *cases 1 & 2* (a), and *3 & 4* (b). The speed disturbances are higher, and last longer, for cases with SCIG than for cases with DFIG.

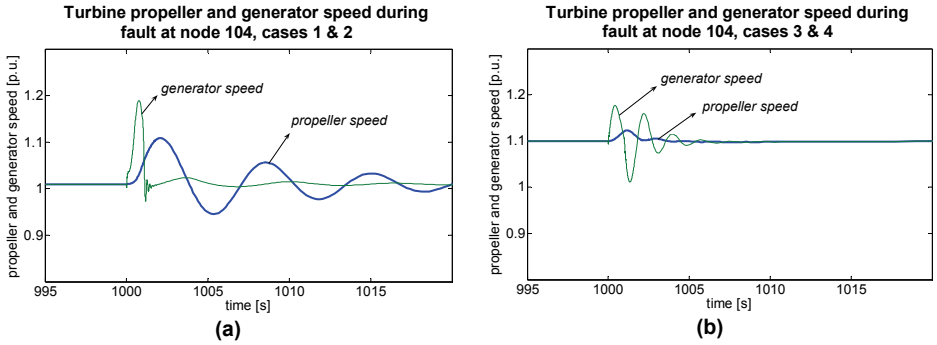

Figure 5.22. Propeller and generator speed during grid fault at node 104, for *cases 1 & 2* (a), and *cases 3 & 4* (b)

Figure 5.23 shows the turbine active (a) and reactive (b) power injection during the fault at node 104, for the cases with the SCIG. It shows high and long lasting transients. Especially the reactive power peak consumption, up to 5 times rated value, at the moment of voltage restoration is to be noted. It causes the slower voltage restoration after fault clearance (Figure 5.21b). However, the effect is only small due to the relatively high grid strength.

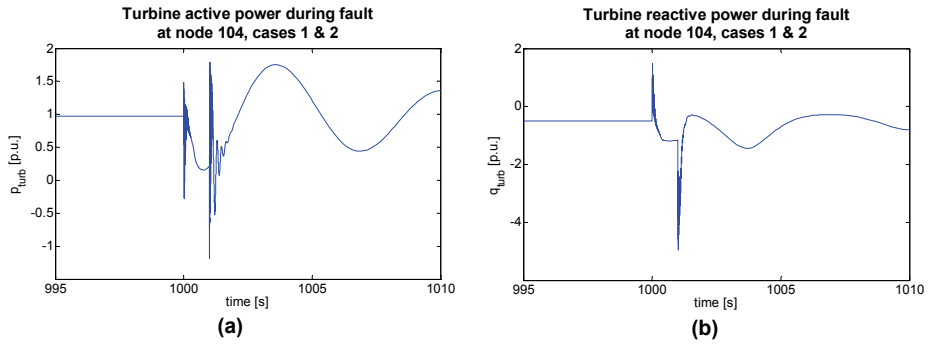

Figure 5.23. Turbine active (a) and reactive (b) power during grid fault at node 104, for *cases 1 & 2*

Figure 5.24 shows active and reactive power injection by the turbine, for *cases 3 & 4*, the cases with DFIG. The transients are much faster damped than with SCIG. The active power keeps decreasing during the fault in *case 4*. It is reminded that in *case 3* the power factor is kept constant at unity, while in *case 4* the voltage is controlled by the turbine reactive power. In order to have the full current rating available for reactive power compensation, the active power is decreased by the pitch controller. The turbine pitch angle is shown in Figure 5.25. Whereas in *case 3*, the pitch angle is increased only to compensate for the speed disturbances during the grid fault, it is further increased during the entire fault and its restoration in *case 4*, in order to provide full reactive power support by decreasing the active current.

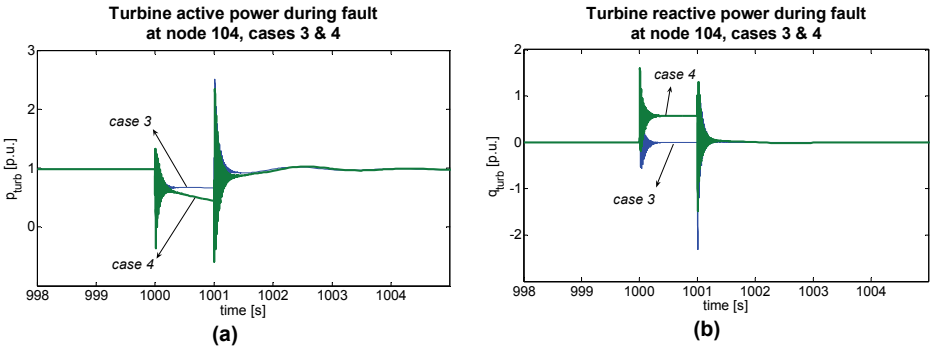

Figure 5.24. Turbine active (a) and reactive (b) power during grid fault at node 104, for *cases 3 & 4*

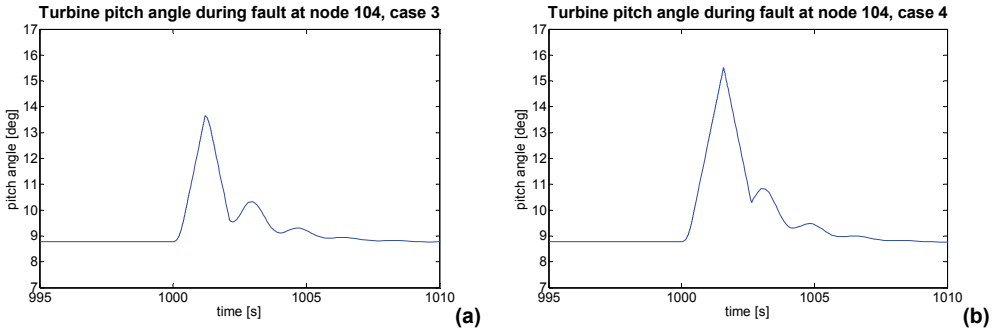

Figure 5.25. Turbine pitch angle during grid fault at node 104, for *cases 3* (a) and *4* (b)

The active and reactive current for *cases 3* & *4* are shown in Figure 5.26 (i_{sd} and i_{totq} from Figure 5.10). In *case 4*, various control options are open for the reactive current control, and its allowed margin. In this simulation example, the reactive current is controlled immediately towards its maximum value to provide voltage support, while the active current slowly decreases at the speed of the pitch control. As a consequence, the total machine current, being the quadratic sum of active and reactive current, is above its rated value during the fault.

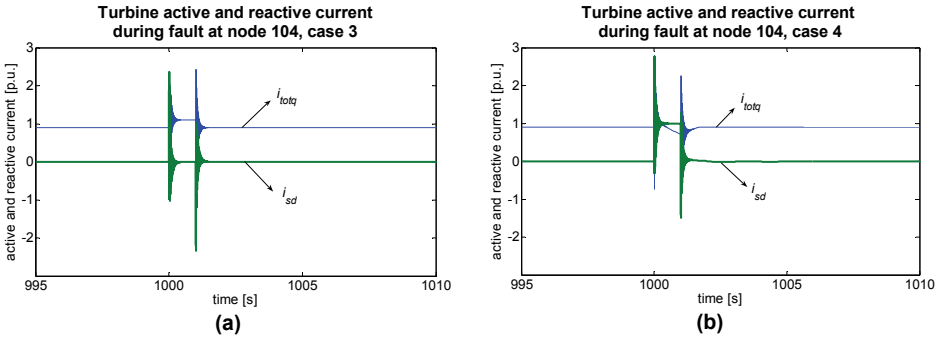

Figure 5.26. Turbine active and reactive current during grid fault at node 104, *cases 3* (a) and *4* (b)

Grid fault with turbine tripping

The same grid fault as in the previous simulation is applied. The turbine tripping equipment is now active, the settings are those from Appendix II. The wind speed is assumed constant during the simulated events and equal to 14 m/s. *Case 4* is simulated: a doubly-fed induction generator with active voltage control. The initial reactive power is zero, the reference voltage for the controller is thus the initial voltage before the fault.

Figure 5.27 shows the rotor current during the fault for *case 4*, the case with active voltage control. The rotor current exceeds its rated value, followed by the bypassing of the rotor frequency converter via the crowbar after 100 ms. According to the tripping settings, the entire turbine is disconnected 300 ms after the crowbar switching. The power system simulator stops calculating the turbine quantities after its disconnection from the grid, as they are irrelevant for the further grid behaviour. The resulting current then immediately jumps to zero.

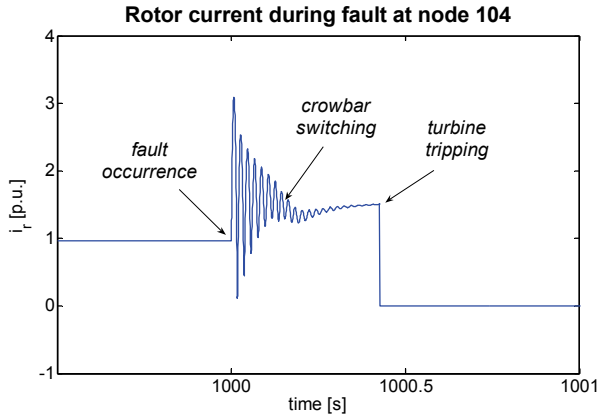

Figure 5.27. Rotor current during grid fault at node 104, *case 4*

Figure 5.28 shows the voltage at the turbine node during the grid fault. On the zoom in (b), the crowbar switching and the turbine tripping can be clearly distinguished. The crowbar switching causes a small additional voltage decrease, as, due to the short-circuiting of the rotor windings, the generator behaves as a SCIG, thus consuming reactive power and causing a voltage drop, until it is tripped.

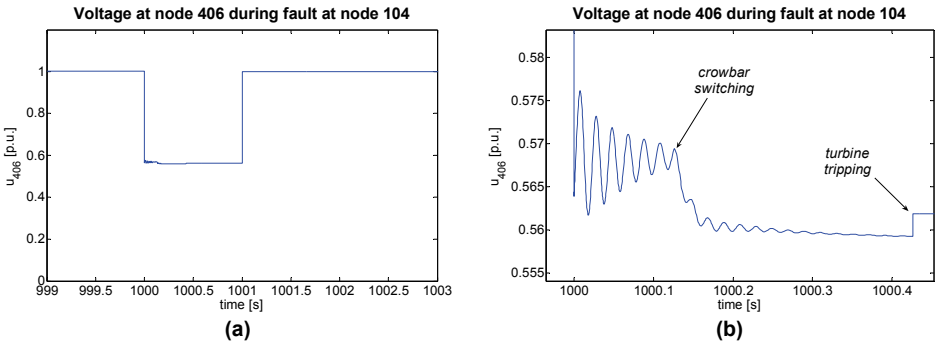

Figure 5.28. Voltage at node 406 during fault at node 104 with turbine tripping, *case 4* (a), zoom on crowbar switching and turbine tripping (b)

The turbine active and reactive power are shown in Figure 5.29. The reactive power generation is initially near zero, then jumps to a positive value in an attempt to

supply voltage control. After short-circuiting the rotor windings, the reactive power becomes negative, thus causing the extra voltage decrease mentioned above.

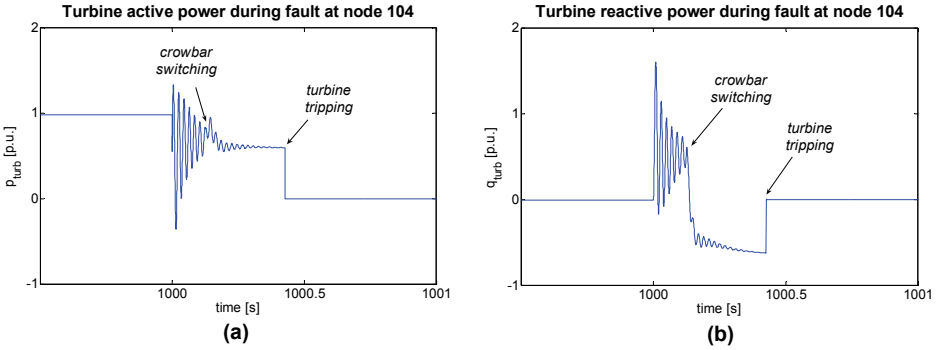

Figure 5.29. Turbine active (a) and reactive (b) power during fault at node 104, *case 4*

The simulation results for *case 3* are very similar to those for *case 4*. The simulation of *cases 1 & 2* simply leads to the disconnection of the turbine by the stator overcurrent protection.

Grid fault with only crowbar switching

For academic interest, the turbine behaviour is investigated during a grid fault followed by the crowbar switching, but not followed by the total disconnection of the turbine. The generator thus continues to operate as a SCIG until the fault is cleared. It is investigated if this is an optional strategy if the loss of active power generation is to be avoided at any cost.

The following figures show the simulation results for *case 4*, with the wind speed constant and equal to 7 m/s, far below rated. The propeller speed before the fault is then equal to its minimum value, being 70% of synchronous speed (Appendix II). These initial conditions allow fully demonstrating the resulting speed disturbances caused by crowbar switching.

Figure 5.30 shows propeller and generator speed during the fault and after its clearance. After crowbar tripping, the generator accelerates during the voltage dip, as a SCIG always does in case of a voltage decrease, due to the loss of electromechanical braking torque. However, also after fault clearance, the generator keeps accelerating, as it evolves towards the supersynchronous speed defined by the torque-speed characteristic of a SCIG, an example of which was given in Figure 4.9. This severe speed disturbance causes torsional oscillations lasting approximately 15 s (Figure 5.30a).

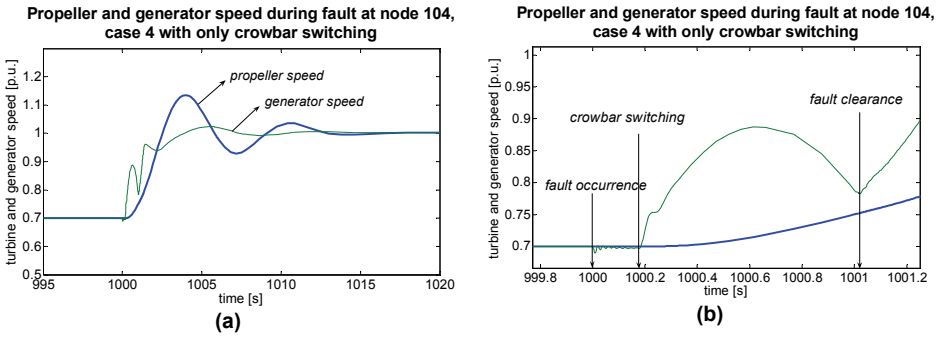

Figure 5.30. Propeller and generator speed during fault at node 104 with crowbar switching not followed by turbine tripping, *case 4* (a), zoom in (b)

The turbine active power is shown in Figure 5.31a, with a close-up at the behaviour during the fault itself in Figure 5.31b. The active power is relatively well controlled until the crowbar is applied. Then, due to the fast acceleration of the turbine during and after the fault, the active power becomes negative: the turbine thus consumes power to reach its supersynchronous speed.

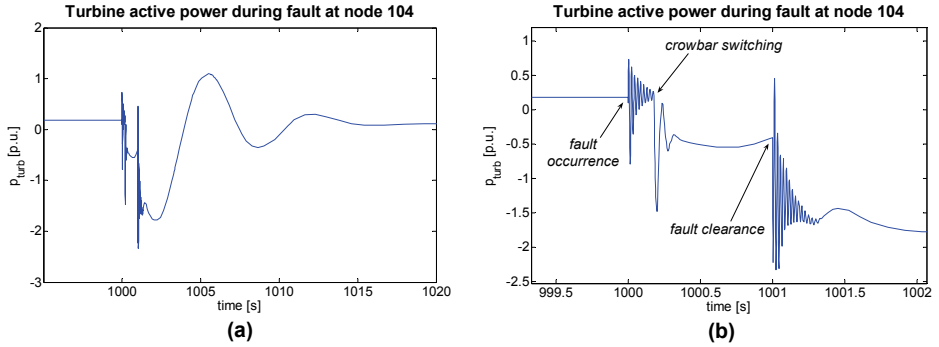

Figure 5.31. Turbine active power during fault at node 104 with crowbar switching not followed by turbine tripping, *case 4* (a), zoom in (b)

The turbine reactive power is shown in Figure 5.32a, with a close-up on the behaviour during the fault itself in Figure 5.32b. Also here, high peaks of reactive power consumption are noted, especially after fault clearance.

The resulting voltage at the turbine node is shown in Figure 5.33a, with a close-up on the fault clearance in Figure 5.33b. Due to the relatively high grid strength, the effect of the high turbine transients on the voltage restoration is rather limited. Nevertheless, the close-up in Figure 5.33b shows a slower return of the voltage to a steady-state value.

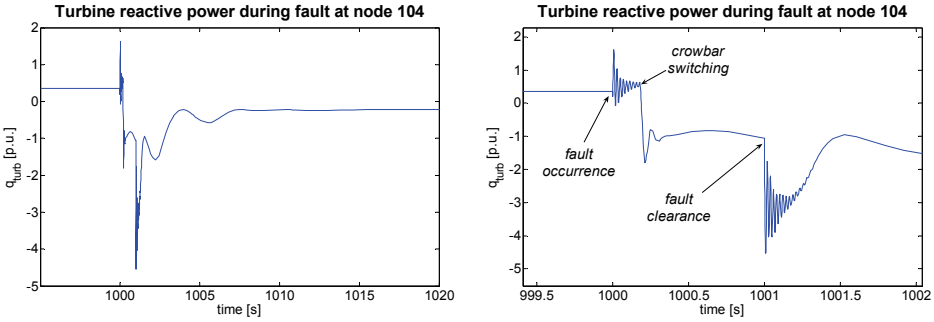

Figure 5.32. Turbine reactive power during fault at node 104 with crowbar switching not followed by turbine tripping, *case 4* (a), zoom in (b)

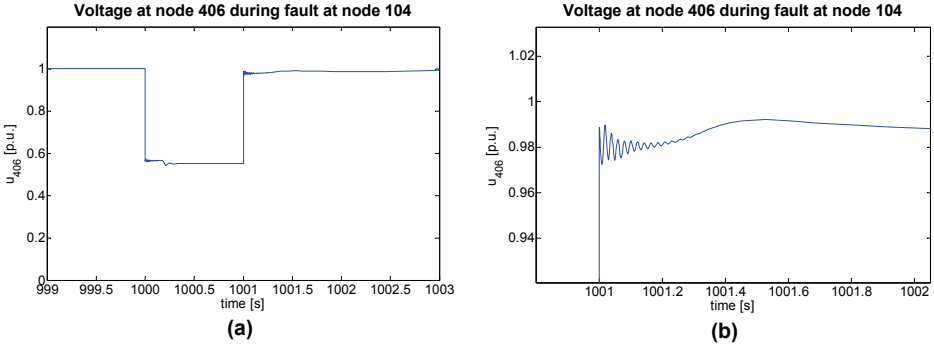

Figure 5.33. Voltage at node 406 during fault at node 104 with crowbar switching not followed by turbine tripping, *case 4* (a), zoom on fault restoration (b)

It is thus concluded that a continued behaviour as a SCIG, after the crowbar switching, is not recommended, as it leads to very high transients that may be harmful for both turbine and grid. Also the option of fast opening of the crowbar again in case of a very short grid disturbance, to continue operation as a DFIG, is difficult. The rotor converter has to be synchronised again with the machine fluxes before reconnecting, in order to avoid high converter inrush currents. This delays the reconnection and the return to controlled turbine behaviour, thus making the return to DFIG operation again more difficult. Figure 5.34 shows active (a) and reactive (b) turbine generator power during a grid fault at node 104, lasting only 150 ms, with crowbar closing and immediate re-opening. In this specific example, the rotor windings are bypassed by the crowbar shortly after fault clearance, as the rotor currents remain above their rated value after fault clearance, thus activating the crowbar. The crowbar is re-opened 300 ms after its closure and the generator continues its operation as a DFIG, as the fault is totally cleared then. However, the re-opening of the crowbar causes high transients in active and reactive power. Their mitigation requires an advanced controller design which is out of the scope of this work.

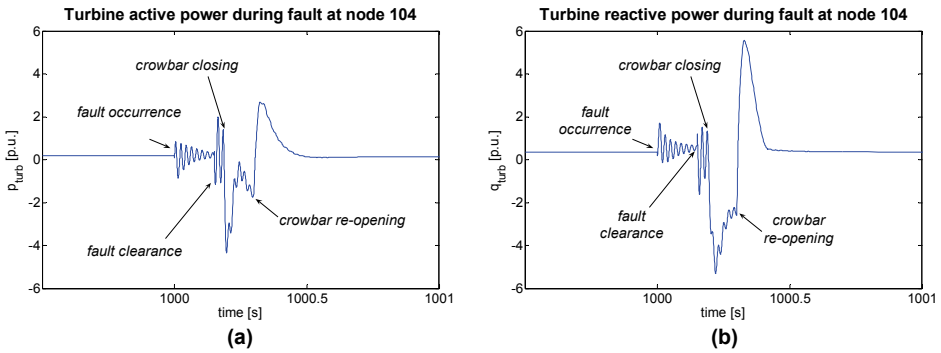

Figure 5.34. Turbine active (a) and reactive (b) power during fault at node 104, *case 4* with crowbar closing and fast re-opening

Figure 5.35(a) shows the voltage at the turbine node, and the generator and propeller speed (b) during the fault at node 104. Note that the time scale in Figure 5.35b is different from the other figures.

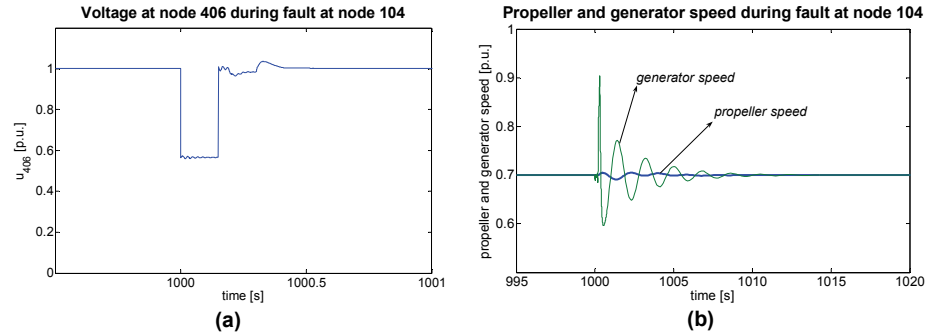

Figure 5.35. Voltage at turbine node (a), and turbine and generator speed (b) during fault at node 104, *case 4* with crowbar closing and fast re-opening

Concluding, the crowbar closing leads to very high transients in both turbine and grid if it is not immediately followed by a total disconnection of the turbine. The closing of the crowbar, being the fastest way to protect the converter from overcurrents, makes the behaviour of a turbine with DFIG very unpredictable during grid disturbances. Although the DFIG is nowadays the most preferred generator type for turbines in the multi-MW range, and although its performance is very high with regard to active and reactive power control for various wind conditions, its capability to ride through severe grid disturbances is limited. This is due to the relatively fragile rotor converter, which is not designed to withstand high currents. As soon as the crowbar has to bypass the rotor converter in case of a grid disturbance, the total turbine behaviour may become unstable.

Manufacturer's solutions are to design the rotor converter to resist short-lasting overcurrents. Also the opening and closing of the crowbar is in modern turbines actually not achieved by mechanical switches but by power electronic switches, making a smooth connection or disconnection of the crowbar possible. A more fault-resistant and advanced design of the crowbar semiconductors or the rotor converter itself however leads to a higher focus on the power electronic components. It is reminded from Chapter 4 that the reduced investment cost for the power electronic components was the main, if not the only, advantage of a DFIG. It is expected that, given the continuously increasing demands concerning the ride-through behaviour of wind turbines, more manufacturers will choose for a completely new generator design, being the direct-drive synchronous generator with fully rated converter.

5.3. Simplified generic dynamic turbine model

5.3.1. Context

The detailed turbine model elaborated in paragraph 5.2 allows examining every physical quantity of the turbine, electrical or mechanical, during the simulation. It would also allow assessing the effect of changing one machine parameter on the total behaviour.

However, modelling and simulation of every single turbine in a power grid requires a lot of programming and computational effort. Alleviating those efforts by aggregating various turbines in one dynamic model, with the same structure as a single turbine model, is often not justified. In [97] it is stated that aggregation of wind turbine models in a single wind park model may lead to a high loss of accuracy. As a compromise between alleviating computational efforts and maintaining satisfactory accuracy, it is proposed in [97] to aggregate all turbine generator models in a single aggregated generator model with adapted parameters, but to maintain the models of the mechanical control blocks for every single turbine. The wind speed, pitch and speed control may differ from turbine to turbine, and their aggregation would result in a too high loss of accuracy. The summarised conclusion in [97] is that the following turbine components may be aggregated in a single model block representing components from various turbines:

- power electronic converters and controls;
- electrical part of the generators.

The following components should be modelled for every turbine separately:

- generator inertia;
- propeller, gearbox, shaft;
- aerodynamics;
- pitch controllers.

All mechanical torques from the single turbine models are then added with a weighting factor, that is well founded on a theoretical basis. The total mechanical torque is then applied to the aggregated model of the electrical part of the generators.

The statement in [97] is considered as a very valuable contribution to the existing wind turbine literature. It contradicts the existing general opinion that an aggregated wind turbine model only consists of a single turbine model with rated power being an integer multiple of a single turbine.

However, the aggregation as proposed in [97], with correct inclusion of the turbine mechanical behaviour, severely decreases the advantage of alleviated programming and calculation effort. Furthermore, many machine and control parameters are often not known, as it is confidential information from the turbine manufacturer. The use of detailed turbine models or adequately aggregated models therefore only makes sense for grid calculations when the exact specifications of a considered wind turbine or wind farm are given, as well as detailed data of the surrounding grid, and when accurate simulations for specific scenarios must be carried out.

For power system simulations only aiming at roughly estimating the potential of the grid to absorb wind power in a given injection point, a more simplified dynamic model can be used that will be developed in this paragraph. The model does not presume a specific turbine technology or generator type, but is a generic model for all variable speed turbines with pitch control.

For the development of the model, an attempt is made to define one single transfer function that directly calculates the active power injection in the grid from the given wind speed signal. This is done by identifying the basic time constants of the v_{wind} - p_{turb} transfer function through examining the frequency response of a detailed turbine model. Then, basic control options are added to the model that may be assumed present for every modern wind turbine, for instance reactive power control and several options for active power control mode. Finally, the model will be validated by simulations.

5.3.2. Development of simplified generic dynamic model

Active power model

Frequency characteristics of the active power model

A detailed turbine model, assembled component by component following the layout from paragraph 5.2, is used as a basis. The turbine and controller parameters are those from Appendix II. The controller parameters are partially taken from [91], which describes the generic dynamic model of a real existing variable speed turbine with DFIG, published by the manufacturer.

Wind speed signals are generated as a superposition of a sine wave (with amplitude 1 m/s and varying frequency) and a constant value. With these wind speed signals as input, the turbine active power, calculated from the detailed model, is also a sine wave of the same frequency as the input signal, superposed on a constant value. This suggests that, for a fixed value of average wind speed, the entire system can be assumed as linear, and can be approximated by a simple transfer function. The amplitude of the power oscillations depends on the mean value of the wind speed signal and on the frequency of its fluctuations.

Figure 5.36 shows examples from wind speed signals with an average value of 50% of $v_{wind,rated}$, i.e. 6.5 m/s (figures a, b and c), and 120% of $v_{wind,rated}$, i.e. 15.6 m/s (figures d, e and f). The corresponding mechanical powers are also shown.

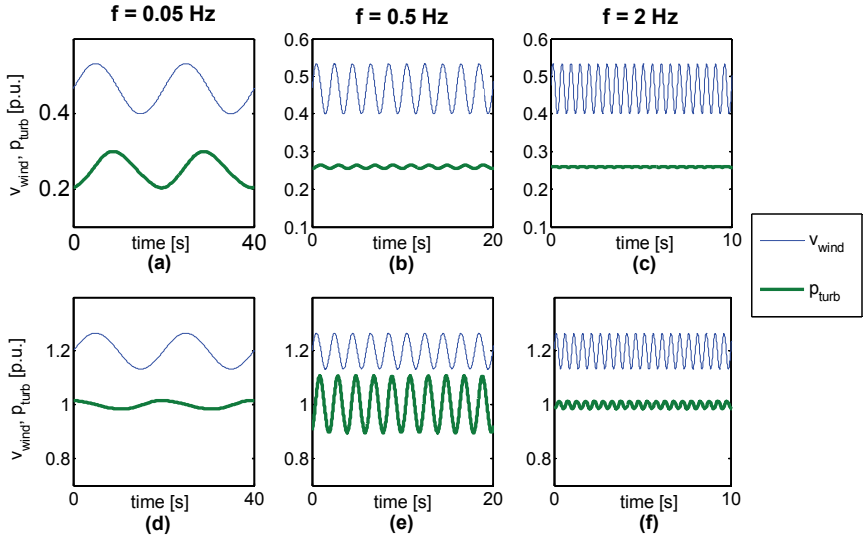

Figure 5.36. Wind speed and mechanical power for two values of average wind speed and three different wind speed fluctuation frequencies

All simulation results, for a large range of frequencies and average wind speeds, are summarised in Figure 5.37. The 10-logarithm of the amplitude of the turbine power oscillations is plotted against the frequency of the wind speed oscillations. This plot can be interpreted as a Bode diagram, and it allows estimating the time constants of the equivalent transfer functions for the variable speed pitch-controlled turbine system.

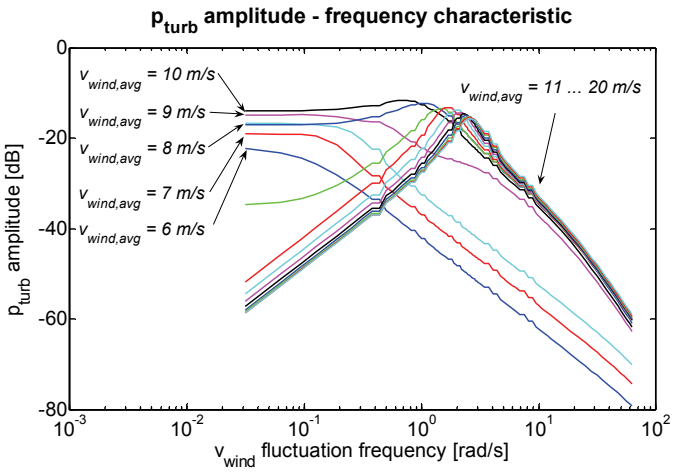

Figure 5.37. Frequency Characteristic of Power Fluctuation Amplitude

In the Bode plot of Figure 5.37, two sets of curves can be distinguished.

1) Low average wind speed (below rated)

The curves for low average wind speeds show the behaviour of a low-pass filter: the amplitude of the output power oscillation remains constant as a function of the frequency, for low fluctuation frequencies. For higher fluctuation frequencies, the amplitude of the power oscillations decreases with a constant slope.

This is explained as follows. At low average wind speeds, the pitch angle remains at 0 degrees to maximise C_p. Only the propeller speed control is active. For slow wind speed fluctuations, the propeller speed is adjusted to obtain the maximum C_p -value, and the optimal propeller speed can be achieved at every moment. The output power is always equal to the maximum power extractable from the wind, given by the power curve. The amplitude of the power output oscillations depends on the average wind speed. This is explained by the non-linearity of the power curve in the low wind speed region.

For fast wind speed fluctuations, the propeller behaves as a flywheel. It accelerates and decelerates to dampen the fluctuations in the output power. The system transfer

function has the characteristic of a low-pass first order filter. The time constant of the filter depends on the average wind speed value but its range is between 1 and 10 s, corresponding to a cut-off frequency of 0.1 to 1 rad/s, the frequency range in Figure 5.37 in which the transition from constant to decreasing behaviour occurs for the considered set of curves.

2) High average wind speed (above rated)

For high average wind speeds, the frequency characteristic is influenced by the action of both the pitch and the speed controllers. The propeller speed is at its maximal rated value, but a small margin for speed variation above and below this speed is still maintained, to dampen power oscillations.

If v_{wind} goes above rated, the pitch control limits the output power. However, the pitch control action is rather slow. Only for very low frequencies of wind speed fluctuations, the pitch control is able to maintain the output power at 1 p.u. at every instant. The amplitude of the power fluctuation is then very low, as can be seen in Figure 5.36d and in the low frequency range of the considered set of curves in Figure 5.37.

For very high frequencies of wind speed fluctuation, the slow pitch control is not able to follow, but the power output fluctuations are then damped by (small) variations of propeller speed. This is again the behaviour of a low-pass filter, and the output power remains approximately constant at 1 p.u, as can be seen in Figure 5.36f and in the high frequency range of the considered set of curves in Figure 5.37.

Between the region of power control by means of pitch angle adjustment on the one hand, and fluctuation damping through speed variation on the other, there is a frequency zone, around 2 rad/s, for which fluctuations of wind speed result in relatively high fluctuations of output power, as can be seen in Figure 5.36e and Figure 5.37. In this frequency zone, speed nor pitch control manage to dampen the power output fluctuations to a large extent.

The transition between low wind speed regime (only speed control) and high wind speed regime (speed and pitch control) would be expected to occur around $v_{wind,rated}$, being equal to 13 m/s. However, during the wind speed peaks, the pitch control becomes active although the average wind speed is lower than $v_{wind,rated}$. Therefore the transition zone between the low wind speed regime and the high wind speed regime is situated somewhat lower than $v_{wind,rated}$. For the turbine simulated here, the transition between the two distinguished frequency behaviour patterns occurs at a wind speed of around 11 – 12 m/s. For wind speeds close to this value, the system behaves strongly non-linear.

Equivalent active power transfer function

From the frequency characteristics in Figure 5.37, it can be concluded that an equivalent transfer function must be a first order low-pass filter for low, and a higher order transfer function for high wind speeds. The equivalent transfer function is shown in Figure 5.38. The function input is v_{wind}. The output is p_{avail}, the mechanical turbine power that is available to produce electrical power. Depending on the operation mode, p_{avail} is fully converted into electrical energy or not, as discussed below.

In the upper part of Figure 5.38, the wind speed is low-pass filtered and converted into active power using the turbine power curve. The time constant of the low-pass filter corresponds to the frequency at which the slope of the first group of Bode plots in Figure 5.37 evolves from 0 to 20 dB/decade. This time constant depends on the average wind speed, but is assumed constant in this simplified model.

The power curve has an upper limit for the output power being the rated power or 1 p.u. The upper input of the summator in Figure 5.38 re
mains constant at 1 p.u. for high wind speeds. The impact of wind speed fluctuations at rated power is taken into account by a 2nd-order transfer function, in the lower part of Figure 5.38. This transfer function represents the second group of curves in Figure 5.37.

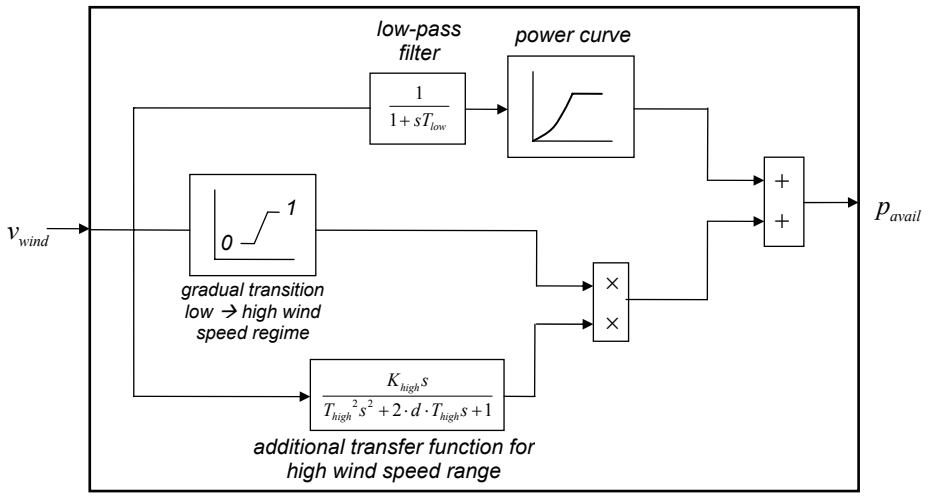

Figure 5.38. Equivalent active power transfer function

The simplified model contains a gradual transition between low and high wind speed region. For wind speeds below 90% of rated wind speed, the transfer function for high wind speeds is not taken into account. For wind speeds above 100% of rated wind speed, the transfer function for high wind speeds is fully taken into account. A linear interpolation is used for the intermediate wind speeds.

The parameters that result in an optimal match between the equivalent transfer function and the plots from Figure 5.38 were found to be:

T_{low}	= 7 s	d	= 0.3
T_{high}	= 0.5 s	K_{high}	= 0.06

The output of the equivalent transfer function is compared with the output of the detailed model for the wind speed signal (Figure 5.39a). The wind speed is first below $v_{wind,rated}$, and rises to a higher value. The resulting power outputs for the detailed model and the equivalent transfer function are shown in Figure 5.39b. They provide a very good correspondence. The output power fluctuations are clearly more damped in the low wind speed region, both with the detailed model and the equivalent transfer function.

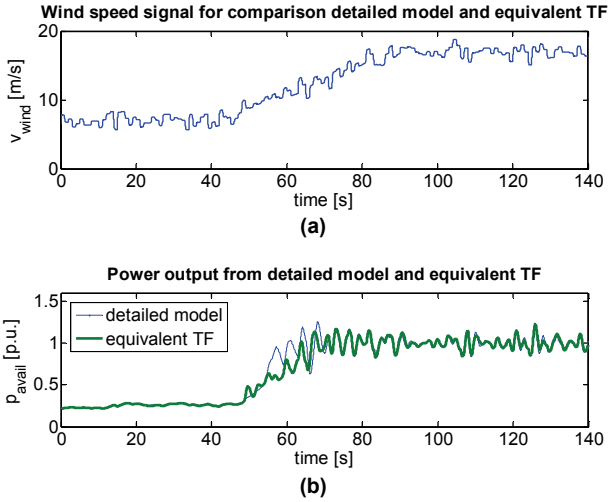

Figure 5.39. Wind speed signal (a) and corresponding power output (b) from the detailed model and the equivalent transfer function

Control modes for active power

In some circumstances, it may be necessary to limit the active power output. This may occur in the following cases.

- The available margin for electrical current of the equipment is needed for the supply of reactive power, when immediate assistance from the turbine is required to mitigate a voltage disturbance. Active power has to be decreased then, in order not to exceed the system's rated current. This is already illustrated with the detailed model (e.g. in Figure 5.26).

- The power lines in the immediate vicinity of the turbines are overloaded. Existing power grids are rarely designed to transport a large amount of

wind power. Basic grid reinforcements are not always sufficient to avoid line overloading at every energy generation and (local) load pattern scenario.

- The grid operator requires that a part of the available wind energy is kept as 'spinning reserve'. Alternatively, the wind turbine operator may take this decision himself, to sell spinning reserves on the ancillary services market. The turbine blades are then partially pitched out of the wind and less energy is generated.

Three control modes for a turbine are proposed here: '*Full*', '*Limited*' and '*Balancing*'. The choice of these control modes is based on (but not the same as) the control modes for the Horns Rev wind farm [98]. The three operation modes are shown graphically in Figure 5.40. The upper line in each graph is the available power from the wind speed. The lower, bold line in the figures '*Balancing*' and '*Limited*' represents the power actually delivered for these operation modes (assuming ideal control).

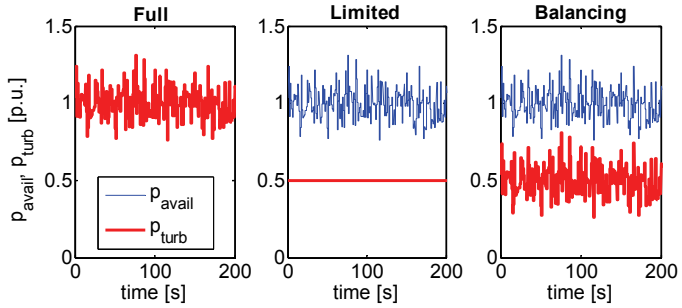

Figure 5.40. Different modes for active power operation

In the '*Full*' power mode, the turbine converts all available mechanical power to electrical, and injects it in the grid. In the '*Limited*' mode, the energy generation does not exceed a maximal value p_{lim}, by permanently controlling the pitch angle of the turbine blades. This can be requested e.g. to prevent overloading of a power line. In the '*Balancing*' mode, the turbine blades are partially pitched out of the wind, to maintain a fixed fraction of available wind energy as balancing power. Only a fraction α of the available wind power is actually produced. Balancing power may have a high economic value for a wind farm operator in the ancillary services market, but is at the moment of writing only very rarely applied, because of the limited accuracy of actual wind speed predictions.

The applicable operation mode is maintained by controlling the pitch angles of the turbines. The transition speed between two operation modes is determined by the pitch variation rate. The proposed dynamic model for the transition is shown in Figure 5.41.

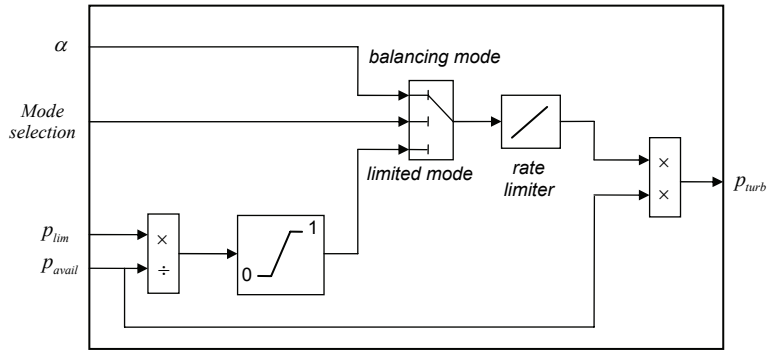

Figure 5.41. Model for transition between active power operation modes

The switch in Figure 5.41 is controlled by the '*Mode selection*'. This determines whether the upper or lower input of the switch must be passed through as output. The switch output is the fraction (between 0 and 1) of the available active power that must be delivered to the grid. The upper switch input represents the '*Balancing*' mode, in which a fraction of available active power can be chosen to be actually produced. The fraction is given by α (between 0 and 1). The lower switch input represents the '*Limited*' mode. Starting from a given maximal value p_{lim} for the output power, the fraction of the available power that must be produced is calculated and is passed through the switch. The most common operation mode ('*Full*') can be reached either by setting p_{lim} to a value equal to 1 p.u., or by setting α in '*Balancing*' mode to '1'.

The transition between the operation modes is modelled as a change of demanded fraction from the available power, through a rate limiter. The maximum rate depends on the pitch variation rate, and is set in this model at 20% per second. The value for the maximum rate may be given by the grid connection requirements. For example, the power output at the Danish offshore wind farm of Horns Rev (160 MW) must be able to reduce from 100% to below 20% within 5 s [99].

The input command for the '*Mode selection*' and reference power may be set by the grid or turbine operator, but may also be set automatically to '*Limited*' by the overcurrent protection, when a large current is required to supply reactive power in case of a voltage disturbance.

Conclusions on the Active Power Model

In the previous sections, a detailed turbine model was replaced by an equivalent transfer function, to calculate the available active power with satisfactory accuracy for simulations of continuous operation of a turbine. Much information on the turbine is lost (e.g. propeller speed, pitch angle) when the equivalent transfer function is used. On the other hand, the integration of this simplified turbine model in a power system model increases the computational efforts for power system

simulations to a far lower extent than the detailed model, and a good assessment of undispatched fluctuating generated power caused by wind turbines can be made. Three operation modes were modelled, as well as the dynamic transition between these modes.

The model parameters, such as the time constants of the equivalent transfer functions, reflect the turbine behaviour only approximately. In general, these parameters are not given by manufacturers. However, they are strongly linked to the fundamental turbine performance characteristics. They summarise the complicated turbine behaviour in a very dense way directly usable for grid operators, project developers or anyone involved in the assessment of wind energy potential in a given grid point. The model can be used for power system simulations in order to calculate:

- specifications for the governor dynamics of conventional generators nearby a wind farm in order to maintain the angular stability of the power system;

- specifications for a turbine's active power control speed, starting from a given grid model;

- specifications for the allowed overloading of any lines, transformers or power electronic devices connected to the wind farm.

The *Active Power Model* assumes variable speed operation of the turbines, but does not prescribe a certain generator type such as doubly-fed induction or synchronous generator. It has already been stated in literature that, for transient power system simulations, the differences between the generator types used in variable speed wind turbines are not seen in their interaction with the grid, because they are compensated by the controllers [100]. Therefore, the model developed here is not applicable for fixed-speed turbines with squirrel cage induction generators.

Reactive power model

The *Reactive Power Model* does not start from a predefined detailed model from literature. With state-of-the art technology, it is generally possible for modern wind turbines to control their reactive power output.

Two control modes for the reactive power generation are suggested here:

- the '*Fixed Power Factor Mode*', i.e. operating at a constant power factor, e.g. unity;

- the '*Voltage Control Mode*', i.e. controlling the reactive power output instantaneously to maintain the voltage at a given node at its reference value, or to provide voltage support in case of a grid disturbance.

As reactive power is the product of grid voltage and reactive current, controlling the reactive power is equivalent to controlling the reactive current. As the turbine is modelled as a current injector in the end, it is more appropriate to immediately act on the reactive current instead of the reactive power.

The reference reactive current for the first operation mode is calculated from the required power factor $cos\ \varphi_{ref}$ and the supplied active power, obtained from the *Active Power Model*:

$$i_{react} = i_{act} \cdot \tan \varphi_{ref} \tag{5.24}$$

For the second operation mode, the required reactive current is calculated by a droop controller (a proportional controller) with gain P_{uctrl}. Optionally a more advanced controller can be implemented.

The actual reactive current is then obtained after an equivalent first-order delay with time constant T_{ictrl} representing the current control loop of the generator. The implementation of a proportional controller and a first-order time delay function is supported by most power system simulation software packages, and does not contain any particularities in its use. Figure 5.42 shows the calculated reactive power output by both the detailed and the equivalent reactive power model. There is a good correspondence between detailed and equivalent model, justifying the assumption that the current control loop can be approximated by a first-order time delay.

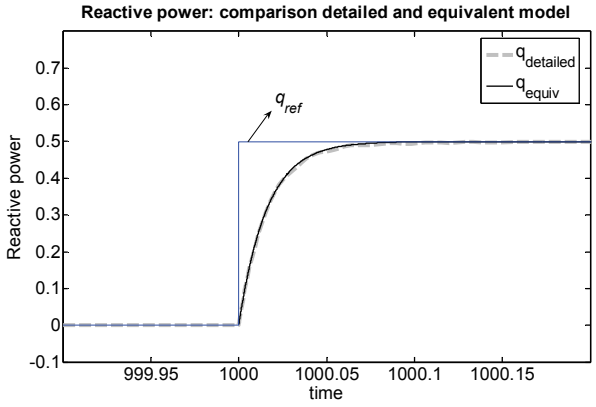

Figure 5.42. Step change in reference reactive power: detailed and simplified model

The structure of the *Reactive Power Model* does not depend on generator technology; however the parameters may depend on it. The speed of reactive power control and the maximum amount of reactive power that can be supported may depend on the generator and power electronics type or additional equipment. The value of T_{ictrl}, the equivalent time delay caused by the current control loop, must be assessed for each category of generator types. Suggested values are:

- T_{ictrl} = 10 ms for a synchronous generator, connected to the grid through a PWM-converter, rated for the entire power, in full control of the current. As the PWM-converter has a direct impact on the grid-sided reactive current, its control speed can be less than a period;

- T_{ictrl} = 20 ms for a doubly-fed induction generator. In this generator type, the power exchange is split over stator and rotor, with the major part supplied by the stator. This stator current is controlled through the magnetic interaction with the rotor current, which is on its turn controlled by a PWM-converter, with a rating of ca. 30% of the turbine rated power. Because of this magnetic interaction, the current control speed is lower, and thus T_{ictrl} is somewhat higher, however still very low compared to the active power time constants.

From the reference reactive current, the maximum allowable active current and active power p_{lim} is calculated to be fed back to the active power controller, in order to never exceed the machine rated current under normal conditions.

$$p_{lim} = u_{grid} \cdot \sqrt{{i_{rated}}^2 - {i_{react}}^2} \tag{5.25}$$

with u_{grid} the grid voltage, i_{rated} the machine's rated current and i_{react} the instantaneous machine's reactive current.

This way of modelling implies that priority is given to the reactive power control, and the active power must be tuned down to achieve reference reactive power. Practically, the circumstances at which the active power must be limited because of reactive power requirements are only during grid disturbances, when full reactive power support is required.

The final block scheme for the equivalent reactive power model is shown in Figure 5.43. The upper input of the switch in the figure is the reference reactive power in the '*Fixed Power Factor Mode*', the lower the '*Voltage Control Mode*'.

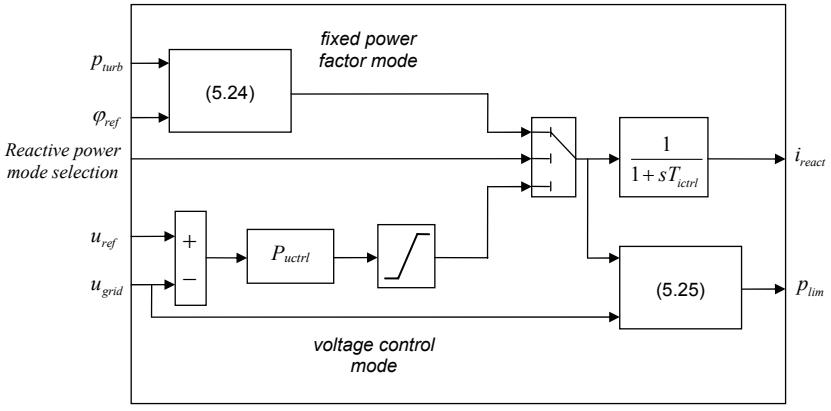

Figure 5.43. Generic reactive power model

Tripping settings

For the tripping settings, only the wind speed, grid voltage and optionally the frequency, is monitored. The propeller speed is not calculated in the simplified model and thus cannot be monitored for tripping settings. The voltage tripping settings are analogous to the detailed model (Figure 5.11).

The model assumes that the state-of-the-art wind turbine technology does not suffer from instable behaviour as long as the grid voltage and wind speed remain in the normal range, defined by turbine specifications.

Interface between turbine model and grid model

Most power system simulation software packages allow dynamic modelling of machines as current injectors, power injectors, or controlled impedances. Modelling a machine as a current injector is the closest approach to the real nature of a machine, and leads also to the least numerical problems during short-circuit simulations.

The exact implementation of the interface between the machine model and a grid model depends on the software used. For the use of the model in EUROSTAG, the active and reactive current are transformed to the *(R,I)* – grid reference frame, by means of the rotational transformation from Figure 5.4, active and reactive current being aligned with respectively the *q*- and *d*-axis of the equivalent turbine model.

5.3.3. Simulation results

Wind speed variations

A 2 MW variable-speed turbine, modelled by the simplified generic dynamic model described above, is connected at node 406 of the Haasrode distribution grid from Figure 5.12. The wind speed signal from Figure 5.13 is again used as input for the simulation. The simulation input parameters are thus the same as for the simulations with the detailed turbine model in paragraph 5.2.

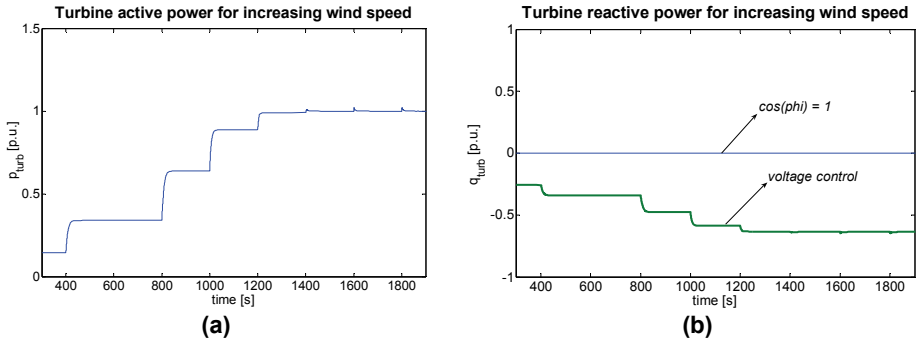

Figure 5.44. Turbine active (a) and reactive (b) power during wind speed variations

The simulated turbine either controls its power factor at a fixed value, being unity, or either provides voltage control by controlling its reactive power output. Those two options are equivalent with *case 3* and *4* from the simulations with the detailed turbine model. Figure 5.44 shows active (a) and reactive (b) power generation by the turbine for the two reactive power control modes. Figure 5.45 shows the resulting voltage at the turbine node. The results are very similar to those in Figure 5.16 and Figure 5.17, presenting the simulation results with the detailed model. This proves the validity of the simplified generic model for the simulation of wind speed changes.

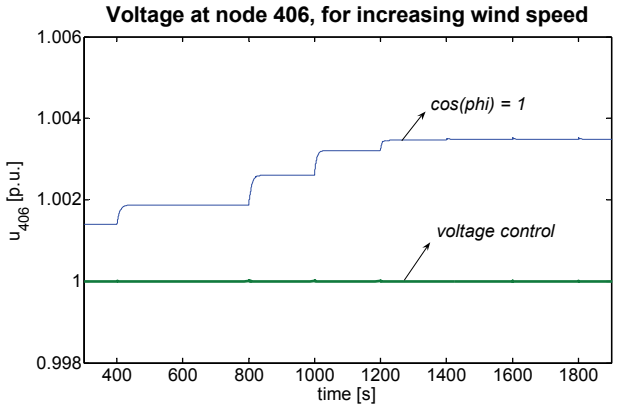

Figure 5.45. Voltage at node 406 during wind speed variations

Voltage transient due to motor start

The start-up of a motor at node 403 is simulated. The simulation parameters are the same as in paragraph 5.2, with the motor active and reactive power shown in Figure

5.18. The voltage at node 406 and the reactive power injection by the turbine, calculated with the simplified generic model, is shown in Figure 5.46. The results are again very similar to those found in paragraph 5.2 (Figure 5.19), proving the validity of the simplified generic model for the simulation of transients caused by switching events.

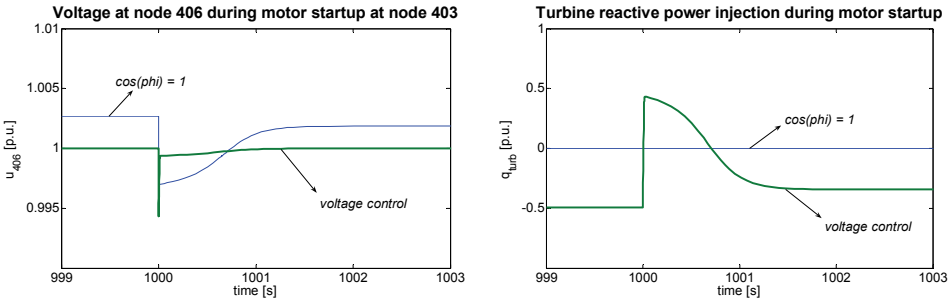

Figure 5.46. Voltage at node 406 during motor start (a), and turbine reactive power injection during motor start at node 403 (b)

Grid fault

A grid fault is simulated at node 104. The fault properties are equal to those in paragraph 5.2, with the voltage at the faulted node shown in Figure 5.20. The voltage at the turbine node, calculated using the simplified generic model, is shown in Figure 5.47a, with a close-up on the voltage during fault restoration in Figure 5.47b. The case with constant turbine generator power factor is simulated, as well as the case with active voltage control, being the equivalents of *case 3* and *4* respectively of the simulations with the detailed turbine model. The tripping settings are inactive.

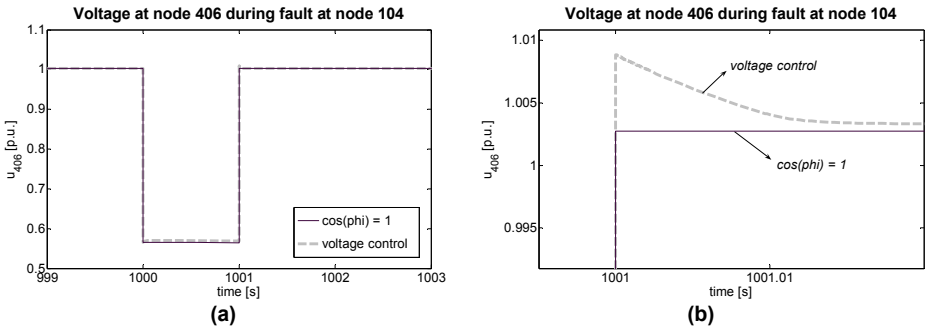

Figure 5.47. Voltage at node 406 (a) of the grid studied, during grid fault at node 104, and close-up on fault restoration (b), with simplified generic dynamic model

Figure 5.48 shows the turbine active (a) and reactive (b) power injection during the fault. The active power decreases during the fault with a slope linked to the maximum pitch rate. The reactive power remains zero for the case with a constant power factor, and is controlled to supply voltage control in the other case. The value of supplied reactive power in this case corresponds to the current rating of the machine.

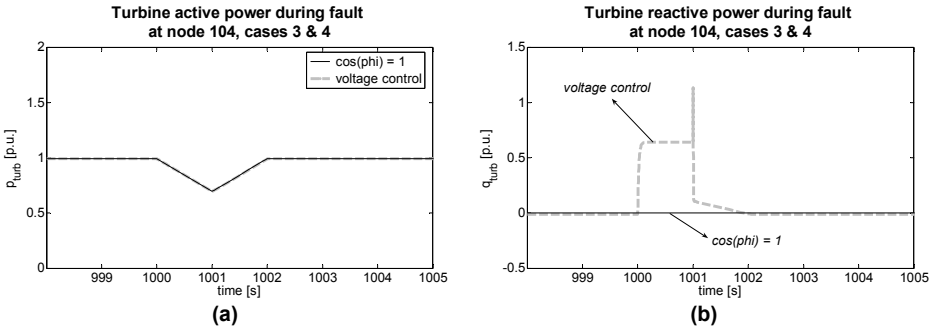

Figure 5.48. Turbine active (a) and reactive (b) power during grid fault at node 104, with simplified generic dynamic model

When comparing Figure 5.47 and Figure 5.48 with Figure 5.21 and Figure 5.24 respectively, it is noted that the simplified model is not able to correctly calculate all transient phenomena. Therefore, care should be taken when using the simplified model for the simulation of grid faults in the close environment of the turbine.

However, the simulations with the detailed model indicated that this heavy disturbance will lead to turbine tripping. With the tripping settings active in the simplified model, the undervoltage protection disconnects the turbine from the grid, making the simulated active and reactive power irrelevant.

It is thus concluded that the simplified and detailed turbine model deliver similar results for light transients, not causing turbine tripping. For heavy transients, the models give different results when the tripping settings are inactive. However, with the tripping settings active, the differences are far less relevant to study the impact of the turbine behaviour on the grid, as the turbine is disconnected in both cases.

5.4. Conclusions

This chapter presents the dynamic models of wind turbines for power system simulation applications. The detailed dynamic model describes the physical behaviour of every turbine component, and allows examining the impact on the turbine behaviour on the grid, as well as the impact of wind speed changes and grid disturbances and wind speed changes on the turbine itself. The torque in the drive train during wind speed changes is shown as an example.

The simplified generic dynamic model reduces the modelling and computational efforts severely. Considering the frequency response characteristics of the detailed model, the main time constants of the entire wind-to-power system are identified and physically explained. The resulting simplified model is basically a single wind-to-power transfer function of 1st or 2nd order, depending on the wind speed region. The model is further extended with some control options for active and reactive power, each with their appropriate time constants and thus simulating the real turbine behaviour in a realistic way. Much information about the physical turbine behaviour is lost when using the simplified model. On the other hand, the model parameters and specifications are directly relevant for grid operators. The model approach also responds to the increasing demand from research institutes and power system operators to extend the power quality standard for wind turbines, IEC 61400-21, in such a way that the turbine response to voltage dips is classified into rigorously defined categories.

Simulating the same events with the simplified model and the detailed model results in very similar grid impact analyses for events causing only ‘light’ transients, e.g. wind speed changes or switching transients. For ‘heavy’ transients, e.g. metallic short-circuits close to the turbine, the simplified model neglects too many transient effects to fully assess the impact on the grid. However those transients mostly lead to the immediate tripping of the turbine, which can easily be included in the simplified model.

It must be noted that many parts of the simplified dynamic model are not specific for wind turbines, but generally applicable for various kinds of distributed generators and loads that are grid-connected through a controlled power electronic interface. Also the strategy for developing the Active Power Model in an equivalent transfer function can be applied if detailed models or measurements of other generating units are available and if model linearisation does not result in excessive approximation errors.

The use of the simplified model is thus well-suited to calculate the impact of more or less severe grid connection and ride-through requirements. It can be used to roughly estimate the impact of wind power injected at a given substation, without knowing yet the technical details of the wind turbines. It is a tool for research institutes and power system operators to estimate the dynamic impact of future wind power that is injected in the grid.

Specific and complete results are difficult to obtain, as the dynamic events and instantaneous grid conditions that can be simulated are numerous. Also, detailed information not only about the wind turbine itself, but also about the dynamic characteristics of the neighbouring grid (generators, loads, circuit breakers etc.) is needed to correctly assess the impact of specific events. This chapter limited itself to offering a library of dynamic turbine models, with application examples of their use in a small grid.

This chapter is thus an attempt to respond to the need for dynamic turbine models by power system operators, in order to find technically feasible grid connection requirements sufficiently guaranteeing the power system's stability on a short term (seconds). The impact of grid events and sudden wind speed changes can be examined.

The modelling of wind turbines has been subject of intensive research by many institutes during the last decade. The author's contribution in this work is the assembly and testing of a well-performing detailed turbine model, using model components previously discussed in different literature sources, and for the first time implemented in the specific software tool Eurostag. The simulations did not show any computational problems in the applied scenarios. The detailed model is very flexible: without changing the model structure, modifications of the parameters allow to examine different control options and different generator types. Furthermore, the development and validation of a simplified generic dynamic model is an entirely new contribution by the author, which lead to publication in an international journal [I].

In the following chapter, the dynamic behaviour of wind turbines is neglected: turbines are modelled by their power curve, and the impact of wind speed changes on the aggregated wind power in the entire control zone is examined. The impact of fluctuating wind power on the system behaviour in terms of hours to days is examined. Chapter 5 and 6 together provide a broad view on the impact of wind power on a power system.

Chapter 6

Aggregated wind power in Belgium

6.1. Introduction

This chapter presents results for the aggregated wind power in Belgium. Wind speed time series at three sites in Belgium, with hourly resolution and over a time span of three years, are used as input. An algorithm is developed to calculate aggregated power time series from the given wind speeds for different scenarios of spatial distribution of wind turbines, ranging from evenly distributed over the control zone of the Belgian TSO Elia to all concentrated in a single (offshore) wind farm. The Elia control zone contains Belgium and a part of Luxemburg.

The resulting power time series are assessed in various ways. The capacity factor of the aggregated wind park is calculated for all scenarios. The annual and daily periodicity is quantified. The hourly fluctuations are treated by means of Markov-matrices. Also the wind power fluctuations during longer time spans, e.g. 24 hours, are handled that way. The dependency of these matrices on the scenario for spatial turbine distribution, as well as on the season, is investigated.

Then, these results are used to estimate the value of wind power. The various ways in which the value of wind power can be quantified was discussed in Chapter 4, and is further elaborated here. The *capacity credit* of the aggregated wind power is calculated, using an approximate approach for the Loss of Load Probability (LOLP) of the existing Belgian generator park.

As discussed in Chapter 4, the capacity credit alone is not able to fully quantify the value of wind power, as it only takes the probability distribution of aggregated wind power generation into account, hereby neglecting the impact of wind power fluctuations. Therefore, the calculated wind power time series are transformed to time series of wind power values continuously available with a given reliability for a given duration. This is called the *reliable wind power generation*, and is, especially for high wind power penetrations, considered as more relevant than the time series of wind power generation itself. Time series of reliable wind power generation are calculated for every scenario of spatial turbine distribution, for various levels of reliability and considered duration. Some summarising results are given in this chapter.

Finally, the value of wind power is expressed in terms of potential *abatement of CO_2-emission*. An existing simulation tool, *PROMIX*, is used to estimate the CO_2-emission abatement for all scenarios. The results diverge, depending on whether the instantaneous wind power time series or the reliable wind power time series are used as input. Given the assembly and the control capabilities of the Belgian generator park, an absolute upper limit of installed wind power is considered, above which the reliable wind power time series must be used rather than the actual time series.

In this chapter, the dynamic turbine behaviour discussed in Chapter 5, such as the reaction on a wind gust or grid disturbance, is neglected. While the previous chapter treated the impact of wind power on the power system on a local level and on a short term (seconds range), this chapter discusses the impact of the aggregated wind power on the power management in a time span of hours to days. The dynamic behaviour of single turbines in the previous chapter and the hourly aggregated wind power fluctuations in this chapter can be treated separately, as the considered time spans are different. Both chapters provide a broad view on the technical impact of wind power on a power system.

6.2. Statistical model for aggregated wind power in Belgium

6.2.1. Wind speed data

Wind speed time series with hourly resolution from three years are available from three sites in Belgium: Ostend, Brussels and Elsenborn (Figure 4.4). At all sites, the anemometer height is 10 m. Some remarks on the characteristics of the measured time series, concerning probability distribution, periodicity and correlation were

made in paragraph 4.2. From the available wind speed time series, the aggregated wind power time series for the Belgian control zone are calculated, assuming various scenarios for the type and geographical spread of wind turbines.

6.2.2. Algorithm

An algorithm is developed to calculate time series of the aggregated wind power output in the Belgian power control zone. Apart from the wind speed time series at the three sites, the algorithm needs the following inputs:

- an arbitrary number of different turbine types, each with their typical power curve and hub height, and an estimate of the relative fraction of this turbine type with regard to the total installed wind power in the area;

- a '*turbine density*' along the Ostend-Brussels-Elsenborn axis, reflecting the geographical spread of the turbines. The user can specify, up to an arbitrary level of detail, whether the turbines are evenly spread over the control zone, or more concentrated at one or more place;

- an estimate of D, i.e. the width of the area over which the turbines are (evenly) spread, orthogonal to the Ostend-Brussels-Elsenborn axis, as a function of the position on this axis. Different functions for all different turbine types can be given;

- an assumption of the average *wind turbulence I* and average *roughness length* z_0, as a function of the position on the Ostend-Brussels-Elsenborn axis. The turbulence intensity [%] is defined as the standard deviation of consecutive instantaneous wind speed values, divided by the average wind speed. Common values vary from 5% to 20%. The roughness length [m] is a parameter that quantifies the landscape roughness (e.g. $z_0 \approx 0{,}0002$ m for sea surface, $z_0 \approx 1$ m in cities [51]).

The algorithm then does the following.

- For every x-position on the Ostend-Brussels-Elsenborn axis, the wind speed is recalculated using a linear interpolation from measured data. The wind speed is also recalculated according to the hub height of each turbine and the roughness length on the x-position, using:

$$v_{wind,h2} = v_{wind,h1} \cdot \frac{\ln \frac{h_2}{z_0}}{\ln \frac{h_1}{z_0}} \tag{6.1}$$

in which $v_{wind,h1}$ is the wind speed at height h_1, $v_{wind,h2}$ the wind speed at height h_2 and z_0 the roughness length.

- A '*multi-turbine power curve*' is calculated for every *x*-position on the Ostend-Brussels-Elsenborn axis and for every turbine type, as a function of *D*, wind speed turbulence *I* and the single turbine power curve of each turbine type. A multi-turbine power curve is a tool to estimate the aggregated wind power in a wide region with evenly spread wind turbines. The methodology assumes a normal distribution of simultaneous wind speeds in the region around a measurement site, with the mean value equal to the instantaneously measured wind speed. The standard deviation depends on the area width *D* and the wind speed turbulence *I*. The result is a smoothed power curve (Figure 6.1, discussed below). Full explanation on the multi-turbine curve methodology is given in [56] and [101].

- The time series for the wind power generation on each *x*-position on the Ostend-Brussels-Elsenborn axis are calculated for each turbine type, using the previously calculated wind speeds and multi-turbine power curves.

- The time series for the aggregated wind power generation in Belgium is then calculated, taking into account the '*turbine density*' given by the user.

- The generated power time series are assessed statistically to quantify the level and fluctuations of wind power output.

6.2.3. Scenarios for installed wind power in Belgium

Turbine types

Two existing turbines have been chosen as representative for the nowadays available technology. Figure 6.1a shows the power curve of a BONUS 600 kW-turbine [104], an example of a fixed speed, stall-controlled turbine; Figure 6.1b of a GE3.6-turbine, an example of a variable speed pitch-controlled turbine [105]. Generally speaking, the turbines of the lower power range (below approximately 1 MW) are mostly fixed speed stall-controlled, all having a power curve very similar to Figure 6.1a. The turbines of the higher power range are variable speed turbines with either pitch or active stall control. Both have a power curve as in Figure 6.1b.

Figure 6.1 also shows the multi-turbine power curve for both cases, for the example of $D = 200$ km (the area width) and $I = 15\%$ (turbulence intensity). The multi-turbine power curve is smoother than the original single-turbine power curve, especially in the high wind speed range. The distinction between both turbine types

becomes very vague when looking at a multi-turbine curve for large values of *D* and *I*.

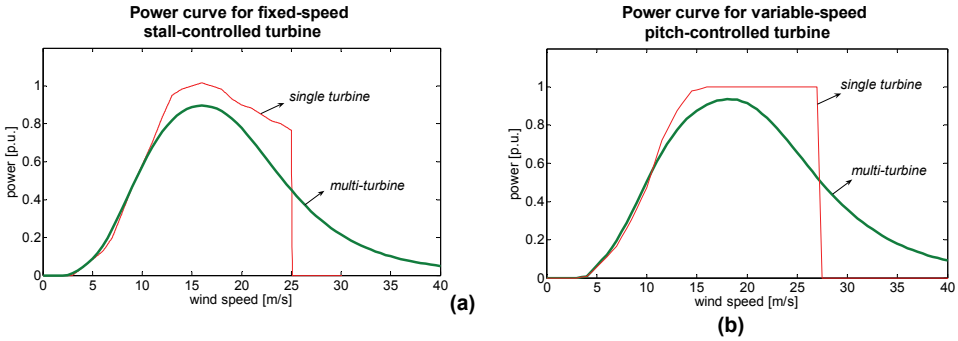

Figure 6.1. Typical power curves for a fixed speed stall-controlled turbine (a), and a variable speed pitch-controlled turbine (b): single and multi-turbine power curve

Scenarios for geographical spread of installed wind power in Belgium

Four scenarios for the '*turbine density*' are assumed, reflecting the geographical spread of wind power in Belgium (Figure 6.2):

Scenario I: even distribution - Figure 6.2(I)

- 50% of the installed wind power consists of fixed speed stall-controlled turbines with hub height 40 m;
- 50% of the installed wind power consists of variable speed pitch-controlled turbines with hub height 80 m;
- all wind turbines are evenly spread over the entire area.

Scenario II: concentration in the west - Figure 6.2(II)

- 60% of the installed wind power consists of variable speed pitch-controlled turbines with hub height 80 m (30% of the installed wind power) and 90 m (30%). These turbines are strongly concentrated in the western part of Belgium, i.e. the region with most wind resources;
- the remaining 40% of the installed wind power consists of fixed speed stall-controlled turbines with a hub height 40 m; half of this wind power is

installed in the western part of Belgium, the other half evenly spread over the rest of the area.

Scenario III: only offshore - Figure 6.2(III)

- one offshore wind farm is installed, consisting of variable speed pitch-controlled turbines with hub height 110 m. The farm width is 5 km. This scenario computes the fluctuation of the large offshore wind farm only, without taking into account possible other wind power onshore.

Scenario IV: on- and offshore - Figure 6.2(IV)

- 60% of the total installed wind power is offshore, as in *scenario III*;
- 40% is onshore, distributed as in *scenario II*.

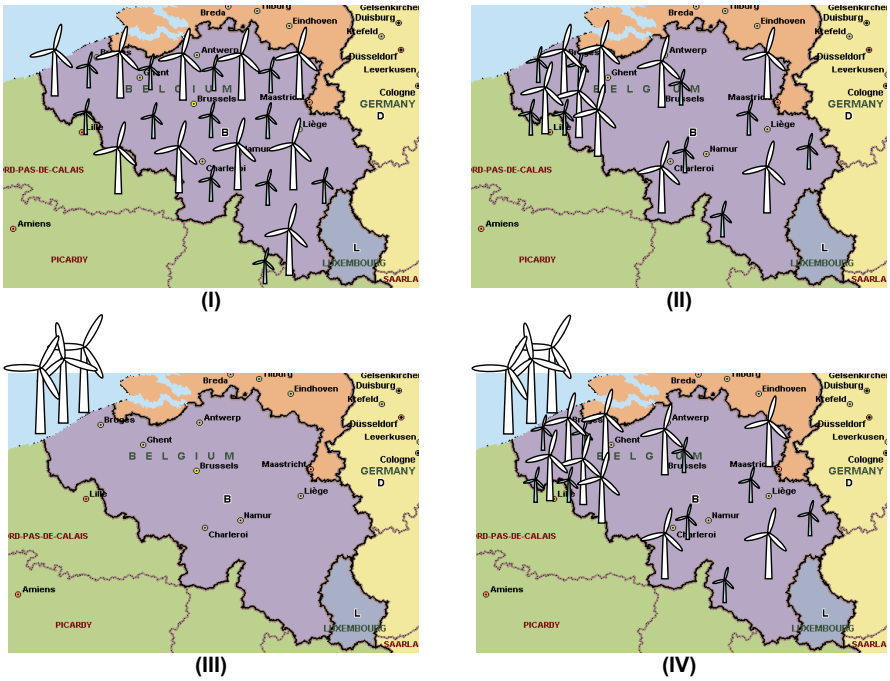

Figure 6.2. Four scenarios for geographical spread of installed wind power in Belgium

As further inputs for the algorithm, the average turbulence intensity I is estimated at 15%, which is a good estimate according to [52], and the roughness length z_0 varies between 0.3 m and 1 m along the Ostend-Brussels-Elsenborn axis onshore, and is estimated at 0.0002 m offshore.

The width D of the region in which the turbines are installed (for calculating the multi-turbine power curve), as a function on the position on the Ostend-Brussels-Elsenborn axis, is 200 km for *scenario I*, varies between 50 and 200 km for *scenario II*, and is 5 km for *scenario III*, the offshore farm scenario.

6.2.4. Results

Aggregated wind power time series

The output of the algorithm is a number of time series for the aggregated estimated wind power generation, as a percentage of the totally installed wind power, with hourly resolution.

Figure 6.3 shows, as an example, the power time series for each scenario, for the first three days of the considered period (2001-2003). It shows the lowest fluctuations for *scenario I*, and the highest for *scenario III*. Furthermore, the average power output is apparently the lowest with *scenario I* and the highest with *scenario III*. These are obvious results, considering the scenario parameters.

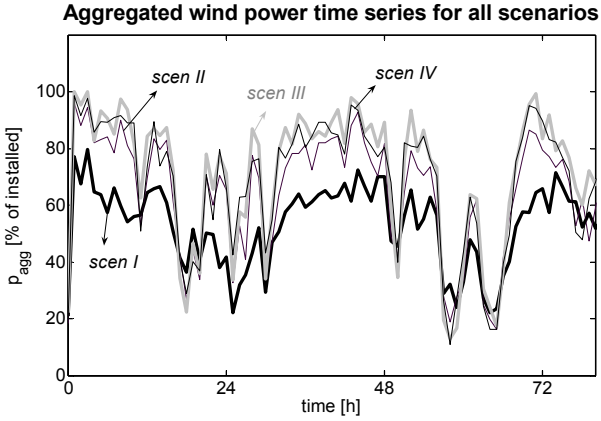

Figure 6.3. Aggregated wind power for all scenarios, for the first three days of January 2001

The resulting power time series are used to calculate histograms and power transition matrices, in order to quantify the power output level and fluctuations for each scenario.

Histograms of power generation, capacity factor

Figure 6.4 shows the histogram of the estimated wind power generation, as a fraction of installed wind power, for each scenario. The *x*-axis has interval widths of 1% of installed wind power. On the vertical axis, the average number of hours per year, in which the aggregated wind power generation falls in a given interval, is given. Note that this value for the power interval 0-1% is out of the figure range for each scenario.

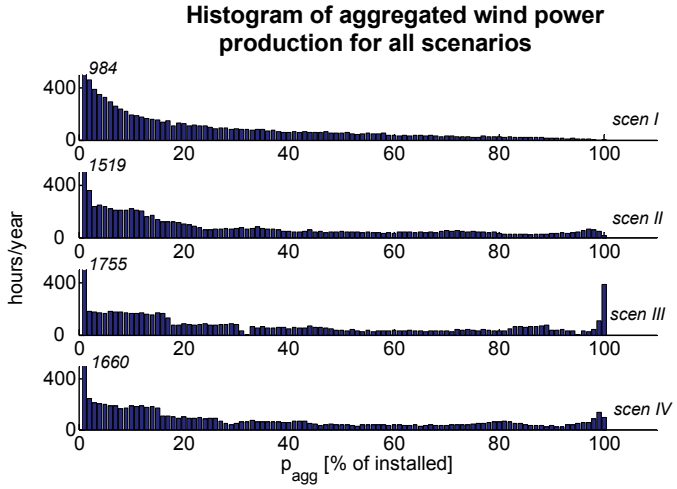

Figure 6.4. Histogram of the estimated wind power generation for each scenario

The average annual power generation, i.e. the capacity factor, and the number of non-operation hours for each scenario are given in Table 6.1. The capacity factor is lowest for *scenario I* and highest for *III*, as *III* faces the best wind resources. The capacity factor for this scenario, i.e. the offshore farm, is estimated at 31%, which is lower than the estimations by the project developers for an offshore farm in the Belgian North Sea (around 37% [21]). This may be explained by a possible underestimation of the offshore wind speeds. The measurements from Ostend were used, as offshore wind speed measurements were not available. Offshore wind speed estimates are further discussed in Chapter 7, however their accuracy and time resolution is insufficient to be used in this chapter.

The offshore wind farm has the highest number of non-operating hours as well as the highest number of full-load hours.

scenario	*capacity factor [%]*	*annual amount of non-operating hours*
I	20	984
II	26	1519
III	31	1755
IV	29	1660

Table 6.1. Annual capacity factor and annual number of non-operation hours for each scenario

Power transition and Markov matrices

Transition matrices and Markov matrices are considered as a suitable tool for statistical assessment of wind speeds ([102], [103], [106]). In the following, transition matrices are calculated for the aggregated wind power, rather than for wind speeds, being of more direct use for the TSO. The power transition matrices count the number of occurrences that the aggregated wind power generation falls in a specified interval, given the power generation in a previous time sample (1st-order transition matrix) or multiple previous time samples (higher order transition matrix). The width of the power intervals, as well as the time span between two samples, can be chosen freely. The power Markov matrices give the probability distribution for the aggregated wind power generation for a time sample, given the generation from the previous time sample.

Table 6.2 to Table 6.5 give the power transition matrices for the four scenarios, in which the power interval width is 20% of installed wind power, and the time span between two samples is 1 hour (hour *H* vs. *H-1*): consecutive samples from the generated power time series with hourly resolution are thus compared. The underlying greyscale plots in the matrices are graphical representations of the same matrices with power interval length of 1%.

scen. I		*Hour H*				
		0%-20%	**20%-40%**	**40%-60%**	**60%-80%**	**80%-100%**
Hour H-1	**0%-20%**	15024	1207	57	0	0
	20%-40%	1206	3132	794	28	1
	40%-60%	58	792	1806	367	5
	60%-80%	1	27	365	1031	115
	80%-100%	0	2	6	113	142

Table 6.2. Power transition matrix for *scenario I*

scen. II		Hour H				
		0%-20%	20%-40%	40%-60%	60%-80%	80%-100%
Hour H-1	0%-20%	13858	1217	200	85	42
	20%-40%	1228	1854	725	168	27
	40%-60%	212	725	961	525	57
	60%-80%	78	182	529	1343	374
	80%-100%	26	24	65	385	1389

Table 6.3. Power transition matrix for *scenario II*

scen. III		Hour H				
		0%-20%	20%-40%	40%-60%	60%-80%	80%-100%
Hour H-1	0%-20%	12199	1253	308	96	113
	20%-40%	1281	1462	741	270	101
	40%-60%	313	748	734	513	239
	60%-80%	95	292	507	557	540
	80%-100%	82	99	257	555	2924

Table 6.4. Power transition matrix for *scenario III*

scen. IV		Hour H				
		0%-20%	20%-40%	40%-60%	60%-80%	80%-100%
Hour H-1	0%-20%	12726	1299	243	126	74
	20%-40%	1322	1631	744	242	49
	40%-60%	256	731	812	559	137
	60%-80%	115	286	547	946	555
	80%-100%	49	41	149	576	2064

Table 6.5. Power transition matrix for *scenario IV*

All tables have their largest elements on the diagonals, meaning that the most probable wind power generation level for a given hour is approximately the same as in the previous one. Large diagonal elements are most pronounced for *scenario I*, and least for *scenario III*.

When normalising the power transition matrix, to make the sum in each row equal to 1, or 100%, the so-called '*1st-order Markov matrix*' is obtained, giving the probability that the aggregated wind power generation falls in a specified interval, given the power generation in a previous time sample. The 1st-order Markov matrices for *scenarios I* and *III* are shown in Table 6.6 and Table 6.7 respectively. Compared to the power transition matrices above, the greyscale images of the Markov-matrices show more clearly the differences between both extreme scenarios, and the extent to which the diagonal elements on the matrices are the largest. It is an obvious result that the single offshore wind farm (*scenario III*) has more power output fluctuations than the aggregation of the evenly distributed wind turbines (*scenario I*). According to Table 6.7, there is a 2%-chance that the power output of an offshore wind farm drops from 80-100% to below 20%. This can be caused by either a strong wind speed decrease or increase, exceeding the cut-out wind speed.

scen. I		Hour H				
		0%-20%	20%-40%	40%-60%	60%-80%	80%-100%
Hour H-1	0%-20%	92	7	0	0	0
	20%-40%	23	61	15	1	0
	40%-60%	2	26	60	12	0
	60%-80%	0	2	24	67	7
	80%-100%	0	1	2	43	54

Table 6.6. Markov matrix [%] for *scenario I*

scen. III		Hour H				
		0%-20%	20%-40%	40%-60%	60%-80%	80%-100%
Hour H-1	0%-20%	87	9	2	1	1
	20%-40%	33	38	19	7	3
	40%-60%	12	29	29	20	9
	60%-80%	5	15	25	28	27
	80%-100%	2	3	7	14	75

Table 6.7. Markov matrix [%] for *scenario III*

However, also in the optimal (but non-realistic) case of evenly distributed turbines (*scenario I*), it must be noted that fluctuations of 20% and more frequently occur from one hour to another. The beneficial effect of even distribution of wind turbines in a small region as Belgium (approximately 300 x 150 km²) must not be overestimated.

Higher-order Markov matrices can be calculated, taking into account the power values of multiple previous time samples, to find the probability distribution of the next time sample. In [106], it is stated that using 2^{nd}-order Markov matrices improves the accuracy of the statistical assessment only slightly, compared to 1^{st}-order.

Power transition and Markov-matrices do not model the natural daily periodical behaviour of wind speed and power, unless matrices of a very high order are used. This is not done in this work. The periodicity of wind power is discussed below.

Seasonal dependency and daily periodicity

Monthly average

There is a clear seasonal dependency of wind power, with the highest generation in late Winter (February) and the lowest in late Summer (August). Figure 6.5 shows the estimated monthly average wind power generation for the four scenarios. The difference between the lowest and highest monthly average is around 20% of installed wind power. The geographical spread of the turbines (i.e. the choice of scenario) does not have much impact on the amplitude of this seasonal periodicity.

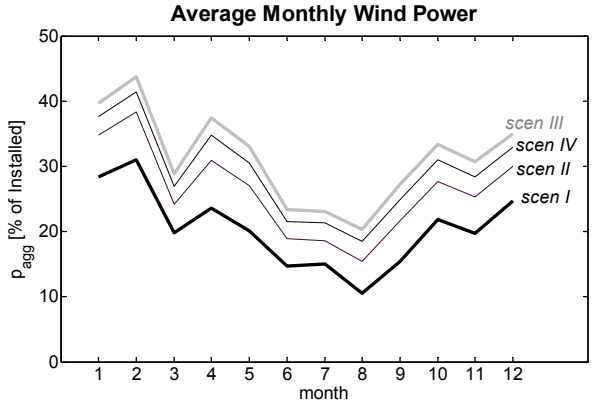

Figure 6.5. Average monthly aggregated wind power for all scenarios

Daily periodicity

Figure 6.6 shows the average, 10-, 50- and 90-percentile of wind power generation for every hour of the day, for Winter (December, January and February) and Summer (June, July and August), for *scenario I*. Figure 6.7 shows the same for *scenario III*. There is a daily periodicity of wind power, with a peak in the afternoon and a low generation in the early morning.

The degree of daily periodicity strongly depends on the season. The daily periodicity is most pronounced in Summer, where the difference between lowest and highest average generation is 10% (*scenario I*) or 20% (*scenario III*) of installed wind power. Spring and Autumn are similar, their characteristics being between Summer and Winter.

The geographical concentration of turbines, with the single offshore wind farm of *scenario III* as the extreme case, leads to a more strongly pronounced daily periodicity, as is seen when comparing Figure 6.6 and Figure 6.7.

Although the average generation in Winter is higher than in Summer, the 10-percentile (i.e. the value of hourly power generation exceeded in 90% of the cases) is higher in Summer. In Winter, this 10-percentile value is virtually zero all day, while in Summer, a peak generation in the afternoon of at least 5% can be 'guaranteed' with a reliability of 90%. This means that in Winter, when wind power generation is generally highest, the guaranteed minimum amount of generation is the lowest. The reliability of wind power generation is discussed further below.

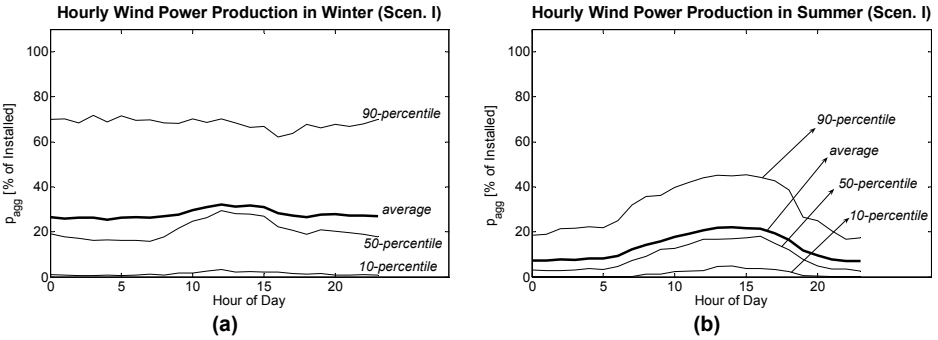

Figure 6.6. Average, 10-, 50- and 90-percentile of produced wind power, for every hour of day, Winter (a) and Summer (b), for *scenario I*

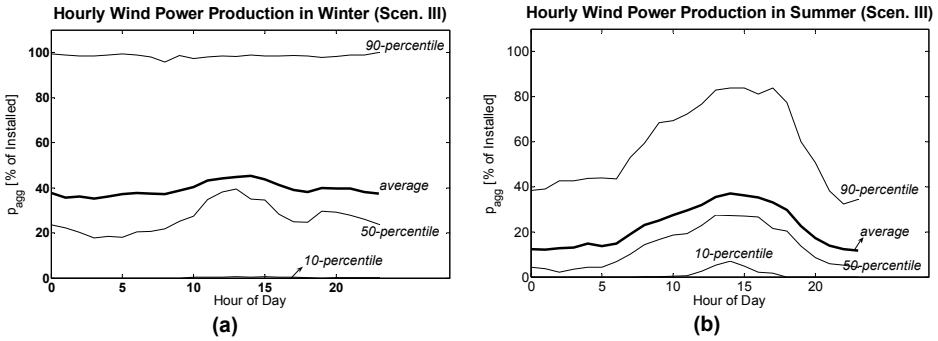

Figure 6.7. Average, 10-, 50- and 90-percentile of produced wind power, for every hour of day, Winter (a) and Summer (b), for *scenario III*

Seasonal histograms and transition matrices

Figure 6.8 shows the histograms of hourly power generation in Winter and Summer separately, for *scenario III*. Clearly, the number of hours with full wind power generation is highest in Winter (202 hours, i.e. almost 10% of the total Winter time). However, the average number of hours of complete wind calm in the three Winter months is still higher: 358 hours, representing 16% of the total Winter time. This indicates the binary behaviour of wind power generation in Winter: the most probable operation modes for a wind farm in Winter are either fully off or fully on.

In Summer, the number of hours with zero generation by the wind farm is equal to 540, representing almost 25% of the total Summer time. During 60% of the total Summer time, the wind farm power generation remains lower than 20% of its rated power. The number of hours with high wind power generation is very low in Summer.

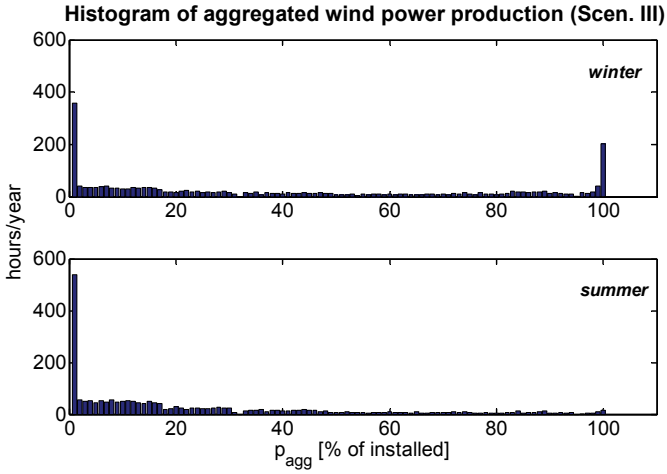

Figure 6.8. Histogram for estimated wind power for *scenario III*, for Winter and Summer separately

Table 6.8 shows the Markov-matrices for Winter and Summer for *scenario I*. Table 6.9 shows the same for *scenario III*. For both scenarios, not much difference between the seasons is noted.

Winter Scen. I		*Hour H* 0%-20%	20%-40%	40%-60%	60%-80%	80%-100%
Hour H-1	0%-20%	91	9	0	0	0
	20%-40%	21	61	18	0	0
	40%-60%	2	23	61	14	0
	60%-80%	0	1	19	71	10
	80%-100%	0	0	2	39	59

(a)

Summer Scen. I		*Hour H* 0%-20%	20%-40%	40%-60%	60%-80%	80%-100%
Hour H-1	0%-20%	94	6	0	0	0
	20%-40%	27	61	12	0	0
	40%-60%	3	29	60	7	0
	60%-80%	0	3	47	48	2
	80%-100%	0	0	0	50	50

(b)

Table 6.8. Markov-matrices [%] for Winter (a) and Summer (b), *scenario I*

To check daily fluctuations, the probability distribution of the aggregated wind power generation is calculated, given the wind power generation during the same hour of the previous day (hour *H* vs. *H*-24). The resulting matrices are shown for *scenario I* in Table 6.10 for Winter and Summer. Table 6.11 shows the same for *scenario III*. Note that, for *scenario III*, the highest two values of every row in the Winter matrix are in the first and last column, indicating the binary behaviour of the farm: it often occurs that a wind farm switches between zero and full generation or vice versa in a 24-hours time span.

Winter Scen. III	Hour H 0%-20%	20%-40%	40%-60%	60%-80%	80%-100%
Hour H-1 0%-20%	87	9	3	1	1
20%-40%	28	41	19	9	3
40%-60%	11	30	28	21	10
60%-80%	7	14	23	28	29
80%-100%	2	1	5	11	81

(a)

Summer Scen. III	Hour H 0%-20%	20%-40%	40%-60%	60%-80%	80%-100%
Hour H-1 0%-20%	88	9	2	1	0
20%-40%	37	38	18	5	2
40%-60%	13	32	29	19	7
60%-80%	4	17	32	27	20
80%-100%	2	4	12	22	61

(b)

Table 6.9. Markov-matrices [%] for Winter (a) and Summer (b), *scenario III*

Winter Scen. I	Hour H 0%-20%	20%-40%	40%-60%	60%-80%	80%-100%
Hour H-24 0%-20%	67	17	9	6	1
20%-40%	43	25	18	11	3
40%-60%	32	22	23	18	5
60%-80%	18	21	27	27	7
80%-100%	21	25	20	23	11

(a)

Summer Scen. I	Hour H 0%-20%	20%-40%	40%-60%	60%-80%	80%-100%
Hour H-24 0%-20%	82	14	4	0	0
20%-40%	60	26	12	2	0
40%-60%	50	26	21	3	0
60%-80%	42	23	26	8	2
80%-100%	0	0	100	0	0

(b)

Table 6.10. Markov-matrices [%] for Winter (a) and Summer (b), hour *H* vs. *H*-24, *scenario I*

For the Summer matrix, the by far largest elements in each row are all in the first column, indicating that, whatever the generation of the wind farm is, it is likely to decrease back below 20% after 24 hours.

Winter Scen. III	Hour H 0%-20%	20%-40%	40%-60%	60%-80%	80%-100%
Hour H-24 0%-20%	61	14	8	5	12
20%-40%	44	16	11	10	19
40%-60%	38	15	11	10	25
60%-80%	28	14	13	14	31
80%-100%	22	13	10	12	43

(a)

Summer Scen. III	Hour H 0%-20%	20%-40%	40%-60%	60%-80%	80%-100%
Hour H-24 0%-20%	71	14	7	4	5
20%-40%	56	19	12	8	5
40%-60%	49	21	13	9	8
60%-80%	39	20	15	11	14
80%-100%	42	20	15	10	14

(b)

Table 6.11. Markov-matrices [%] for Winter and Summer, hour *H* vs. *H*-24, *scenario III*

Summary of results

The simultaneous wind speeds at various locations in Belgium are strongly correlated. The beneficial effect of a geographical spread of wind turbines on the expected power fluctuations is proven in this work. *Scenario I*, the best-case scenario, shows clearly less fluctuating aggregated wind power generation than *scenario III*, the worst case with regard to wind power fluctuations. However, this effect should not be overestimated for a small area like Belgium. With a perfectly even distribution of wind turbines over the entire Belgian surface, hourly power steps over 20% of installed wind power still frequently occur.

The wind power generation depends on the season. In general, the average wind power generation is higher in Winter than in Summer. Also, the wind power generation shows a daily periodical behaviour, most pronounced in Summer, with the highest generation in the late afternoon and the lowest in the early morning. Both seasonal and daily periodicities more or less coincide with the normal load fluctuations in a power system, with the highest loads in Winter and in the late afternoon.

It must be noted explicitly that all calculations in this work assume a 100%-availability of the wind turbines. Furthermore, the wind turbines are considered perfectly resistant against minor grid disturbances, such as voltage dips or swells. It is of high importance that the grid operator issues sufficiently severe grid connection requirements that specify ride-through requirements for wind turbines in case of grid faults, as well as the obligation to provide grid support (e.g. voltage support by reactive power control) when demanded, as discussed in Chapters 3, 4 and 5. If wind power plants have insufficient ride-through capabilities, a higher occurrence of

sudden power drops can be expected, especially when the turbines are concentrated in a small area.

6.3. Value of aggregated wind power in Belgium

6.3.1. Capacity credit

Methodology

For each scenario described above, the capacity credit of the aggregated wind power is calculated. The definition of capacity credit was given in paragraph 4.4 and it is reminded here that its calculation requires knowledge of the *Loss of Load Probability (LOLP)* of the considered power system.

Information about the LOLP for Belgium is difficult to obtain, as, due to market liberalisation, information on expected loads and reliabilities of existing power plants is fragmented amongst various market participants and mostly confidential.

From [84] and from discussions with the Belgian TSO Elia, the model shown in Figure 6.9 is considered as a realistic approach for the LOLP. It shows the probability *H(D)* [hours/year] that the electrical demand exceeds the instantaneously available generation capacity by more than *D* [MW]. Negative values for *D* indicate the availability of surplus capacity. By definition, *H(0)* is the LOLP. Typical values for the LOLP in the Belgian control zone are between 4 and 25 h/year. This does not include power import from neighbouring countries.

The course of *H(D)* depends on the available power generation park, and the reliability of the individual power plants. For the Belgian case, it was discussed with Elia that *H(D)* is well approximated by an exponential function:

$$H(D) = H(0) \cdot \exp\left(-\frac{\lambda D}{Q_{peak}} \right) \tag{6.2}$$

with λ a decay factor, assumed equal to 30, and Q_{peak} the peak demand in Belgium, assumed equal to 13500 MW.

The addition of a new power plant to the existing power system results in a new course for *H(D)*, called $H_2(D)$.

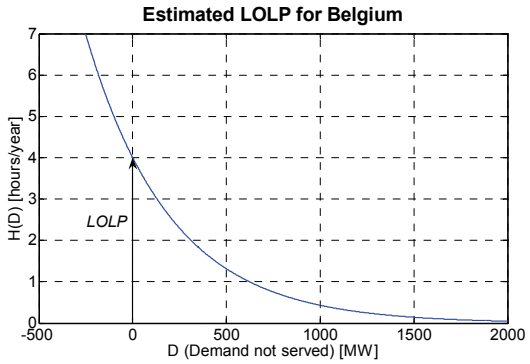

Figure 6.9. Estimated LOLP for the Belgian control zone

The following equation is valid for all D:

$$H_2(D) = \sum_{P_{plant}} H(D + P_{plant}) \cdot p\left(P_{plant}\right) \tag{6.3}$$

with $p(P_{plant})$ the probability that the new power plant produces at least the power P_{plant}. P_{plant} covers the entire power range that can be generated by the new plant.

The aggregated wind park, geographically spread according to one of the four scenarios described in paragraph 6.2, is considered as a single new power plant. The probability distribution P_{plant} is derived from the histograms such as Figure 6.4, considered over an entire year or for every season separately. Various assumptions for the total installed wind power in each scenario are made, ranging from 100 to 5000 MW.

Figure 6.10 shows, as an example, $H_2(D)$ when the generation park is extended with an aggregated wind park with installed power 1000 MW, spatially evenly distributed (*scenario I*).

As stated in paragraph 4.4, the value of wind power can be quantified in different ways. In Figure 6.10, the following quantities are marked:

- *Capacity credit*: the amount of conventional power plants that can be replaced by wind power without an increase of the LOLP. Assuming a 100% availability of the power plants replaced by wind turbines, the capacity credit is the horizontal distance between $H(D)$ and $H_2(D)$ at the level of the original LOLP. For the considered scenario in Figure 6.10, the capacity credit is equal to 175 MW.

- Amount of extra conventional power plants that would result in the same LOLP improvement as the installed wind power does. Assuming a 100% availability for the extra conventional power plants, it is given by the

horizontal distance between *H(D)* and $H_2(D)$ at the level of the new LOLP (170 MW in Figure 6.10).

- The improvement of the LOLP thanks to wind power, being 1.1% in Figure 6.10)

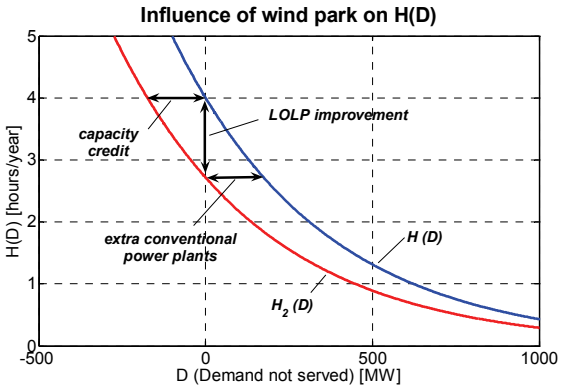

Figure 6.10. Influence of aggregated wind park on *H(D)*, for the case of evenly distributed turbines, installed wind power 1000 MW

Capacity credits for all scenarios

Capacity credit per year

Following the methodology described above, the capacity credit of the aggregated wind park in Belgium is calculated, for all scenarios of geographical spread introduced in paragraph 6.2, and installed wind power ranging from 100 MW to 5000 MW.

Figure 6.11 shows the capacity credits of the aggregated wind park in absolute (a) and relative (b) terms, for all scenarios of geographical spread introduced in paragraph 6.2.

It is concluded that the capacity credit of wind power decreases monotonically for increasing values of installed power, to below 10% for an installed power of 5000 MW. For low values of installed power, the capacity credit for a given scenario is well approximated by, although not equal to, the annual capacity factor as given in Table 6.1.

It is further noticed that the capacity credit for *scenario I* is the lowest of all scenarios for low values of installed wind power, but becomes the highest when the installed power increases. The benefit of the geographical spread of the turbines in

scenario I and the resulting smoothened power time series then outweigh the disadvantage of lower overall wind resources and the resulting lower capacity factor. This effect is however only noticed for very large values of installed wind power. It was already concluded in paragraph 6.2 that the beneficial effect of geographical spread must not be overestimated, as simultaneous wind speeds are highly correlated in the entire Belgian control zone.

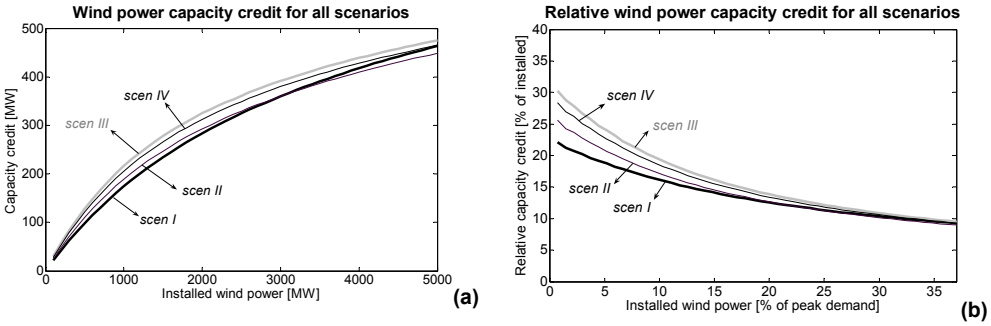

Figure 6.11. Capacity credit of aggregated wind park for all scenarios, in MW (a) and as percentage of installed wind power (b)

Capacity credit per season

The capacity credit for all scenarios is calculated per season separately. For this, the approximation is made that the LOLP of the original power system is constant in time. This means that, if the LOLP is 4 h per year, it is assumed equal to 1 h per season. The cumulative probability density of the wind power generation is recalculated for each season separately, based on the histograms as Figure 6.8.

The resulting capacity credit for all scenarios is given in Figure 6.12 for Winter (a) and Summer (b). For all scenarios, the capacity credit is higher in Winter than in Summer. The results for Spring and Autumn are between the extreme cases of Winter and Summer.

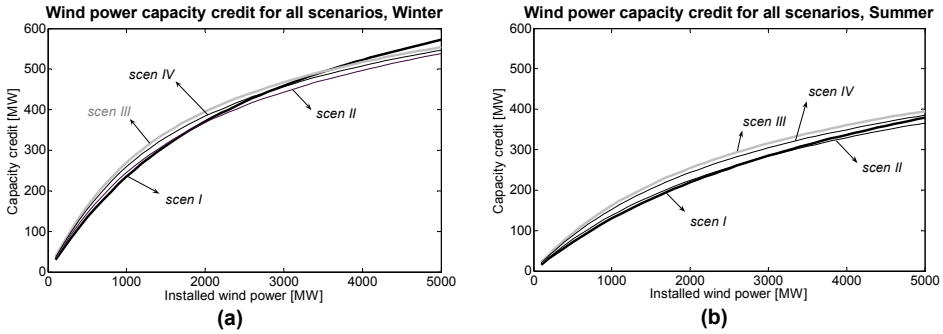

Figure 6.12. Capacity credit of the aggregated wind park for all scenarios, Winter (a) and Summer (b)

6.3.2. Reliable wind power generation during given time span

Methodology

An attempt is made to validate wind power, taking into account its fluctuating behaviour.

From the power time series in paragraph 6.2, matrices are calculated for each scenario, indicating the reliability with which a minimum relative amount of aggregated wind power is available during consecutive time samples, given the actual power generation. The number of consecutive time samples *t* during which the amount of wind power must be available can be arbitrarily chosen by the user.

Table 6.12 shows the wind power reliability matrices for *scenario I*, for a time span of 1 hour (a) and 6 hours (b) respectively. Table 6.13 shows the same matrices for *scenario III*. The matrices for a time span of 1 hour can also be derived from the Markov-matrices (Table 6.6 and Table 6.7).

The use of the matrices is illustrated by the following example: if the aggregated wind power generation in *scenario III* at a given hour is between 60% and 80% of the rated value, then the reliability for the power in the next hour not decreasing below 80% is 27%, not below 60% is 55%, not below 40% is 81% etc. (Table 6.13a). The reliability for the power not decreasing below 80% of rated within the next 6 hours is 5%, not below 60% is 15% etc. (Table 6.13b).

	scen. I	0%-20%	20%-40%	40%-60%	60%-80%	80%-100%
t = 1 hour	0%-20%	100	8	0	0	0
	20%-40%	100	77	16	1	0
	40%-60%	100	98	72	12	0
	60%-80%	100	100	98	74	7
	80%-100%	100	100	99	97	54

(a)

	scen. I	0%-20%	20%-40%	40%-60%	60%-80%	80%-100%
t = 6 hours	0%-20%	100	3	0	0	0
	20%-40%	100	39	4	0	0
	40%-60%	100	71	30	3	0
	60%-80%	100	91	68	33	1
	80%-100%	100	99	89	64	5

(b)

Table 6.12. Wind power reliability matrices for *scenario I*, for time span = 1 hour (a) and 6 hours (b)

The matrices from Table 6.12 and Table 6.13 are calculated using the power time series of the entire measurement period (2001-2003). Alternatively, they can be calculated for each season separately, using only power time series from a specific season. The power interval width in the matrices (20% in Table 6.12) can also be arbitrarily chosen.

	scen. III	0%-20%	20%-40%	40%-60%	60%-80%	80%-100%
t = 1 hour	0%-20%	100	13	4	1	1
	20%-40%	100	67	29	10	3
	40%-60%	100	88	58	30	9
	60%-80%	100	95	81	55	27
	80%-100%	100	98	95	89	75

(a)

	scen. III	0%-20%	20%-40%	40%-60%	60%-80%	80%-100%
t = 6 hours	0%-20%	100	4	1	0	0
	20%-40%	100	28	7	2	0
	40%-60%	100	47	18	6	2
	60%-80%	100	61	33	15	5
	80%-100%	100	78	64	49	33

(b)

Table 6.13. Wind power reliability matrices for *scenario III*, for time span = 1 hour (a) and 6 hours (b)

Time series of reliable wind power

From the time series of aggregated power for each scenario, calculated in paragraph 6.2, new time series are calculated, indicating the minimum wind power generation that is produced continuously during a given number of hours starting from the considered hour, with a given reliability. For this, the wind power reliability matrices described above are used, calculated for each season separately and with power intervals of 1% of installed wind power.

Figure 6.13 shows as an example the time series of the instantaneous wind power, as calculated in paragraph 6.2, for a Summer day (June 1st 2001) for *scenario I*. Furthermore, the instantaneous wind power levels continuously guaranteed with a 90% reliability for the next 2, 6 and 24 hours are plotted. A 90% reliability of the future wind power generation on a short term is considered a relevant requirement, still lower than the accuracy of the hourly load forecasts in a power system.

It is concluded that the reliable wind power rapidly decreases for an increasing time span. This is partially explained by the daily periodicity of wind power, which is most pronounced in Summer, as was concluded in paragraph 6.2.

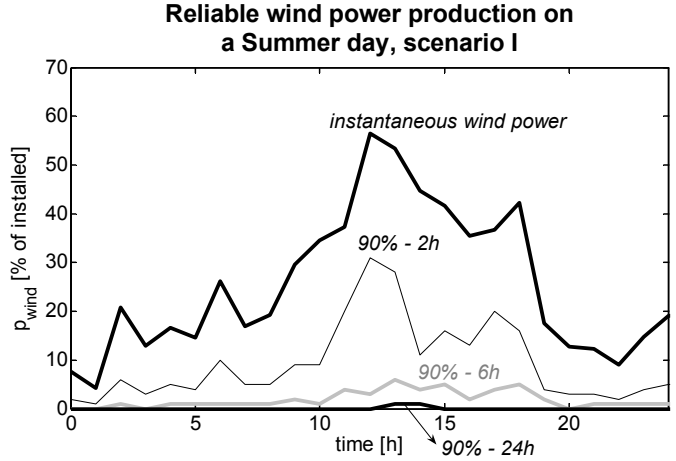

Figure 6.13. Estimated instantaneous wind power generation on a Summer day (June 1st 2001) and guaranteed wind power generation level (90% reliability) for the next 2, 6 and 24 hours

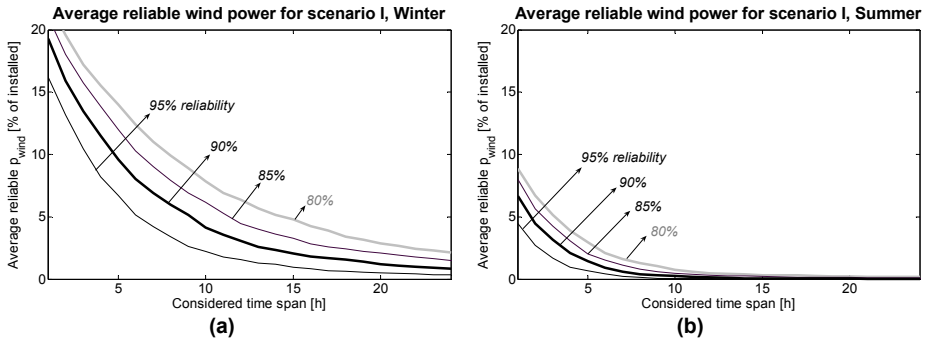

Figure 6.14. Hourly average reliable wind power generation for the Winter (a) and Summer (b) months of *scenario I*

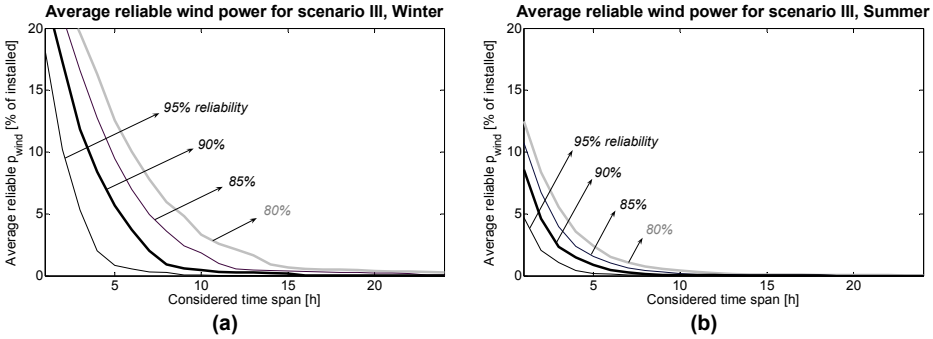

Figure 6.15. Hourly average reliable wind power generation for the Winter (a) and Summer (b) months of *scenario III*

Figure 6.14 shows the hourly average reliable wind power generation for the Winter (a) and Summer (b) months of *scenario I*, as a function of the time span, and for various levels of reliability. Figure 6.15 shows the same for *scenario III*. The results for Spring and Autumn, as well as the results for *scenario II* and *IV*, are between these for the extreme cases presented in the figures.

The figures lead to the following conclusions:

- the average reliable wind power generation in Winter is much higher than in Summer, for all scenarios and reliability levels;

- comparing *scenario I* with *III*, the average reliable wind power generation level is higher in *III* for relatively low reliability levels and short time spans. The decrease for increasing reliability level and time span is however much steeper in *scenario III*;

- for all scenarios and seasons, the reliable wind power generation during a time interval of 24 hours is very low, virtually zero for a single offshore wind farm (*scenario III*);

6.3.3. Potential abatement of CO_2-emission by wind power

Methodology

As a last attempt to quantify the value of wind power, the potential contribution of wind power to the abatement of the CO_2-emission by the power generation park in Belgium is estimated.

The results in this paragraph are calculated with the simulation tool *PROMIX*. *PROMIX* stands for '*Production Mix*' and refers to the composition of the electricity generation system in a particular control area. Based on the primary energy composition, the fuel costs and other zone-specific parameters, *PROMIX* calculates the cost-optimal use of the available power plants to cover the electricity demand in a control area. Also, patterns for the aggregated demand, with hourly resolution, are needed.

PROMIX also takes into account time, costs and emissions for starting up, shutting down or controlling a power plant of a given type, being an important input for determining continuously the optimal generation allocation. The power system generation pattern is thus simulated in a dynamic way, with a time step being one hour.

PROMIX analyses the impact of demand patterns on energy use and emissions in a given electricity generation system. The output consists of time series with hourly resolution of the electric power generated by each separate power plant, as well as the corresponding primary energy use, costs and emissions.

Potential grid bottlenecks within the control area, that could possibly obstruct optimal unit commitment schemes for the available power plants, are not considered. This is a reasonable assumption when considering Belgium only.

Also it must be noticed that *PROMIX* only calculates the generation pattern for covering the total system load, not taking into account the continuous need for primary and secondary reserve, which will however be influenced by future wind power. This is compensated by using the time series of reliable wind power rather than the time series of instantaneous wind power generation as input for *PROMIX*, as is discussed below.

More information about *PROMIX* is found in [107] and [108]. The development of *PROMIX*, as well as the fine-tuning of the large set of input parameters, is the main subject of the PhD thesis by Voorspools [108].

The input data for PROMIX are extensive, and not all listed here. The minimum and maximum hourly load in the Belgium control zone are respectively 5.9 GW and 13.5 GW (before compensation by pumped hydro storage). The available generation park in the Belgian control zone is given in Table 6.14 [109], subdivided by technology. In *PROMIX*, these categories are further subdivided. For instance, the classic thermal power plants are subdivided into 26 subcategories, depending on the fuel (liquid, solid, gas or combined), heat carrier (steam, gas) and the thermodynamic cycle (Rankine, Brayton, combined), each with their unit sizes, and typical starting/stopping times, controllability, fuel consumption and emissions.

Generation technology	***Installed capacity [MW]***
Nuclear	5801
Classic thermal	6800
Biogas	26
Waste	201
Combined heat and power	1341
Hydro (storage excluded)	108
Pumped storage	1307
Wind	93
Total	***15677***

Table 6.14. Generation capacity in the Belgian control zone (2004)

The existing *PROMIX* tool with its input data is used as a start to assess the impact of wind power on the total CO_2-emission. The already installed wind power (93 MW in 2004) is subtracted from the *PROMIX* input, in order to find the total CO_2-emissions by the generation park without wind power as a reference value.

The way in which wind power injection is considered in the power system is not straightforward. For small penetration ratios of wind power, all injected wind power can be considered as an equal reduction of the total system load for every time sample. For larger amounts of wind power, the system load is not decreased to the same extent as the wind power injection. Due to the relatively low reliability of continuous wind power injection during consecutive hours found above, various power plants in the system have to remain stand-by during high wind power injection. The time series of equivalent load decrease due to wind power injection are then better approximated by time series of reliable wind power generation for a given time span, an example of which was given in Figure 6.13.

Results

The CO_2-emission abatement is calculated for *scenarios I* and *III*, the two extreme scenarios, as a function of installed wind power. The installed wind power is normalised by the system peak demand, being 13500 MW in the Belgian control zone. The total CO_2-emission calculated by *PROMIX* without taking wind power into account is $26 \cdot 10^6$ ton/year, used as a reference to calculate the relative emission abatement.

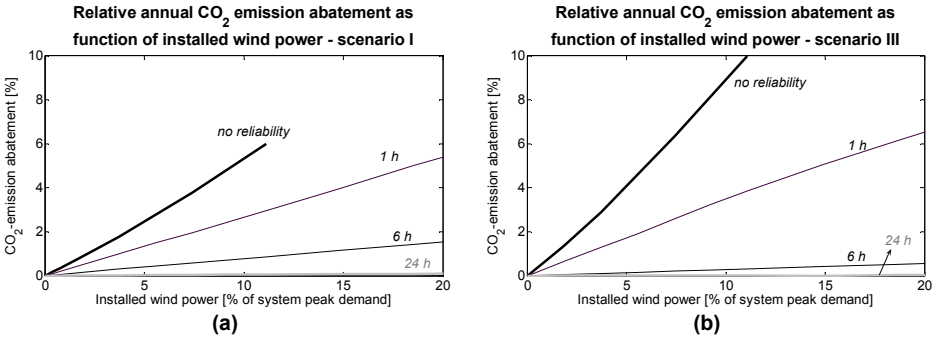

Figure 6.16. Relative annual CO_2-emission abatement as a function of installed wind power, *scenario I* (a) and *scenario III* (b)

Figure 6.16 shows the various estimates, depending on the time span for wind power reliability, for the CO_2-emission abatement as a function of installed wind power for *scenario I* (a) and *III* (b). The '*no reliability*' – plot shows the relative abatement of CO_2-emission abatement by the total Belgian generation park, considering the time series of produced wind power itself as equivalent negative load. This plot is only

calculated for installed wind power up to 10% of system peak load, as higher wind power penetration implies an extensive reorganisation of the entire generator park and unit commitment decisions, due to the increased power reserve requirements, making the input data and algorithms used by *PROMIX* less relevant.

The other plots in Figure 6.16 take only the reliable wind power into account for a time span shown in the legend and a reliability level of 90%, which is considered as relevant, however still lower than the average predictability of the total system load.

The results lead to the following conclusions.

- The estimates of the CO_2-emission abatement by wind power strongly depend on the assumed or required reliability levels for continuous wind power generation. The absolute upper limit for relative CO_2-emission abatement by wind power is 10%, occurring in the case of a single offshore wind farm (*scenario III*) representing around 10% of the total system peak demand, with no required reliability for continuous wind power feed-in.

- When taking the instantaneous wind power generation fully into account, or when only 1 h continuous reliable wind power generation is required, the single offshore wind farm from *scenario III* has a higher emission abatement potential than the evenly distributed turbines from *scenario I*, due to the better wind resources.

- When a reliable continuous wind power production for a long time span (6 h – 24 h) is required, the potential CO_2-emission abatement strongly decreases. The best results are then obtained in *scenario I*, e.g. 1.7% for an installed wind power of 20% of system peak demand, and a reliability time span of 6 hours.

The required time span of reliable wind power generation, as a function of installed wind power, is very difficult to assess unambiguously. In the limit case of a very low value of installed wind power, all instantaneous generation can be considered as negative load, leading to the highest relative estimates of emission abatement. For higher wind power penetrations, the required reliability of wind power must be considered against the available generation park in Belgium from Table 6.14.

From the generation capacity in this table, only the pumped storage and the classic thermal power plants provide the availability to regulate the power output in an economically viable way. Pumped hydro storage can control its energy output within a very short time span (minutes). Classic thermal plants need 4 to 24 hours to cover their entire control range, depending on the subcategory. Turbojets that serve especially to cover peak demand can be put into operation within less than one hour, but consume a high amount of fuel. Their use should be limited to some hours per year.

To the author's view, only the pumped hydro storage can be considered as a resource to compensate for the instantaneously fluctuating wind power generation. A more intense use of the entire operating range of classic thermal plants, thus

frequently deviating from their optimal operation regime, would lower their overall efficiency to such an extent that the effect of wind power on emissions is reversed: higher needs of reserve generation capacity increase the emissions more than the decrease realized by wind power generation. Furthermore, when the required energy reserves must be supplied by the classical thermal plants needing some hours to control their power output, a 90%-reliability level of continuous wind power generation for at least one hour, but more realistically four to six hours, is required.

The absolute upper limit of wind power generation that can be considered as arbitrarily fluctuating negative load is thus 1300 MW (i.e. 10% of the system peak demand), being the total capacity of pumped hydro storage plants in the Belgian power system. However, the total capacity of 1300 MW is only available for a maximum duration of 4 h when the hydro buffers are full. Furthermore, a more intense use of the hydro storage for compensating wind power fluctuations limits its availability for classic peak load shaving and as a primary and secondary reserve resource.

Taking a roughly estimated safety margin into account, the allowed level of installed wind power without reliability requirements can cover half of the maximum hydro storage capacity, around 5% of system peak load. For this level, the estimated potential of CO_2-emission abatement ranges from 2% (*scenario I*) to 4% (*scenario III*). When reliable wind power is required, this abatement level is only exceeded when the installed wind power is at least doubled and when a reliability for only one hour is required. For lower values of installed wind power or with higher reliability requirements, the emission abatement never exceeds 4%; this level is therefore considered as a realistic maximal potential contribution of wind power to CO_2-emission abatement.

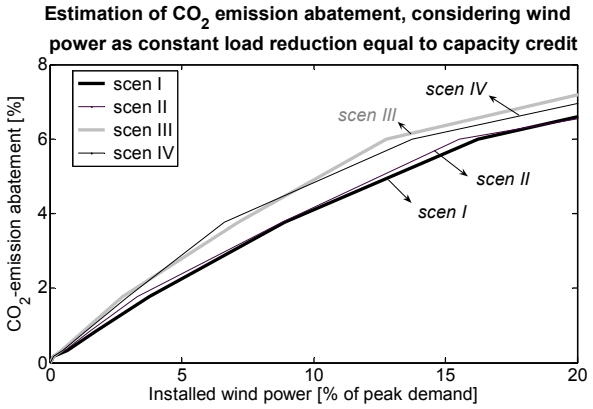

Figure 6.17. Estimated CO_2 emission abatement by the aggregated wind park for all scenarios, by considering wind power as constant load reduction equal to its capacity credit

As a final attempt to estimate the emission abatement by wind power, simulations in *PROMIX* are performed in which the load time series are decreased by a constant value, equal to the capacity credit of the aggregated wind park shown in Figure 6.11.

The resulting estimated relative CO_2-emission abatement is shown in Figure 6.17 for all scenarios of geographical distribution of wind power. The results are of the same order of magnitude as those found above, well situated between the most optimistic and most pessimistic estimates from Figure 6.16.

It is concluded that the realistic potential of CO_2-emission abatement due to wind power is estimated at 2% to 4% of the emissions by the total generation park in the Belgian control area (excluding already installed wind power). This level is realised for an installed wind power of 5% of the system peak load, i.e. around 0.7 GW. The abatement level of 4% is achieved in *scenario III*, the scenario with the single offshore wind farm, as this scenario faces the best wind resources. The total amount of avoided CO_2-emissions is then $1.04 \cdot 10^6$ ton/year, or $1.54 \cdot 10^3$ ton/year per installed MW.

As already mentioned above, the beneficial effect of the even spatial distribution of wind power from *scenario I* on the increased reliability levels of wind power becomes only apparent for higher levels of installed wind power. However, as higher levels of installed wind power again require a higher reliability of continuous power generation, at least for some hours, the estimated emission abatement does not exceed 4%.

Therefore, it is concluded that the recommended policy with regard to the abatement of CO_2-emission is to allow wind power, preferentially offshore, up to a level of approximately 0.7 GW. When this level is achieved, the added value of further installing offshore or onshore wind power is very low. It must be noticed that an installed power of more than 600 MW offshore would also confront the transmission capability of the Belgian power system with its limits, as discussed in the Chapter 7.

Costs of CO_2-emission abatement by wind power

Concerning the costs of CO_2-emission avoidance by wind power, it is noted that the installation cost of wind power strongly depends on project-specific parameters. In [110], the cost estimates range from 800 euro/kW (onshore) to 1850 euro/kW (offshore). In [XVI], it is between 900 and 2400 euro/kW for offshore wind power, as discussed in Chapter 7. For wind turbines of state-of the-art technology, the annual operation and maintenance costs are estimated between 1.5 and 2% of the investment costs ([51], [XVI]).

The annual CO_2-emission abatement is estimated above at $1.54 \cdot 10^3$ ton per installed MW. Given these data, and assuming a turbine lifetime of 20 years, the estimated cost of CO_2-emission abatement ranges between 36 euro and 105 euro/ton. This does not include the costs of unexpected turbine failures, neither does it include the costs of optional grid reinforcements or increased reserve requirements.

For comparison, the costs of CO_2-emission abatement are estimated by the DENA-study at 104.7 euro/ton (in 2007) to 58.9 euro/ton (in 2015) [4], which corresponds well with the results found in this work.

For further comparison, the market price of *EU Emission Allowances* (*EUAs*) that are traded until July 2005 is shown in Figure 6.18 [111]. EUAs are traded within the *EU Emission Trading Scheme* (*EU ETS*), which formally entered into operation on January 1 2005. However some companies started engaging in demonstration trades of spot and forward EUAs in anticipation of entry into force of the EU ETS [112]. One EUA is the allowance of emitting one ton of CO_2-equivalent greenhouse gas. The allowances are issued by the Member States, following the European Directive 2003/87/EC [113], and can be traded internationally amongst the exploiters of CO_2-emitting installations.

The EUA price has steeply increased during the first half of 2005, with a maximum price of 29 euro (Figure 6.18). This instable price indicates that the EU emission trading scheme has not yet reached the state of maturity, although it is stated in [112] that the EUA market price at a given point in time is almost unique, with very low spread in the price of individual transactions. Until July 2005, the EUA market price is clearly lower than the estimated costs per ton of CO_2-emission abatement by wind power calculated above, indicating that cheaper technologies exist for emission abatement. These technologies are mainly the optimisation of industrial processes, and the optimisation of classic thermal power plants, leading to higher efficiencies and lower emissions per unit of energy output.

Figure 6.18. Market price for EU emission allowances (EUAs) for use in 2005 [111]

6.4. Conclusions

Results for aggregated wind power time series

Based on calculated time series of aggregated wind power in Belgium, this chapter discusses the average wind energy output, as well as its fluctuations within hours to days. Making abstraction of grid bottlenecks and the dynamic behaviour of wind turbines during abnormal grid conditions, only the total wind power output is considered.

Wind speed measurements at three sites in Belgium with hourly resolution over a period of three years (2001-2003) are used as input. An algorithm for calculating the aggregated wind power on a solid theoretical basis is developed. Four scenarios for the spatial distribution of wind turbines are considered, ranging from evenly distributed across the entire Belgian control zone to all concentrated in a single offshore farm.

Estimates for the annual capacity factor of the aggregated wind park range from 20% (evenly distributed turbines) to 31% (single offshore farm).

Special attention is given to the characteristics of the fluctuations of the aggregated wind power injection. They are quantified by Markov-matrices for every scenario, for different time intervals. It is concluded that the beneficial effect of spatial distribution of wind turbines on the smoothening of power generation is proven, but should not be overestimated, as the simultaneous wind speeds in Belgium are all strongly correlated. Fluctuations of more than 20% of installed wind power within an hour frequently occur, around 20% of the time, for the most optimistic scenario of evenly distributed wind turbines. Over a time span of 24 hours, the wind power output may fluctuate over its entire range. Especially in Winter and for the scenario of a single offshore wind farm, the power output frequently switches from 0% to 100% of installed wind power and vice versa within 24 hours.

The periodical fluctuations of wind power are considered as well. It is concluded that the highest wind power output occurs in Winter and the lowest in Summer. The daily periodicity of wind power is most pronounced in Summer, with the highest generation late afternoon and the lowest early morning. The average difference between lowest and highest generation during a day is 10% to 20% of installed wind power, depending on the spatial distribution of the turbines. The daily periodicity is virtually inexistent in Winter.

Results for the value of wind power

The value of wind power is quantified in three ways:

1) capacity credit of the aggregated wind park;

2) instantaneous reliable wind power generation for various reliability levels;

3) potential CO_2-emission abatement.

The *capacity credit* of the aggregated wind park is calculated using a simplified model for the *Loss of Load Probability* for the existing generator park in Belgium. It ranges from 30% for very low values of installed wind power to 10% for very high values (up to 5000 MW). However, as was already mentioned in Chapter 4, the capacity credit only uses the probability distribution of wind power injection as input, without taking into account the extent of fluctuation between the various wind power injection levels, which is however a fundamental characteristic with regard to power system management. Therefore, the capacity credit alone does not reveal all information on the value of wind power.

The *reliable wind power generation* is determined using the time series of aggregated wind power calculated. For every hour of the time series, the wind power continuously available for a given duration after the considered hour, with a given reliability, is calculated. These time series of reliable wind power are calculated for every scenario of spatial turbine distribution, for time spans ranging from 1 to 24 hours and for reliability levels from 80% to 95%. The average reliable wind power highly depends on the scenario for spatial distribution, season, and required reliability level and duration. For every scenario, the reliable wind power generation is virtually zero if a duration of 24 hours is considered.

The *potential of wind power to reduce the CO_2-emissions* by the entire generator park in the Belgium control zone is quantified using the simulation tool *PROMIX*. The way in which wind power is considered in the simulation of the entire Belgium power system is not unambiguous. For very low wind power penetration, it can be considered as equivalent negative load. For higher penetration levels, the equivalent load reduction is lower than the instantaneous wind power injection, due to the increased need for primary and secondary reserve. The time series of reliable wind power, calculated above, are then considered as the equivalent load reduction. The duration during which wind power must be available with a given reliability increases for increasing levels of installed wind power. This must be considered as a function of the assembly of the available generator park in Belgium. Only a limited fraction of the available generator park, i.e. the pumped storage and to a lesser extent the classic thermal plants, can be rapidly controlled over a wide operation range and can compensate for both the fluctuating system load and wind power injection. It is assumed that from a wind power installation level of 5% of peak demand, the reliable wind power must be considered as equivalent load reduction, rather than the instantaneously produced wind power.

As a global conclusion, the CO_2-emission abatement potential by wind power is estimated at 4% ($1.04 \cdot 10^6$ ton/year) of the total CO_2-emission by the Belgian generator park. This is realised when the installed wind power is 5% (0.7 GW) of the system peak load and situated offshore. Higher levels of wind power installation

do not result in a higher emission abatement due to the higher required reliability levels. The even distribution of turbines over the entire control zone only results in higher reliable wind power levels than the offshore case for very high values of installed power. However, for these values, the reliability requirements for wind power increase as well, especially the number of consecutive hours during which the wind power must be available, resulting in the conclusion that the emission abatement potential by a spatially evenly distributed wind park always remains below 4%.

Therefore, if the abatement of emissions is considered as the most important value of wind power, the recommended policy is to allow wind energy up to an installed level of 0.7 GW, preferentially offshore or where wind resources are optimal. The added value of further installation of wind power is low. The estimated costs of emission abatement by wind power strongly depend on the project-specific installation costs, but range between €36 and more probably €105 per ton of avoided CO_2-emission, without taking the costs of possible grid reinforcements into account.

Final remarks

This chapter has made abstraction of various aspects.

- The value of wind power may increase when larger control areas are considered. However, the transmission bottlenecks in the UCTE-grid limit the exchangeability of wind power over control areas large enough to fully take profit of spatial distribution of wind turbines. It is assumed that every control zone in the UCTE-area must be responsible for its own instantaneously available power reserves; also when influenced by wind power.

- The impact of different market mechanisms is not discussed. It is assumed that all available wind power in Belgium is injected in the system, and that the remaining system demand is covered by the available power plants in the most efficient way.

- The impact of wind speed forecasts is not taken into account. As discussed in Chapter 4, wind power forecasting sees a very promising evolution, but is still considered not accurate enough for solid grid management. The most difficult aspect of wind power forecasting is predicting the moment at which increases or decreases of wind power occur, which is a very critical aspect for power system operation. Further research concerning the impact of wind power forecasts on the wind power reliability is however recommended.

- The dynamic short-term behaviour of wind turbines, as discussed in Chapter 5, is neglected: the turbines are considered perfectly resistant to

grid disturbances. Furthermore, a 100% availability of the turbines is assumed, which is, especially for offshore turbines, a very severe requirement.

- Instead of considering only control capacities of the available generator park, also the potential of active demand side management as complementary to the fluctuating wind power production must be investigated. This is not done in this work, but is a recommended subject for further research.

Chapter 7

Prospects for offshore wind power in Belgium

7.1. Introduction

The prospects for offshore wind energy in the Belgian Continental Shelf (BCS) have been the subject of a joint study supported by the Federal Government of Belgium [5]. The report of the full study is available in reference [XVI]. A summarising paper is given in [XIII].

The study looked into the site-specific physical and zoning opportunities and constraints and into the scope and limitations with respect to integration in the Belgian high-voltage grid. Besides, it has taken into account expected developments of offshore wind energy until the year 2015. Due to the multidisciplinary nature of the study and the consecutive large extent of results, this chapter can only aim at presenting a summary review of the overall work. The availability of resources will be discussed with regard to the available area in the Belgian North Sea territory, the wind resources, and the availability of the high voltage grid to absorb wind power. Then the total offshore wind power potential is discussed, with an estimate of the costs.

7.2. Resource availability

7.2.1. Available area in the Belgian North Sea territory

The Belgian Continental Shelf (BCS) is protruding at maximum some 70 km out of the Belgian coast, with a total surface of 3600 km². It has borders with the sea zones connected to The Netherlands, France and UK.

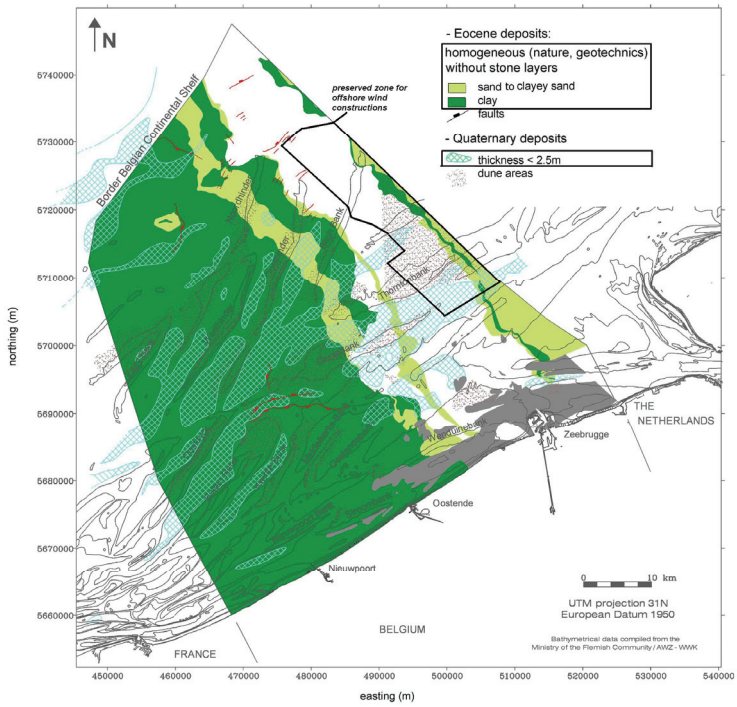

Figure 7.1. Map of the subsoil of the BCS. The areas with quaternary deposits layer thickness < 2.5 m in Eocene sand layers are considered the most suitable for the case of monopile turbine foundations.

From the geological point of view, determining which zones of the BCS are suitable for offshore wind constructions is difficult because of the large number of parameters, especially the type of foundation chosen (monopile, tripod or gravity based structure) and their further technological developments. Therefore, a sound

knowledge base of the most relevant geo-parameters has been developed and maps have been provided with the spatial distribution [114]. Combinations of various parameters are possible, enabling to produce scenarios, for example according to the type of foundation selected. Only as an example, Figure 7.1 indicates the most suitable areas when monopile foundations are considered, being the areas in Eocene sand layers (rather than clay) where the quaternary deposits layer thickness is less than 2.5 m. Also the zone that is actually preserved by the government for wind farm constructions is indicated. This preserved zone has an area of 270 km². This figure only considers the seabed properties and leaves the water depth out of consideration. The water depth in the BCS is shown in Figure 7.2 (as far as data are available).

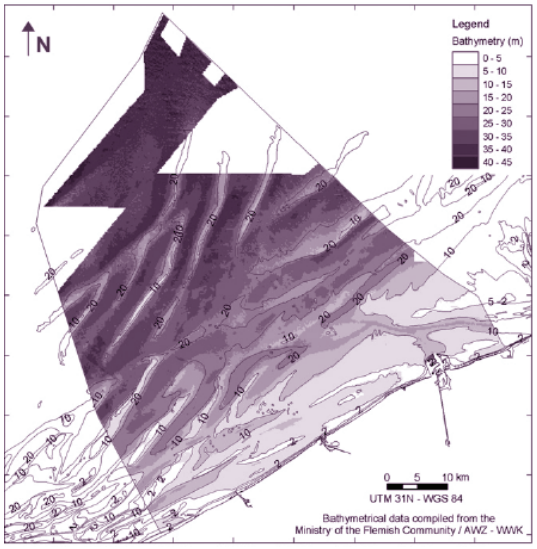

Figure 7.2. Water depth in the BCS

Figure 7.3 shows the main zones of the BCS preserved for other activities, and thus excluded for wind farm constructions. The zone within three nautical miles from the coast is by default excluded, as it is unlikely that the visual impact of a near-shore wind farm will be accepted by the public opinion.

The research in [XVI] leads to the conclusion that an area of at most 2100 km² remains theoretically available for offshore wind activities. The nowadays designated area is 270 km².

Concerning specific projects, the C-power offshore wind project which is in a far planning stage at the moment of writing consists of 60 turbines of 3.6 MW [21], and is situated at the Thornton Sandbank, in the designated area.

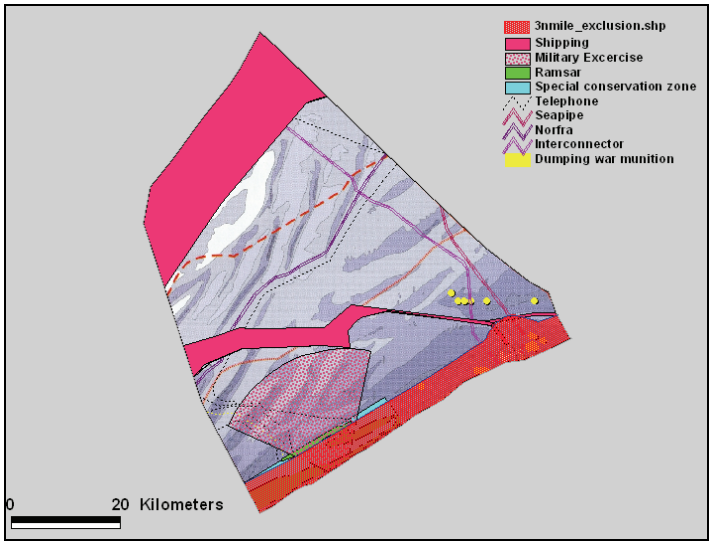

Figure 7.3. Map of the BCS, with exclusion zones for wind farms

7.2.2. Wind resources

The wind mapping is based on the POWER method, a software tool for offshore wind mapping in the European seas developed within the European RTD project JOR CT-98-0268 [115]. The distribution over the BCS of the long-term average wind speed has been derived from seven data positions of the POWER database and linearly interpolated as function of the distance from the coastline. Maps of the average wind speed have been constructed with a resolution of 1x1 km and for five relevant altitudes, from 70 to 150 m for the whole BCS. The resulting long term average wind speed varies between 8.4 m/s at 70 m height near the coast to 10.1 m/s at 150 m height far offshore. In the preserved zone for offshore wind energy, the values vary between 9.1 and 10.0 m/s, depending on altitude and distance from the coast. In the first 20 km from the coast, the average wind speed increases relatively fast with distance, while from 20 km distance on the increase it is very modest. These results are compatible with the data from the meteorological station of Ostend, discussed in paragraphs 4.2 and 6.2, assuming a roughness length in Ostend of 0.4 m.

In addition, the increase of wind speed with height is very moderate from 70 m altitude onwards. In this respect, it is recommended to try to exploit the resource not too far offshore and to be modest with tower heights.

7.2.3. Availability of high-voltage grid

A high amount of wind power injection at the high-voltage substations at the Belgian coast, being Koksijde, Slijkens or Zeebrugge, may have an impact on the risk of *system overload*, *(N-1)-contingency* and *static voltage instability*. This has been investigated by performing static load-flow calculations. *System overload* occurs when the transmitted power through certain lines or transformers is above the capacity of these lines or transformers. *(N-1)-contingency* means that the failure of one single element in the system may not cause a succession of other failures, leading to a total system collapse. Together with avoiding constant overloading of grid elements, (N-1)-contingency is a main concern for the grid operator. *System static voltage instability* may be caused by a high reactive power demand of wind turbine generators. When induction generators are used, the reactive power demand can be as high as 40% of the generated active power. Options for wind turbine generator types are discussed in paragraph 4.3. Generally speaking, a high reactive power demand causes the system voltage to drop. The static load flow calculations study the system voltage at steady state.

For the static load flow calculations, a worst case scenario has been used, i.e. wind turbines equipped with induction generators without compensation for the high reactive power demand, injecting their power in the high voltage substation of Koksijde, Slijkens or Zeebrugge. As further input, a model of the Belgian high-voltage-grid, shown in Figure 7.4a is used. This model includes every Belgian node in the range from 400 kV down to 70 kV and also the main nearby foreign nodes. Figure 7.4b shows a close-up on the high-voltage grid near to the coast, with the three coastal 150kV-substations indicated. The arrows represent injections of offshore wind power, and the power flow further inland.

The parameters of lines, transformers and capacitor banks are known and included in the model. For the load and generation pattern, 24 reference scenarios are considered, representing peak and off-peak situations in Winter, Summer, day and night. The highest peak load (Winter weekday) in Belgium is assumed to be 13.5 GW, the lowest off-peak load (Summer weekend night) 5.9 GW. Furthermore, the international power flows, e.g. from France to the Netherlands, partially passing through Belgium and partially through Germany, are taken into account. This international power transit is modelled by an extra power flow from the nodes Avelin (F) to Avelgem (B) and from Lonny (F) to Achène (B), ranging from 0 MW (level ‘T1’) gradually to 2000 MW (level ‘T5’) in steps of 500 MW, and an extra power demand at the Dutch border nodes.

The impact of a grid reinforcement in the coastal region, i.e. a cable link between Koksijde and Slijkens, is studied. This link will be in operation by the time of possible production from offshore wind turbines. Also the impact of a reinforcement of the Rodenhuize-Heimolen connection, further in-land, is studied.

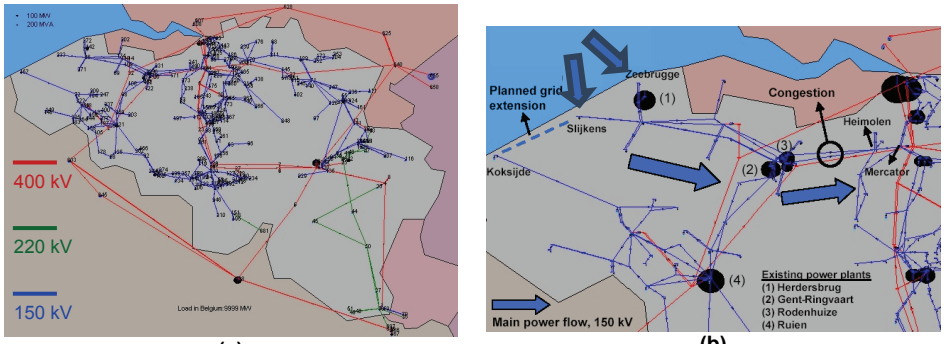

Figure 7.4. Belgian high-voltage grid (a) and close-up on coastal region (b)

Given all input data, the maximum power injection that can be injected in the coastal nodes before system overload or *(N- 1)*-contingency problems occur is calculated. Static voltage instability appeared never to occur, even not when uncompensated induction generators are used for the wind farms. This maximum power injection depends on the scenario for load and generation pattern, and for cross-border power flows.

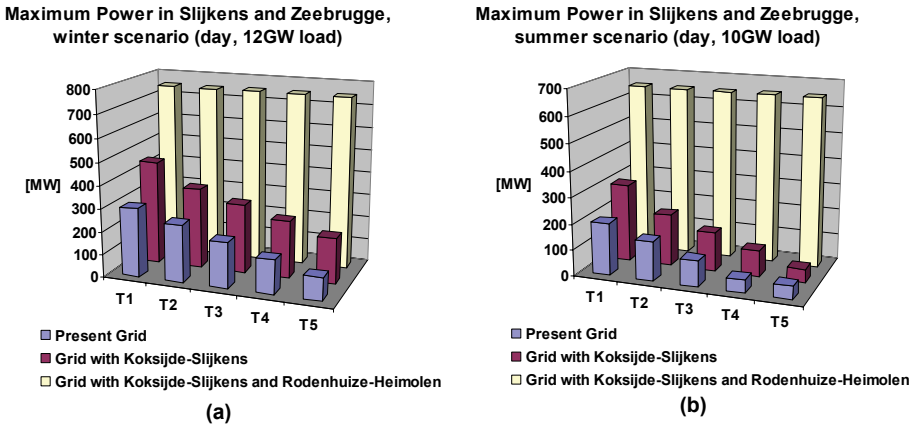

Figure 7.5. Maximum Power injection from offshore wind farms in Slijkens and Zeebrugge, Winter day scenario (12 GW load) and Summer day scenario (10 GW load), resulting from the static load flow calculations, for increasing power transits T1 (400 MW)… T5 (2000 MW).

Figure 7.5 shows for instance the results for the Winter (12 GW load) and Summer day scenario (10 GW load). With the present grid, system overload or contingency problems may already occur with an extra power injection from offshore wind of 150 MW to 50 MW, depending on the level of international power transit. The installation of the link Koksijde-Slijkens in the coastal region slightly alleviates this problem. A reinforcement of the critical link between Rodenhuize and Heimolen inland further alleviates the problem: due to the power plant of Herdersbrug and

Ruien very near to the coast (Figure 7.4b), there is already a net power flow from the coast to in-land, aggravated by offshore wind power, and causing congestion on the link Rodenhuize-Heimolen further inland.

Figure 7.5 shows the results for only one scenario. The general conclusion of the study, taking into account all scenarios, is that offshore wind power in Belgium requires relatively small grid reinforcements of critical links up to an installed wind power of ca. 600 MW. More installed power requires an extension of the 400 kV-grid towards the coast, a very costly operation and probably provoking opposition because of the impact on the landscape. This study was done in 2002. The Belgian TSO was since long aware of the local congestion problems, which are meanwhile alleviated, after the partial decommissioning of some generators (e.g. Rodenhuize).

7.3. Offshore wind potential and costs

Offshore wind energy potential

Given the wind speed resources and a description of expected 2005 and 2015 technology described and commented in [XVI], a generic farm power curve is developed using the wind farm design tool WindPro®. For 2005 as well as for 2015 technology, the maximum installed power per km² is estimated at 10 MW. This estimate starts from the assumption that the distance between turbines should be at least 5D orthogonal to the prevailing wind speed, and 7D parallel with the prevailing wind speed, with D the turbine rotor diameter. Smaller distances between turbines lead to higher farm losses, i.e. the losses due to wind disturbances caused by the turbines themselves. Taking into account the available sea area discussed above, the upper limit for installed wind power is 21 GW.

The calculation of the economic potential is also discussed in [XVI]. It assumes that wind turbines can be installed in 15% to 30% of all available area with maximum water depth 20 m and within 40 km distance to shore. The resulting potential varies then between 2.1 GW and 4.2 GW.

When considering the designated area for offshore constructions, being 270 km², the maximum installed wind power is 2.7 GW. When only the area with water depth less than 20 m and distance to shore less than 40 km is considered as economically feasible, only two sandbanks remain available within the designated area, representing a surface of approximately 30 km² or an installed power of 0.3 GW.

It must be noted however that the offshore wind project under development intents to install 216 MW on an area of only 13.8 km², however split in two parts [21]. This project aims at installing 60 turbines with rotor diameter 100 m, and an installed power of 3.6 MW per turbine. The rule of thumb to determine the distance between turbines within a farm is thus not fully obeyed, probably leading to increased farm losses and to a lower annual farm capacity factor.

The potential annual energy generation by offshore wind power is estimated at 66 – 79 TWh, the range depending on the used type of technology. The economic potential corresponding to the above described zone delimitation varies between 6 and 13 TWh. When considering only the designated area for offshore wind constructions, the potential is approximately 8 TWh, or 0.93 TWh when only the sandbanks with water depth less than 20 m are considered.

All results are summarised in Table 7.1. As a reference number, also the total installed power and annual energy demand in Belgium are given.

Wind power potential		**Installed power [GW]**	**Annual energy generation [TWh]**
Potential in BCS	Total	21	66 - 79
	Economic	2.1 – 4.2	6 - 13
Potential in designated area	Total	2.7	8.5 - 10.1
	Economic	0.3	0.9 - 1.1
Belgian generation park		**Installed power [GW]**	**Annual energy consumption [TWh]**
		15.7	83.7

Table 7.1. Maximum and economic offshore wind power potential in Belgium

Estimated costs of offshore wind power

The costs of offshore wind power depend on numerous parameters, extensively discussed in [XVI]. Only the general conclusions of this study are presented here. In the area of the BCS considered to determine the economic potential, the estimated investment costs range from 1500 to 2400 euro/kW with 2005 technology and from 900 to 1600 euro/kW with 2015 technology. The estimated generation costs range from 65-90 euro/MWh with 2005 technology and 36-54 euro/MWh with 2015 technology. The ranges mainly depend on water depth, distance to the coast and hub height.

The breakdown of the investment costs is shown in Figure 7.6, for the example of a wind farm with 70 m turbine hub height, 40 km shore distance and 2005 technology.

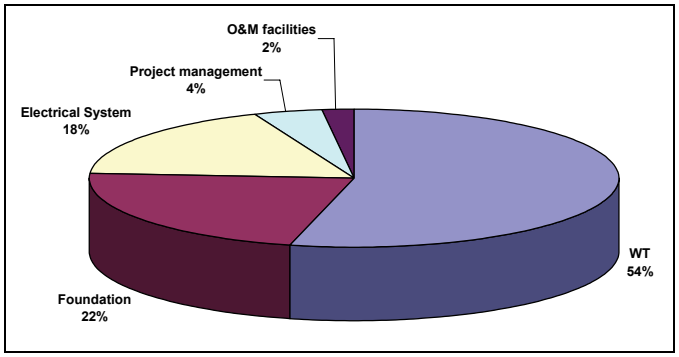

Figure 7.6. Breakdown of investment costs, for hub height 70 m, and distance to shore 40 km (total investment cost €1815/kW) [XVI]

The cost of the electrical system, consisting of transformers, a power transmission cable and optionally power electronic devices, strongly depends on the distance to shore and is estimated at 2 Meuro/km. It only slightly depends on the installed power, up to a power transmission level of 500 MW. Higher power levels would probably require multiple parallel cables, having a higher impact on the costs. The costs estimates do not include necessary reinforcements of the Belgian high voltage grid.

7.4. Conclusions

This chapter recapitulates the results of a multidisciplinary research project, treating the offshore wind power potential in the Belgian Continental Shelf, considering the expected technological developments until 2015. More results and argumentations for the used methodologies can be found in [XVI].

It is concluded that the total potential for offshore wind power is 21 GW when using all available area in the BCS for wind power applications. A more realistic potential estimate is 2.1 to 4.2 MW, considering only the available area with water depth less than 20 m and distance to shore less than 40 km. The 'immediately available' potential, i.e. within the zone designated for wind power applications and in water depths less than 20 m, is approximately 300 MW.

The potential is further limited by the available capacity of the high voltage grid. Without strong grid reinforcements, i.e. an extension of the 400 kV grid towards the coast, the maximum amount of offshore wind power that can be injected in the grid is 600 MW, however depending on the generation and load pattern of the power system in Belgium and its neighbouring countries.

The investment costs are estimated between 1500 and 2400 euro/kW for the state-of-the art technology. This only implies the costs of the wind farm itself and the connection to shore. The cost of reinforcement of the power system onshore is difficult to estimate. The public resistance for new power lines is very high, making the permitting procedure for grid upgrades very slow and with uncertain outcome. This negatively influences the budget planning of a wind farm project.

It is reminded from Chapter 6 that the added value of any installed wind power level above 0.7 GW is relatively low, due to the higher demands on the reliability of wind power generation. Considering the fact that already 95 MW onshore wind power was installed in Belgium at the end of 2004 of which 28 MW in 2004, and that the annual growth of onshore wind power is not expected to decrease for the next years, the 300 MW economic offshore potential within the designated area of the BCS is probably sufficient to reach a total of 0.7 GW installed power on- and offshore. Before further exploiting the available area resources, higher performances of wind power forecasting must be achieved. Also the development of an international market for balancing power is necessary to further use the available potential in the BCS. An international balancing market however requires a strong reinforcement of the UCTE-grid, with special attention to the power lines crossing national borders, which were originally not designed for high international power exchanges.

The author's contribution in this multidisciplinary research project covers the aspects related to the grid availability. Also, input was given for defining the expected 2005 and 2015 technology, concerning turbines and cables. For the estimation of the costs of offshore wind, the author gave input with regard to the expected technological developments of turbines and transmission cables, and the expected transmission losses. This is discussed in more detail in [XVI].

The research project also lead to the development of both a detailed and simplified dynamic wind turbine model, for use in power system simulations. This is entirely the author's work and is discussed in Chapter 5.

Chapter 8

General conclusions

8.1. Outcome of the thesis

In its introductory chapters, this thesis provides an overview of the structure of the liberalised power market, as well as the political context and support mechanisms for renewable energy in the European Union.

Chapter 3 and 4 describe the technical aspects of distributed generation and wind power. They cover a wide range of literature sources, all brought together in a dense overview. Original contributions by the author include the study concerning the operating range of doubly-fed induction generators, the estimate of potential line loss reduction by distributed generation (elaborated in Appendix I) and the comments on the existing definitions for 'value of wind power'.

The author's study with regard to distributed generation in general lead to the international publications [II], [VII], [XI]. The study concerning the operating range of doubly-fed induction generators lead to the publication [VI].

The author's own contributions are mainly situated in Chapter 5 to 7.

Chapter 5 provides a library of fundamental models for wind power that can be used by research institutes, system operators or project developers to assess the impact of wind power on a system. Detailed models allow studying a single turbine's dynamic behaviour during normal and abnormal grid conditions. It allows, among other things, to simulate whether a specific turbine with given parameters is able to 'ride through' a specific grid fault, or to support voltage control by means of

reactive power in a specific system. The impact of the turbine behaviour on the grid parameters can be simulated, as well as the impact of a grid disturbance on the mechanical loading of the turbine components. A simplified turbine model, developed in Chapter 5, allows simulating large power systems without the need for extensive programming or computational effort.

For dynamic simulations, the accuracy of the grid model in which the turbine is installed is of equal importance as the turbine model itself. General results and recommendations are hard to obtain, as the number of scenarios for the status of the grid, and the events inducing transient behaviour, are numerous. Therefore, the work is limited to a thorough description of the turbine modelling, and a simulation example of a single turbine in a specific distribution grid, demonstrating the equivalence of detailed and simplified model.

The innovative aspects in Chapter 5 include the assembly of a well-functioning detailed turbine model, using turbine model components obtained from various resources. The model is for the first time implemented in EUROSTAG, a specific software tool for power system simulations. It is easily convertible to other simulation tools. The model is originally implemented for a variable-speed pitch-controlled turbine with doubly-fed induction generator, but can be used for other turbine types by parameter modification only. The model is not based on data of a specific turbine manufacturer, but its generic implementation covers a large range of typical turbines. It is thus widely usable for power system simulations.

The methodology to develop a simplified generic dynamic model, using an equivalent transfer function with time constants derived from a detailed turbine model, is an original contribution by the author.

The research results from Chapter 5 lead to the international publications [I], [III], [V], [VIII], [IX], [X], [XII] and [XV].

The following chapters focus on the Belgian case, resulting in more specific conclusions and recommendations.

In **Chapter 6**, wind speed time series with hourly resolution, measured at three sites over a three-year period, are used to calculate the aggregated wind power time series for various scenarios of installed wind power in Belgium, ranging from evenly spread over the entire country to a single (offshore) wind farm.

These time series allow estimating the annual *capacity factor* of the aggregated wind park, ranging from 20% for the evenly distributed turbines to 31% for the single farm.

The power time series also allow estimating the general impact of the geographical spread of turbines on the fluctuations of the aggregated power. The beneficial effect of evenly spreading the turbines is proven in this work, but should not be overestimated, due to the high correlation of simultaneous wind speeds in the entire Belgian region. Fluctuations of more than 20% of installed power within an hour still frequently occur, around 20% of the time.

An attempt to quantify the value of wind power is done in three ways: by determining the *capacity credit* of the aggregated wind park, by determining the time series of *reliable wind power generation*, and by estimating the potential *abatement of CO_2-emission*. This is elaborated in Chapter 6, and it is concluded that wind power in Belgium is preferentially installed concentrated in the regions where the wind resources are best, i.e. offshore.

It is estimated that up to an installed power of 0.7 GW, wind power has a positive impact on the CO_2-emission abatement, being the most meaningful quantification of the value of wind power. The maximum reduction of CO_2-emission by wind power is one million tonnes a year, being 4% of the total emissions by the generation park in Belgium. For higher values of installed wind power, the reduction of CO_2-emission is lower due to the increased needs of balancing power and spinning reserves.

The beneficial effect of smoothed power time series by wind turbines evenly spread over Belgium only outweigh the disadvantage of lower overall wind resources for very high values of installed wind power, in which case the requirements on the reliability of wind power generation are severely higher, and not fulfilled by any scenario for installed wind power.

Therefore, it is recommended that policy makers promote wind power up to an installed power level of approximately 0.7 GW where the wind resources are highest, i.e. preferentially offshore.

The algorithms to calculate the wind power time series, as well as the quantification methods of estimating the value of wind power, are entirely the author's original work. By adding the calculated wind power time series to the input of the existing PROMIX – tool for estimating CO_2-emissions by power generation parks, a new application of PROMIX was presented. The research results in Chapter 6 lead to the international publication [XIV].

Chapter 7 summarises a multidisciplinary research project, in which the potential of offshore wind power in the Belgian Continental Shelf is estimated. The results vary from a potential 21 GW installed offshore power when all available area is used, to a more realistic 2,1 GW when only the available area with water depth less than 20 m and distances from shore less than 40 km is considered. The potential in the Belgian North Sea area designated by the government for offshore wind constructions at the moment of writing ranges from 2.7 GW (full potential) to 0.3 GW (limited water depth and distance from shore). It must be noted that the offshore wind projects in planning or early construction stage at the moment of writing intent to install turbines in a very dense layout, leading to higher potential values of installed power in the designated area (around 0.5 GW) but probably resulting in a lower relative energy output due to increased farm losses.

The author's contribution in the multidisciplinary project presented in Chapter 7 covered all aspects related to grid availability and static and dynamic impact of wind

power on the high voltage grid. The results lead to the international publications [IV], [XIII] and [XVI], in addition to those mentioned for Chapter 5.

Given the conclusions from Chapter 6 and Chapter 7, the author calls policy makers to allow and create incentives for a full use of the economic potential in the designated offshore area. The high voltage grid has the technical capacity to absorb an amount of approximately 0.5 GW offshore power, however strongly depending on many parameters. Thus, severe grid upgrades, i.e. an extension of the 400 kV grid towards the coast, are not a conditio sine qua non for fully making use of the economic potential in the designated area.

The actual installed wind power in Belgium, all onshore, already exceeds by far 100 MW at the moment of writing. Although the author does not urge on a further explosive growth of onshore wind power, a continuous fast development can be expected. A saturation point of 200 MW onshore is called for. When the realistic offshore potential of 300 to 500 MW offshore is then fully exploited, the maximal benefits of wind power in Belgium can be achieved, as quantified above, without requiring severe grid upgrades.

8.2. Recommendations for further research

This thesis quantified an upper limit for installed wind power in Belgium, before its added value would severely decrease due to the need for extra ancillary services and balancing power on the one hand, and for severe grid upgrades on the other hand.

With regard to balancing power, research is recommended on how more wind power can be integrated in the system without putting higher demands on balancing power.

- The concept of *demand side management*, as an economical alternative to addressing expensive power reserves, offers a high potential for additional contribution by wind power and distributed generation in general. Particularly the topic of *load shedding*, i.e. gradually disconnecting loads in situations of high electrical demand or low power generation, and its potential to reduce generation reserves requirements, is a recommended subject for further research.

- Forecasting of wind power is only very briefly discussed in this thesis. Its improvement is strongly necessary for the further development of wind power. The impact of wind speed forecasts, and its possible errors, on the

maximum level of wind power penetration in a system is a recommended subject for further research.

- Increased possibilities of energy storage may prove very valuable as complementary to wind power generation. Energy storage has since long been the subject of much research, and progress in this topic is very slow. Storage of energy can be done through electrochemical batteries, regenerative fuel cells, flywheels, supercapacitors, inductances, compressed air etc. The largest installed storage device, pumped hydro storage excluded, is a 120 MWh, 15 MW plant at Innogy's Little Barford Power Station in the UK (2003), with an efficiency of 75%, consisting of regenerative polysulfide bromide batteries ([116], [117]). The project was however terminated due to financial problems. These capacities are however still very low compared to pumped hydro storage plants, of which Coo (1300 MW, 4h) was mentioned in Chapter 6 for the Belgian case. The potential of large-scale development of storage devices is thus yet to be fully exploited, however only realisable on a very long term.

With regard to the need for grid upgrades, it is an interesting study to evaluate the impact of wind power on the European power system, especially on the loop flows, i.e. power flows through various control areas that were not nominated in advance, and being due to the existence of various parallel electrical paths between two control areas. However, such a study requires much information about power systems, load and generation patterns, installed wind power and wind speeds. These data are mostly confidential and scattered among a number of parties. Such a study would thus require a solid international coordination and support for gathering and extracting all necessary data.

Bibliography

Chapter 1

[1] European Wind Energy Association: *http://www.ewea.org* (last consulted in July 2005).

[2] Statistics on national electricity consumption and production of UCTE countries, 2004, *available at http://www.ucte.org*.

[3] *http://www.wilmar.risoe.dk* (last consulted in July 2005).

[4] 'Energiewirtschaftliche Planung für die Netzintegration von Windenergie in Deutschland an Land und Offshore bis zum Jahr 2020,' Konsortium DEWI / E.ON Netz / EWI / RWE Transportnetz Strom / VE Transmission, February 2005, *available at http://www.deutsche-energie-agentur.de*.

[5] Federal Science Office, *http://www.belspo.be*.

[6] Institute for the Promotion of Innovation by Science and Technology in Flanders, *http://www.iwt.be*.

[7] *http://www.elia.be*.

[8] Fund for Scientific Research - Flanders (Belgium), *http://www.fwo.be*.

Chapter 2

[9] Directive 96/92/EC of the European Parliament and of the Council of 19 December 1996 concerning common rules for the internal market in electricity, Official Journal of the European Union, 1997, L 27, pages 20-29.

[10] Directive 2003/54/EC of the European Parliament and of the Council of 26 June 2003 concerning common rules for the internal market in electricity and

repealing Directive 96/92/EC, Official Journal of the European Union, L 176, 2004, pages 37-55.

[11] S. Stoft, 'Power system economics, designing markets for electricity', John Wiley & Sons; 1st edition, May 2002, 496 pages.

[12] L. Meeus, K. Purchala, R. Belmans, 'Development of the Internal Electricity Market in Europe,' Regulatory Round Table and Annual Conference, Florence School of Regulation, Firenze, May 2005, *available at http://www.esat.kuleuven.ac.be/electa/publications/search.php*.

[13] European Commission EC (2005a), Fourth benchmarking report, Annual Report on the Implementation of the Gas and Electricity Internal Market, Communication from the Commission, COM(2004) 863, *available at http://europa.eu.int/comm/energy*.

[14] L. J. de Vries: "Capacity Allocation in a Restructured Electricity Market: Technical and Economic Evaluation of Congestion Management Methods on Interconnectors, Proc. of IEEE Power Tech Conference, Porto, 2001.

[15] K. Purchala, L. Meeus, R. Belmans, Implementation Aspects of Coordinated Auctions for Congestion Management, Proc. IEEE Bologna Power Tech Conference, 2003.

[16] K. Skytte, P. Meibom, M.A. Uyterlinde, D. Lescot, T. Hoffman, P. del Rio, 'Challenges for investment in renewable electricity in the European Union: Background report in the ADMIRE-REBUS project,' November 2003, *available at: http://www.admire-rebus.net/publications.html*.

[17] Communication from the Commission - ENERGY FOR THE FUTURE: RENEWABLE SOURCES OF ENERGY - Green paper for a Community Strategy COM/96/0576/, 20 November 1996.

[18] Communication from the Commission - Energy for the future: renewable sources of energy - White Paper for a Community strategy and action plan COM/97/0599; 1997.

[19] Directive 2001/77/EC of the European Parliament and of the Council of 27 September 2001 on the Promotion of Electricity Produced from Renewable Energy Sources in the Internal Electricity Market, Official Journal of the European Union, L 283 , 27 October 2001, pages 33 – 40.

[20] British Wind Energy Association: *http://www.bwea.org* (last consulted in July 2005).

[21] *http://www.c-power.be* (last consulted in July 2005).

Chapter 3

[22] 'Distributed Generation in Liberalised Electricity Markets,' International Energy Agency IEA, 2002.

[23] G. Pepermans, J. Driesen, D. Haeseldonckx, R. Belmans and W. D'haeseleer, Distributed generation: definition, benefits and issues, Energy Policy, Volume 33, Issue 6, April 2005, pages 787-798.

[24] N. Jenkins *et al*., 'Report of CIRED Working Group No 4 on Dispersed Generation,' Proceedings of CIRED '99 conference, Nice, 1-4 June 1999.

[25] T. Ackermann, G. Andersson and L. Söder, 'Distributed generation: a definition,' Electric Power Systems Research, Volume 57, Issue 3, 20 April 2001, pages 195-204.

[26] W. El-Khattam and M. M. A. Salama, 'Distributed generation technologies, definitions and benefits,' Electric Power Systems Research, Volume 71, Issue 2, October 2004, pages 119-128.

[27] T. Feck, R. Steinberger-Wilckens, K. Stolzenburg, 'Hydrogen as a Storage and Transportation Vector for Offshore Wind Power Production,' Proceedings of the 3rd International Workshop on Transmission Networks for Offshore Wind Farms, Stockholm, April 11-12, 2002.

[28] *http://www.fuelcells.org* (last consulted in May 2005).

[29] T. Gönen, Electric power distribution system engineering, MacGraw-Hill New Tork (N.Y.), 1989, 739 pages.

[30] P. Kundur, 'Power System Stability and Control,' Electric Power Research Institute EPRI, 1994.

[31] N. Jenkins, 'Embedded Generation,' IEE Power and Energy Series 31, 2000, IX, 273 pages.

[32] J. Matevosyan, T. Ackermann, L. Söder, 'Comparison of International Regulations for Connection of Wind Turbines to the Network,' Nordic Wind Power Conference (NWPC04), Chalmers University of Technology, Göteborg, Sweden, March 1-2, 2004.

[33] A. Johnson, N. Tleis, 'The Development of Grid Code Requirements for New and Renewable Forms of Generation in Great Britain,' Fifth International Workshop on Large-Scale Integration of Wind Power and Transmission Networks for Offshore Wind Farms, Glasgow, Scotland, April 7-8, 2005.

[34] 'Specifications for Connecting Wind farms to the Transmission Network,' Transmission System Planning, Eltra, April 2000, *available at http://www.eltra.dk/composite-837.htm*.

[35] 'Ergänzende Netzanschlussregeln für Windenergieanlagen,' E.ON Netz GmbH. Stand: 01. December 2001

[36] 'E.ON Netz Grid Code,' August 2003, *available at http://www.eon-netz.com*.

[37] 'Netzanschluss- und Netznutzungsregeln der Vattenfall Europe Transmission GmbH,' January 2004, *available at http://transmission.vattenfall.de*.

[38] L. Craig, 'Large-scale Integration of Wind Power into Power Systems – the Spanish Experience,' Fifth International Workshop on Large-Scale

Integration of Wind Power and Transmission Networks for Offshore Wind Farms, Glasgow, Scotland, April 7-8, 2005.

[39] 'Procedimiento de Operación del Sistema, 12.2 Instalaciones Conectadas a la Red de Transporte: Requisitos Mínimos de Diseño, Equipamiento, Funcionamiento y Seguridad y Puesta en Servicio,' 11 February 2005, *available at http://www.ree.es*.

[40] Technisch Reglement Distributie Elektriciteit Vlaams Gewest, 30 November 2004, *available at http://www.vreg.be*.

[41] A. Woyte, 'Design Issues of Photovoltaic Systems and their Grid Integration,' PhD-thesis, Faculteit Toegepaste Wetenschappen, Katholieke Universiteit Leuven, December 2003, Leuven, Belgium.

[42] P.M. Anderson, 'Power System Protection,' IEEE Press Power Engineering Series, 1999, 1305 pp.

[43] D. Alvira, 'Integration of Wind Power in the System,' presentation for the CIGRE Working Group C6.08: 'Integration of large share of fluctuating generation', February 2005.

[44] 'Wind Energy is Growing Faster than the Grid,' Interview with Uwe Radtke, Enercon WindBlatt Magazine, June 2002.

[45] M. Didden, 'Techno-economic Analysis of Methods to Reduce Damage due to Voltage Dips,' PhD-thesis, Faculteit Toegepaste Wetenschappen, Katholieke Universiteit Leuven, December 2003, Leuven, Belgium.

[46] International Standard IEC 61400-21, 'Wind Turbine Generator Systems – Part 21: Measurement and Assessment of Power Quality Characteristics of Grid Connected Wind Turbines,' December 2001.

[47] K. De Brabandere, B. Bolsens, J. Van den Keybus, A. Woyte A., J. Driesen, R. Belmans, 'A voltage and frequency droop control method for parallel inverters,' 2004 IEEE 35th Annual power electronics specialists conference, Aachen, Germany, June 20-25, 2004; pages 2501-2507.

[48] International Standard IEC 61000-4-15, 'Electromagnetic compatibility (EMC) – Part 4: Testing and measurement techniques – Section 15: Flickermeter – Functional and design specifications,' November 1997.

[49] R. Belhomme, C. Corenwinder, 'Wind Power Integration in the French Distribution Grid: Regulations and Network Requirements,' Nordic Wind Power Conference (NWPC04), Chalmers University of Technology, Göteborg, Sweden, March 1-2, 2004.

[50] A. Larsson, 'The Power Quality of Wind Turbines', PhD thesis, Department of Elektrical Power Engineering, Chalmers University of Technology, Göteborg, Sweden, 2000.

Chapter 4

[51] *http://www.windpower.org* (last consulted in July 2005).

[52] European Wind Atlas, Risø National Laboratory, 1989.

[53] T. Ackermann *et al*., 'Wind Power in Power Systems,' John Wiley & Sons, 2005.

[54] G. Giebel, 'On the benefits of distributed generation of wind energy in Europe,' PhD-thesis, Carl von Ossietzky Universität Oldenburg, Germany, September 2000.

[55] P. Dowling, B. Hurley, 'A strategy for locating the least cost wind energy sites within an E.U. electrical load and grid infrastructure perspective,' Fifth International Workshop on Large-Scale Integration of Wind Power and Transmission Networks for Offshore Wind Farms, Glasgow, Scotland, April 7-8, 2005.

[56] P. Nørgaard , 'MAWIPOC - a model to simulate the aggregated wind power time series for an area,' European Wind Energy Conference EWEC'04, 22-25 November 2004, London, UK.

[57] H. K. Holttinen, 'Aggregated wind power production and smoothing of hourly variations in the Nordic countries,' European Wind Energy Conference EWEC'04, 22-25 November 2004, London, UK.

[58] Slootweg J.G., H. Polinder, W.L. Kling. 'Dynamic modelling of a wind turbine with doubly-fed induction generator,' 2001 IEEE Power Engineering Society Summer Meeting, Vancouver, 15-19 July 2001, pages 1-6.

[59] *http://www.vestas.dk*, last consulted in July 2005.

[60] L. Schreier, M. Chomát, J. Bendl, 'Working Regions of Adjustable-Speed Units with Doubly Fed Machines', IEMDC Conference, Seattle, USA, May 1999.

[61] J.L Rodriguez-Amenedo, S. Arnalte, J.C. Burgos, 'Design criteria of variable speed wind turbines with doubly-fed induction generator,' European Wind Energy Conference (EWEC'01), Copenhagen, Denmark, 2-6 July 2001.

[62] E. De Vries, 'Global wind technology – overview of developments 2003 – 2004,' Renewable Energy World, July 2004.

[63] M.R. Dubois, H. Polinder, J.A. Ferreira, 'Comparison of Generator Topologies for Direct-Drive Wind Turbines,', IEEE Nordic Workshop on Power and Industrial Electronics (NORPIE2000), Aalborg, Denmark, June 13-16, 2000.

[64] M.R. Dubois, 'Review of Electromechanical Conversion in Wind Turbines,' internal report, Technical University of Delft, April 2000.

[65] S. Jockel, 'Gearless Wind Energy Converters with Permanent Magnet Generators- An Option for the Future?' European Wind Energy Conference (EWEC'96), Gothenburg, Sweden. 20-24 May 1996.

[66] J. Luo, D. Qin, T.A. Lipo, S. Li and S. Huang, 'Axial Flux Circumferential Permanent Magnet (AFCC) Machine,' IEEE IAS Annual Meeting, St. Louis, Oct.1998, pages 144-151.

[67] E. Muljadi, C.P. Butterfield, Y. Wan, 'Axial-Flux Modular Permanent-Magnet Generator with a Toroidal Winding for Wind-Turbine Applications,' IEEE Transactions on Industry Applications, Vol. 35, No 4, July/August 1999, pages 831-835.

[68] E. Spooner, A.C. Williamson, 'Direct coupled, permanent magnet generators for wind turbine applications,' IEE-Proceedings Electric Power Applications. vol.143, no.1; Jan. 1996; p.1-8.

[69] A. Grauers, Design of Direct-driven Permanent-Magnet Generators for Wind Turbines, PhD-Thesis, 1996, Chalmers University of Technology, Gothenburg, Sweden.

[70] D. A. Torrey, 'Variable-reluctance generators in wind-energy systems,' IEEE PESC'93, 1993, pages 561–567.

[71] D. A. Torrey, 'Switched Reluctance Generators and Their Control,' IEEE Transactions on Industrial Electronics, Vol.49, No. 1, February 2002, pages 3-14.

[72] A. K. Wallace, R. Spee, G.C. Alexander, 'The brushless doubly-fed machine: its advantages, applications and design methods,' IEMDC'93, London, UK; 1993, pages 511-517.

[73] E. Wiedenbrug, M.S. Boger, A.K. Wallace, D. Patterson, 'Electromagnetic mechanism of synchronous operation of the brushless doubly-fed machine,' 1995 IEEE Industry Applications Conference, IEEE, New York, NY, USA; 1995.

[74] S. Williamson, A.C. Ferreira, A.K. Wallace, 'Generalised theory of the brushless doubly-fed machine. I. Analysis,' IEE Proceedings Electric Power Applications. vol.144, no.2; March 1997; p.111-122.

[75] D. Zhou, R. Spée, G.C. Alexander, 'Experimental evaluation of a rotor flux oriented control algorithm for brushless doubly-fed machines,' IEEE-Transactions on Power Electronics. vol.12, no.1; Jan. 1997; p.72-78.

[76] R. Li, A. Wallace; R. Spée, 'Dynamic simulation of brushless doubly-fed machines', IEEE-Transactions on Energy Conversion. vol.6, no.3; Sept. 1991; p.445-452.

[77] S. Bhowmik, R. Spée, J.H.R. Enslin, 'Performance optimisation for doubly fed wind power generation systems,' IEEE Transactions on Industry Applications. vol.35, no.4; July-Aug. 1999; p.949-958.

[78] F. Runcos, R. Carlson, A. M. Oliveira, P. Kuo-Peng N. Sadowski, 'Performance Analysis of a Brushless Double Fed Cage Induction

Generator,' Nordic Wind Power Conference (NWPC04), Chalmers University of Technology, Göteborg, Sweden, March 1-2, 2004.

[79] 'Wind Energy, the Facts: an Analysis of Wind Energy in the EU-25', EWEA, *available at http://www.ewea.org/.*

[80] *http://www.jeumont-framatome.com* (last consulted in July 2005).

[81] R M.G. Castro, L.A.F.M. Ferreira, 'A Comparison Between Chronological and Probabilistic Methods to Estimate Wind Power Capacity Credit,' IEEE Transactions on Power Systems, Vol.16, No.4, November 2001, pages 904-909.

[82] J. Sontow, M. Kaltschmitt, 'Capacity Effects of Wind Power Generation Quantification and Economic Assessment,' Wind Power for the 21st Century, the Challenge of High Wind Power Penetration for the New Energy Markets, Kassel 25-27 Sep. 2000, pages 259-262.

[83] G. Giebel, 'A Variance Analysis of the Capacity Displaced by Wind Energy in Europe,' Wind Power for the 21st Century, the Challenge of High Wind Power Penetration for the New Energy Markets, Kassel 25-27 Sep. 2000, pages 263-267.

[84] B. Raison, S. Dupuis, 'Capacity credit evaluation of wind energy conversion systems,' IEEE Young researchers symposium in electrical power engineering - Distributed generation, Leuven, Belgium, February 7-8, 2002.

Chapter 5

[85] V. Akhmatov, 'Analysis of Dynamic Behaviour of Electric Power Systems with Large Amount of Wind Power,' PhD- thesis, Technical University of Denmark, November 2003.

[86] J.G. Slootweg, 'Wind Power: Modelling and Impact on Power System Dynamics,' PhD-thesis, Technische Universiteit Delft, December 2003.

[87] V. Akhmatov, H. Knudsen, A. H. Nielsen, 'Advanced Simulation of Windmills in the Electric Power Supply,' International Journal of Electrical Power & Energy Systems, Volume 22, Issue 6, August 2000, pages 421-434.

[88] V. Akhmatov, 'Modelling of Variable-Speed Wind Turbines with Doubly-Fed Induction Generators in Short-Term Stability Analysis', Third International Workshop on Transmission Networks for Offshore Wind Farms, Stockholm, April 11-12, 2002.

[89] Slootweg J.G., H. Polinder, W.L. Kling; 'Dynamic modelling of a wind turbine with doubly-fed induction generator'. 2001 IEEE Power Engineering Society Summer Meeting (Vancouver, 15-19 July 2001), IEEE Power Engineering Society, S.l., 2001, pages 1-6.

[90] 'Dynamic Modelling of Doubly-Fed Induction Machine Wind-Generators', DigSilent GmbH Technical Documentation, 2003, available at *http://www.digsilent.de*.

[91] R. W. Delmerico, N. Miller, W. W. Price, J. J. Sanchez-Gasca, 'Dynamic Modelling of GE 1.5 and 3.6 MW Wind Turbine-Generators for Stability Simulations,' IEEE Power Engineering Society PES General Meeting, 13-17 July 2003, Toronto, Canada.

[92] M. Pöller, S. Achilles, 'Direct Drive Synchronous Machine Models for Stability Assessment of Wind Farms', Fourth International Workshop on Large Scale Integration of Wind Power and Transmission Networks for Offshore Wind Farms, Billund, Denmark, October 20-21 2003.

[93] Hafzullah Aksoy, Z. Fuat Toprak, Ali Aytek, N. Erdem Unal, 'Stochastic generation of hourly mean wind speed data,' Renewable Energy, Volume 29, Issue 14, pages 211-213, November 2004.

[94] P.C. Krause. O. Wasynczuk, S.D. Sudhoff, 'Analysis of Electric Machinery', IEEE Press, New York, 1995.

[95] D.W. Novotny, T.A. Lipo, 'Vector Control and Dynamics of AC Drives', Oxford University Press, 1996.

[96] S. Müller, M. Deicke, R. W. De Doncker, 'Adjustable Speed Generators for Wind Turbines based on Doubly-fed Induction Machines and 4-Quadrant IGBT Converters Linked to the Rotor,' Conference Record of the 2000 IEEE Industry Applications Conference, 8-12 October 2000, vol. 4 pages 2249 - 2254.

[97] M. Pöller, S. Achilles, 'Aggregated Wind Park Models for Analyzing Power System Dynamics,' Fourth International Workshop on Large Scale Integration of Wind Power and Transmission Networks for Offshore Wind Farms, Billund, Denmark, October 20-21 2003.

[98] P. Christiansen, 'The Wind Farm Main Controller and the Remote Control System in the Horns Reef Offshore Wind Farm', OWEMES 2003 Conference, Naples, Italy, 12-14 April 2003.

[99] P. Christiansen K.K. Jorgensen, A. G. Sorensen, 'Grid Connection and Remote Control for the Horns Rev 160MW Offshore Wind Farm,' August 2002, *available at http://www.hornsrev.dk*.

[100] G. Slootweg, S.W.H. de Haan, H. Polinder, W.L. Kling, 'General model for representing variable speed wind turbines in power system dynamics simulations,' IEEE Transactions on Power Systems, Volume: 18 , Issue: 1, Feb. 2003, pages:144 – 151.

Chapter 6

[101] P. Nørgaard, H. Holttinen, 'A Multi-Turbine Power Curve Approach', Nordic Wind Power Conference, 1-2 March 2004, Chalmers University of Technology, Göteborg, Sweden.

[102] A. D. Sahin, Z. Sen, 'First-order Markov chain approach to wind speed modelling,' Journal of Wind Engineering and Industrial Aerodynamics, Volume 89, Issues 3-4, March 2001, pages 263-269.

[103] Hafzullah Aksoy, Z. Fuat Toprak, Ali Aytek, N. Erdem Ünal, 'Stochastic generation of hourly mean wind speed data,' Renewable Energy, Volume 29, Issue 14, November 2004, pages 2111-2131.

[104] BONUS 600 kW power curve, *available at http://www.bonus.dk.*

[105] GE 3.6 MW power curve, *available at http://www.gepower.com*.

[106] A. Shamshad, M.A. Bawadi, W.M.A. Wan Hussin, T.A. Majid, S.A.M. Sanusi, 'First and second order Markov chain models for synthetic generation of wind speed time series,' Energy, Volume 30, Issue 5, April 2005, pages 693-708.

[107] K.R. Voorspools, W. D. D'haeseleer, 'An evaluation method for calculating the emission responsibility of specific electric applications,' Energy Policy, Volume 28, Issue 13, November 2000, pages 967-980.

[108] K.R. Voorspools, 'The modelling of large electricity-generation systems with applications in emission-reduction scenarios and electricity trade,' PhD-thesis, Faculteit Toegepaste Wetenschappen, Katholieke Universiteit Leuven, May 17, 2004.

[109] Federation of the electricity companies in Belgium (*http://www.bfe-fpe.be* - last consulted in July 2005).

[110] M. Junginger, A. Faaij, 'Cost reduction prospects for the offshore wind energy sector,' European wind energy conference EWEC, Madrid, Spain, June 16-19, 2003.

[111] *http://www.pointcarbon.com* (last consulted in July 2005).

[112] F. Lecock, K. Capoor, 'State and Trends of the Carbon Market 2005,' International Emission Trading Organisation (IETA), May 9, 2005, available at *http://www.ieta.org* (last consulted in July 2005).

[113] European Directive 2003/87/EC of the European Parliament and of the Council of 13 October 2003 establishing a scheme for greenhouse gas emission allowance trading within the Community and amending Council Directive 96/61/EC (Text with EEA relevance) Official Journal L 275 , 25/10/2003 pages 32 – 46.

Chapter 7

[114] S. Le Bot, V. Van Lancker, S. Deleu, M. De Batist, J.P. Henriet, W. Haegeman, 'Geological characteristics and geotechnical properties of Eocene and Quaternary deposits on the Belgian continental shelf: synthesis in the context of offshore wind farming,' Netherlands Journal of Geosciences – Geologie en Mijnbouw, volume 84, N°2, pages 147-160.

[115] G. M. Watson, J. A. Halliday, J P. Palutikof, T. Holt, R. J. Barthelmie, J. P. Coelingh, E. J. van Zuylen, J. W. Cleijne, 'Predicting offshore wind energy resources (POWER),' JOR3-CT98-0286, July 2001.

Chapter 8

[116] *http://www.electricitystorage.org* (last consulted in July 2005).

[117] *http://www.regenesys.com* (last consulted in July 2005).

List of Publications

All publications are available at

http://www.esat.kuleuven.ac.be/electa/publications/search.php

Reviewed journal

[I] J. Soens, J. Driesen, R. Belmans, 'Equivalent Transfer Function for a Variable-speed Wind Turbine in Power System Dynamic Simulations,' International Journal of Distributed Energy Resources, Volume 1 Number 2, April-June, 2005; pages 111-133.

International conferences

[II] C. Dragu, J. Soens, R. Belmans: 'Small-Scale Renewable Energy in The Next Century Market Hydro Plants - State of The Art and Applications,' International conference on renewable energies and power quality (ICREPQ '03), Vigo, Spain, April 9-12, 2003.

[III] J. Soens, J. Driesen, R. Belmans: 'A comprehensive model of a doubly-fed induction generator for dynamic simulations and power system studies,' International conference on Renewable energies and power quality (ICREPQ),, Vigo, Spain, April 9-12, 2003.

[IV] P. Van Roy, J. Soens, J. Driesen, R. Belmans: 'Impact of offshore wind power on the Belgian HV-grid,' European wind energy conference EWEC, Madrid, Spain, June 16-19, 2003.

[V] J. Soens, T. Vu Van, J. Driesen, R. Belmans: 'Modelling wind turbine generators for power system simulations,' European wind energy conference EWEC, Madrid, Spain, June 16-19, 2003.

[VI] J. Soens, K. De Brabandere, J. Driesen, R. Belmans: 'Doubly-fed induction machine: Operating regions and dynamic simulation,' 10th European Conference on Power Electronics and Applications (EPE 2003), Toulouse, France, September 2-4, 2003.

[VII] T. Vu Van, A. Woyte, J. Soens, J. Driesen, R. Belmans: 'Impacts of distributed generation on distribution system power quality,' Electrical Power Quality and Utilisation, EPQU 03, Cracow, Poland, September 17-19, 2003; pages 585-591.

[VIII] J. Soens, J. Driesen, R. Belmans: 'Generic dynamic wind farm model for power system simulations,' Nordic Wind Power Conference, Chalmers University of Technology, Göteborg, Sweden, March 1-2, 2004.

[IX] J. Soens, J. Driesen, R. Belmans: 'Wind turbine modelling approaches for dynamic power system simulations,' IEEE Young Researchers Symposium in Electrical Power Engineering - Intelligent Energy Conversion, Delft, The Netherlands, March 18-19, 2004.

[X] J. Soens, J. Driesen, D. Van Hertem, R. Belmans: 'Generic aggregated wind farm model for power system simulations - impact of grid connection requirements,' International Conference on Renewable Energy and Power Quality (ICREPQ), Barcelona, Spain, March 31-April 1, 2004.

[XI] T. Vu Van, D. Vandenbrande, J. Soens, D.M. Van Dommelen, J. Driesen, R. Belmans: 'Influences of large penetration of distributed generation on N-1 safety operation,' IEEE Power engineering society, Denver, Colorado, USA, June 6-10, 2004.

[XII] J. Soens, J. Driesen, R. Belmans: 'Interaction between electrical grid phenomena and the wind turbine's behaviour,' Noise and Vibration Engineering (ISMA 2004), Leuven, Belgium, Sept.20-22, 2004; pages 3969-3987.

[XIII] F. Van Hulle, Y. Cabooter, S. Le Bot, V. Van Lancker, S. Deleu, J. Driesen, J. Soens: 'Prospects for offshore wind energy from the Belgian continental shelf,' European wind energy conference (EWEC), London, Nov. 22-25, 2004.

[XIV] J. Soens, J. Driesen, R. Belmans, 'Estimation of fluctuation of wind power generation in Belgium,' Fifth International Workshop on Large-Scale Integration of Wind Power and Transmission Networks for Offshore Wind Farms, April 7-8, 2005, Glasgow, Scotland.

[XV] J. Soens, S. Geerts, J. Driesen, C. Hirsch, R. Belmans, 'Entire wind-to-power representation of a wind turbine unit in electrical power system studies,' CIRED 18th International Conference on Electricity Distribution, June 6-9, 2005, Turin, Italy.

Book

[XVI] S. Le Bot, V. Van Lancker, S. Deleu, J.P. Henriet, Y. Cabooter, G. Palmers, L. Dewilde, J. Soens, J. Driesen, P. Van Roy, R. Belmans, F. Van Hulle, 'Optimal offshore wind energy developments in Belgium,' Part 1: Sustainable production and consumption patterns, final report CP/21-SPSD II, May 2004; 153 pages.

Appendix I

Potential line loss reduction by distributed generation

Optimal power injection and location of one generator

In paragraph 3.3.1, the general statement was made that distributed generation can severely reduce the line losses along a feeder line. A general formula is now developed to find the optimal rating and location of a distributed generator along a line, with the assumption that the load along the cable is evenly distributed.

In Figure 3.1b, the active power flow P_{flow} through the distribution line, as a function of the distance x from the distribution transformer, is:

$$P_{flow}(x) = \left(P_L - P_G\right) - p_l x \qquad \text{for} \quad 0 < x < x_G \qquad \text{(I.1)}$$

$$P_{flow}(x) = (L - x)\, p_l \qquad \text{for} \quad x_G < x < L \qquad \text{(I.2)}$$

with

- L line length;
- P_L total load along the line;
- p_l electrical load along the line per unit of length:

$$P_L = p_l L \tag{I.3}$$

- P_G power injected by the distributed generator.

When only ohmic losses are considered, and when reactive power transport is considered very small compared to active power transport along the feeder line, the local losses in the feeder line are proportional to the square of the power flow.

In a single-phase system, the following equation applies:

$$p_{loss}(x) = K \cdot P_{flow}(x)^2 \tag{I.4}$$

with K a constant factor, equal to:

$$K = \frac{r_{line}}{U^2} \tag{I.5}$$

and with

- $p_{loss}(x)$ the losses in the feeder line, per unit length;
- r_{line} the ohmic line resistance, per unit length;
- U the line voltage, which is, as a first approach, considered constant along the distribution line.

The total power losses P_{loss} in the distribution line are then calculated using (I.1) to (I.4):

$$P_{loss} = K \cdot \left[\int_0^{x_G} \left(\left(p_l L - P_G \right) - p_l x \right)^2 dx + \int_{x_G}^{L} \left(\left(L - x \right) p_l \right)^2 dx \right] \tag{I.6}$$

After some calculations, the following result is obtained:

$$P_{loss} = K \cdot \left[p_l P_G {x_G}^2 + \left({P_G}^2 - 2 p_l P_G L \right) x_G + \frac{{p_l}^2 L^3}{3} \right] \tag{I.7}$$

For a given generator power injection P_G, its position resulting in the minimal line losses is calculated from:

$$\frac{\partial P_{loss}}{\partial x_G} = 0 \tag{I.8}$$

yielding

$$x_G = \frac{2p_l L - P_G}{2p_l} \tag{I.9}$$

It is seen that x_G increases for decreasing power injection P_G.

Alternatively, (I.7) can be used to find the optimal generator power P_G for a given location x_G:

$$\frac{\partial P_{loss}}{\partial P_G} = 0 \tag{I.10}$$

yielding

$$P_G = \frac{2p_l L - p_l x_G}{2} \tag{I.11}$$

The further the generator is located from the distribution transformer (i.e. the higher x_G), the lower P_G must be for line loss minimisation.

The absolute optimum is found when both x_G and P_G can be optimally chosen. For this, (I.9) is replaced in (I.7) and partially derived with respect to P_G.

After some calculations, the following result is obtained:

$$P_G = \frac{2}{3} p_l L = \frac{2}{3} P_L \tag{I.12}$$

Replacing (I.12) in (I.9) yields

$$x_G = \frac{2}{3} L \tag{I.13}$$

In Figure 3.1b, both P_G and x_G are optimally chosen, resulting in the power flow profile along the line as shown.

Optimal power injections and location of multiple generators

The conclusions from the previous paragraph may be generalised as follows. For the case of n generators, and with optimisation of all generator positions and power injections, the generators are located at a distance $x_{G,I}$, with

$$x_{G,i} = \frac{2i}{2n+1} L, \qquad i = 1...n \tag{I.14}$$

The power injection $P_{G,i}$ of each generator is:

$$P_{G,i} = \frac{2}{2n+1} P_L, \qquad i = 1...n \tag{I.15}$$

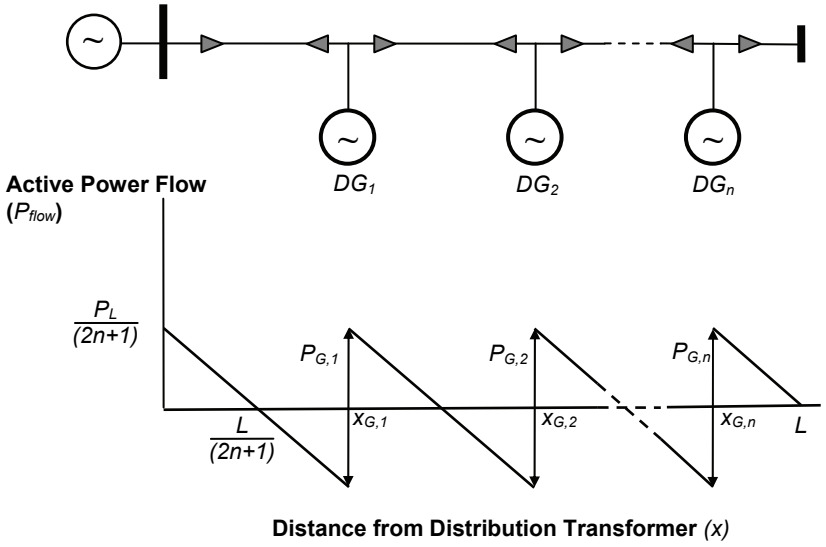

Figure I.8.1. Power flow along radial line, with *n* distributed generators

These equations are intuitively explained in Figure I.8.1, showing the power flow along a radial line for the general case of *n* distributed generators and taking (I.14) and (I.15) into account. From the optimal power injections and location follows a periodical pattern of the local power flow, resulting in the lowest overall losses.

Relative line loss reduction

Maintaining the assumption that the local line losses are proportional to the square of the local power flow, and assuming (I.14) and (I.15) satisfied, the total line losses are written from Figure I.8.1 as proportional to:

$$P_{loss} \sim (2n+1) \int_0^{\frac{L}{2n+1}} \left(\frac{P_L}{2n+1} - \frac{P_L}{L} x \right)^2 dx \tag{I.16}$$

yielding:

$$P_{loss} \sim \frac{{P_L}^2 L}{3(2n+1)^2} \tag{I.17}$$

The total line losses are inversely proportional to the square of the number of distributed generators.

Setting the line losses for the reference case without distributed generators as 100%, the relative line losses for increasing values of n are given in Table I.1.

Number of distributed generators *n*	0	1	2	3	4
Relative line losses [%]	100	11	4	2	1

Table I.1. Relative losses in a distribution line, as a function of the number of distributed generators

More general, the optimal location of a generator is calculated from (I.14) by considering $x_{G,i} / L$ not as the relative distance of the generator from the distribution transformer, but as the line impedance between the distribution transformer and the generators, normalised with respect to the total transformer and line impedance. This allows taking into account varying line impedances along its length. Mostly, the line cross-section is smaller at the end, as the transported power and thus the necessary line rating are lower in the case without distributed generation. Also, now the impedance of the distribution transformer can be included, as it represents a large fraction of the losses.

The equations calculated above are however highly theoretical, as the assumption of an evenly distributed load along a line is a firm approximate. Also, as distributed generation is mostly intermittent, the optimal power injection can not be instantaneously achieved at every moment. Furthermore, reminding that distributed generation is not dispatched and not owned by grid operators, the choices for location and power injection levels of generators are often based on business opportunities and environmental conditions, and not on issues regarding grid losses. Finally, due to the unbundling of electricity generation and grid management, the operators of distributed generators do not have an incentive to optimise their generators as a function of line losses.

Nevertheless, it is concluded from Table I.1 that distributed generation has the potential to considerably reduce line losses. Especially the difference between the

case without distributed generation and with one generator must be noted, with a total line loss reduction of almost 90%.

Appendix II

Parameters for the detailed turbine model

The parameters below refer to the detailed turbine model used in Chapter 5.

Turbine propeller			
P_{rated}	= 2 MW	R_{turb}	= 38 m
Ω_b	= 1.81 rad/s	$v_{wind,rated}$	= 13 m/s
Ω_{min}	= 1.25 rad/s = 11.9 rpm = 0.7 p.u.	ρ_{air}	= 1.225 kg/m³
Ω_{max}	= 1.96 rad/s = 18.7 rpm = 1.1 p.u.		
J_{turb} =	= $6 \cdot 10^6$ kgm²	H_{turb}	$= \frac{J_{turb} \cdot \Omega_b^{\,2}}{2 \cdot P_{rated}}$ = 5 s
Generator			
Generator base values			
S_b	= 2 MVA	U_b	= 3000 V
Ω_s	= 157.07 rad/s (1500 rpm)	Z_{base}	$= \frac{U_b^{\,2}}{S_b}$ = 4.5 Ω
ω_b	= 2π·50 rad/s	p_p	= 2

Generator parameters			
real values (all impedances referred to stator quantities)		***normalised values***	
R_s	= 0.0473 Ω	r_s	$= \frac{R_s}{Z_b}$ = 0.0105 p.u.
R_r	= 0.0387 Ω	r_r	$= \frac{R_r}{Z_b}$ = 0.0086 p.u.
L_{sd}	= 0.0652 H	x_{sd}	$= \frac{L_{sd} \cdot \omega_b}{Z_b}$ = 4.5547 p.u.
L_{rd}	= 0.0637 H	x_{rd}	$= \frac{L_{rd} \cdot \omega_b}{Z_b}$ = 4.4497 p.u.
L_{md}	= 0.0627 H	x_{md}	$= \frac{L_{md} \cdot \omega_b}{Z_b}$ = 4.3760 p.u.
L_{sq}	= 0.0652 H	x_{sq}	$= \frac{L_{sq} \cdot \omega_b}{Z_b}$ = 4.5547 p.u.
L_{rq}	= 0.0637H	x_{rq}	$= \frac{L_{rq} \cdot \omega_b}{Z_b}$ = 4.4497 p.u.
L_{mq}	= 0.0627 H	x_{mq}	$= \frac{L_{mq} \cdot \omega_b}{Z_b}$ = 4.3760 p.u.
J_{gen}	= 80 kgm²	H_{gen}	$= \frac{J_{gen} \cdot \omega_b^2}{2 p_p^2 \cdot S_b}$ = 0.5 s
$\Omega_{gen,min}$	= 110 rad/s = 1050 rpm	$\omega_{gen,min}$	= 0.7 p.u.
$\Omega_{gen,max}$	= 173 rad/s = 1650 rpm	$\omega_{gen,max}$	= 1.1 p.u.
Shaft coupling and gearbox			
gearbox ratio	= 88.2 : 1		
$K_{shaft,real}$ (low speed side)	= 77.7·10⁶Nm/rad	$K_{shaft,real}$ (high speed side)	= 10³ Nm/rad
$K_{shaft,base}$ *(low speed side)*	$= \frac{P_{rated}}{\Omega_b} \cdot (gearbox\ ratio) \cdot p_p$ = 1.942·10⁸ Nm	$K_{shaft,base}$ *(high speed side)*	$= \frac{P_{rated}}{\Omega_s} \cdot p_p$ = 2.546·10⁴ Nm
K_{shaft} *normalised: [torque p.u. / electral radian]*	$= \frac{K_{shaft,real}}{K_{shaft,base}}$ = 0.4 p.u.	K_{shaft} *normalised: [torque p.u. / electral radian]*	$= \frac{K_{shaft,real}}{K_{shaft,base}}$ = 0.4 p.u.
C_{shaft}	= 1 p.u.		
Speed Controller			
K_ω	= 5	$T_{em,max}$	= 1/ $\omega_{gen,max}$
T_ω	= 0.5 s	$T_{em,min}$	= -1/ $\omega_{gen,max}$

Pitch Controller			
K_β	= 200	β_{max}	= 30°
T_β	= 200 s	β_{min}	= 0°
Current Controller			
K_{ird}	= 0.05	$u_{rd,max}$	= 1.5 p.u.
T_{ird}	= 0.05 s	$u_{rd,min}$	= -1.5 p.u.
K_{irq}	= 0.05	$u_{rq,max}$	= 1.5 p.u.
T_{irq}	= 0.05 s	$u_{rq,min}$	= -1.5 p.u.
Rotor frequency converter			
T_{conv1}	= 0.005 s	η_{conv}	= 0.95
T_{conv2}	= 0.200 s		
Tripping settings			
$u_{under,1}$	= 0.2 p.u.	$i_{s,over}$	= 1.3 p.u.
$t_{u,under,1}$	= 0.15 s	$t_{is,over}$	= 1.2 p.u.
$u_{under,2}$	= 0.8 p.u.	$i_{r,over}$	= 1.2 p.u.
$t_{u,under,2}$	= 3 s	$t_{ir,over}$	= 0.1 s
$u_{over,1}$	= 1.3 p.u.	r_{cb}	= 0.05 p.u.
$t_{u,over,1}$	= 3 s	t_{cb}	= 0.3 s
$\omega_{over,1}$	= 1.3 p.u.		
$t_{\omega\_over,1}$	= 0.5 s		

Short Curriculum

Joris Soens

Born:
21 September 1978
Ninove (Belgium)

Secondary School:
1990-1996: Sint-Aloysiuscollege Ninove

Universitary Education:
1996 - 2001: Burgerlijk Werktuigkundig-Elektrotechnisch Ingenieur, Richting Elektrotechniek, Optie energie, at the Katholieke Universiteit Leuven

Work:
2001-2005: Research Assistant and PhD-student at the Katholieke Universiteit Leuven, Electrotechnical Department (ESAT-ELECTA), funded by *Fonds voor Wetenschappelijk Onderzoek (F.W.O.) – Vlaanderen*
Research interests: power system management, distributed generation, wind power

since 2005: Technisch Toezichthouder at the Vlaamse Reguleringsinstantie voor Elektriciteits- en Gasmarkt (VREG), the regulator for the electricity and gas market in the Flemish region.